NEONOR
Neotectonics in Norway

NGU
Geology for Society since 1858

NORSAR

STATENS
KARTVERK

AMOCO

HYDRO

PHILLIPS 66

Statkraft

Norges forskningsråd

IKU
SINTEF GROUP

RF
ROGALAND RESEARCH

N T N U
Trondheim

NGU Report 99.007

Neotectonics in Norway

Annual Technical Report 1998

NGU Norges geologiske undersøkelse Geological Survey of Norway	Geological Survey of Norway P.O.Box 3006 - Lade N-7002 Trondheim, Norway	**REPORT**

Report no.: 99.007	ISSN 0800-3416	Grading: Confidential until 1/7-2001

Title:

Neotectonics in Norway, Annual Technical Report 1998

Editors:	Client:
John Dehls and Odleiv Olesen	Amoco, Norsk Hydro, Phillips Petroleum, Statkraft, NFR, NGU, NORSAR, NPD and SK

Contributors:	Contributing institutes:
L.H. Blikra, L. Bockmann, H. Bungum, J. Dehls, S. Fanavoll, P. Goldsmith, E. Hicks, B. Hilmo, T. Klemetsrud, Æ. Jóhannsson, C. Lindholm, E. Mauring, O. Olesen, L. Olsen, F. Riis, L. Rise, D. Roberts, J.S. Rønning, A. Sylvester	NGU, NORSAR, NPD, SK, SINTEF, Rogaland Research, Phillips Petroleum, NTNU, UiO

Deposit name and grid-reference:	Number of pages: 206 Price (NOK): Map enclosures: 7

Fieldwork carried out:	Date of report:	Project no.:	Person responsible:
1998	12/03-1998	2757.00	

Summary:

The NEONOR project represents a national effort by several national research and mapping institutions to study neotectonic phenomena through a multidisciplinary approach. Information on present land uplift, seismicity, rock stress and postglacial faults is compiled in a 1: 3 million map of Norway and adjacent areas. There is good evidence for a conjugate set of normal faults perpendicular to the extensive system of NE-SW trending reverse faults in northern Fennoscandia. The Nordmannvikdalen fault in northern Troms and the Stuoragurra Fault in western Finnmark constitute the Norwegian part of this fault province. Nine other faults occur in northern Finland and northern Sweden. Trenching of the Stuoragurra Fault in Masi has revealed that the seven metre high scarp was formed in one seismic event (magnitude 7.4-7.7) during the very last part of the last deglaciation in Finnmark (i.e. c. 9,300 years BP) or shortly afterwards. Large-scale rock avalanches and gravitational faulting in northern Troms are most likely triggered by one or more earthquakes (magnitude larger than 6) immediately after the last deglaciation. New seismic mini-arrays in the Ranafjord and Bremangerlandet areas have revealed areas of increased seismicity. Several hundred earthquakes have been detected in the outer Ranafjord area during the last one and a half years, with magnitudes up to 2.8. This is very high for onshore Baltic shield areas. Neotectonic activity in the Rana, Masi and Kåfjord areas seems to influence the ground water flow. Several distortions in the Quaternary reflectors have been mapped in the northern North Sea area. Some of the subtle features may represent tectonic faults resembling the postglacial faulting previously reported by Hovland (1983). No conclusive evidence for a tectonic cause of the structures can, however, be drawn from the interpretation of the 3D seismic data. There is increasing evidence for a major seismic pulse in Fennoscandia and Scotland accompanying each of the deglaciations following the multiple glaciation cycles during the last 600.000 years. It is possible that the interaction of the contraction and dilation of fissures associated with the seismic cycles may assist in concentrating hydrocarbons from their source rocks and pumping them to potential reservoir formations.

Keywords: Geofysikk	Geologi	Seismologi
Neotektonikk	Geologisk risiko	Forkastning
Skred	Landhevning	Fagrapport

CONTENTS

LIST OF TABLES

LIST OF FIGURES

1 INTRODUCTION

By Odleiv Olesen, NGU

The initiative for a national neotectonic research project was taken in 1995 by NORSAR and the Geological Survey of Norway (NGU). The Norwegian Petroleum Directorate (OD) and NGU did at the same time make plans for compiling a neotectonic map of Norway at the scale 1:3 million. These two initiatives were merged into the 'Neotectonics in Norway - NEONOR Project in 1996. The Norwegian Mapping Authority (SK) has joined the project and is contributing with expertise on geodesy. The Norwegian Research Council (NFR) has financed three years of a four-year Doctoral fellowship (Dr. Scient for Erik Hicks at NORSAR/UiO and a two-year Post Doctoral fellowship for John Dehls at NGU, until 1 June, 1999). The project will continue for one more year and will be finished in December 1999. Mark Shahly (Amoco), Chris Dart (Norsk Hydro), Philip J. Goldsmith (Phillips Petroleum; Robert Hunsdale after August 1998) and Ivar Hågensen (Finnmark Energiverk) are representatives of the four industrial partners in the steering committee. Mark Shahly replaced Philip J. Goldsmith as chairmain after August 1998. NGU, NORSAR, OD and SK are represented by Odleiv Olesen, Hilmar Bungum, Fridtjof Riis and Lars Bockmann, respectively. Stein Fanavoll (SINTEF Petroleum Research), Willy Fjeldskaar (Rogaland Research), Ægir Jóhannsson (SINTEF Civil and Environmental Engineering) and Terje Skogseth (NTNU, Dept. of Surveying and Mapping) are carrying out substantial parts of the research project on a contract basis. Conrad Lindholm and Hilmar Bungum (NORSAR) were instrumental in the planning phase of the project proposal.

The project started in June 1997 and the activities during 1997 were reported in the NEONOR Annual Technical Report 1997 (NGU Report 98.016). The present report documents the status for the activities that have been carried out by NGU, NORSAR, NPD, SK, NTNU, Sintef and RF during 1998 (task numbers refer to the project proposal):

1. Classification and quality assessment of reported neotectonic phenomena.

2. Collation and interpretation of marine seismic data (both 2D and 3D) from Sintef Petroleum Research (former IKU), Norwegian Petroleum Directorate and the petroleum industry, aimed at mapping recent offshore faulting.

3. Production of a 1:3 million scale map on neotectonic phenomena in Norway.

4. Geological and geophysical investigations .

5-7. Acquisition and interpretation of local and regional high-resolution geodetic data, also by means of GPS networks .

8. Drilling through faults; *In situ* stress measurements.

9. Trenching of postglacial faults.

10. Acquisition of local seismological data by means of new seismic stations (micro-networks).

11. Joint interpretation of acquired neotectonic data and geodynamic modelling aimed to understand the recent and present day crustal dynamics.

One Dr. Scient fellowship and one post Doctoral fellowship are essential parts of the project, and these will run over four and two years, respectively.

The NEONOR activities in 1998 have generally followed the lines of the NEONOR Project Document. There have been some delays in the interpretations of the 3D seismic data but this work is now included in the present report. A combined NEONOR Project Meeting in Alta and excursion to the Stuoragurra postglacial fault was arranged in August, 1998. A similar arrangement with project meeting in Tromsø and excursion to the Nordmannvikdalen postglacial fault is scheduled for August, 1999. Studies of the Øygarden Fault Zone and ground water occurrence in the postglacial Stuoragurra Fault, which were both suggested by the sponsors at the 1997 NEONOR Project Meeting, have been given high priority. A summary of the 1998 activities and 1999 plans is included in Appendix 1. This annual report was presented to the NEONOR participants at the Project Meeting at NPD, Stavanger on 4 January, 1999.

A detailed investigation involving quality analysis of existing reports, improved understanding of the characteristics of crustal deformations through more and better observations, and a unified interpretation of the observations, is a prerequisite for a better understanding of the dynamic processes that are active in Norwegian regions at present. Such understanding is desirable from a scientific point of view, but also has practical implications, including various aspects of geological risks, both onshore and offshore. Active faulting in the offshore region can, amongst other effects, lead to major submarine landslides, and may also have implications for migration and sealing properties of faults (with consequences for petroleum potential). The study of the postglacial faults on land could lead to a better understanding of the offshore faults, as the on-land faults are more readily available to study.

The final phase of the NEONOR project will involve an integrated interpretation of the compiled neotectonic data sets. We will especially pay attention to the study the large-scale earthquakes (with magnitudes 7-8) that followed immediately after the last deglaciation of Fennoscandia. It is important to investigate if similar earthquakes (occurring after each of the numerous glaciations during the last 600,000 years) have increased the migration of hydrocarbons from the relatively impermeable source rocks up into reservoir rocks on the Norwegian continental shelf. The relationship between large earthquakes and rock-avalanches/submarine slides in the Storegga, Rana and Troms areas will also be a matter of more detailed studies.

2   CLASSIFICATION AND QUALITY ASSESSMENT OF REPORTED NEOTECTONIC PHENOMENA (TASK 1)

By Odleiv Olesen & John Dehls, NGU

2.1   INTRODUCTION

Neotectonics are, according to the International Association for Quaternary Research (INQUA), defined as "Any earth movement or deformations of the geodetic reference level, their mechanisms, their geological origin (however old they may be), their implications for various practical purposes and their future extrapolations (INQUA 1982)". Neotectonic crustal deformations have been reported at a large number of locations in Norway (both on local and regional scales). Documentation of large scale postglacial faulting (with up to 150 km length and 30 m offset) in northern Fennoscandia (Table 2.2.1) has also justified a re-evaluation of the previously reported evidences of Quaternary deformation in Norway. The NEONOR project represents an effort to investigate and classify these phenomena through a multidisciplinary approach. The definition of postglacial faulting is tectonic faulting that has occurred since the end of the last glaciation. Criteria for identification of postglacial faulting have been presented earlier by Fenton (1991, 1994) and Muir Wood (1993):

1) Offset of an original continuous surface or sediment of postglacial or late glacial age.

2) Reasonably consistent direction and amount of slip along the length of the fault.

3) The ratio of displacement to overall length of the feature should be less than 1/1000. For most faults this ratio is between 1/1000 and 1/10.000.

4) Exclusion of gravity sliding as the driving mechanism of faults in areas of moderate to high relief.

5) No signs of glacial modification (such as striation or ice-plucking) of fault scarps especially those controlled by banding, bedding or schistosity.

6) Exclusion of mechanisms such as glaciotectonics (ice push features), collapse due to ice melting, differential compaction or deposition over a pre-existing erosional scarp being the cause of an apparent offset in overburden.

Slight glacial modification of scarps suggests late glacial or interglacial age for a fault scarp.

We can when applying these criteria, objectively rank neotectonic claims similar to the review of seismotectonics in Sweden by Muir Wood (1993). He classified the claims into five grades;

(A) Almost certainly neotectonics,

(B) Probably neotectonics,

(C) Possibly neotectonics,

(D) Probably not neotectonics

(E) Very unlikely to be neotectonics.

2.2   REPORTED NEOTECTONIC ACTIVITY IN NORWAY

Muir Wood (1993, 1995) reported 13 claims in Norway, (7 offshore and 6 on mainland Norway, incl. Hjeltefjorden and Tjeldsundet) to the Swedish Nuclear Fuel and Waste Management. We have added 36 more onshore accounts to form the list in Table 2.3.1 and 3 offshore account to form Table 3.3.1. An assessment of the claims is also included. Ten of the claims are situated in the offshore area and the 42 others are located on mainland Norway.

The locations of 16 reported claims of neotectonic activity in Norway were visited for closer geological and geomorphological examination during the initial phase of the NEONOR Project (Dehls & Braathern 1998 and Olesen & Dehls 1998): Lygre (Fusa), Mosvatnet (Suldal), Ragnhildnuten (Sandnes), Yrkje, Vindafjorden, Ulvegrovene (Forsand), Rana, Austerdalsisen, Beiarn, Skjomen, Vassdalfjell, Kåfjord, Nordreisa, Masi, Gæssajavri and Skipskjølen (Varanger Peninsula). An evaluation of neotectonic claims in Tjeldsundet and Hjeltefjorden has been carried out by Longva *et al*. (1998) and Rise *et al*. (this report).

The locations of two reported neotectonic phenomena in southern Norway were visited for more detailed studies in 1998. The field work in northern Gudbrandsdalen has shown that the proposed postglacial faults by Werenskiold (1931) can be related to erosion (plucking) along steeply dipping fracture zones (Gnedden between Otta and Kvam) and gravity-induced sliding (Rudihø between Lalm and Heidal). The results from this study are included in Table 2.3.1. Reconnaissance studies have been carried out in the northern Østerdalen area in 1998 for planning of a re-levelling in 1999 of the shore-lines utilising a high-precision differential GPS receiver.

Three more locations in southern Norway are scheduled for field studies in 1999: Spronget (Krossvatn, Suldal), Grytehorgi (Vøringsfossen, Ullensvang) and Ytre Byrknes Archipelago (Gulen). The latter locality was added to the list of neotectonic claims during the autumn of 1998. A more detailed account from the studies of Rudihø and Gnedden will be included with the four other localities in southern Norway in the next Annual Technical Report.

A total of 7 and 12 claims were classified as grade A and B, respectively in the tentative assessment included in the NEONOR Project proposal (both offshore and onshore locations). After one and a half years of studies the present status is 5 and 2 claims with grade A and B, respectively. Claims with grade C, D and E has increased in number from 15 to 42 (onshore and offshore). Note that additional 15 claims are added to the list. An evaluation of the offshore claims is listed in Table 3.3.1. The present grade A claims include the postglacial faults in Masi and Kåfjord and the eartquake swarms in Steigen, Meløy and Sjona-Ranafjord. We plan to study the two grade B localities in more detail during the field season of 1999.

Table 2.2.1. Summary of properties of the documented postglacial faults within the Lapland province. The major faults are NE-SW trending reverse faults and occur within a 400x400 km large area in northern Fennoscandia. The Nordmannvikdalen and Vaalajärvi faults are minor faults trending perpendicular to the reverse faults. The former is a normal fault and the latter is a potential normal fault. The scarp height/length ratio is generally less than 0.001. The Merasjärvi Fault has a scarp height/length ratio of 0.002. This fault represents, however, an antithetic fault to the major Pärve Fault. . *Moment magntitudes of accompanying earthquakes from Bungum & Lindholm, 1997.

Fault	Country	Length	Max. scarp	Height length	Trend	Type	Moment magnitude*	Comment	Reference
Suasselkä Fault	Finland	48 km	5 m	0.0001	NE-SW	reverse	7.4		Kujansuu 1964
Pasmajärvi-Venejärvi Fault	Finland	15 km	12 m	0.0008	NE-SW	reverse		two separate sections	Kujansuu 1964
Vaalajärvi Fault	Finland	6 km	2 m	0.0003	NW-SE	??			Kujansuu 1964
Pärve Fault	Sweden	150 km	13 m	0.0001	NE-SW	reverse	8.1		Lundquist & Lagerbäck 1976
Lainio-Suijavaara Fault	Sweden	55 km	30 m	0.0005	NE-SW	reverse	8.0		Lagerbäck 1979
Merasjärvi Fault	Sweden	9 km	18 m	0.002	NE-SW	reverse		secondary fault to the Pärve Fault	Lagerbäck 1979
Pirttimys Fault	Sweden	18 km	2 m	0.0001	NE-SW	reverse			Lagerbäck 1979
Lansjärv Fault	Sweden	50 km	22 m	0.0004	NE-SW	reverse	7.9		Lagerbäck 1979
Burträsk-Bastuträsk Fault	Sweden	60 km	c. 10 m	0.0002	NE-SW N-S	??		two separate sections	Lagerbäck 1979
Stuoragurra Fault	Norway	80 km	7 m	0.0001	NE-SW	reverse	7.7	three separate sections	Olesen 1988
Nordmannvikdalen Fault	Norway	2 km	1 m	0.0005	NW-SE	normal			Tolgensbakk & Sollid 1988

An evaluation of the offshore neotectonic claims is included in the next chapter (Offshore faulting, Task 2)

2.3   CONCLUSIONS

Field checking of neotectonic reports and claims has shown that the majority of these can be attributed to other effects than tectonic faulting. In northern Norway there are now documented postglacial crustal deformation in Rana, Meløy, Beiarn, Kåfjord, Steigen and Masi. The extensional faults in Beiarn are, however, gravity-induced and classified as a sackung feature which has earlier been reported from mountainous areas in western US and Canada, Alps and New Zealand (Savage and Varnes, 1987). It is a matter of debate if these features are caused by slow creep or triggered by earthquake shaking. The normal NW-SE trending fault in Kåfjord represents a normal fault perpendicular to the system of NE-SW trending reverse faults in northern Fennoscandia (Lapland postglacial faults).

The present study of neotectonic claims on-land Norway suggest that they can be classified into five groups:

(1) Neotectonic faults (examples: Stuoragurra in Masi and Nordmannvikdalen in Kåfjord)

(2) Gravitationally induced faults (examples: Vassdalsfjell, Kvasshaugen, Rudihø, Ringja and Ulvegrovene)

(3) Erosional along older zones of weakness (examples: Nordreisa, Skjomen, Austerdalsisen, Gnedden and Lygre)

(4) Uverburden draping of underlying bedrock features (example: Gæssagielas in Karasjok)

(5) Stress release features (examples: Lebesbye, Kobbelv and Ødegården).

Table 2.3.1. Reported evidences of neotectonics on the mainland of Norway and tentative assessments of the claims. The locations are ordered from north to south. The criteria for classification of postglacial faulting by Fenton (1991, 1994) and Muir Wood (1993) have been utilised for grading the claims into the classes: (A) Almost certainly neotectonics, (B) Probably neotectonics, (C) Possibly neotectonics, (D) Probably not neotectonics and (E) Very unlikely to be neotectonics. The most likely cause of the proposed neotectonic deformation have been included as 'TYPE' in the fifth column: (1) Tectonic fault; (2) Gravity-induced faults, (3) Erosional phenomena (4) Overburden draping of bedrock features, (5) Stress release features.

NO.	LOCATION AND REFERENCE	OBSERVATION	COMMENT	GRADE / TYPE
1	Lebesby, Laksefjord, Finnmark Roberts (1991).	A road-cut drillhole penetrating cleaved phyllites has been observed to be offset in a reverse fault sense by 5.8 cm along a 40° dipping fault surface. This displacement occurred at some time during the period 1986 to 1989.	Stress release phenomena of surficial character. The direction of offset indicates the direction of maximum horizontal stress (Roberts, this report).	E5
2	Tanafjord, Finnmark (no exact location) by J.E. Rosberg according to Tanner (1907).	Postglacial fault (no published description).		
3	Skipskjølen, Varanger peninsula, Finnmark Olesen et al. (1992b)	WNW-ESE trending 4 km long escarpment within the Trollfjord-Komagelv Fault Zone has been observed from aerial photographs. The northern block seems to be downfaulted.	The scarp has been sculptured and rounded by the moving inland ice. The height of the scarp is varying considerable along the scarp (Olesen & Dehls, 1998).	E3
4	Gæssagielas, Karasjok, Finnmark Olsen (1989)	E-W trending 1.5 km long assumed Late Quaternary fault. The northern block is depressed.	The scarp is interpreted to represent a till draped escarpment in the underlying bedrock (Olesen & Dehls, 1998).	E4

NO.	LOCATION AND REFERENCE	OBSERVATION	COMMENT	GRADE / TYPE
5	Masi-Iešjav'ri area, Finnmark Olesen (1988), Muir Wood (1989a), Olesen *et al.(1992a, 1992b, 1992c)*, Bungum & Lindholm (1997) Roberts *et al.* (1997), Olsen *et al.* (this report).	The NE-SW trending postglacial Stuoragurra Fault extends for 80 km in the Masi-Iešjav'ri area in the Precambrian of Finnmarksvidda. The fault is manifested in the surface as a fault scarp up to 7 metres high and is situated within the regional Proterozoic Mierujavri-Sværholt Fault Zone. The Stuoragurra Fault is a southeasterly dipping reverse fault. A c. 1 m thick zone containing several thinner (a few cm wide) zones of fault gouge represents the actual fault surface. The 21 January earthquake (M 4.0) in the Masi area was most likely located along the Stuoragurra Fault at a depth of c. 10 km.	The age of the SF is constrained in that it crosscuts glaciofluvial deposits northeast of Iešjav'ri and an esker northeast of Masi. Thus it formed after the deglaciation which is estimated to approximately 9,300 yrs. BP (Olsen *et al.* this report).	A1
6	Storslett, Nordreisa, Troms Wontka (1974)	An up to 150 m high scarp to the southeast of Storslett is interpreted in terms of a postglacial reactivation of the Caledonian Jyppyrä fault which has an apparent accumulated displacement of approximately 700 m.	The height of the scarp varies considerably and also appears to be rounded by glacial erosion. The scarp is most likely formed by plucking of the moving inland ice along a Caledonian fault (Olesen & Dehls 1998).	D3
7	Lyngen, Troms and Øksfjord-Alta, Finnmark Holmsen (1916)	Postglacial uplift has been estimated from levelling of shore-lines in northern Troms and western Finnmark. The uplift shows negative anomalies from the regional trend in the order of 5 metres in the Lyngen and Øksfjord areas. This effect has been attributed to gabbro massifs.	The interpretation is hampered by poor age control on the formation of the shorelines.	C

NO.	LOCATION AND REFERENCE	OBSERVATION	COMMENT	GRADE / TYPE
8	Nordmannvik-dalen,Kåfjord, Troms Tolgensbakk & Sollid (1988), Sollid & Tolgensbakk (1988)	NW-SE trending postglacial faults in the Kåfjord area, North Troms. Normal faults dipping 30-50º to the northeast (Olesen & Dehls 1998). The height and length of the main escarpment is approximately 1 m and 2 km, respectively.	The fault is sub-parallel to the Nordmannvikdalen valley. The slope of the terrain is 10-12º and the elevation difference between the fault scarp and valley bottom is 150-200 m. According to Varnes *et al.* (1989) gravity induced sliding is less likely to occur when the elevation difference is less than 300 m. We do therefore favour a tectonic origin of the fault.	A1
9	Tjeldsundet, Troms Grønlie (1922), Vogt (1923)	Displacement of Holocene shorelines (an offset of c. 2.2 m down to the west). Lower shorelines appeared to be unbroken indicating that the inferred faulting occurred immediately after the deglaciation. Vogt (1923) pointed at the striking coincidence of the young faulting occurring in an old regional fault-zone along Tjeldsundet.	Multibeam echo-sounding data and marine seismic profiling (Longva *et al.,* 1998) do not reveal any fault scarps in the sediments or bedrock at the sea floor of Tjeldsundet. The different altitudes of the shorelines may therefore be due to variations of the currents through the sound during deposition of the shorelines.	D

NO.	LOCATION AND REFERENCE	OBSERVATION	COMMENT	GRADE / TYPE
10	Vassdalfjellet, 4 km east of the E6 in Kvanndalen north of Bjerkvik, Nordland Bargel *et al.* (1995)	A series of parallel east-west-oriented open fractures can be observed on the western part of the top of the ridge. Some of these are over 1 m wide and many are so deep that their depth is difficult to assess. There have been vertical movements along some of the fractures	The most continuous fault is 600 m long. They are situated close to a steep 600 m high wall along the south-ernmost slope of Vass-dalfjellet. The faults are interpreted to be effects of gravity-induced slid-ing (Olesen & Dehls 1998). The faults may resemble a small scale sackung feature (Varnes *et al.,* 1989) due to gravity spreading of Vassdal-fjellet.	E2
11	Reinneset, Skjomen, Nordland Bargel *et al.* (1995)	A 1.5 to 10 m high escarpment on the headland between Skjomen and Sørskjomen is interpreted in terms of a reverse postglacial fault dipping to the north. The fault continues to the west on the other side of Skjomenfjorden. Foliated granite can be observed in a few dm wide zone at the foot of the escarpment. The high, sharp-edged fault wall facing the direction of the moving inland ice points to a young age.	An inspection of the lo-cality has shown that the top of the escarpment is rounded and that the height of the escarpment varies considerable over short distances along the fault. These observations point towards a forma-tion due to erosion along an older zone of weak-ness (Olesen & Dehls, 1998.	D3
12	Tysfjord-Kobbelv area, Nordland Myrvang (1993)	Large-scale rock bursting and even buckling at the surface due to high horizontal stress in the order 30-40 MPa.	Stress release phenom-ena of superficial char-acter.	E5

NO.	LOCATION AND REFERENCE	OBSERVATION	COMMENT	GRADE / TYPE
13	Steigen, Nordland Atakan *et al.* (1994)	The earthquake swarm occurred in 1992 and contained 200 shocks but no main shock was recorded. The magnitude of the shocks was up to 3.6.	Earthquake swarms usually occur in volcanically or tectonically active areas such as plate boundaries but have also been reported from passive continental margins surrounding the northern part of the Atlantic Ocean and the Arctic Sea.	A1
14	Meløy, Nordland Bungum *et al.* (1979), Bungum & Husebye (1979) and Gabrielsen & Ramberg (1979)	The spectacular earthquake swarm on Meløy was located within the seismicity zone of the Nordland coast. The swarm occurred in 1977/1978 and contained 10,000 shocks, but no main shock was recorded. The magnitude of the shocks was up to 3.2.	These swarms are generally interpreted to be related to the formation of new zones of weakness in relatively competent bedrock (R. Muir Wood, pers. comm.).	A1
15	Kvasshaugen mountain between the valleys of Beiardalen and Gråtådalen, Nordland Grønlie (1939), Johnsen (1981), Muir Wood (1993)	NNE-SSW trending clefts occur along an approximately 5 km long NNE-SSW trending zone. These clefts are up to 20 m wide and 10 m deep and the eastern sides are locally down-faulted.	The faults may be classified as sackung features (Varnes *et al.,* 1989) due to gravity spreading of the 500 m high ridge along Gråtåhaugen, Kvasshaugen and Monsfjellet (Olesen & Dehls, 1998). The initiation of movements may, however, be triggered by large earth-quakes	D2

11

NO.	LOCATION AND REFERENCE	OBSERVATION	COMMENT	GRADE / TYPE
16	Austerdalsisen, Rana and Handnesøya, Nesna, Nordland Olesen *et al.* (1994, 1995)	Interpretation of aerial photographs unveiled two areas of north-south trending, vertical dipping fractures and faults in the Austerdalsisen area to the NW of Mo i Rana and on Handnesøya, north of Nesna. There seems to be a vertical offset of the bedrock surface across these structures. The foliation of the mica schist is sub-parallel to the bedrock surface.	Field inspected revealed that the features are probably of erosional origin. The moving inland ice has most likely been plucking blocks from the bedrock along steeply dipping N-S trending fractures (Olesen & Dehls, 1998).	D3
17	Sjona-Ranafjord area, Nordland Hicks *et al.* (1998, this report), Helzen (1834), Muir Wood (1989b)	A total of 400 earthquakes have occurred within the Sjona-Raanfjord area during the last 18 months. Four main clusters of earthquakes have been observed in time and space. The earthquakes range in magnitude from 0.1-2.8 and hypocenter depths are shallow, mainly around 5-12 km.	The clusters resemble the previously observed earthquake swarms in Meløy and Steigen, though on a smaller scale. The Sjona region coincides with the area of strongest effects from the 1819 earthquake (M 5.8-6.2) and accompanying eathquake swarms (Helzen, 1834 and Muir Wood, 1989b)	A
18	Ranafjord area, Nordland Helzen (1834), Grønlie (1923), Muir Wood (1989b), Bakkelid (1990), Olesen *et al.* (1994, 1995) Hicks *et al.* (1998, this report).	The Båsmoen Fault consists of SSE-dipping (40-70º) fault segments within a 2-km wide and 50 km long zone. There is evidence for anomalous land uplift along the Båsmoen Fault at the locations Utskarpen, Straumbotn, Båsmoen on the northern shore of Ranafjorden and Hemnesberget and on the Hugla and Tomma islands. The fault bears resemblance to the postglacial faults reported from the Lapland area of northern Fennoscandia.	It has not yet been found any conclusive evidences for postglacial movements along specific fault scarps. A new seismic mini-array has registered numerous earthquakes in the outer Ranafjord area. They do, however, not seem to be attributed to the Båsmoen fault (Hicks *et al.,* 1998, this report). We do therefore favour an erosional origin of the scarps along the Båsmoen Fault.	D3

NO.	LOCATION AND REFERENCE	OBSERVATION	COMMENT	GRADE / TYPE
19	Romsdalen Anda (1995), Anda & Blikra (1998)	Concentration of rock-avalanches correlates with a 500-700 m high regional escarpment of the land surface. This large-scale geomorphic feature is attributed to a fault zone associated with the Cenozoic uplift of Norway.	It is likely that the regional escarpments reflect fault segments along the Mesozoic Møre-Trøndelag Fault Zone. Mesozoic sediments may have filled local basins along the fault zone (similar to the basins in Beistandfjorden and Trondheimsleia). Glacial erosion will more easily remove these soft sediments (than the more competent basement rocks) subsequent to the Cenozoic exhumation of Norway.	D
20	Breisunddjupet, Møre og Romsdal Holtedahl (1959)	The elevation of the strand flat to the north of the NW-SE trending Breisunddjupet seems to be lower than the strand flat to the south.	Later, more detailed studies by H. Holtedahl (pers. comm. 1995) and Holthedal (1998) have questioned this observation. Inspection of the topographic maps (1:50.000) in the area has not revealed any altitude change of the strandflat across Breisunddjupet.	D
21	Northern Øster-dalen, Hedmark Holmsen (1916)	Local postglacial uplift has been estimated from levelling of shorelines left by ice-dammed lakes. Gabbro massifs (Tron and Klettene) have been subject to separate postglacial upheaval on the order of 3 metres.	The shorelines will be relevelled during the summer 1999.	C

NO.	LOCATION AND REFERENCE	OBSERVATION	COMMENT	GRADE / TYPE
22	Rudihø, Heidal, Oppland Werenskiold (1931)	Two 100-200 metres long and one metre wide SE-NW trending fractures. One side seems to be down-faulted and the fractures are 1-2 metres wide and up to 6 metres deep. The clefts are arc-shaped with the concave side facing a 500 m high, almost vertical mountain side. The distance from the fractures to the steep mountain side is 10-40 metres.	The fractures are inter-preted to be gravity-induced.	E2
23	Gnedden, Holsætrin, Sel, Oppland Werenskiold (1931)	Up to 7 metres high and 1 km long escarpment trending in the ENE-WSW direction (N65°) across a small moun-tain crest. Large variation in scarp height along the western part of the scarp, more con-stant to the east (3-5 m). The escarpments seem to be sculptured by the inland ice.	The escarpment is most likely formed by erosion by the inland ice along a pre-existing fracture in the bedrock.	D3
24	Ytre Byrknes Archipelago Michelsen *et al.* (1986)	NNE-SSW trending open fractures 0.5- 3 m wide and 50-100 m apart. Some are normal faults with vertical displacement of 0.5-2 m. One of the faults cuts a glacial splay channels.	The interpretation of Holocene displacement is plausible. The location will be visited for a de-tailed investigation in 1999.	B
25	Grytehorgi and Vøringfossen, Hordaland Reusch (1901)	NNE-SSW trending fault on Grytehorgi .The down-faulted block is to the west. Ice-striation seems to be offset by 1 metre (normal fault). Other N-S sharp escarpments in the Vøringsfossen area are also suggested to be effects of postglacial faulting.	Løset (1981) questioned the postglacial age of the Grytehorgi fault since it is filled with till and er-ratic blocks. Neotectonic movements along the N-S trending faults are, however, possible.	D3
26	Finse - Geilo area, Hordaland - Buskerud Anundsen *et al.* (in prep.)	Anomalous uplift from re-peated levelling.	A careful analysis of the levelling methods is pending.	

NO.	LOCATION AND REFERENCE	OBSERVATION	COMMENT	GRADE / TYPE
27	Hjeltefjorden, 30 km northwest of Bergen Unpublished NTNF-NORSAR and NGI (1985)	At the northern end of Hjeltefjorden a boomer seismic survey was undertaken in the mid-80's for a possible tunnel crossing. Several E-W lines between Seløy and Uttoska, appeared to show a consistent offset of the superficial sediments in the floor of the fjord, along a NNW-SSE trending dislocation, involving down to the west displacement of 5-10m (Muir Wood 1993).	The offset-length ratio of the fault scarp is 1/80 (height 5-9 m/length 400 m) which is much higher than the required 1/1000 ratio (Fenton, 1991).	D
28	Lygre, northern side of the mouth of Hardanger-fjord Reusch (1888)	Potential postglacial fault occurring as a N-S trending escarpment. The western block seems to be down-faulted. The length of the escarpment is not reported, but an accompanying drawing indicates a length of approximately 1 km.	There is no evidence for displacement. The scarp is an erosional feature along a fracture zone, which may be part of a regional lineament (Dehls & Braathen, 1988).	D
29	Etne, Rogaland Karpuz *et al.* (1991)	The 4.25 (±0.25) magnitude Etne earthquake (29 Jan. 1989) occurred as a result of predominately normal faulting on a NW-SE trending fault. Secondary effects of the earthquake were observed as surface fissures in Quaternary sediments. The basement and walls of a farmhouse were damaged as a result of this slope instability.	The structure is most likely caused by ground shaking and is not a deep-seated tectonic fault.	D

NO.	LOCATION AND REFERENCE	OBSERVATION	COMMENT	GRADE / TYPE
30	Vindafjorden - Ølen area, Rogaland, Anundsen (1989)	A 7 km wide and c. 30 km long N-S trending active half-graben has been reported. Along the eastern slope of Vindafjord, and on the mountain plateau to the east of the fjord, a series of long sub-parallel crevasses is observed. A present subsidence is supported by precision levelling (20 mm movement over 19 years)	The sub-parallel crevasses, along with an orthogonal set, can be explained by gravitational sliding along a very strong foliation dipping towards the fjord. The step-like nature of the fjord walls appears to be an erosional feature (Dehls & Braathen, 1998). The benchmark with anomalous high uplift is most likely emplaced in an unstable slab of rock (Bockmann, this report).	D2-3
31	Yrkjefjord Anundsen *et al.* (in prep.)	Levelling in combination with repeated triangulations between concrete pillars, showed that both horizontal and vertical displacements in the order of 0.1-0.9 mm/year take place along the Yrkjefjord fault zone. Annual measurements during a period of 10 years indicate that movements change, i.e. are reversed in some periods.	The displacements are very small and are not consistent in time (alternating normal and reverse faulting).	D
32	Yrkje area Anundsen (1982), Anundsen & Fjeldskaar (1983) and Anundsen (1985)	A 7-10 metre offset (since 10,400 B.P.) of the Younger Dryas transgression level across a NE-SW trending fault. The observation is based on a study of the marine isolation of six basins and one of these basins show anomalous uplift.	The offset is only observed at one location. No further work has been undertaken to study other lake basins in this area. From a limited set of dates and cores the fault explanation for the apparent variation in isolation levels, is not unique (Muir Wood, 1993).	D

NO.	LOCATION AND REFERENCE	OBSERVATION	COMMENT	GRADE / TYPE
33	Ulvegrovene, north of Røssdalen, Rogaland Anundsen (1988a)	Active subsidence of a narrow zone. The turf along the escarpments seems to be torn apart. The structure is parallel to the valley of Røssdalen.	Most likely a gravity induced structure (Dehls & Braathen, 1998).	E2
34	Mosvatnet, Suldal, Rogaland Anundsen (1988b)	The sides of open fractures in the bedrock are located at different levels indicating vertical movements along the fractures.	Erosion of a fine-grained amphibolitic dyke (Dehls & Braathen, 1998).	E3
35	Spronget, Krossvatnet, Suldal, Rogaland Anundsen (1988b)	The sides of open fractures in the bedrock are located at different levels indicating vertical movements along the fractures.	The locality will be visited in 1999 for closer inspection	D
36	Karmøy, Rogaland and Fjøsanger, Hordaland Mangerud *et al.* (1981) and Sejrup (1987)	A considerable long-term neotectonic uplift, 10-40 m, of western Norway during the last 125,000 years is based on investigations of marine sediments from interglacials.		C

NO.	LOCATION AND REFERENCE	OBSERVATION	COMMENT	GRADE / TYPE
37	Gannsfjord lineament, Jæren, Rogaland Abandoned clay pit at about 10-30 m above sea level at Gann, on the western side of the Sandnes Harbour. Opstad and Høgemork at about 200 above sea level to the east of the Gannsfjord lineament. Feyling-Hanssen (1966), Fuggeli & Riis (1992)	Subsurface boreholes revealed a NE-SW trending boundary, steeper than about 60 degrees, between mostly marine clay to the west and sand to the east. The clay is overlain by Weichselian till. Glaciomarine clays of Weichselian age to the east of the Gannsfjord fault appear to uplifted by recent tectonic movements.	Recent work indicates that the N-S trending escarpment separating 'Høg-Jæren' from 'Låg-Jæren' is formed by the northwards moving Skagerrak glacier (Larsen *et al.,* 1998).	D3
38	Ragnhildnuten, Sandnes, Rogaland Feyling-Hanssen (1966),	Postglacial fault (with dip-slip and sinistral offsets of 30 m each) splitting a 'mountain' in two.	The hill has a 50 m high escarpment along the western side, due to erosion along a fracture zone. The escarpment is part of a NNW-SSE lineament through 2 other ridges, about 3-4 km away (Dehls & Braathen, 1998).	E3
39	Egersund, Rogaland Bakkelid & Skjøthaug (1985) Bakkelid (1986) Bakkelid (1989)	Part of the town of Egersund was uplifted approximately 4 cm relative to the other part of the town during 34 years.	S. Bakkelid (pers. comm. 1998) has concluded that a 40 mm error in the bench mark B39N9-Eide measured by the consultantcy company Ing. Dahls Oppmåling in 1951/52 spread out along several levelling lines in the area.	E

NO.	LOCATION AND REFERENCE	OBSERVATION	COMMENT	GRADE / TYPE
40	Egersund-Flekkefjord area, Rogaland Anundsen (1989), Anundsen *et al.* (in prep.)	The Egersund Anorthosite-Gabbro Province shows a subsidence of 2-2.5 mm/yr. The zone of maximum subsidence coincides with a zone of maximum gravity anomaly.		C
41	Haukeligrend, Telemark Anundsen *et al.* (in prep.)	Anomalous subsidence from repeated levelling	A careful analysis of the levelling methods is pending.	C
42	Ødegården, Bamle, Telemark Brøgger (1884)	Approximately 0.2 metre sinistral offset of a 0.5 by 0.6 m pothole along a WNW-ESE trending fault. The pothole is estimated to be of Quaternary age.	Probably blasted away, not possible to find today (Løset, 1981, Selnes, 1983). Represents most likely a stress release phenomenon since it was located in the vicinity of an open pit.	D5

2.4 REFERENCES

Anda, E. 1995: Romsdalen og Romsdalsfjorden. Hovedtrekkene i landskapet. *In* Sanden, J., (ed.) *Romsdalen, natur og kultur.* Romsdalsmuséet, årbok 1995, *14-34.*

Anda, E. & Blikra, L.H. 1998: Rock-avalanche hazard in Møre & Romsdal, western Norway. Norwegian Geotechnical Institute Publication 203, 53-57

Anundsen, K. 1982: Undersøkelser vedrørende mulige kvartære forkastninger i Sørvest-Norge. Report to Norwegian Geotechnical Institute (NGI), 39 pp.

Anundsen, K. 1985: Changes in shore-level and ice-front position in Late Weichsel and Holocene, southern Norway. *Norsk geografisk Tidsskrift 38*, 205-225.4

Anundsen, K., 1988a: Jordskorpebevegelser. *In: Geologi for fjellvandrere.* Stavanger Turistforening, Årbok 1988, 86-87.

Anundsen, K., 1988b: Landskapet forandrer seg fremdeles. *In: Geologi for fjellvandrere.* Stavanger Turistforening, Årbok 1988, 88-89.

Anundsen, K., 1989: Late Weichselian relative sea levels in southwest Norway: observed strandline tilts and neotectonic activity. *Geologiska Föreningens i Stockholm Förhandlingar* 111, 288-292.

Anundsen, K. & Fjeldskaar, W. 1983: Observed and theoretical late Weichselian shore-level changes related to glacier oscillations at Yrkje, south-west Norway. *In: Schroeder-*

Lanz, H. (ed.), *Late- and postflacial oscillations of grlaciers: glacial and periglacial forms.* A.A. Balkema, Rotterdam, The Netherlands, 133-170.

cursion. *Structural Geology Group, UiB/NRSC Report 5*, 29 p

Anundsen, K., Grimstveit, L., Harsson, B.G. & Holsen, J. in prep.: Measurements of neotectonic movements in southern Norway: Implications for former ice thickness estimates.

Atakan, K., Lindholm, C. D. & Havskov, J., 1994: Earthquake swarm in Steigen northern Norway: an unusual example of intraplate seismicity. *Terra Nova* 6, 180-194.

Bakkelid, S. 1986: The discovery in Norway of a strongly active geological fault and some of its practical consequences. *Proceedings of the 10th General Meeting of the Nordic Geodetic Commission,* Sept.-Oct., Helsinki, 237-245.

Bakkelid, S. 1989: Kontrollmålinger av forkastningssone i Eigersuns i 1987 - 1988. *Statens kartverk Rapport 2/1989,* 7 pp.

Bakkelid, S., 1990: Innmåling av rur- og tangrandmerker i Nordland. *Statens kartverk report 3/1990*, 90 p

Bakkelid, S. & Skjøthaug, P. 1985: Aktive geologiske forkastninger i Eigersund – foreløpige resultater. *Norges geografiske oppmåling, Publikasjon 2,* 23 pp.

Bargel, T. H., Boyd, R. & Dahl, R., 1995: The geology of the Narvik District, A journey in time and space*, Geological Survey of Norway*, *Trondheim, 351 p.*

Brøgger, W. C., 1884: Spaltenverwerfungen in der Gegend Langesund-Skien. *Nyt Magazin for Naturvidenskaberne* 28, 253-419.

Bungum, H. & Husebye, E.S. 1979: The Meløy, northern Norway, earthquake sequence - a unique intraplate phenomenon. *Nor. Geol. Tidsskr. 59,* 189-193.

Bungum, H., Hokland, B. K., Husebye, E. S. & Ringdal, F., 1979: An exceptional intraplate earthquake sequence in Meløy. *Nature* 280, 32-35.

Bungum, H. & Lindholm, C., 1997: Seismo- and neotectonics in Finnmark, Kola Peninsula and the southern Barents Sea. Part 2: Seismological analysis and seismotectonics. *Tectonophysics* 270, 15-28.

Dehls, J. & Olesen, O. (eds.) 1998: Neotectonics in Norway, Annual Technical Report 1997. *NGU Report 98.016,* 161 pp.

Dehls, J. & Braathen, A. 1998: Neotectonic phenomena in southern Norway. *In:* Dehls, J. & Olesen, O. 1998 (eds.) *Neotectonics in Norway, Annual Technical Report 1997,* NGU Report 98.016, 31-39.

Fenton, C., 1991: *Neotectonics and palaeoseismicity in North West Scotland.* Ph.D. thesis, University of Glasgow Glasgow, 403.

Fenton, C., 1994: Postglacial faulting in eastern Canada. *Geological Survey of Canada, Open file report 2774*, 98 p

Feyling-Hanssen, R. W., 1966: Geologiske observasjoner i Sandnes-området. *Geological Survey of Norway* 242, 26-43.

Fugelli, E. & Riis, F., 1992: Neotectonism in the Jæren area, southwest Norway. *Norsk Geologisk Tidsskrift* 72, 267-270.

Gabrielsen, R.H. & Ramberg, I.B. 1979: Tectonic analysis of the Meløy earthquake area based on Landsat lineament mapping. *Nor. Geol. Tidsskr. 59,* 183-187.

Grønlie, O. T., 1922: Strandliner, moræner og skjælforekomster i den sydlige del av Troms fylke. *Norges geologiske undersøkelse Nr. 94*

Grønlie, O. T., 1923: Har Høgtuva steget i vor tid? *Naturen* 7, 139-141.

Grønlie, O. T., 1939: Some remarks on the land area in Nordland between the glacier Svartisen, and the frontier. *Norsk Geogr. Tidsskr* 7, 399-406.

Heltzen, I. A., 1834: Ranens Beskrivelse*, Rana Museums og Historielag*, Mo i Rana, 290 p

Hicks, E. Bungum, H. & Lindholm, C. 1998: Seismicity in the Ranafjord area. *In:* Dehls, J. & Olesen, O. 1998 (eds.) *Neotectonics in Norway, Annual Technical Report 1997,* NGU Report 98.016, 122-135.

Holmsen, G., 1916: Om strandlinjers fald omkring gabbroomraader (Summary in English). *Norsk Geologisk Tidsskrift* 4, 7-20.

Holtedahl, H., 1959: Den norske strandflate med særlig henblikk på dens utvikling i kystområdene på Møre. *Norsk Geogr. Tidsskr.* 16, 285-305.

Holtedahl, H., 1998: The Norwegian strandflat – a geomorphological puzzle. *Norsk Geologisk. Tidsskrift* 16, 47-66.

INQUA, 1982: International Association for Quaternary Research (INQUA) Commission Reports 1978-1982. *In Striolae 1982:1 (INQUA Newsletter 4)*, 36-38.

Johnsen, E., 1981: Kvartære trekk fra Beiarns geologiske historie. *In: Årbok for Beiarn, Beiarn historielag*. Egil Trohaugs Forlag a.s, Bodø, 93-106.

Karpuz, M. R., Gabrielsen, R. H., Engell-Sørensen & Anundsen, K., 1991: Seismotectonic significance of the 29 January 1989 Etne earthquake, SW Norway. *Terra Nova* 3, 540-549.

Kujansuu, R., 1964: Nuorista sirroksista Lapissa. Summary: Recent faults in Lapland. *Geologi* 16, 30-36.

Lagerbäck, R., 1979: Neotectonic structures in northern Sweden. *Geol. Fören. Stockh. Förh* 100 (1978), 271-278.

Larsen, E., Riis, F., & Rise, L. 1998: Offshore and onshore studies of the Jæren area, southwest Norway. *In:* Dehls, J. & Olesen, O. 1998 (eds.) *Neotectonics in Norway, Annual Technical Report 1997,* NGU Report 98.016, 82-85.

Longva, O., Rise, L. & Dehls, J. 1998: Marine geological investigations of neotectonic features in the Rana and Tjeldsundet areas. *In:* Dehls, J. & Olesen, O. 1998 (eds.) *Neotectonics in Norway, Annual Technical Report 1997,* NGU Report 98.016, 93-103.

Løset, F., 1981: Neotectonic movements in Norway. Literature review of neotectonic movements in Norway, and results from field investigations on Hardangervidda. *Norwegian Geotechnical Institute (NGI), Internal Report 40009-7*, 13 p

Lundquist, J. & Lagerbäck, R., 1976: The Pärvie Fault: A late-glacial fault in the Precambrian of Swedish Lapland. *Geol. Fören. Stockh. Förh.* 98, 45-51.

Mangerud, J., Sønstegaard, E., Sejrup, H.-P. & Haldorsen, S., 1981: A continuous Eemian-Early Weichselian sequence containing pollen and marine fossils at Fjøsanger, western Norway. *Boreas* 10, 137-208.

Michelsen, J.K., Lind, T. & Hansen, H.J: 1986: The geology of the Devonian Fensfjord Basin. Unpubl manuscript. Univ. of Bergen, 41 pp.

Muir Wood, R., 1989a: Extraordinary deglaciation reverse faulting in northern Fennoscandia. *In:* Gregersen, S. & Basham, P. W. (ed.), *Earthquakes at North-Atlantic passive margins: neotectonics and postglacial rebound.* Kluwer Academic Publishers, Dordrecht, The Netherlands, 141-173.

Muir Wood, R., 1989b: The Scandinavian Earthquakes of 22 December 1759 and 31 August 1819. *Disasters* 12, 223-236.

Muir Wood, R., 1993: A review of the seismotectonics of Sweden. *Swedish Nuclear Fuel and Waste Management Co. Technical Report 93-13*, 225 p

Muir Wood, R., 1995: Reconstructing the tectonic history of Fennoscandia from its margins: The past 100 million years. *Swedish Nuclear Fuel and Waste Management Co. Technical Report 95-36*, 107 p

Myrvang, A., 1993: Rock stress and rock stress problems in Norway. *In:* Hudson, J. A. (ed.), *Comprehensive rock engineering. Vol. 3, Rock testing and site characterization.* Pergamon Press, 461-471.

NTNF/NORSAR and Norwegian Geotechnical Institute 1985: Mongstad Earthquake Criteria Study. Unpublished report. *69 pp.*

Olesen, O., 1988: The Stuoragurra Fault; evidence of neotectonics in the Precambrian of Finnmark, northern Norway. *Norsk Geologisk Tidsskrift* 68(2), 107-118.

Olesen, O. & Dehls, J. 1998: Neotectonic phenomena in northern Norway. *In:* Dehls, J. & Olesen, O. 1998 (eds.) *Neotectonics in Norway, Annual Technical Report 1997,* NGU Report 98.016, 3-30.

Olesen, O., Gjelle, S., Henkel, H., Karlsen, T. A., Olsen, L. & Skogseth, T., 1994: Neotectonic studies in the Ranaford area, northern Norway. *Geological Survey of Norway, Report 94.073*

Olesen, O., Gjelle, S., Henkel, H., Karlsen, T. A., Olsen, L. & Skogseth, T., 1995: Neotectonics in the Ranafjorden area, Northern Norway. *Bulletin - Norges Geologiske Undersøkelse* 427, 5-8.

Olesen, O., Henkel, H., Lile, O. B., Mauring, E. & Ronning, J. S., 1992a: Geophysical investigations of the Stuoragurra postglacial fault, Finnmark, northern Norway. *Journal of Applied Geophysics* 29(2), 95-118.

Olesen, O., Henkel, H., Lile, O. B., Mauring, E., Rønning, J. S. & Torsvik, T. H., 1992b: Neotectonics in the Precambrian of Finnmark, northern Norway. *Norsk Geologisk Tidsskrift* 72, 301-306.

Olesen, O., Roberts, D. & Olsen, L., 1992c: Neotectonic studies in Finnmark 1992. *Geological Survey of Norway Report 92.325*, 15 p

Olsen, L., 1989: Bæivašgied'di, 2033 III kvartærgeologisk kart - M 1:50 000. Geological Survey of Norway.

Reusch, H., 1888: Bømmeløen og Karmøen med omgivelser*, Geological Survey of Norway*, 423 p

Reusch, H., 1901: Nogle bidrag til forstaaelsen af hvorledes Norges dale og fjelde er blevne til. *Geological Survey of Norway Bulletin* 32, 125-217.

Roberts, D., 1991: A contemporary small-scale thrust-fault near Lebesbye, Finnmark. *Norsk Geologisk Tidsskrift* 71, 117-120.

Roberts, D., Olesen, O. & Karpuz, M. R., 1997: Seismo- and neotectonics in Finnmark, Kola Peninsula and the southern Barents Sea; Part 1, Geological and neotectonic framework. *Tectonophysics* 270(1-2), 1-13.

Savage, W. Z. & Varnes, D. J., 1987: Mechanics of gravitational spreading of steep-sided ridges ('sackung'). *International Association of Engineering Geologists Bulletin* 35, 31-36.

Sejrup, H.-P., 1987: Molluscan and foraminiferal biostratigraphy of an Eemian-Early Weichselian section on Karmøy, southwestern Norway. *Boreas* 16, 27-42.

Selnes, P. B., 1983: Possible neotectonic fault movements in Norway. *In:* Ritsema, A. R. & Gürpinar, A. (ed.), *Seismicity and seismic risk in the offshore North Sea*. D. Reidel Publishing Company, 47-48.

Sollid, J. L. & Tolgensbakk, J., 1988: Kvartærgeologisk og geomorfologisk kartlegging på Svalbard og fastlands-Norge utført ved Geografisk institutt, Univ. i Oslo. Abstract 18. *Nordiske Geologiske vintermøte, København*, 380-381.

Tanner, V., 1907: Studier öfer kvartärsystemet i Fennoskandias nordliga delar. I: Till frågan om Ost-Finmarkens glaciation och nivåförändringar. Résymé en francais. *Bull. Comm. Géol. Finl. 18*, 165 p

Tolgensbakk, J. & Sollid, J. L., 1988: Kåfjord, kvartærgeologi og geomorfologi 1:50 000, 1634 II. Geografisk institutt, Universitetet i Oslo.

Varnes, D. J., Radbruch-Hall, D. H. & Savage, W. Z., 1989: Topographic and structural conditions in areas of gravitational spreading of ridges in the Western United States. *USGS professional paper 1496*

Vogt, T., 1923: En postglacial jordskjælvs-forkastning. *Naturen* 7, 65-71.

Werenskiold, W., 1931: Ett sprekkesystem i Gudbrandsdalen. *Norsk Geologisk Tidsskrift* 12, 575-576.

Wontka, J. F., 1974: *Zur Geologie und Tektonik des Gebietes zwischen nördlichem Reisadal und Oksfjorddal, Nordreisa Kommune, Troms, Nord-Norwegen*. Diploma thesis, University of Mainz Germany, 58.

3 OFFSHORE FAULTING (TASK 2)

3.1 INTERPRETATION OF SWATH BATHYMETRY AND SEISMIC DATA FROM THE ØYGARDEN FAULT ZONE

By Leif Rise (NGU), Fridtjof Riis (NPD), John Dehls (NGU), Philip J. Goldsmith (Phillips Petroleum) and Odleiv Olesen (NGU)

3.1.1 Introduction

The study area is 3 by 10 km, and located along the Øygarden Fault Zone off the coast northwest of Bergen (Fig. 3.1.1). This extensive fault complex is paralleling the southwestern coast from approximately 59° N to 61° 30' N (> 300 km), and comprises the most landward N-S striking fault zone of major throw in the northern North Sea sedimentary province. The zone marks a sharp transition in crustal thickness from the mainland to the adjacent Horda Platform. The fault complex has probably been active in several periods since Paleozoic times (Eynon 1981), and according to Færseth et al. (1995) present day movements are indicated from seismological observations and in situ stress measurements. In the study area and further north, the Øygarden Fault Zone represents the boundary between Mesozoic sediments and the crystalline basement rocks. South of approximately 61° N, however, Jurassic sediments are preserved on the basement rocks east of the fault zone (Rokoengen & Rønningsland, 1983; Fossen *et al.*, 1997).

The major scarp that has developed along the fault has some of the appearance of a fault-scarp slightly north of 61°N (with vertical offset up to 150m), and although offsets have not been observed in the overlying sedimentary section itself, sediments onlap the scarp, with some suggestion of dips steeping towards the fault (Muir Wood & Forsberg 1988, Muir Wood 1993). Færseth et al. (1995) did also report indications of neotectonic movements along the Øygarden fault. Due to these reports and indications of postglacial reactivation on seismic lines from Phillips Petroleum (Figs. 3.1.2-7), it was decided to acquire a multibeam echo-sounding survey to investigate for evidence of postglacial movements on the seafloor images.
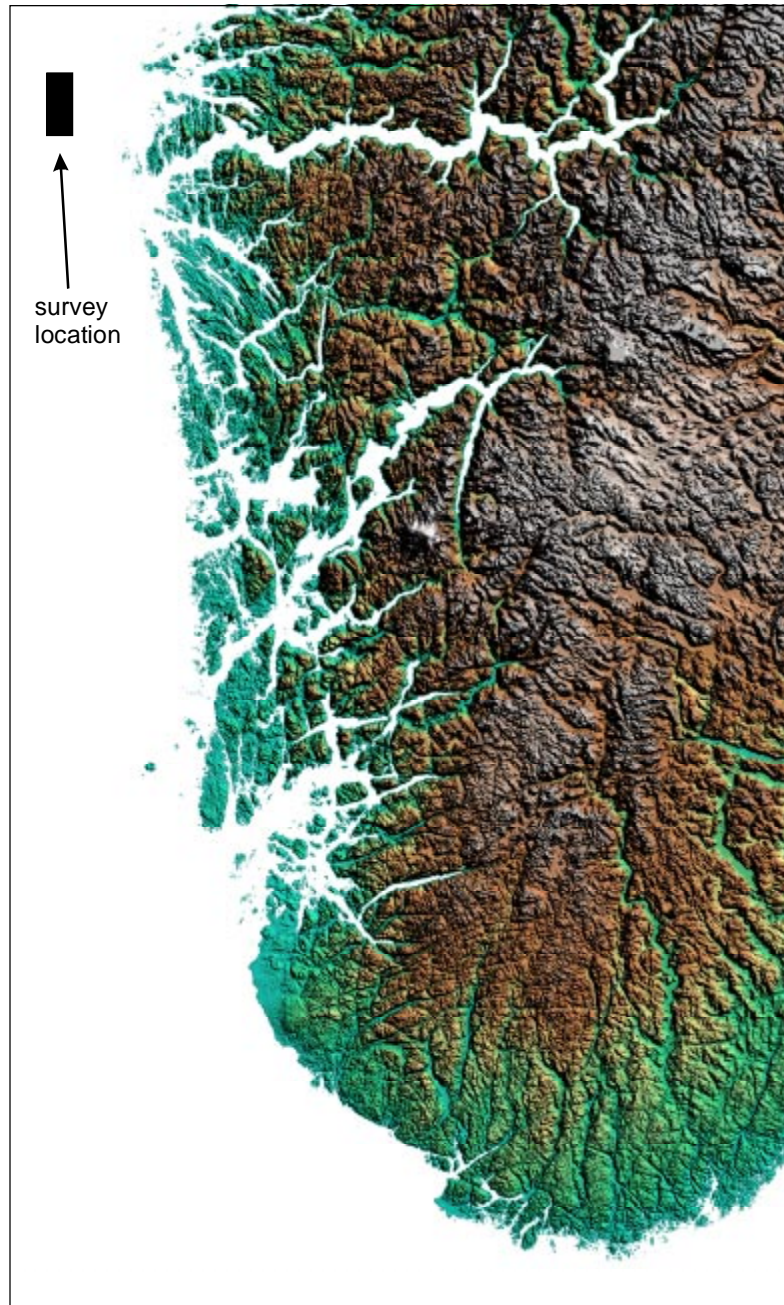
Fig. 3.1.1.   Map showing the study area west of Sognefjorden.

3.1.2   Database

The Norwegian Hydrographic Survey was contracted to carry out an echo-sounding survey in the study area. The data was collected during good weather conditions during the first days of May 1998 using a multibeam echo-sounder (Simrad EM-100) from the vessel M/S Sjømålaren. The data were processed by the Norwegian Hydrographic Survey. The bathymetric data were of very high quality, and the digital model was based on a 2 m x 2 m grid produced by a minimum curvature gridding method. The ER- Mapper software was applied to produce an artificial shaded relief image map (Fig. 3.1.9).

Sections of six interpreted digital seismic lines (Figs. 3.1.2-7) across the fault zone (E-W) were made available by Phillips Petroleum. The shot points of these lines are marked on the

bathymetric image map. Two analogue sparker lines across the study area were made available from IKU.
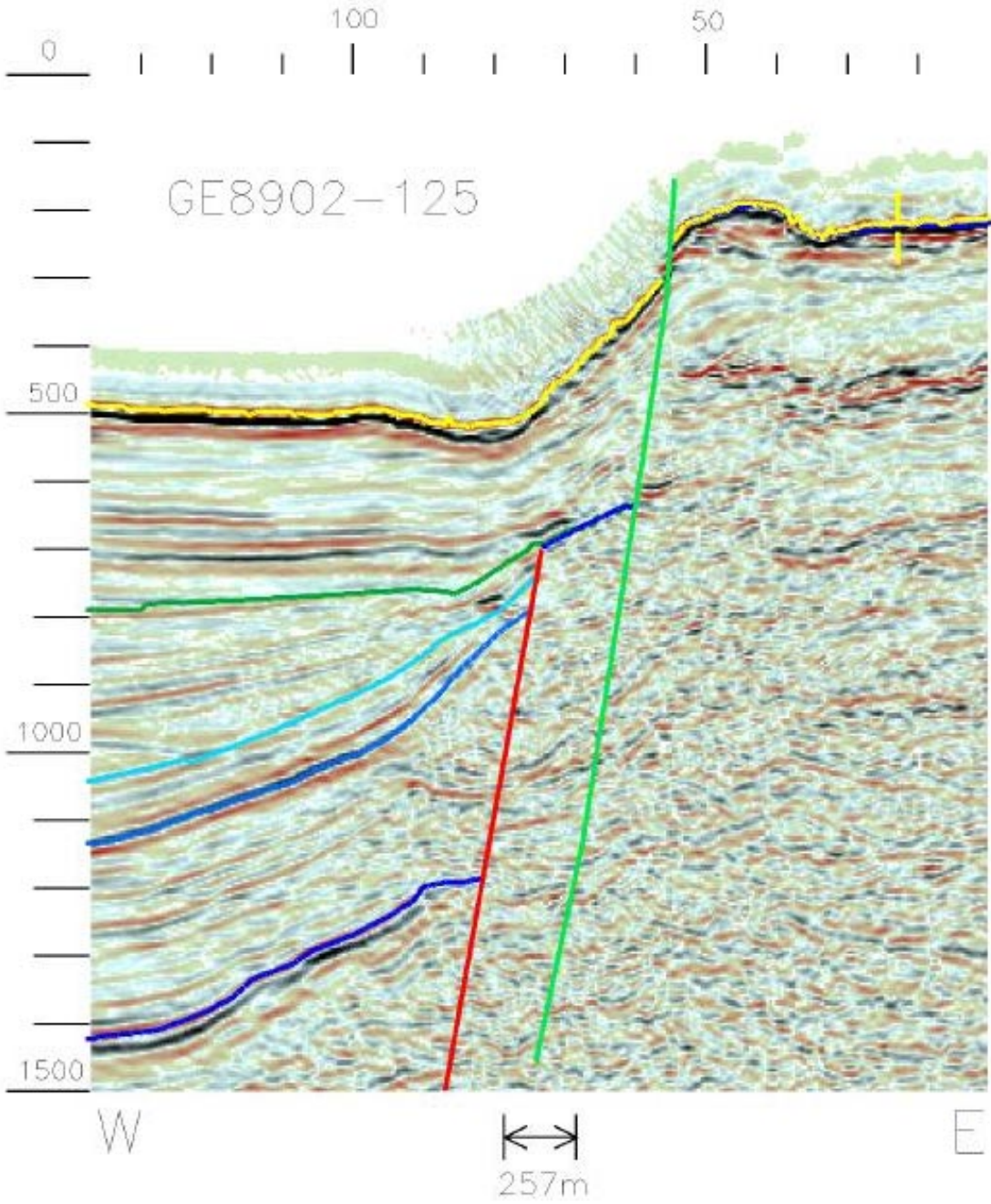
Fig. 3.1.2.   Section of digital seismic line GE8902-125. Interpretation by Phillips Petroleum. Base of Quaternary is interpreted at approximately 800 ms below sea level. The tracks of this and the following lines are shown in Fig. 3.1.9. For recognition of drumlins see Fig. 3.1.10.
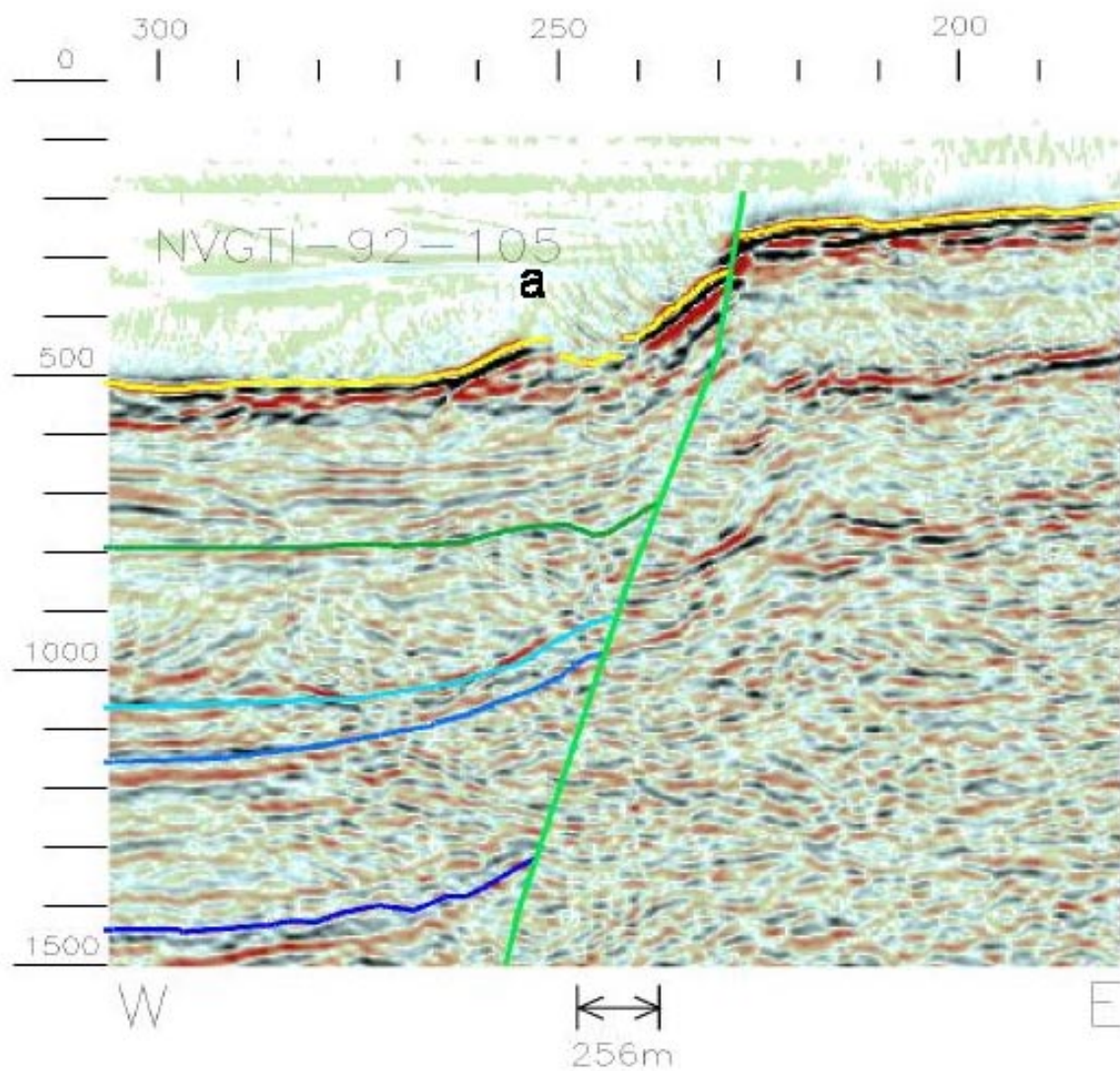
Fig. 3.1.3.   Section of digital seismic line NVGTI92-105. Interpretation by Phillips Petro-leum.
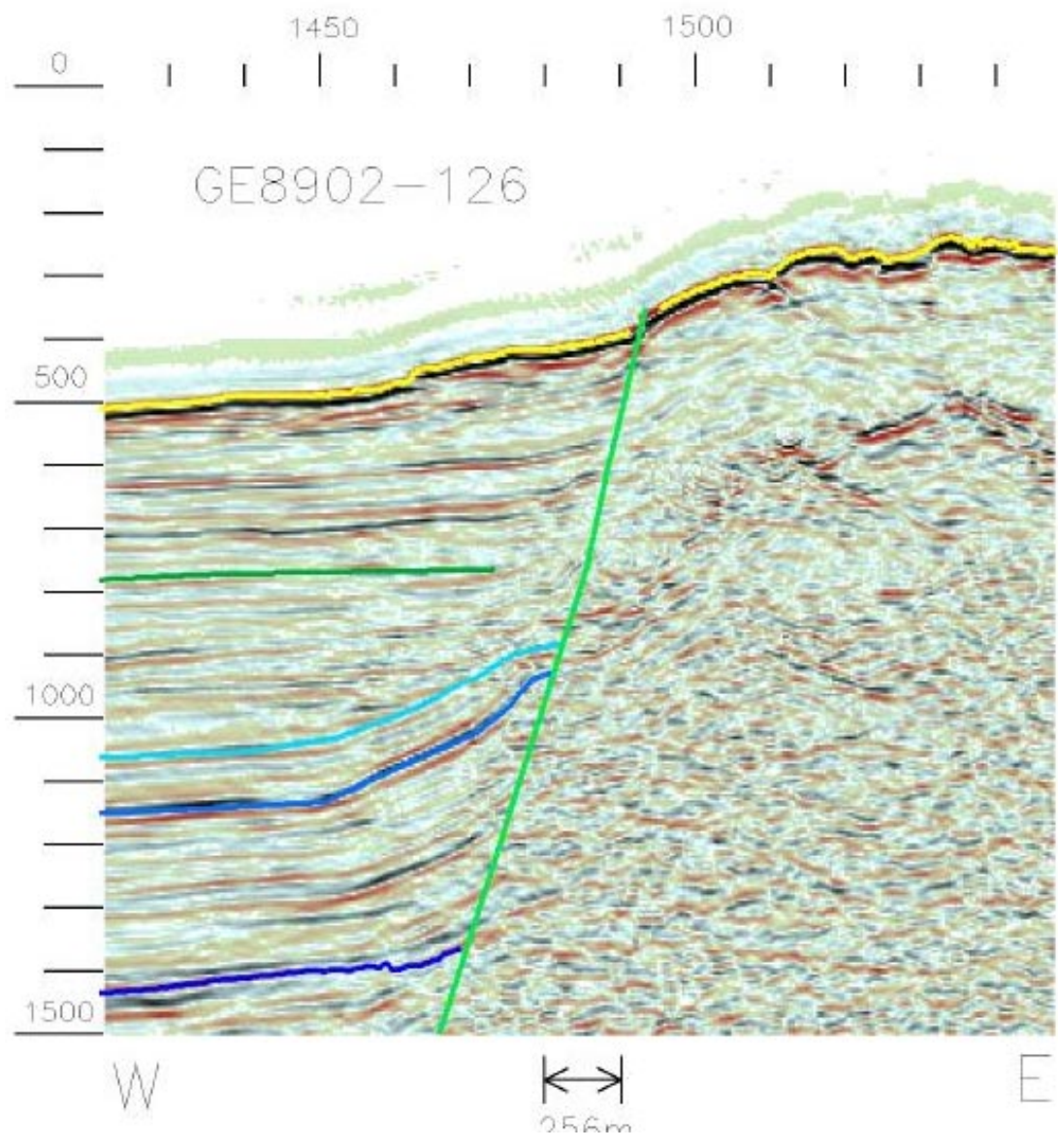
Fig. 3.1.4.   Section of digital seismic line GE8902-126. Interpretation by Phillips Petroleum.
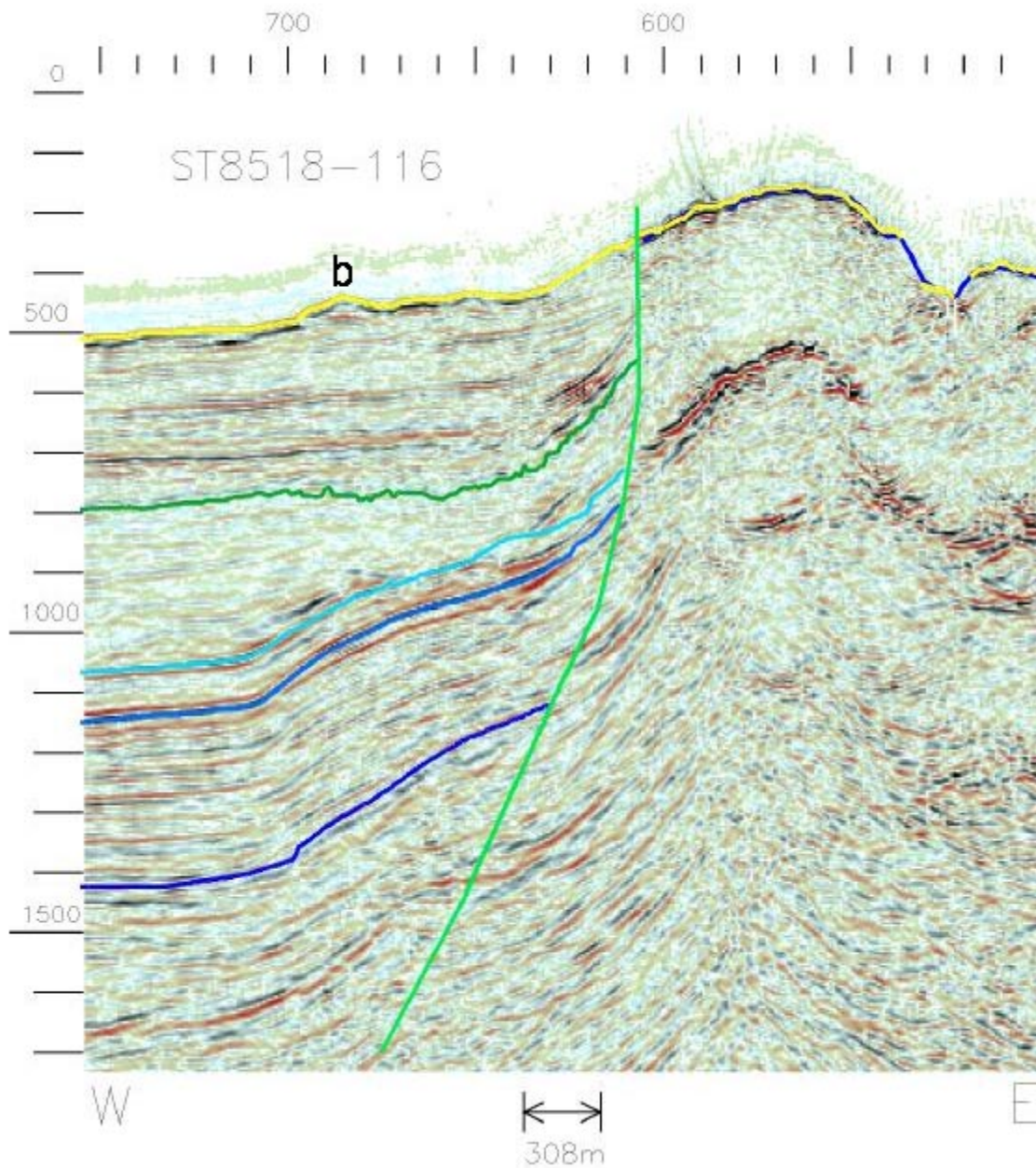
Fig. 3.1.5.   Section of digital seismic line ST8518-116. Interpretation by Phillips Petroleum.
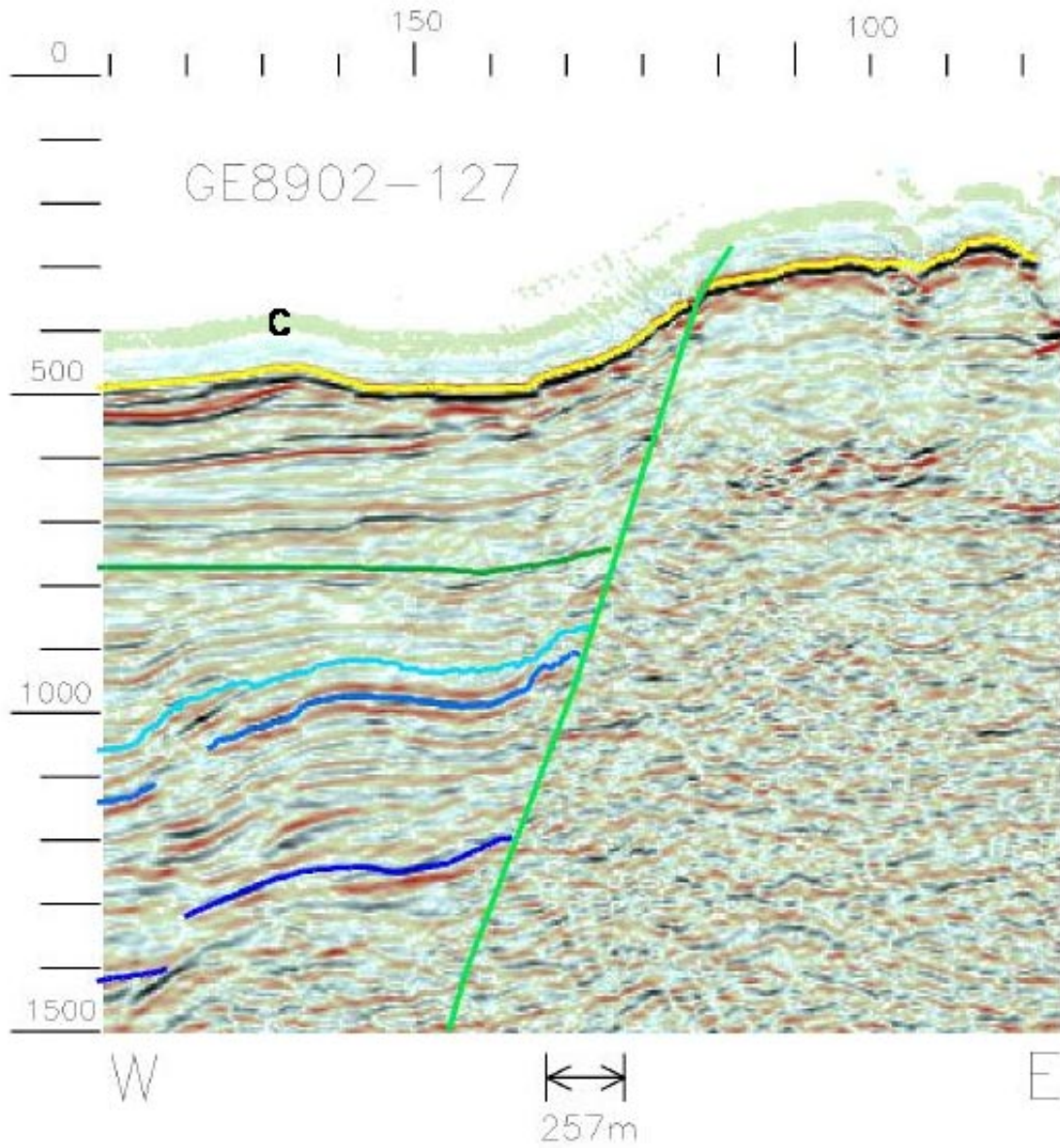
Fig. 3.1.6.   Section of digital seismic line GE8902-127. Interpretation by Phillips Petro-leum.
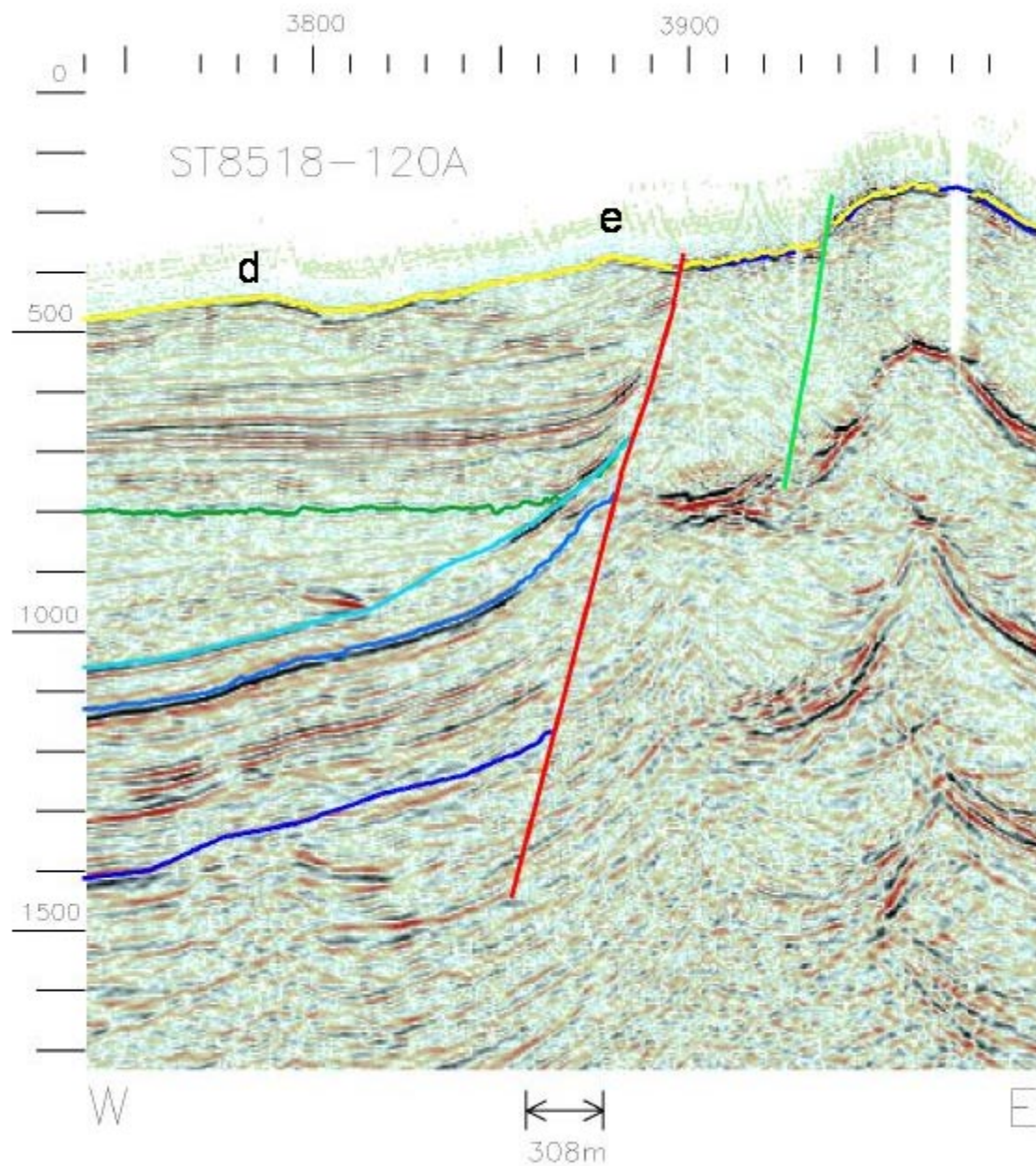
Fig. 3.1.7.   Section of digital seismic line ST8518-120A. Interpretation by Phillips Petroleum.
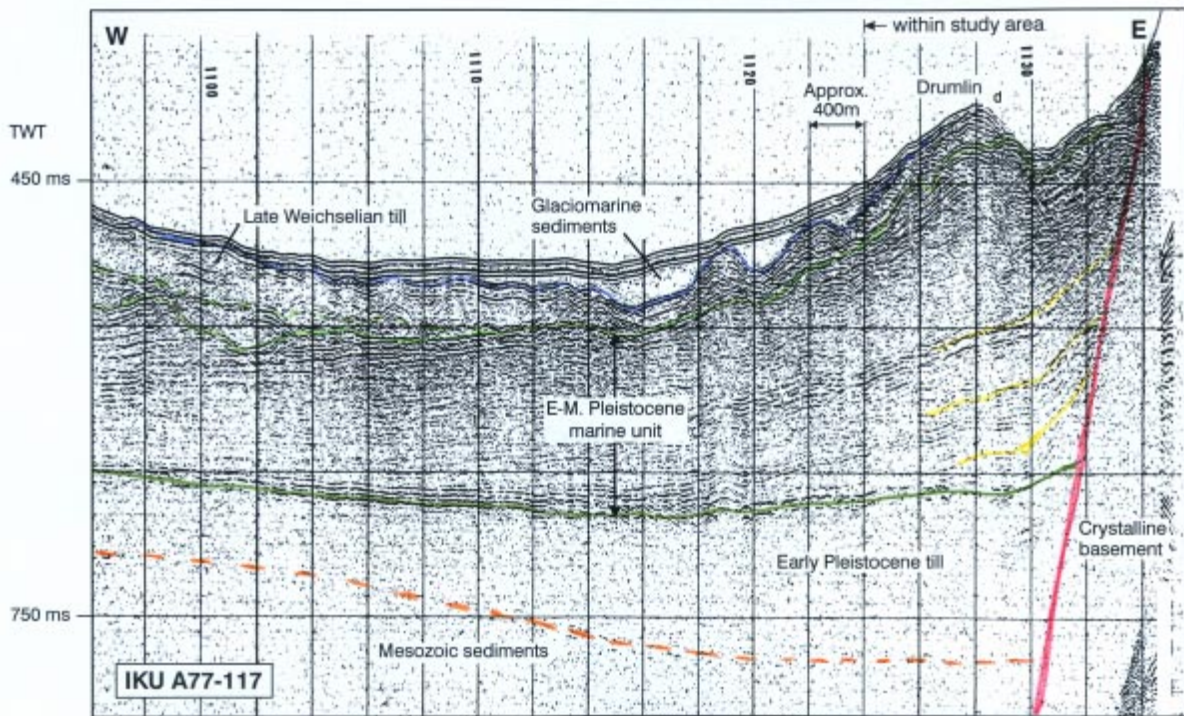
Fig. 3.1.8.   Interpreted section of analogue sparker line IKU A77-117. The track of the line is shown in Fig. 3.1.9.

3.1.3   Quaternary geology and bathymetry in the study area

The Quaternary sediments west of the Øygarden fault zone are around 300 ms thick, where an early Pleistocene glacial erosion event has cut deeply into the sedimentary succession. The base of the Quaternary represents an angular unconformity, which is well developed west of the study area. Only a thin and discontinuous layer of Quaternary sediments is deposited on top of the crystalline basement rocks. These rocks have been more resistant to glacial erosion, and crop out commonly at shallower depth with a more pronounced seafloor relief.

Although the water depth in general is much shallower where the crystalline rocks outcrop (at 200-300 ms depth) compared to west of the fault plane, the last phase of glacial movement across the area and later glaciomarine deposition have resulted in a gradual and variable change of the morphology across the boundary. The northwest striking ridges west of the crystalline rocks represents drumlins, which partly are buried below glaciomarine sediments in the westernmost part of the area (Figs. 3.1.9, 10). These are mainly created on the lee side of basement ridges (crag and tail type features), and thus the basement morphology is partly extended also west of the fault plane. It is therefore difficult to imagine the basement boundary from the bathymetric images. Only in the southernmost part of the study area where a very pronounced slope is developed, can the exact position of the boundary be inferred.

Above the angular unconformity, which is visible as a very faint reflector on the E-W sparker line across the study area, the lowermost Quaternary unit probably represents an early Pleistocene glacial deposit, probably partly consisting of till (Fig. 3.1.8). A tentative correlation to a deep Quaternary borehole at the Troll Field southwest of the study area, possibly indicates that the age of this unit is around 1 million years (Sejrup et al. 1995). The parallell layered seismic unit above is very thick (150-180 ms) close to the basement boundary. The reflections onlap the basement, and the lower part of the unit apparently progrades out from the basement area, thins and downlap the glacial unit below in the eastern part of the trench (Fig. 3.1.8). The up-

32

per part of the unit is strongly glacially eroded in the through directly west of the study area, and has previously been thicker also in the study area. Also the upper part of the unit seems to have been built out from the basement areas, rapidly thinning in the "prodelta" area and gradually thinning westwards before it pinches out close to the eastern slope of the Norwegian Trench (Rise et al. 1984). The upper part of this sequence is correlated to a 50m thick fine grained normal marine unit, encountered in the Troll borehole. According to Sejrup et al. (1995) this unit was deposited during Early/Middle Pleistocene in a long period (in the order of 500 000 years) when the climate was not sufficiently extreme to facilitate the growth of the Fennoscandian ice sheet to the offshore areas. Late Weichselian till and glacial marine sediments are deposited (up to 40-50 ms thick) above the marine layered unit in the study area. The thickness of the Holocene clays (<10 000 years old) is only in the order of maximum 1-2 m.
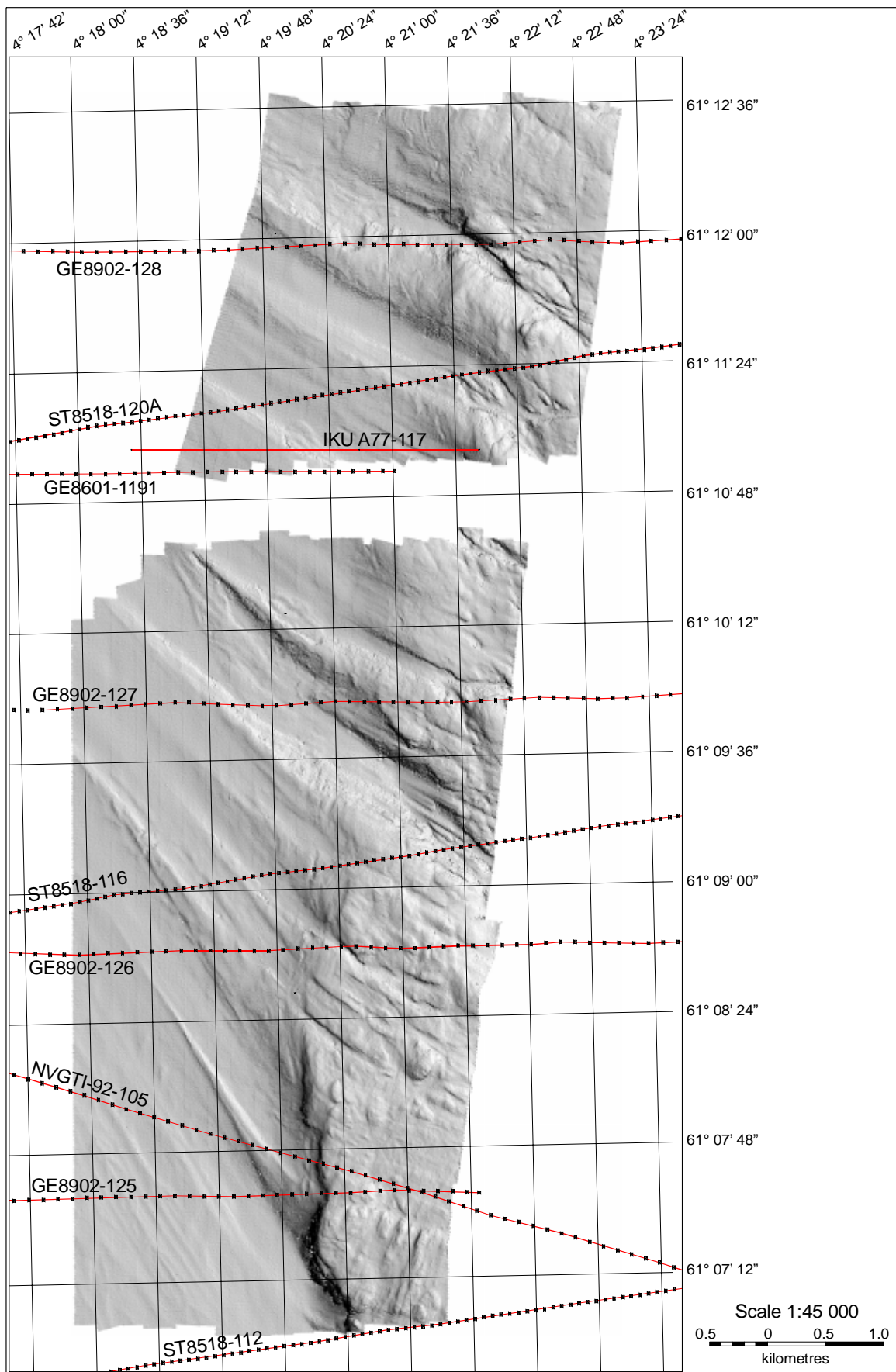
Fig. 3.1.9.   Sea floor relief image map in the study area based on swath bathymetric data.

3.1.4 Interpretation focusing on Quaternary reactivation of the fault zone

Some of the digital seismic lines are suspicious from a neotectonic point of view. On line NVGT92-105 for instance (Fig. 3.1.3), a marked westward slope is developed where the fault plane is extended to the seafloor, and a possible antithetic fault can be imagined from the sea-floor morphology. These features can easily be understood from the bathymetric relief image, which shows that the ridges represents drumlins striking north-westwards from the basement boundary (Fig.3.1.10). The interpretation of the digital seismic lines and the E-W sparker line do indicate limited glacial erosion of the fault plane, and the apparent basement boundary seems to coincide with the extended fault plane (Figs. 3.1.2-7). The interpretation of the basement boundary on the seismic lines is marked on the seafloor relief image map, and drawn between the lines (Fig. 3.1.10). However, no lineaments along this boundary have been observed, which convincingly can be related to neotectonic movements.

On the E-W sparker line, several of the parallel reflections seen in the Early to Middle Weichselian marine unit, can be followed close to the basement where the sediments show an increased westward dip towards the extended fault plane (Fig. 3.1.8). The apparent dip seen on the sparker line is in the order of 8 degrees. There is no evidence for seismic disturbances in this unit indicating water escape features, debris flows, etc., which possibly could have been related to earthquakes.

On the slopes of some drumlins, arc-shaped features can be observed, indicating small slides. One of the best-developed features is 250-300 m across, located slightly north of line GE8902-128 (Fig. 3.1.11). Interpretation of these slides as triggered by earthquake loading is speculative, and they can be collapse features created immediately after the ice became buoyant, when the glacial sediments lost their lateral support.
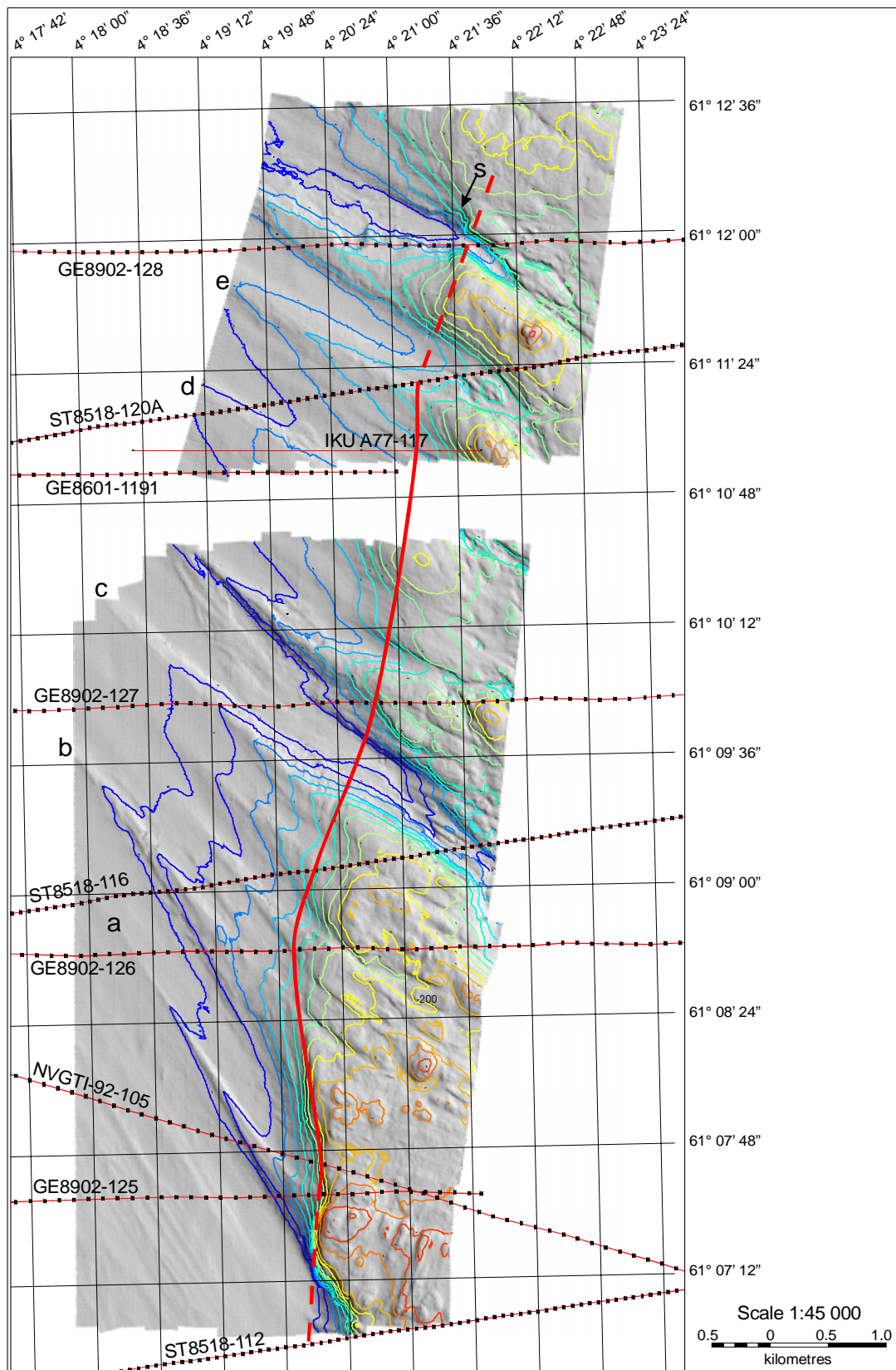
Fig. 3.1.10. Sea floor relief image map in the area with superimposed bathymetric contour lines (20 m contour distance). The interpreted basement boundary (i.e. extended fault plane in Figs. 3.1.2-7) is marked on the track lines, and interpreted between the lines. The letters marked on the drumlins refer to letters on the corresponding features seen on the seismic lines (Figs. 3.1.2-8). The slide denoted S is shown in greater detail in Fig. 3.1.11.

36
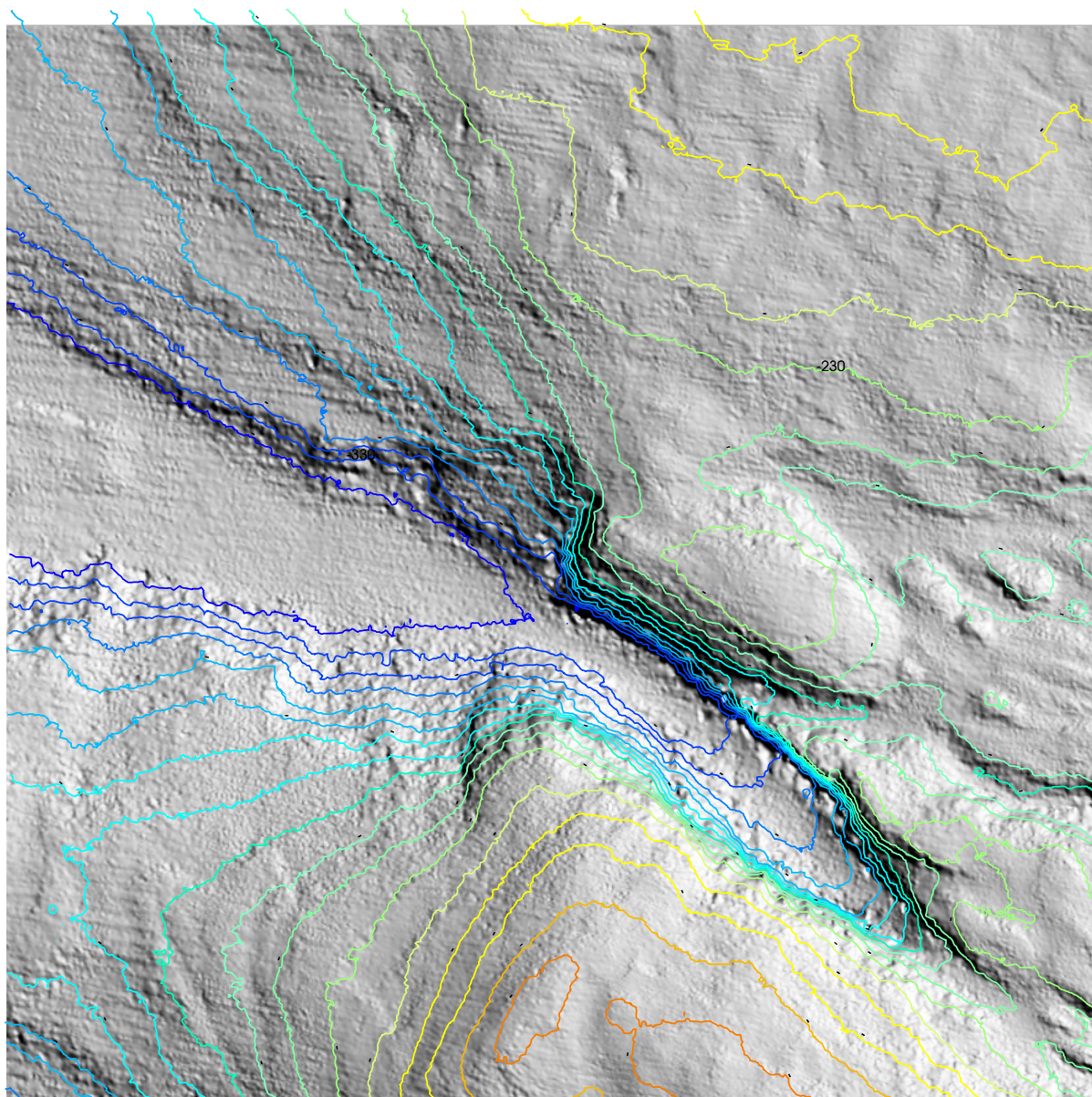
Fig. 3.1.11.   Sea floor relief image of a wide slide 250-300 m across. For location of the feature, see "s" in Fig. 3.1.10.

3.1.5   Conclusion

Based on the investigated data we have no indications of neotectonic movements at the Øygarden Fault zone.

3.1.6   References

Eynon, G. 1981: Basin development and sedimentation in the Middle Jurassic of the Northern North Sea. In: Illing, L.V. and Hobson, G.D. (eds.): Petroleum Geology of the Continental Shelf of North-West Europe. pp.196-204.

Fossen, H., Mangerud, G., Hesthammer, J., Bugge, T. and Gabrielsen, R. H. 1997: The Bjorøy Formation: a newly discovered occurrence of Jurassic sediments in the Bergen Arc System. Norsk Geologisk Tidsskrift, Vol. 77, pp. 269-287.

Færseth, R.B., Gabrielsen, R. H. and Hurich, C. A. 1995: Influence of basement in structuring of the North Sea basin, offshore southwest Norway. Norsk Geologisk Tidsskrift, Vol. 75, pp. 105-119.

Muir Wood, R., 1993: A review of the seismotectonics of Sweden. Swedish Nuclear Fuel and Waste Management Co. Technical Report 93-13, 225 å

Muir Wood, R. & Forsberg, C. F., 1988: Regional crustal movements on the Norwegian continental shelf, ELOCS (Earthquake Loading on the Norwegian Continental Shelf) Report 1-3, Norwegian Geotechnical Institute, Oslo, NTNF/NORSAR, Kjeller and Principia mechanica Ltd., London, 148 p

Rise, L., Rokoengen, K., Skinner, A.C. and Long, D. 1984: Northern North Sea. Quaternary geology map between 60° 30' N and 62° N, and east of 1° E (M 1.500 000). Institutt for kontinentalundersøkelser (IKU), Norway.

Rokoengen, K. and Rønningsland, T. M. 1983: Shallow bedrock geology and Quaternary thickness in the Norwegian sector of the North Sea between 60° 30' N and 62° N. Norsk Geologisk Tidsskrift, Vol. 63, pp. 83-102.

Sejrup, H.P., Aarseth, I., Haflidason, H., Løvli, R., Bratten, Å., Tjøstheim, G., Forsberg, C.F.and Ellingsen, K.L. 1995: Quaternary of the Norwegian Channel: glaciation history and paleooceanography. Norsk Geologisk Tidsskrift, Vol. 75, pp. 65-87.

3.2 INTERPRETATION OF SEISMIC DATA FROM HJELTEFJORDEN

By Leif Rise (NGU), Fridtjof Riis (NPD) and Odleiv Olesen (NGU)

3.2.1 Introduction

Hjeltefjorden represents a major geological boundary striking NNW-SSE, on the east side of the Øygarden islands, NW of Bergen. The northernmost part of the fjord is named Fedjefjorden, on the eastern side of the Fedje Island (Fig. 3.2.1).

During the last 2 million years western Norway has been heavily eroded by glaciers, and the zones of regional fractures and faults have been overdeepened by erosion. These zones are today mainly exposed as deep fjords such as Hjeltefjorden/Fedjefjorden.

In connection with a pipeline feasibility study from Oseberg to the Mongstad site, an extensive site investigation was made in the Hjeltefjorden between the islands Seløy/Alvøy and Uttoska. This investigation included seismic refraction and sparker/boomer profiling combined with rock coring in the fjord (reported by Noteby in 1984). In the deepest part of the fjord, a 1 km wide low velocity zone indicated a possible down-faulted basin of Mesozoic rocks. Rock coring from a drillship showed, however, that the bedrock consisted of a serpentinite breccia of Cambro-Silurian age belonging to the Bergen arc metamorphic rocks. The bedrock at the Øygarden islands consists mainly of Precambrian gneisses.

Close to the island Bjorøy, located within the Øygarden Fault zone approximately 30 km southeast of our study area, Late Jurassic sediments were encountered during the construction of a subsea road tunnel (Fossen *et al*. 1997). According to Fossen *et al*. (1997) the westerly dip of the Mesozoic strata west of Sotra/Øygarden requires a post-Middle Jurassic down to the east throw component (up to a few hundred meters) on the Hjeltefjorden Fault zone for the strata of this age to reappear in the Bjorøy area.

In the "Mongstad earthquake criteria study" (NTNF/NORSAR and NGI, 1985) some interesting observations were made on boomer lines, which could be related to postglacial deformation. On several SW-NE lines crossing the fjord between Alvøy and Uttoska, a possible offset of 5-10 m were inferred in the post-glacial sediments, with the southwestern side apparently down-faulted.

As the scope of the NTNF/NORSAR/NGI-study was too limited to go further in detail with these interesting data, and because Statoil recently has collected swath bathymetry in the same area, the NEONOR project decided to examine the existing database to look for evidences of postglacial reactivation of the Øygarden Fault zone.
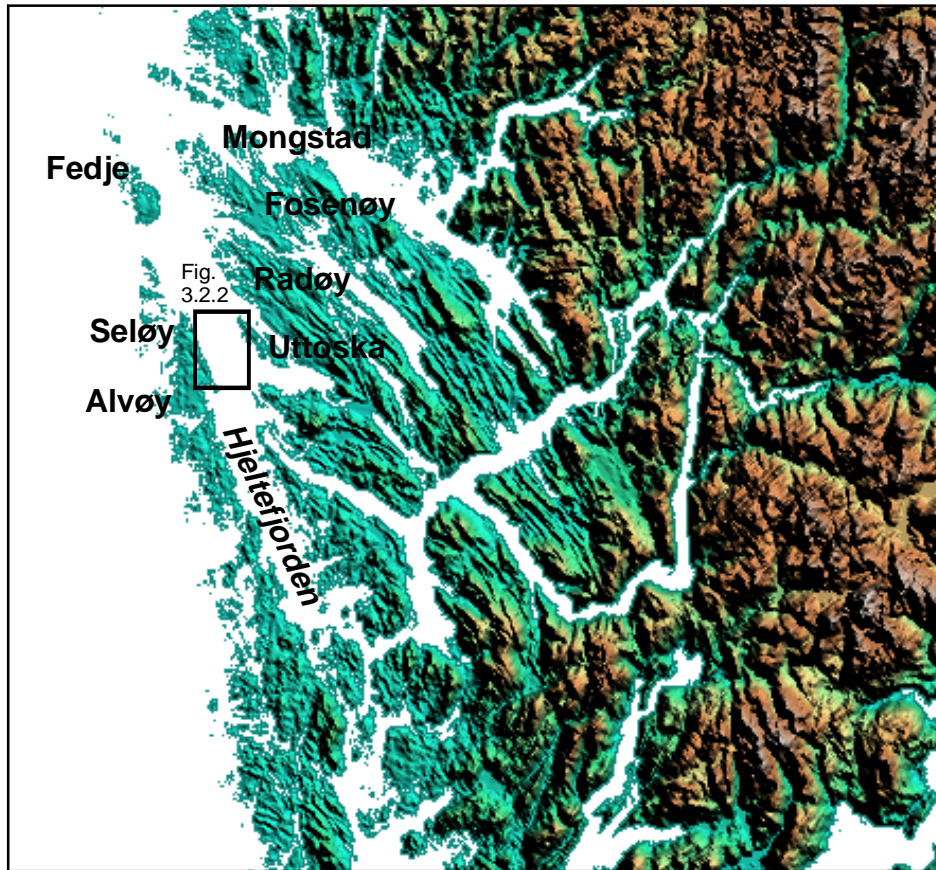
Fig. 3.2.1.   Map showing the study area in Hjeltefjorden.

3.2.2 Database

The boomer data in Hjeltefjorden were collected by a.s Geoconsult in 1980 and 1983. During a visit to NGI in June 1998, the 1983 data set was interpreted. All lines are run in SW-NE direction, 100 m apart, perpendicular to the axis of Hjeltefjorden. The seismic data are of fairly good quality, but side echoes/diffractions partly make an exact interpretation difficult at marked slopes/ridges. The lines are named E3000, E3100 etc., increasing numbers towards the south-east. The only available map (1:10000) shows the track of the lines, but no line identification or shot/fix points are annotated. An important question is therefore: Where exactly are the interesting observations located? Requests to the client (Norsk Hydro) and the involved contractors (Noteby/Geoconsult) gave negative results. By comparing the bathymetry of the map (5 m contour distance) and the bathymetry seen from the seismic lines, we believe to have obtained a fairly good control of the line identification (+/- 100 m, Fig. 3.2.2). However, as no fix numbers/shot points are marked on the map, it is impossible to map the exact position of where the assumed neotectonic observations are made.
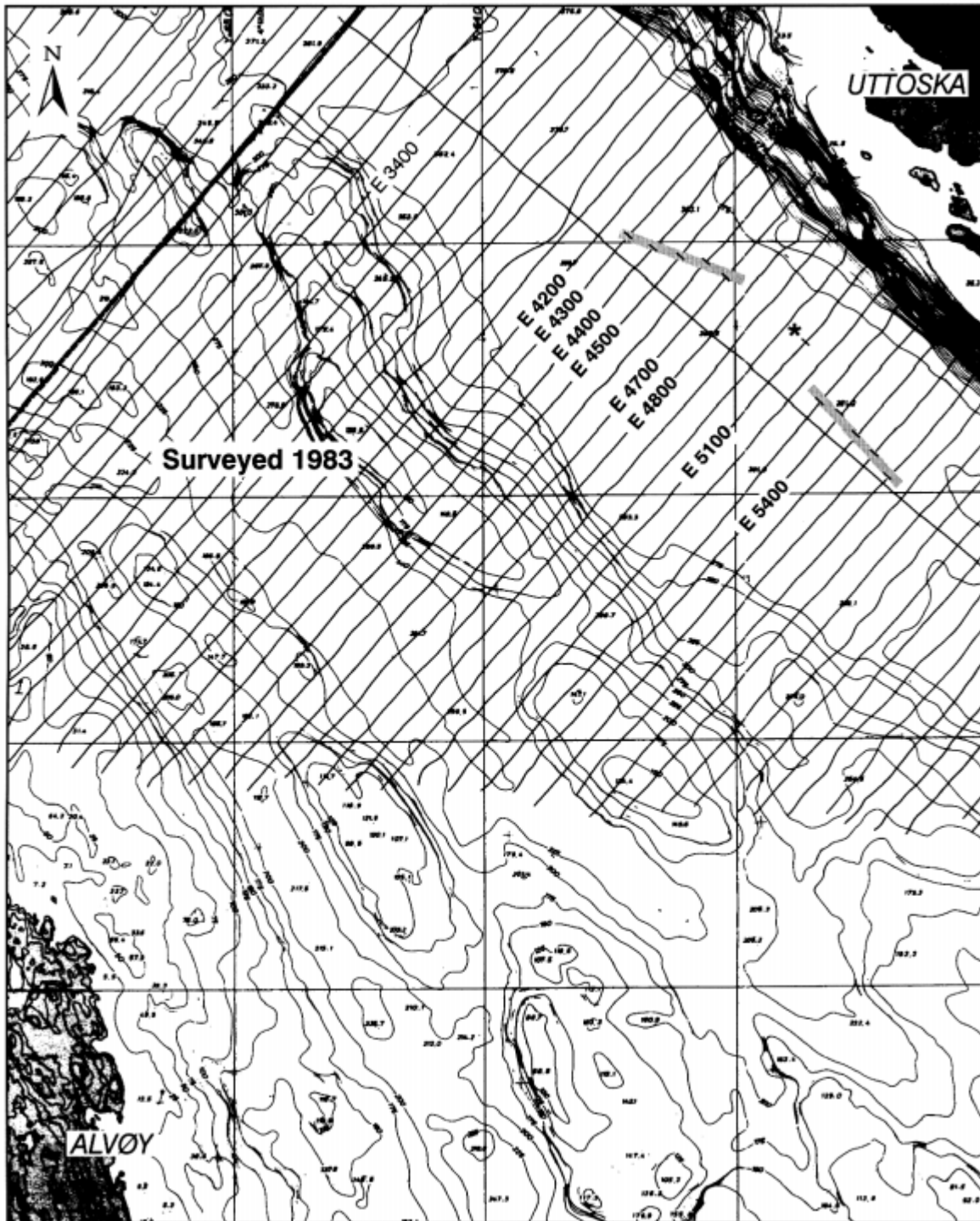
Fig. 3.2.2.   Part of Geoconsult`s drawing no.11028-210, showing the track of the boomer lines. Approximate location of the inferred fault seen on lines E4300-4700 (Fig. 3.2.3), apparent step of Unit A on line E5100 (Fig. 3.2.5) and the pronounced seabed slope seen on line E5300-5700 (Fig. 3.2.6) are shown.

In the actual area multibeam echo-sounding (swath bathymetry) has been carried out, and we visited the premises of Statoil to study the seafloor image relief map. Unfortunately, the data were muted due to military restrictions in a small area where the best observations of possible neotectonic movements were made.

3.2.3 Quaternary geology and bathmetry

In Hjeltefjorden the deepest section is infilled with 40-70 ms (c. 35-60 m) of Quaternary sediments, mainly glaciomarine clays. A till unit is probably deposited on top of the crystalline basement, but this unit is too thin or discontinuous to be clearly identified on the seismic. The lowermost seismic Unit A has both incoherent and weak parallel reflections. The parallel reflections are apparently best developed in the north-eastern part of the fjord. In the uppermost part of Unit A the reflections become more continuous and get higher amplitudes. Unit B above, has mainly weak incoherent reflections, resulting in a medium light structureless seismic pattern. Units A and B are interpreted to represent dominantly glaciomarine sediments, deposited approximately 13000 to 10000 years before present. The uppermost seismic Unit C, is acoustically transparent with no apparent parallel reflections. We believe that this unit represents the Holocene sedimentation in the area (last 10000 years).

The seafloor at the deepest part of the fjord (1-1.5 km wide) is fairly even in the investigated area. The water depth increases from approximately 370 m in the north-western part to more than 400 m in the south-eastern part. Both the north-eastern and the south-western slope of the fjord are steep, and here limited amounts of Quaternary sediments have been deposited.

3.2.4 Interpretation: Neotectonic faulting or current controlled deposition ?

Looking separately on 5 of the seismic lines (E4300 - E4700, each 100 m apart), a possible neotectonic movement can be inferred. The approximate position of the inferred fault has been plotted based on the distance between the foot of the slopes, assuming that the survey vessel kept constant speed. The plotted positions indicate a WNW- ESE lineament (Fig. 3.2.2). The most "convincing" observations are seen on lines E4300 - E4500 (see Fig. 3.2.3), where the top of Unit A apparently is down-thrown 11-13 ms in the south-western part of the fjord (assuming that the sea floor was flat before the faulting). The crystalline basement forms a ridge directly below the inferred fault, and Unit A is 10-20 ms thicker in the depression to the north-east of the ridge. The top of Unit A is fairly flat on both the north-eastern and south-western side of the fjord. If a neotectonic explanation of the observed features is correct, the movement must have happened shortly after Unit A was deposited, because Unit B shows an apparently "sharp" increase in thickness to the south-west of the inferred fault (in the order of 8-10 ms). With respect to the evaluation of "sharpness" of incidents, it should be kept in mind that the vertical exaggeration of the seismic lines is approximately three times.

The neotectonic explanation becomes less evident looking at the lines directly to the north-west and north-east of lines E4300 - E4700 (Fig. 3.2.4). On line E4200 to the north-west, the top of Unit A is shallowest in the central part of the deep fjord, reflecting vaguely the bedrock ridge below. The top of Unit A is 6-7 ms higher on the north-eastern side of the ridge, and no marked change of reflections or paleo-topography indicate any neotectonic movement. Although the topography of the basement ridge has changed on profile 100 m to the south-east (E4300), it is possible to imagine a similar gradual change in the depositional pattern across the ridge on this line. Comparison of line E4700 (south-easternmost line where a possible neotectonic movement can be inferred) and the neighbour line E4800 (Fig. 3.2.4) gives also impression of a gradual change in depositional development. On profile E4800 it is no indication of any neotectonic movement, but also on this line the top of Unit A is 6-7 ms higher on the north-eastern side.
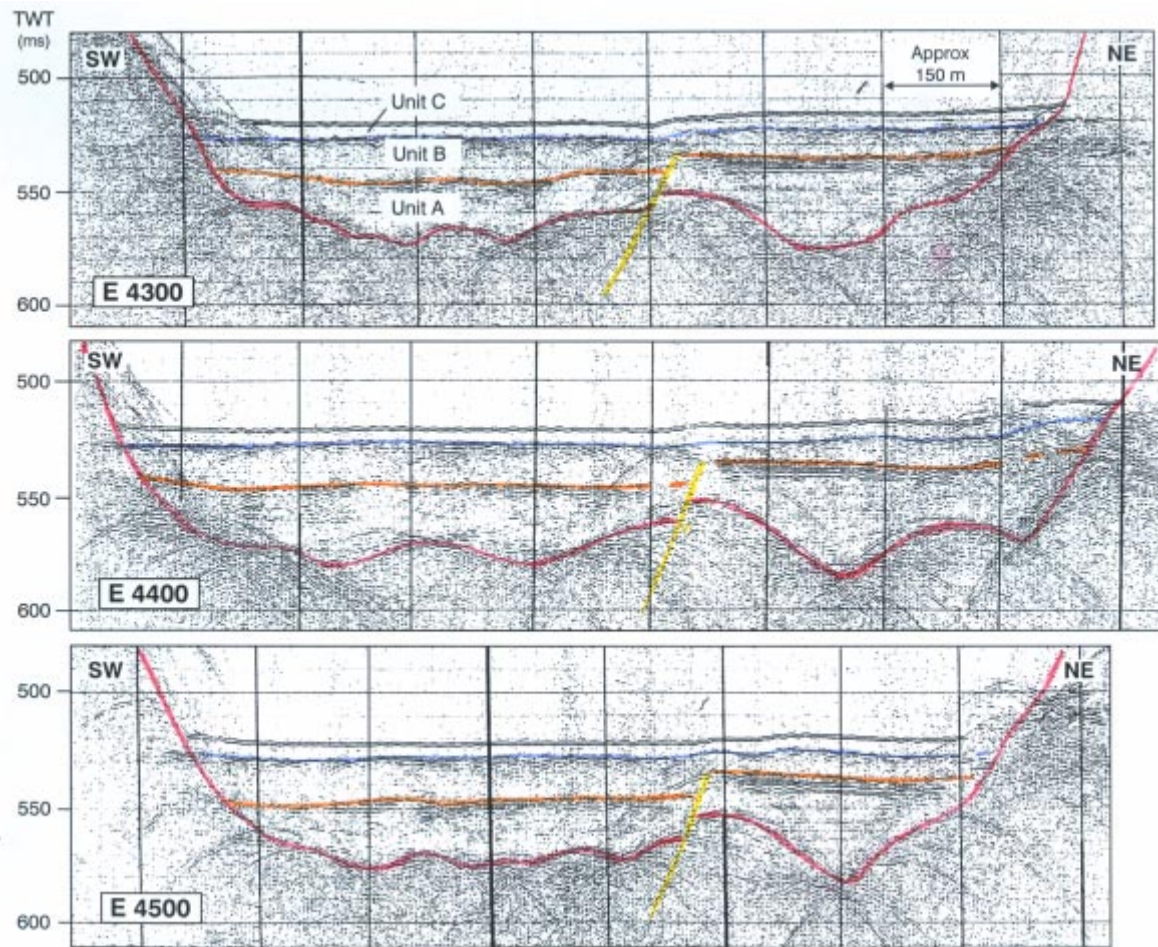
Fig. 3.2.3. Seismic interpretation of three boomer lines across the deep section of the fjord (each 100 m apart), assuming postglacial faulting of Unit A. Units A and B represent glacio-marine sediments deposited approximately 13000 - 10000 years before present, with Holocene sediments above (Unit C). See Fig. 3.2.2 for location of the inferred fault.

43
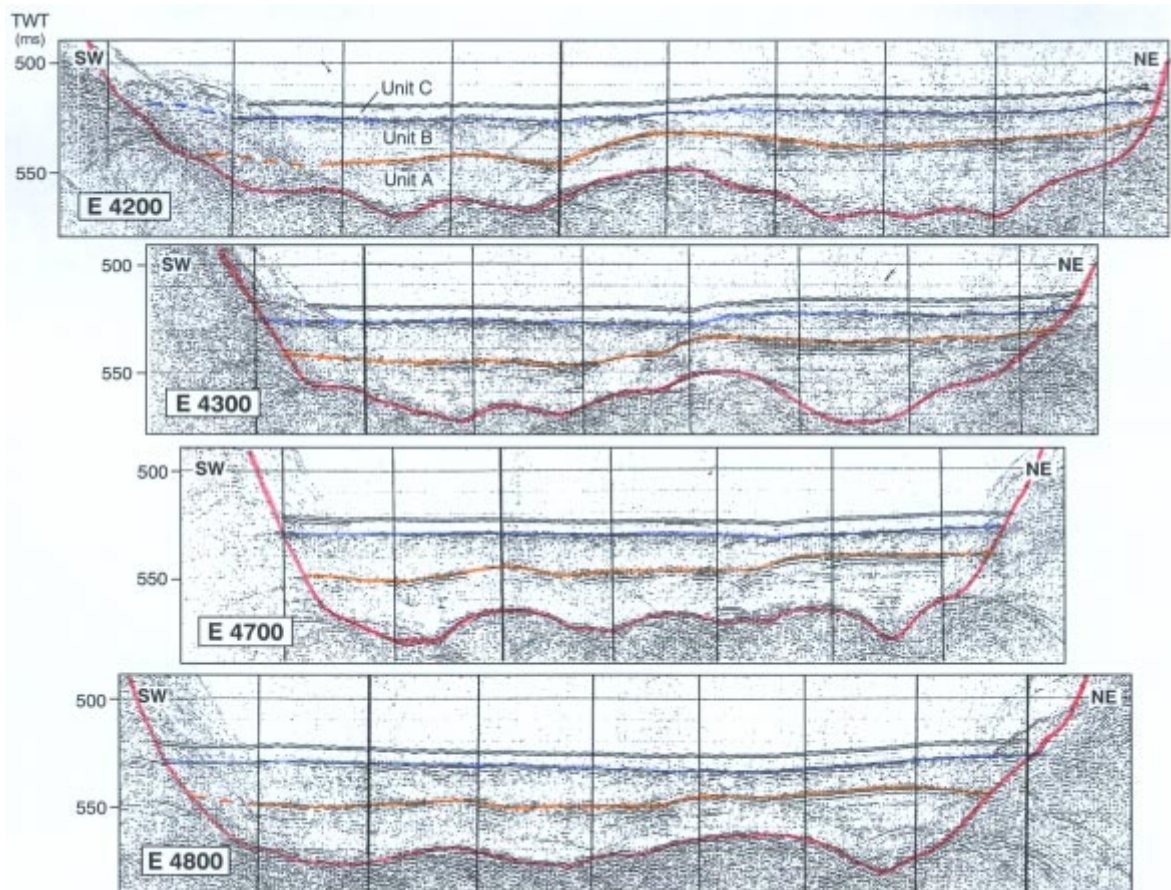
Fig. 3.2.4.   Seismic interpretation of the line E4200 (upper section) and E4800 (lower section), respectively 100 m northwest and 100 m southeast of the area of inferred neotectonics (E4300-E4700), indicates a gradual change of the top Unit A-level, from NE to SW (following the SW slope of the underlying basement ridge).

Fig. 3.2.5 shows that the depositional environment has changed very rapidly in the fjord, indicating that a varying current regime controlled the deposition. Between profile E3400 and E4300 (NW to SE) the thickness of Unit A decreases from approximately 50 ms to 25 ms on the south-western side of the fjord (distance only 900 m). The change in thickness is less on the north-eastern side, particularly because the top of Unit A is built up to a higher level in this part, indicating that the currents were weaker, or that backcurrents which favoured deposition existed here.

The current regime shifted totally at the boundary to Unit B, resulting in a different depositional pattern. Where the thickness of Unit A decreased from 50 ms to 25 ms, Unit B increases from 7 ms (partly 0 ms) to 20 ms (between lines E3400 and E4300, south-western side of the fjord). On the north-eastern side of the fjord, Unit B increases from 7 ms to 12 ms. In general the depositional environment during the sedimentation of Unit B, tried to flatten the existing relief formed at the top of Unit A.

The deposition of Holocene sediments in the fjord (Unit C) is very uniform, showing a slight increase in the investigated area from 5 ms (NW) to 8 ms (SE) (see Fig. 3.2.5).

Between line E4300 and E5100 the change in thickness of the units is less, and the basement topography becomes more symmetrical with the deepest glacial erosion in the middle of the fjord. The top of Unit A shows an apparent "step" on line E5100 to a 7-8 ms shallower level (Fig. 3.2.5), but the neighbour line E5200 indicates that the surface of Unit A is mirroring the

general shallower basement topography. A more pronounced bedrock slope to a 25-30 ms shallower level on the NE side of the fjord is seen in lines E5300-5700. Above this slope the seafloor shows a marked slope up to an approximately 10 ms shallower level (Fig. 3.2.6). These observations are candidates for interpretation of a neotectonic fault, but the neighbour lines to the south-east indicate that the seabed mirror the underlying topography and thus results in an most likely apparent fault. The direction of the seabed slope is NW-SE.
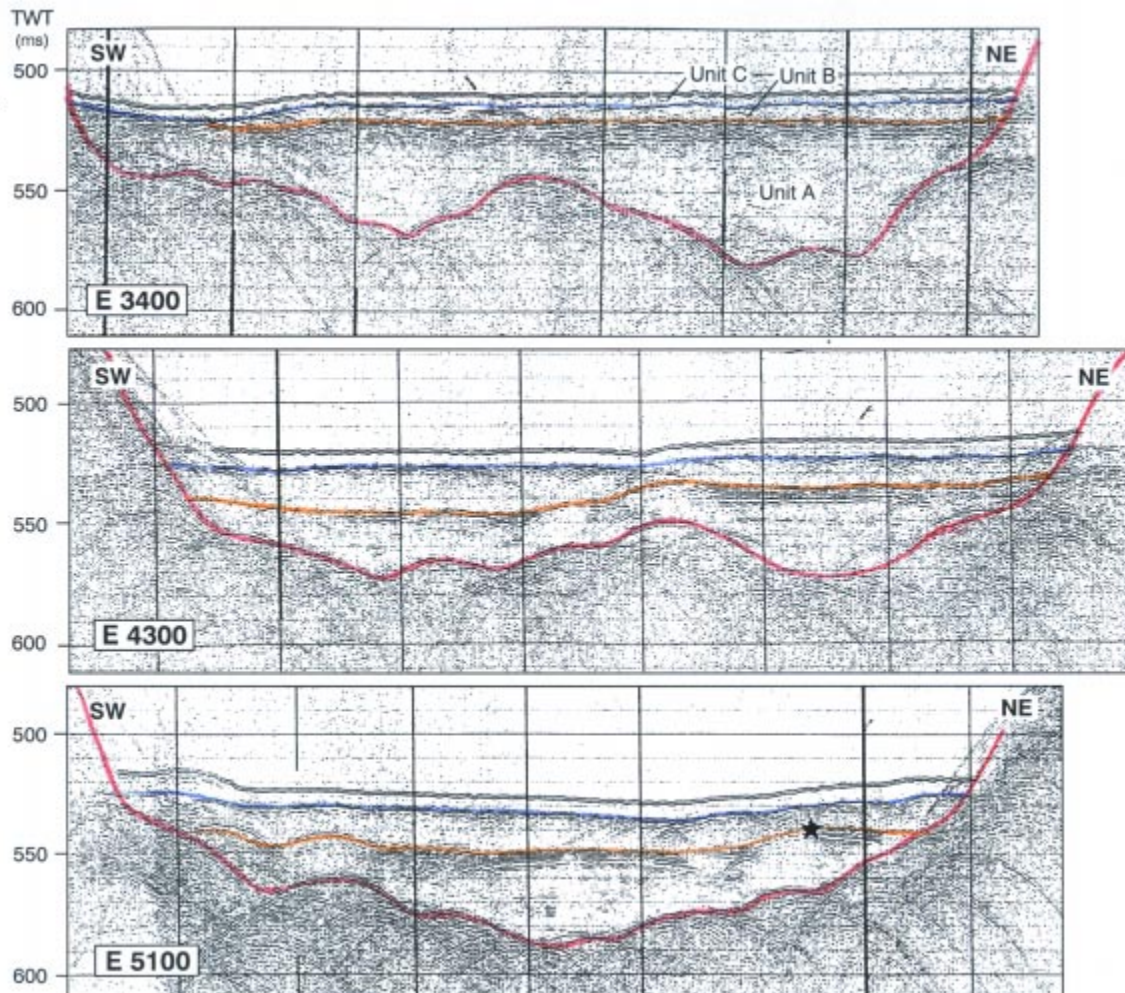
Fig. 3.2.5. Seismic interpretation of the lines E3400 (NW) and E4300 (900 m apart), shows a marked (and opposite) change in thickness of Units A and B along the fjord axis, and partly across the fjord. Line E5100 (800 m to the southeast) demonstrates that the basement morphology in the deep section of the fjord varies. The location of the apparent step on top of Unit A is shown in Fig. 3.2.2.
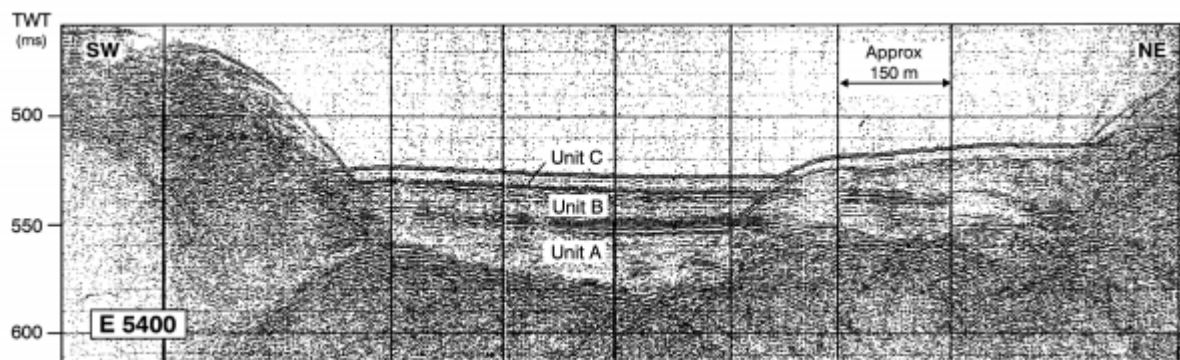
Fig. 3.2.6. Seismic line E5400 shows a marked seabed slope which mirror the bedrock slope below. See Fig.2 for location of the slope seen on lines E5300- E5700.

3.2.5 Summary and conclusion

Although an interpretation of a neotectonic fault is possible on five of the profiles (E4300-E4700, see Fig. 3.2.3), we believe this is very unlikely. On the profiles north-west and south-east of the interesting observations (Fig. 3.2.4), it is not possible to infer any neotectonic movement. The offset/length ration of the inferred fault is therefore 1/80 (height 5-9 m/length 400 m), which is far from filling the requirements of 1/1000 (Fenton 1991). The shaded relief image map of the seafloor were unfortunately muted in a small square, exactly where the observations were done. However, no linear features indicating neotectonic faulting were observed on the seafloor relief image near by.

The deposition of units A and B shows a marked and gradual change both along and across the deep section of the fjord in the north-western part of the studied area. It is obvious that the current regime and depositional pattern shifted totally at the boundary between the units in the north-western part of the studied area (Fig. 3.2.5). Our interpretation is that this resulted in a peculiar geometric constellation of units A and B, particularly well illustrated on some of the profiles (Fig. 3.2.3).

The pronounced seabed slope seen on the profiles E5300-E5700 looks apparently as a recent fault on the seismic lines (Fig. 3.2.6), but we favour the interpretation that the seabed topography mirror the basement topography.

Our conclusion is that the examined data not convincingly indicate neotectonic movements in the Hjeltefjorden. However, we will not based on the present data totally exclude the possibility that the "fault" lineament (WNW-ESE) and the "slope" lineament (NW-SE) located 600 m apart could be fragmentary expressions of an *en echelon* fault system in the Hjeltefjorden (see Fig. 3.2.2).

3.2.6 References

Fossen, H., Mangerud, G., Hesthammer, J., Bugge, T. and Gabrielsen, R. H. 1997: The Bjorøy Formation: a newly discovered occurrence of Jurassic sediments in the Bergen Arc System. *Norsk Geologisk Tidsskrift*, Vol. 77, pp. 269-287.

Fenton, C., 1991: *Neotectonics and palaeoseismicity in North West Scotland*. Ph.D. thesis, University of Glasgow, Glasgow, 403.

GEOCONSULT (1983): Pipeline Oseberg-Mongstad. Track chart boomer (map scale 1:10000). Survey 1980 and 1983. Drawing no. 11028-210.

NTNF/NORSAR and Norwegian Geotechnical Institute 1985: Mongstad Earthquake Criteria Study. Unpublished report. *69 pp.*

3.3 INTERPRETATION OF 3D SEISMIC SURVEYS IN THE NORTHERN NORTH SEA AND NORDLAND II AND VI AREAS

By Odleiv Olesen (NGU), Fridtjof Riis (NPD) and Stein Fanavoll (Sintef Petroleum Research)

3.3.1 Introduction

A total of eight 3D surveys (Fig. 3.3.1) from the northern North Sea and the Norwegian Sea have been interpreted within the frame of the NEONOR Project. The objective of the study has been to identify and evaluate possible neotectonic features offshore Norway. The northern North Sea and the Norwegian Sea have been the focus of interest since these areas reveal increased seismicity and have extensive 3D seismic coverage. The interpretation was carried out utilising Charisma workstations at NPD and IKU. Faulting of the Quaternary sediments in the northern North Sea have previously been well documented by Hovland (1983). This report is included in Table 3.3.1, where an evaluation of previous neotectonic claims in offshore Norway is listed.

The 3D seismic surveys NH9101 and SG9202 in the Troll area and the 2D surveys NPD-KYST-96 and NPD-SK-95 were interpreted by Fridtjof Riis, NPD and reported in the NEONOR Annual Technical Report 1997 (Riis 1998). Indications of Quaternary faulting and flexing were observed on both 2D and 3D data, especially in the northeastern Troll area. The interpretation of additional six surveys has been carried out along the same lines as the interpretation by Riis (1998) and is presented in the present report. We used the following set of criteria (Riis 1998):

1) Faults should be recognisable in the time slices and in the mapped surfaces

2) One fault should be recognised in a number of time slices

3) Fault orientation should be oblique to the line direction (because of static shifts).

4) Glacially induced structures, such as grooves or plough-marks must not be interpreted as faults.

Table 3.3.1.   Reported evidences of neotectonics offshore Norway and tentative assessments of the claims. The locations are ordered from north to south. The criteria for classification of postglacial faulting by Fenton (1991, 1994) and Muir Wood (1993) have been utilised for grading the claims into the classes: (A) Almost certainly neotectonics, (B) Probably neotectonics, (C) Possibly neotectonics, (D) Probably not neotectonics and (E) Very unlikely to be neotectonics. List of onshore neotectonic claims is presented in Appendix 2.1.

NO.	LOCATION AND REFERENCE	OBSERVATION	COMMENT	GRADE / TYPE
1	Barents Sea, 50 km east of Edgeøya Fanavoll & Dahle (1990)	A fault seems to offset the sea-floor on the seismic line BFB-76-35.	The Quaternary is very thin in the northern Barents Sea area and the hard sea floor is causing strong multiples. The poor quality of the seismic data reduces the reliability of the claim. Neither have any indications of postglacial faulting been observed on the neighbouring seismic lines NPD 7730-80B and NPD-2600-80B.	D
2	Bjørnøyrenna, Barents Sea margin Fiedler (1992), Muir Wood (1995)	Offset of shallow reflectors along the southern Barents Sea margin has been interpreted as effects from sea floor instability and postglacial strike-slip faulting by Fiedler (1992) and Muir Wood (1995), respectively.	There is no offset of the reflectors below the scarp at the sea floor. We do therefore favour a gravity-induced mechanism.	D
3	Malangsdjupet, offshore Malangen, Troms Fanavoll & Dahle (1990) and Fanavoll & Dehls (1998)	An offset of Quaternary reflectors can be observed on IKU shallow sparker line IKU-C84-306. A step at the sea floor marks the shallow termination of the fault. Multi-beam data reveal a bulge in the bathymetry corresponding to the fault on the seismic line. The extent of the fault as expressed on the sea bottom is limited to ~0.5 km.	Multi-beam echo-sounding data acquired in the NEONOR Project reveal a limited extent of the fault (0.5 km) which reduces the grade of this claim (Fanavoll & Dehls 1998). It is, however, a possibility that the short fault scarp is a secondary structure to strike-slip movements along the NW-SE trending Bothnian-Senja Fault Complex	D

NO.	LOCATION AND REFERENCE	OBSERVATION	COMMENT	GRADE / TYPE
4	NW of the island of Røst, Nordland Rokoengen & Sættem (1983) and Fanavoll & Dehls (1998)	The sea floor relief shows several abrupt changes in level and slope that were interpreted in terms of potential postglacial faults. The main escarpment is located 1.2 km beyond the steep boundary between the crystalline basement and deformed sedimentary sequences.	Multi-beam echo-sounding data acquired in the NEONOR Project indicate that the scarps are effects of erosion rather than tectonic processes (Fanavoll & Dehls 1998).	E
5	Continental slope, Røst Basin, Nordland Mokhtari (1991) and Mokhtari & Pegrum (1992)	Evidence of recent downslope gliding along the continental slope.	This fault is most likely not caused by a deep-seated tectonic process but rather by gravity gliding.	D
6	Fulla Ridge, Vøring Basin Muir Wood (1995)	Muir Wood (1995) interpreted seismic data by Granberg (1992) in terms of a mid-late Quaternary reverse fault, activating Miocene faults along the Fulla Ridge.	The Pliocene reflectors beneath the potential offset Quaternary reflector do not seem to be offset, contradicting the hypothesis of a young faulting	D
7	Southern end of the Klakk Fault Complex, about 100 km to the west of Hitra island Muir Wood & Forsberg (1988), Muir Wood (1993)	On a NW-SE regional seismic reflection profile (B-4-72) a faulted offset of Tertiary reflectors appears to pass up through the youngest base Quaternary (?) reflector (c.63.7ºN.-6.6ºE). The fault involves downward displacement to the west and the reflector offset is several tens of metres. The underlying fault appeared to be near vertical in dip and probably trends approximately N-S.	Muir Wood (pers. comm., 1999) has studied more modern 2D seismic data from the area and has not been able to identify the fault on other seismic profiles. The area has also been covered with 3D seismic surveys lately.	D

NO.	LOCATION AND REFERENCE	OBSERVATION	COMMENT	GRADE / TYPE
8	Øygarden Fault Rokoengen & Rønningsland (1983), Muir Wood & Forsberg (1988)	The northern half of the N-S trending Øygarden Fault (between 61° and 61°45'N) runs parallel with the coast of western Norway and marks a significant change in the depth of the bedrock surface beneath the thick Quaternary sedimentary cover. The major scarp that has developed along the fault has some of the appearance of a fault-scarp (with vertical offset up to 150m), and although offsets have not been observed in the overlying sedimentary section itself, sediments onlap the scarp, with some suggestion of dips steeping towards the fault (Muir Wood 1993).	The fault bounds crystalline basement in the east from relatively soft Cretaceous sediments in the west. A combined interpretation of multi-beam echo-sounding data (acquired in the NEONOR Project) and 2D seismic lines shows that the Quaternary sediments are draped along the fault scarp (Rise *et al.* this report).	D
9	Western slope of the Norwegian Trench, offshore Øygarden Hovland (1983)	A N-S trending normal fault-zone with 1-2 m offset. The fault-zone has a length of minimum 2 km and consists of 2-4 parallel faults often forming a subsided internal zone. The eastern zone is generally down-faulted. The faults are detected with a deep-towed boomer during the Statpipe route survey in 1981. The fault cuts soft, silty, cohesive clay.	The fault is occurring in an area with abundance of pockmarks and Hovland (1983) has suggested a genetic between the two phenomena. Release of gas does, however, that explain the 1-2 m offset of the seafloor. A tectonic cause is therefore probable.	B
10	Holene, west of northern Karmøy, close to the British sector Hovland (1984)	Several faults are cutting the seafloor within a more than 2 km long and 10 m deep N-S trending depression (Holene). The faults are trending NE-SW, NNW-SSE and N-S and have approximately a length of 100 m.	The faults are most likely of superficial character, because of the limited scarp length. Hovland (1984) has related the faulting to gas seepage.	D

NO.	LOCATION AND REFERENCE	OBSERVATION	COMMENT	GRADE / TYPE
11	Karmsundet, 20 km northwest of Stavanger, Rogaland Bøe *et al.* (1992)	The Karmsundet Basin is a small half-graben bounded to the east by the major Kvitsøy Fault and filled with sediments of assumed Jurassic age. Overlying Quaternary sediments show plentiful evidence of instability including slump scars, rotated sedimentary units and superficial fault structures.	The majority of these superficial features do not correspond with underlying faults in till and bedrock and hence cannot be considered as direct evidence of outcropping fault-rupture (Muir Wood 1993, Rise & Bøe 1998). A land slide to the southwest of Vestre Bokn is most likely triggered by an earthquake since the slope gradient is very low and there is no indication of extraordinary strong bottom currents in this area (Rise & Bøe 1998).	D

3.3.2 Seismic data

Norsk Hydro has made three 3D surveys available for interpretation: NH9202 and NH9405 in the northern North Sea (mainly block 35/9), and NH9604 in Nordland VI (block 6710/6). The shallow parts of the three surveys were interpreted by Stein Fanavoll at IKU. Additional three surveys have been interpreted at NPD by Odleiv Olesen and Fridtjof Riis during the one year stay of Odleiv Olesen at NPD. The 3D seismic surveys SG9603M and BPN9401 to the south and north, respectively, of the two Norsk Hydro surveys in the northern North Sea and the ST9203 survey from the Nordland II area (Norne) were selected for interpretation. The surveys in the northeastern North Sea are partly overlapping each other (Fig. 3.3.2). The surveys were shot with a 12.5 m CDP distance and a 12.5 m line distance. There are some variations in data quality of the surveys. The automatically picked Quaternary reflectors do therefore show deviations in quality.

The three Norsk Hydro surveys were also loaded into the Charisma workstation at NPD from Petrobank. Every second point was loaded and the cubes consist consequently of 25m x 25m x 4ms voxels. Comparison and classification of features in the different surveys were easier to carry out when all 3D-surveys were available simultaneously. IKU and NPD utilised two different Charisma methods to interpret the Quaternary reflectors, the auto-tracking and the ASAP (automatic seismic area picker) methods (Schlumberger GeoQuest 1998), respectively. The former method is doing a loop line-by-line interpretation while the latter is working directly on the seismic cube. Some adjustments were made manually where the automatic tracking or ASAP methods did not work satisfactorily, like for instance where one unit

pinches out above another. Up to four horizons (including sea bed) have been interpreted in the North Sea and Nordland II surveys, while only seabed and partly base Quaternary could be interpreted on the Nordland VI survey (NH9604, mainly in block 6710/6) due to thin Quaternary overburden and processing problems. The interpretations of the SG9603M and BPN9401 surveys in the northeastern North Sea have been merged with data from NH9202 and NH9405 to generate a continuous coverage of the area (Enclosures 2-5).

The time structure maps from the Nordland II and IV areas (ST9203 and NH9604) are presented without any further modification. The interpreted reflectors from the four surveys in the northern North Sea were, however, filtered using the cosine de-corrugation filter (Geosoft 1994) to remove static shifts along the original seismic acquisition lines. The filtering was carried out before the surveys were merged since the direction of the acquisition profiles varied from survey to survey. The interpreted reflectors were gridded to a regular grid consisting of 50x50 m cells using the minimum curvature method (Geosoft 1997) and subsequently merged using the GRIDSTICH algorithm (Desmond Fitzgerald and Associates 1996) which also utilises the minimum curvature method. The three reflectors are presented as shaded relief maps (artificial illumination from the NE) in Enclosures 2, 3 and 5. Because of the small relief on the horizons, minor variations show up as contrasts in the colouring of the map. Observations from each reflector are described separately below. The subtle details of the flute structures on the base Elster reflector have been enhanced even more by applying a Butterworth high-pass filter (500 m wave-length) on the grid. The enhanced data set has been used to look for tectonic structures, and is shown in Enclosure 4.
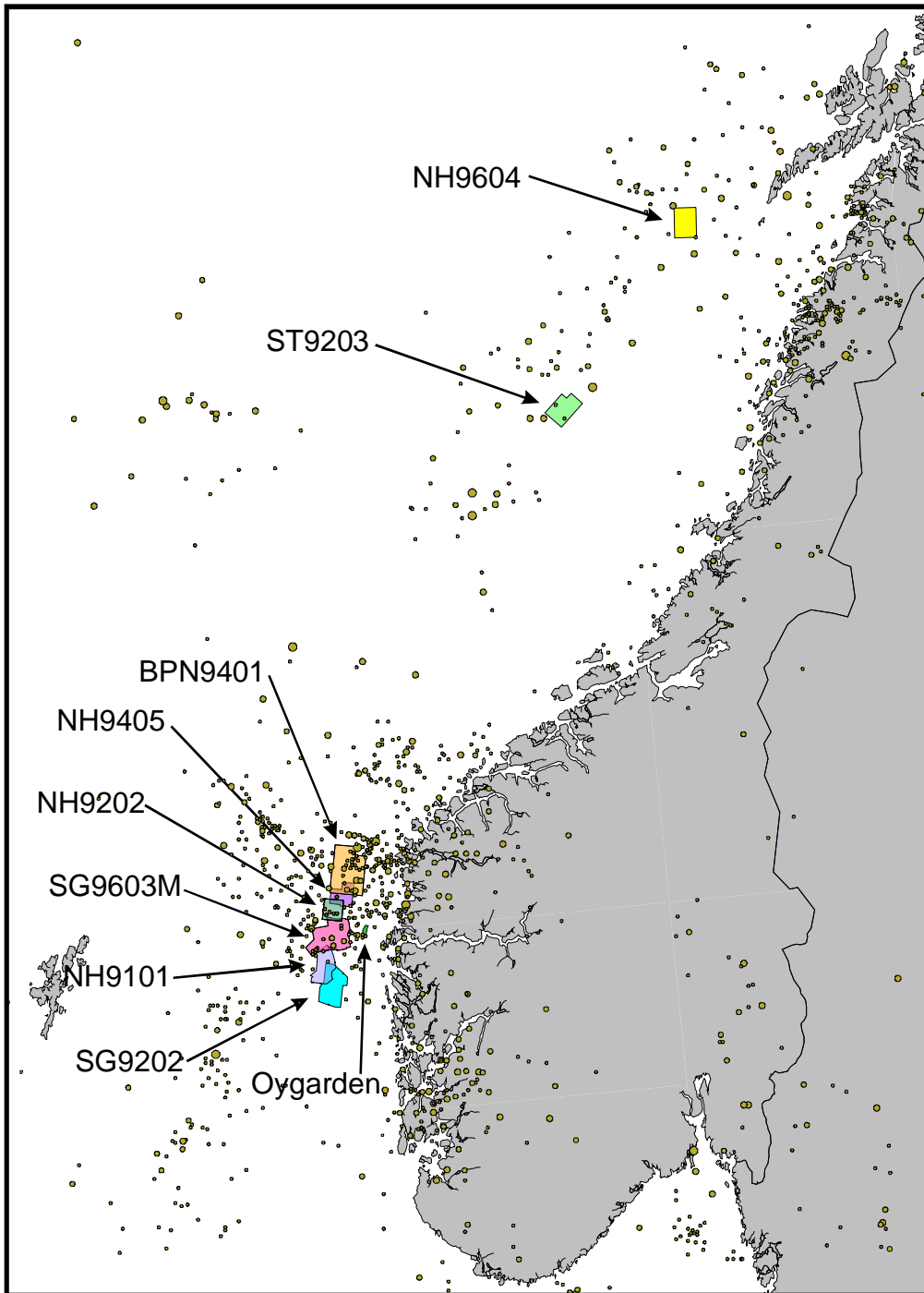
Fig. 3.3.1. Location of the interpreted 3D surveys in the northern North Sea (SG9202, NH9101, SG9603M, NH9202, NH9405 and BPN9401) and Norwegian Sea (ST9203 and NH9604). Riis (1998) has reported the interpretations of the SG9202 and NH9101 surveys. The outline of the multibeam echo-sounding survey (Rise et al., this report) across the Øygarden Fault Zone is also included on the map. Locations of earthquakes (small circles) are provided by NORSAR.
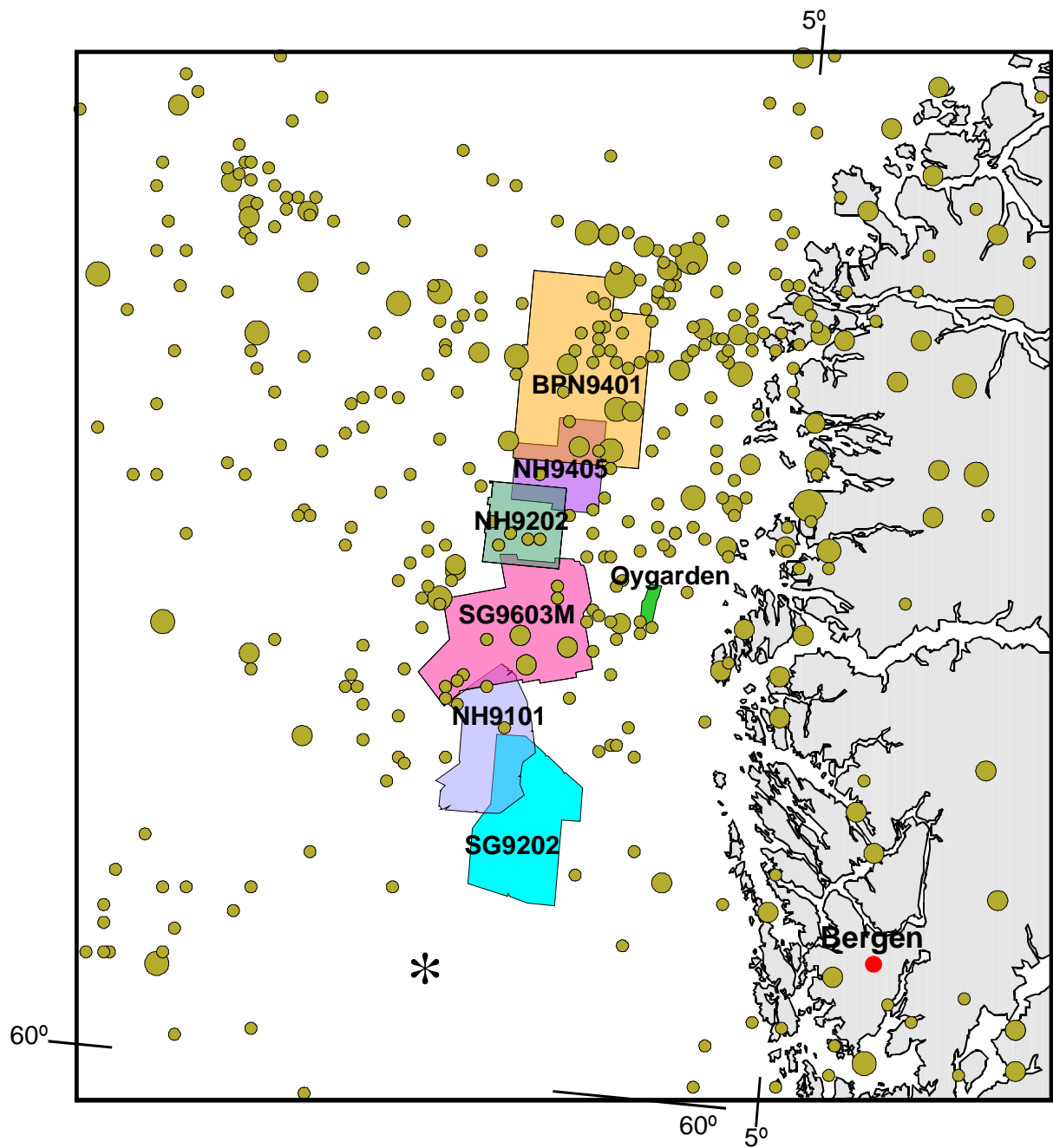
Fig. 3.3.2.   Location of the interpreted 3D surveys in the northern North Sea (SG9202, NH9101, SG9603M, NH9202, NH9405 and BPN9401). Interpretations of the latter four surveys are presented in the present report. Riis (1998) has reported the results from the SG9202 and NH9101 surveys. The area of the multibeam echo-sounding survey (Rise et al. present volume) across the Øygarden Fault Zone is shown with dense green colour. Locations of earthquakes (yellow circles) are provided by NORSAR. The star (*) shows the location of the postglacial faulting reported by Hovland (1983) to the SW of the SG9202 survey.

3.3.3 Northern North Sea

Study area and stratigraphy

The study area (Fig. 3.3.2) consists of four 3D surveys and covers the blocks 35/6, 35/9, 35/11, 35/12, 36/4 and parts of adjacent blocks. The thickness of the Quaternary sediments increases from 200 ms. in the southern and central survey area to 400 ms to the northeast (beyond the eastern slope of the Norwegian Channel). The Quaternary stratigraphy from well 31/6-U-21 (Sejrup *et al.* 1995) has been adapted in the interpretation of the 3D seismic surveys. The well is situated in the Troll gas field within the 3D survey SG9202 that was interpreted by Riis (1998). The stratigraphy can be traced from this southernmost survey through the five other interpreted 3D surveys in the northeastern North Sea. The lithologies consist of alternating glacio-marine sediments and tills. The lowermost till is lying on top of the base Quaternay unconformity and represents an age of 1.1 Ma. (Sejrup *et al.* 1995).

Seismic interpretation

The glaciomarine sediments which were deposited in the time period between the two major glaciations at 0.6 and 1.1 Ma are characterised by continuous, parallel reflectors with moderate to low amplitudes (Riis 1998). The reflection patterns of the tills are more variable, often with irregular, high amplitude reflectors defining the boundaries and with an interior of low reflectivity or chaotic reflections. The top surfaces of the tills have an irregular morphology. Time slices and reflectors from the bases of the tills typically show a pronounced linear pattern of grooves (Figs. 3.3.3-4 and Enclosure 3-4). The direction of the grooves indicates the movement direction of the glaciers. The grooves of the base Elster till (Mid-Pleistocene age) are typically E-W to ESE-WNW in the southern part of the survey area (SG9603M on Enclosure 3-4). These grooves were most likely formed by a glacier flowing out of the Sognefjorden due east of this area. The trend of the grooves rotates gradually to N-S in the northernmost survey area (BPN9401). This N-S trend is also found in the westernmost part of the survey area and is representing the direction of the Norwegian Channel ice stream. The Base Elster reflector is the most distinct reflector within the Quaternary sedimentary sequence and can be traced as a reference horizon through all six 3D surveys. It is important to note that its age is approximately 0.5 Ma, and thus it is 50 times older than the late-glacial sediments (9.000-10.000 years old) in northern Fennoscandia which are cut by numerous postglacial faults with throws that reach 30 metres.
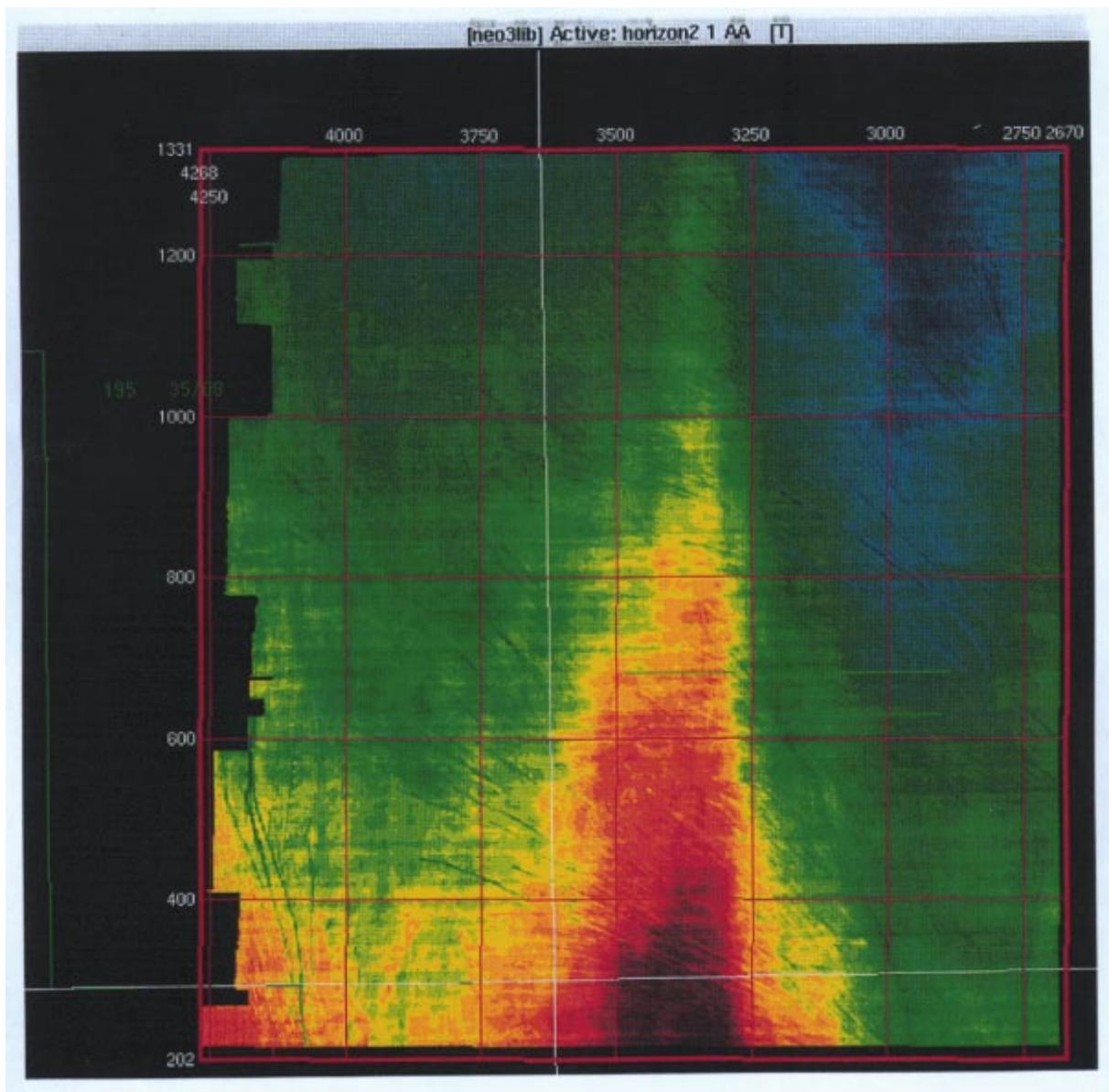
Fig. 3.3.3.   Map of Horizon 2, NH9202. Several sets of ice scouring are observed. The seismic example in Fig. 3.3.4 is from the south-western corner.
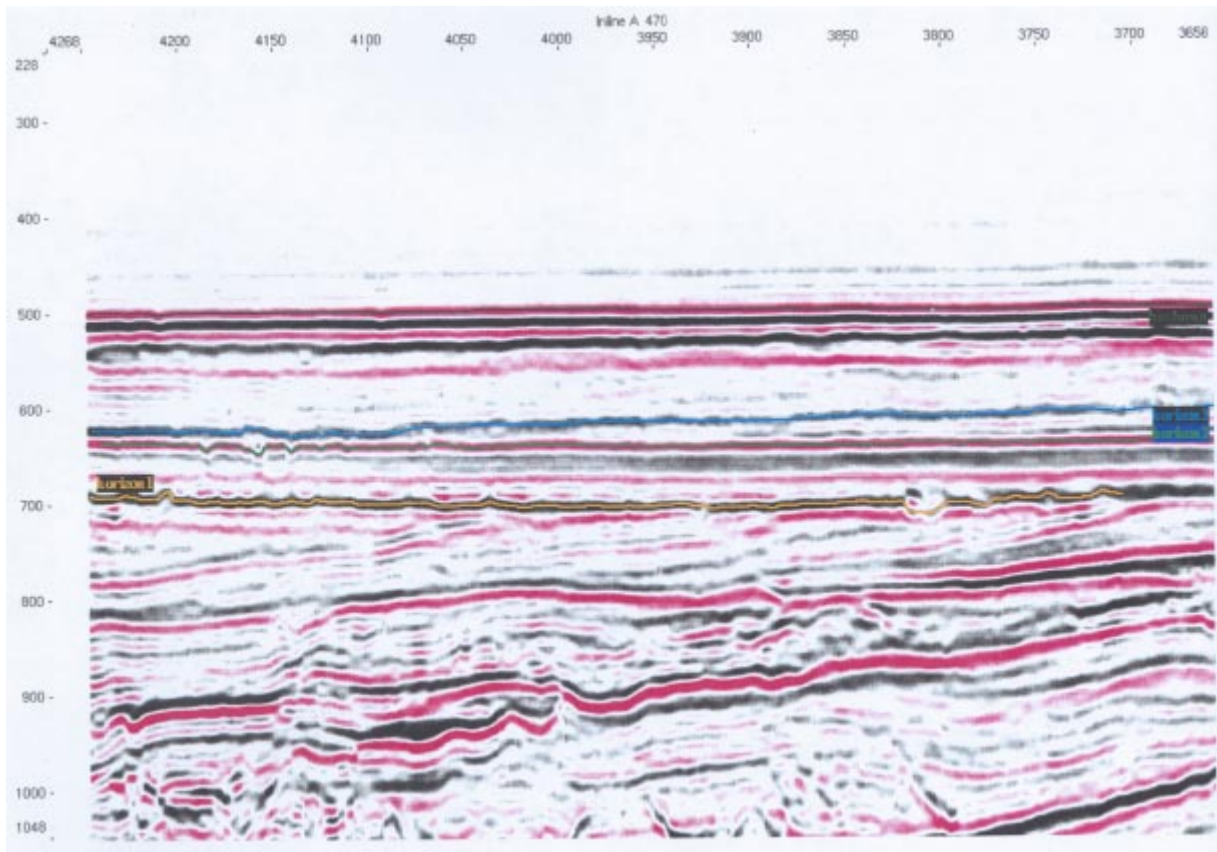
Fig. 3.3.4.   Seismic expression of scour marks (sp 4050 - 4200).
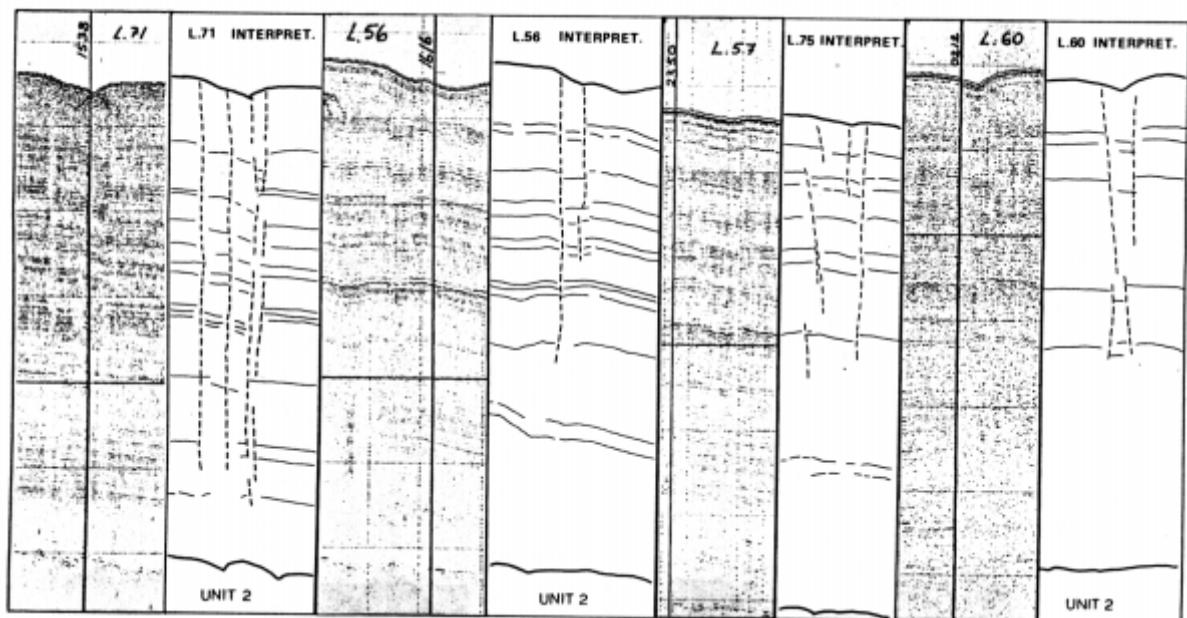
Fig. 3.3.5.   Example of postglacial faulting of a soft, silty clay at the foot of the western slope of the Norwegian Channel (Hovland 1983). A total of nine parallel boomer profiles have been acquired along a 2 km wide corridor as part of the Statpipe route survey. The net slip of the vertical fault is in the order 1-2 m (Hovland 1983). The fault is trending N-S (parallel to the slope of the Norwegian Trench) and is evident on nearly all boomer profiles run in the corridor.

Indications of neotectonic movements

1. Previous studies.

Hovland (1983) reported normal faulting of Quaternary deposits on the western slope of the Norwegian Channel (Fig. 3.3.5). The location shown in Fig. 3.3.2 is situated 30 km to the south of the SG9202 survey in the Troll area (i.e. due west of Bergen). The fault zone is trending N-S parallel to the western slope of the Norwegian Channel. The fault zone consists of 2-4 parallel faults with a net slip in the order of 1-2 metres. The interior of the fault zone has partly subsided supporting the interpretation of a normal fault. Studies of 2D exploration seismic surveys have shown that, within the seismic resolution, there are no faults at depth below the shallow faulting indicating that the deformation may be of superficial character. There are no abrupt changes in the thickness of Quaternary sediments across the fault. It is therefore not likely that these young faults are caused by differential compaction in the underlying sediments. Since the slope of the western margin of the Norwegian Trench is gentler than 0.5° it is not probable that the faulting is due to gravity sliding. Hovland (1983) argues that the faulting is associated with release of shallow gas that has been mapped in the Quaternary sediments. It is, however, difficult to conceive that this mechanism alone should cause a 1-2 m offset at the sea floor. A tectonic cause can therefore not be ruled out. Release of gas could be linked, however, with tectonic movement.

The area investigated by Hovland is situated south of the Kvitebjørn field. A brief study of the 3D seismic on the field indicated north-south trending lineaments within the Pleistocene section. The lineaments may be correlated with the faults observed by Hovland.

2. Main study area

Four reflectors have been interpreted: "Base Quaternary" (Horizon 1), base of the Elsterian glacial wedge (Horizon 2), top of the Saalian glacial wedge (Horizon 3), and Seabed. The horizons are shown on Fig. 3.3.5 and each horizon is described below (mainly NH9202 survey).

The seismic resolution is controlled by the sampling interval of the 3D seismic data of 4 ms. This implies that faults with throws smaller than approximately 2 m in the Quaternary overburden will be difficult to identify. The postglacial faults in northern Fennoscandia have vertical throws up to 30 m and 5-10 m high fault escarpments are common (Kujansuu 1964, Lagerbäck 1979, Olesen 1988). Faults with a comparable size have not been observed in the studied area. Such features would easily be recognised on the interpreted seismic reflectors.

Subtle linear features have been identified by inspection of time slices and the maps on the base Elster level (Fig. 3.3.6). They seem to be more common in the northern and southern parts of the study area (surveys BPN9401and SG9202). Many lineaments are artefacts or caused by draping or pull-up effects. Lineaments that are considered to be of possible tectonic origin are plotted in Fig. 3.3.6, which shows the seven interpreted surveys in the study area.
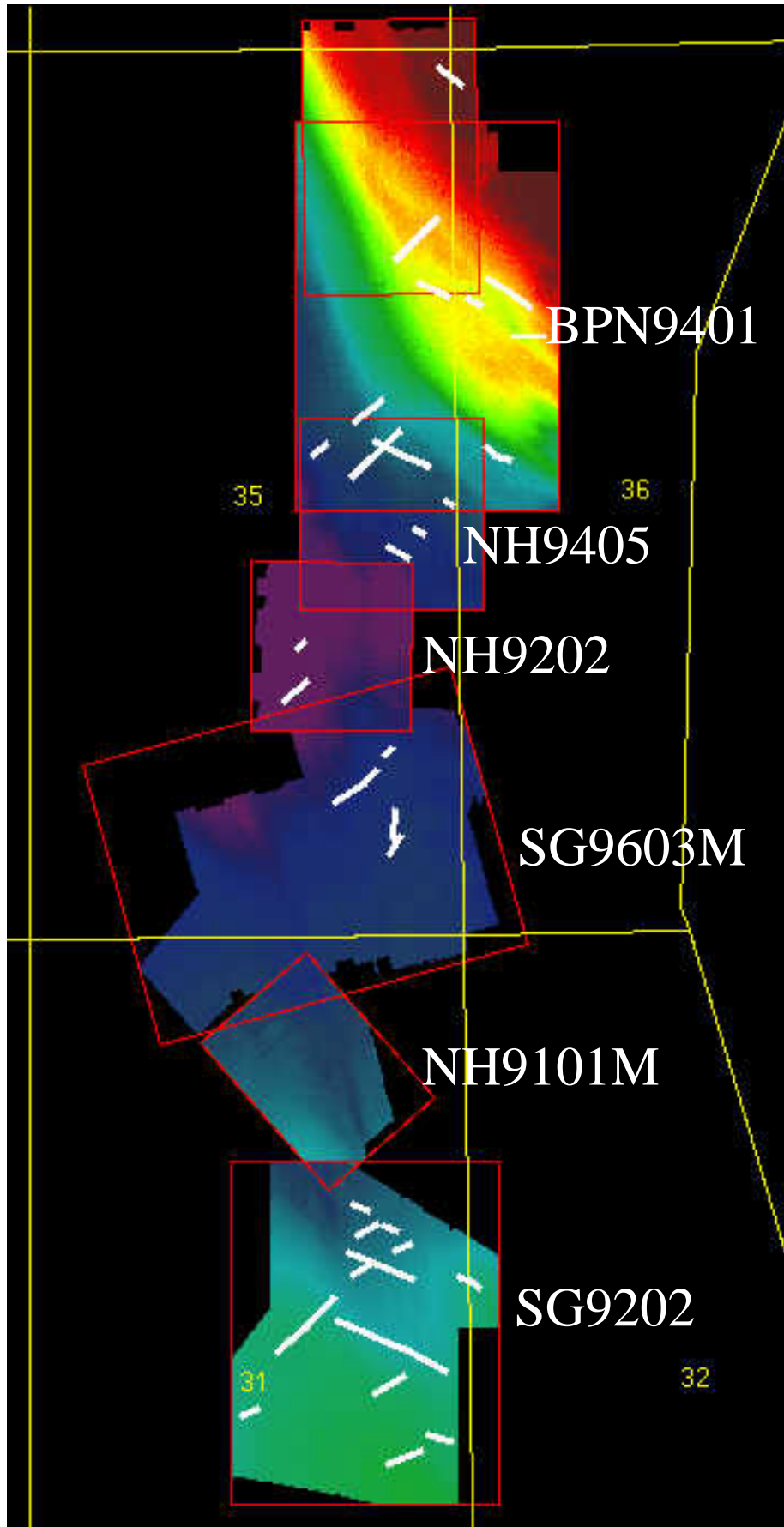
Fig. 3.3.6.   Interpretation of two way travel time to seabed on the 3D surveys in the north-ern North Sea, including the observed subtle lineaments in the lower Pleistocene.

60

Base Quaternary (Horizon 1):

In the western part of NH9202, there is an irregular topography (Fig. 3.3.7 and Enclosure 2), with low and high areas. From the seismic data, we can see that this is most likely to be channels. Whether they are subaerial or submarine/subglacial has not been decided. A seismic example of this is shown in Fig. 3.3.8.

Another striking feature on the base Quaternary map of NH9202 is a north - south trending ridge, most likely caused by a sub-cropping unit of a more competent rock which has resisted the glacial erosion (Fig. 3.3.16). An alternative mechanism for formation of the ridge is compressional deformation prior to the deposition of Quaternary sediments. Since the ridge is coinciding with the sub-cropping Oligocene sandstone, an erosional formation model is favoured. The base Quaternary unconformity is illustrated in Fig. 3.3.7. The ridge is draped by overlying sediments and therefore it forms a positive structure on the maps for the other horizons.
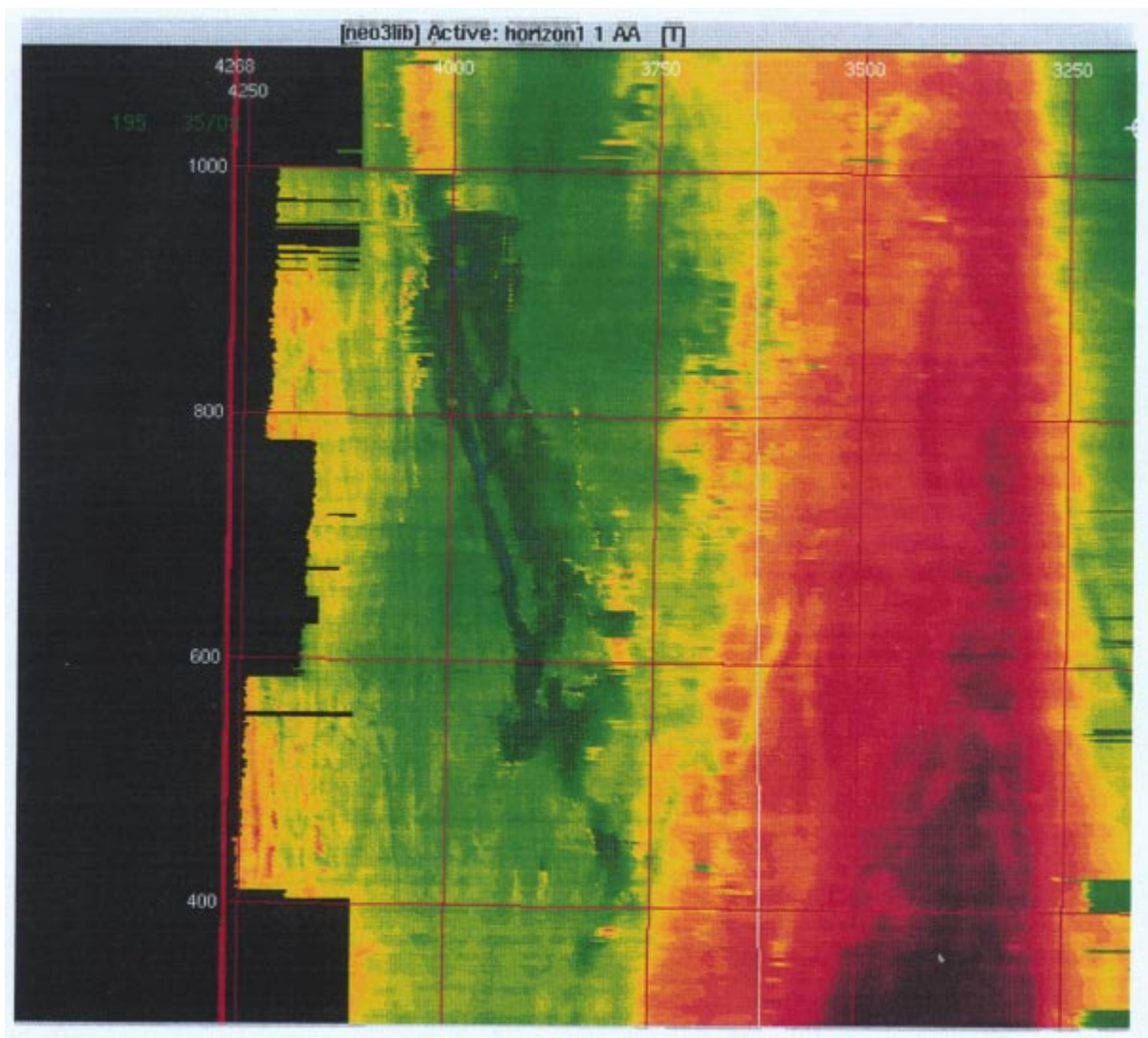
Fig. 3.3.7.   Map of base Quaternary (Horizon 1), NH9202 (eastern part not shown). The dark green area defines an area of channelling. To the right, the erosional ridge is seen.
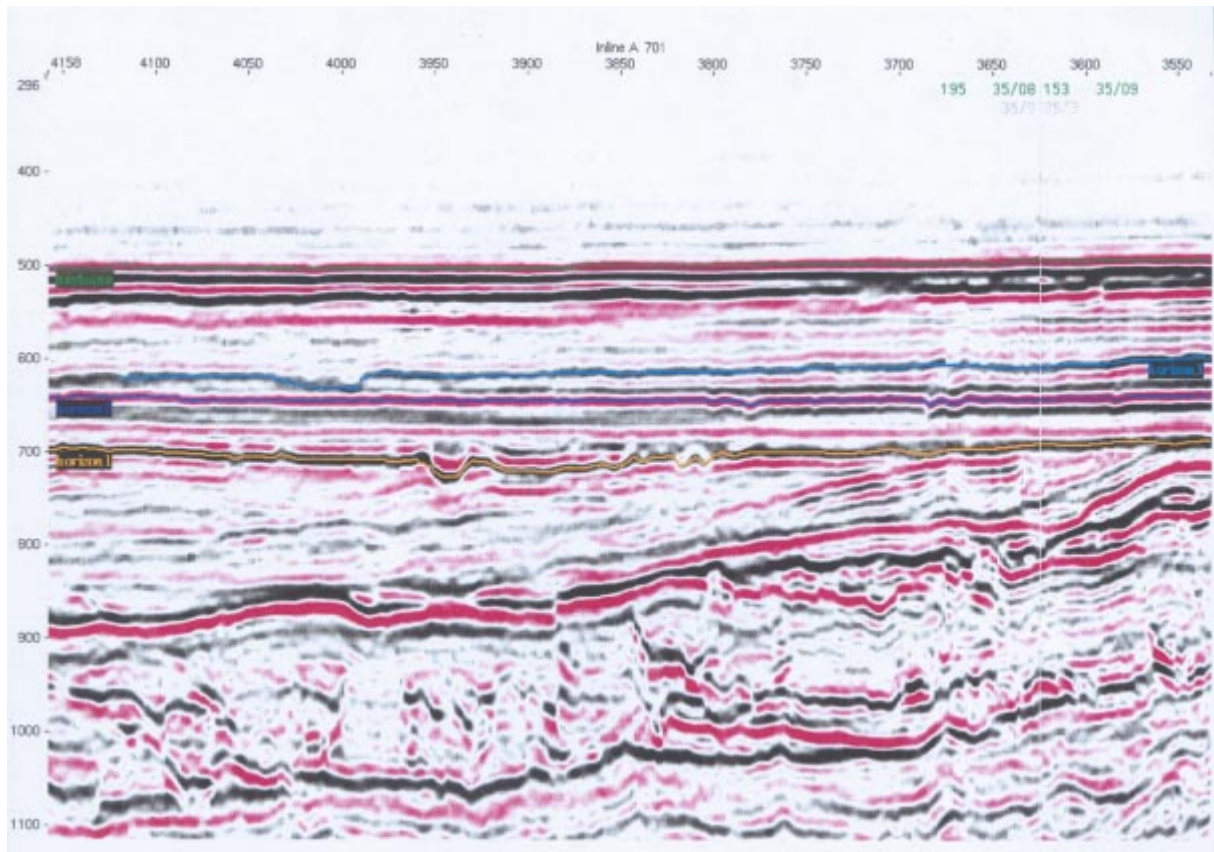
Fig. 3.3.8.   Seismic expression of deep channelling of base Quaternary (Horizon 1), sp 3800 – 3950.

Base Elster (Horizon 2):

Apart from the ridge in the central part of the NH9202 survey (Fig. 3.3.8), the Horizon 2 surface is dominated by the glacially derived scour marks. Several sets of marks are identified, with slightly different directions. All these observations are interpreted to be of glacial origin. On Figs. 3.3.3 and 3.3.4, examples of the scour marks are shown.

A few very subtle NW-SE trending lineaments can be observed in the northeastern part of the survey. Two of these are marked with arrows. No rupture through the sediments is observed, however. The observations are shown in Figs. 3.3.9–12. These lineaments coincide with till drumlins in the overlying sediments and are therefore interpreted as 'pull-up' effects due to a higher seismic velocity in the till as compared with glaciofluvial deposits.

Some NW-SE and NE-SW trending subtle lineaments (Fig. 3.3.6) cannot, however, be attributed to any of the effects listed above, and may consequently represent small scale faulting or flexing similar to the structures reported by Hovland (1983) and Riis (1998).

The mapped subtle lineaments are analogous to those that penetrate the lower part of the Pleistocene in the other surveys in the study area.
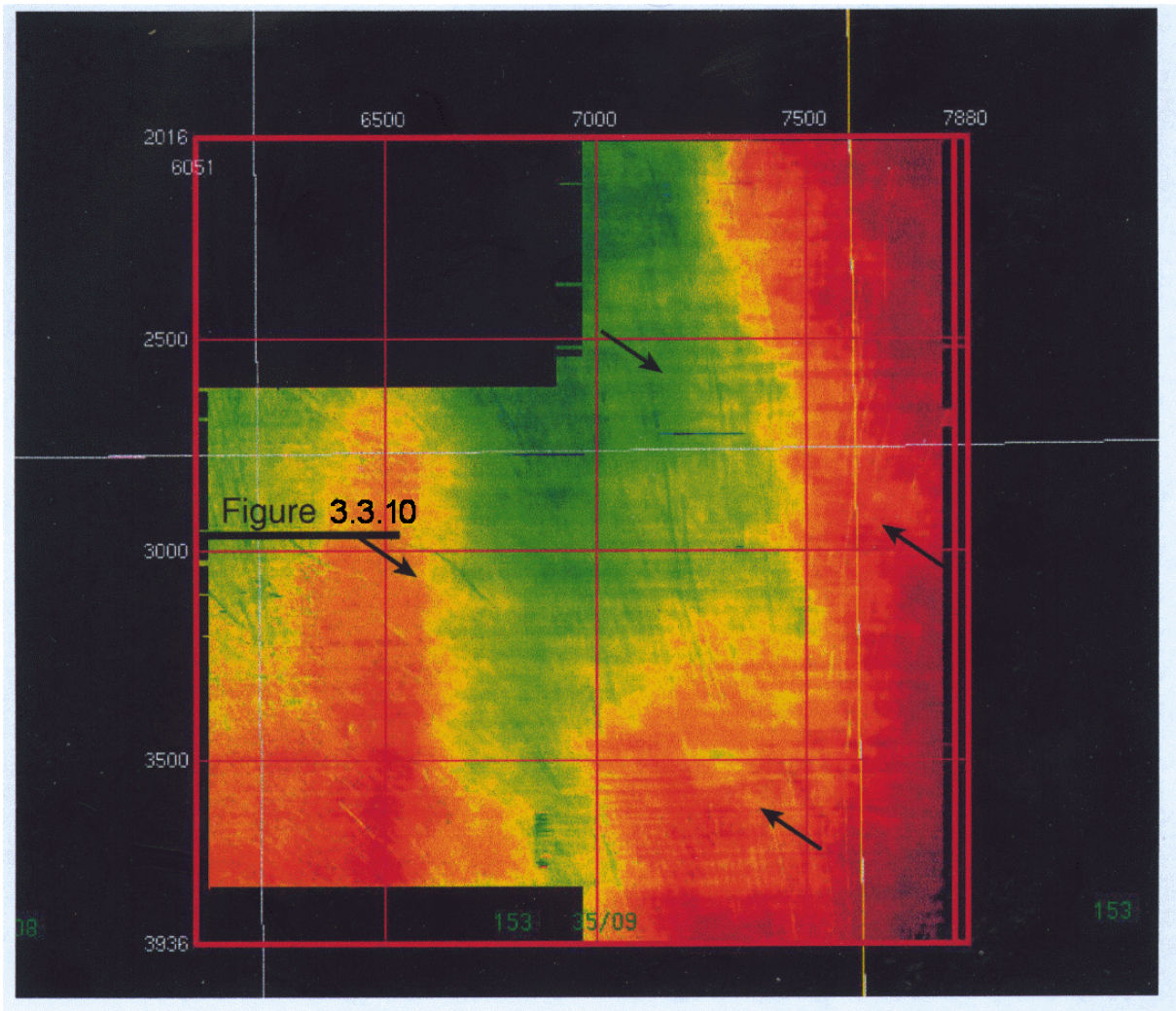
Fig. 3.3.9.   Map of Horizon 2, NH9405. Position of seismic example is indicated . Sets of ice flow trajectories are easily recognised. Arrows point at NW-SE trends that is interpreted to be a 'pull-up' effect of above-lying high-velocity drumlines with a NW-SE trend.
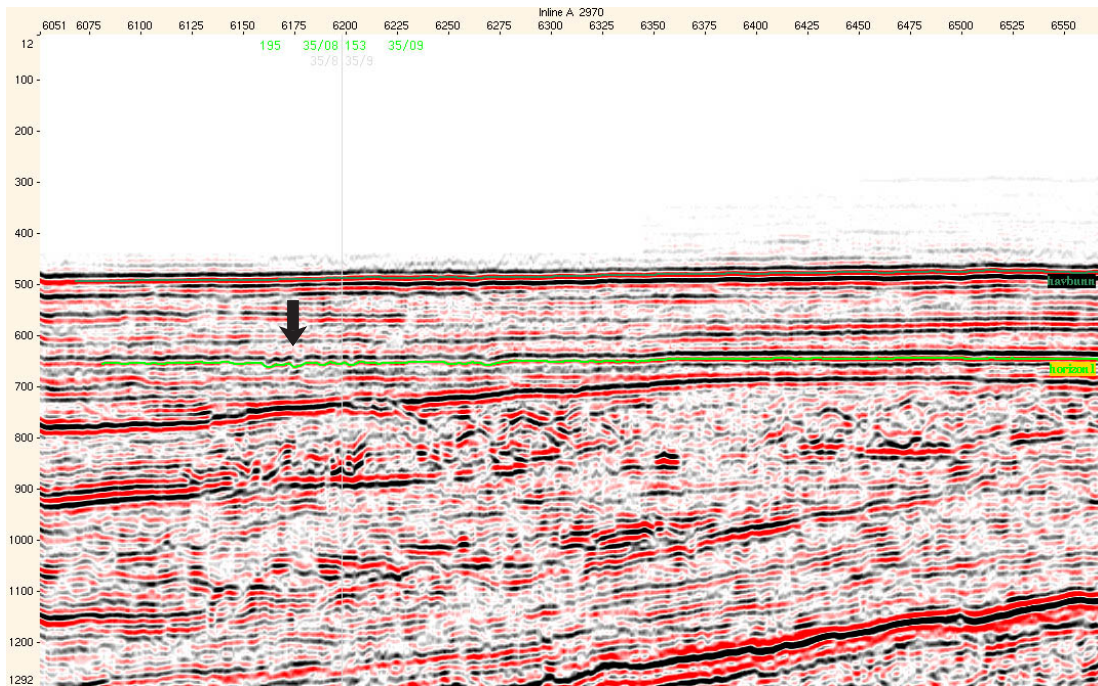
Fig. 3.3.10.   Seismic example of ice scouring of Horizon 2.
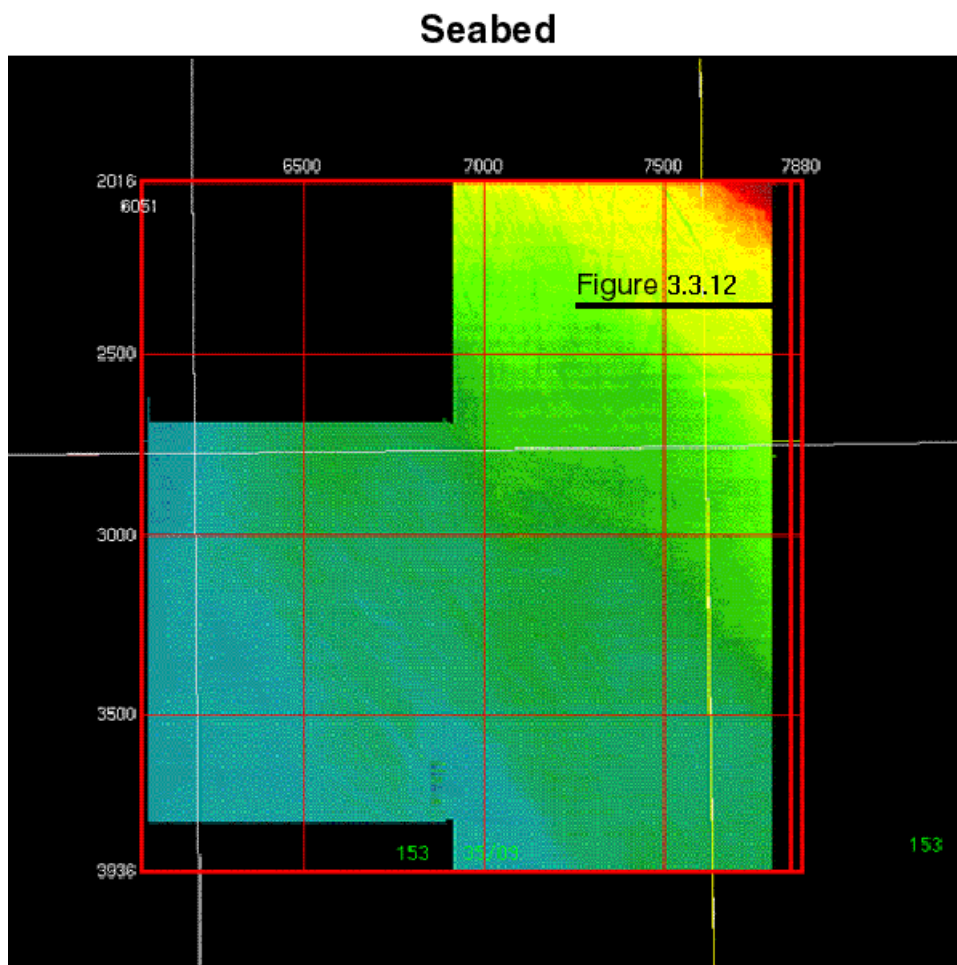
Fig. 3.3.11.   Map of Seabed, NH9405. Position of seismic example indicated.
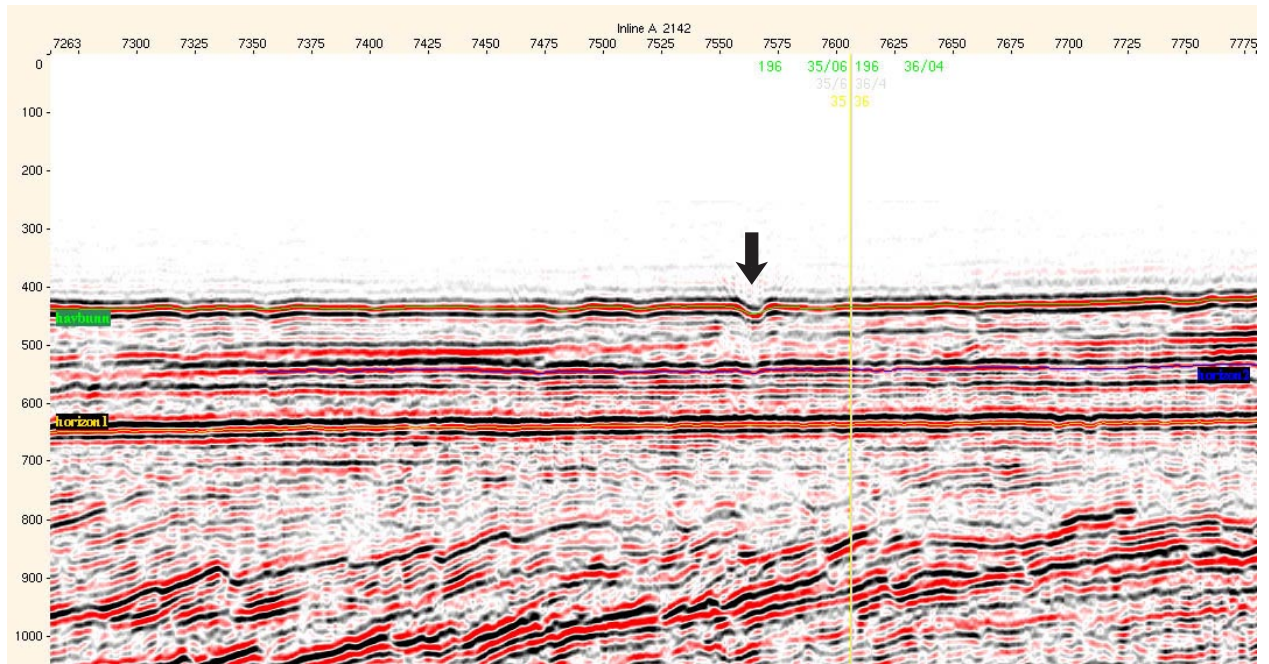
Fig. 3.3.12.   Depression on seafloor caused by ice scouring (plough mark?).

Saale (Horizon 3):

This horizon does not show any signs of scour marks as seen on Horizon 2 (Fig. 3.3.3 and Enclosure 3), which could indicate a more marine influence than for the surface below. The most striking features on NH9202 are some depressions, which could have been caused by either erosion or fluid escape (pockmarks) (Figs. 3.3.13 and 3.3.14).
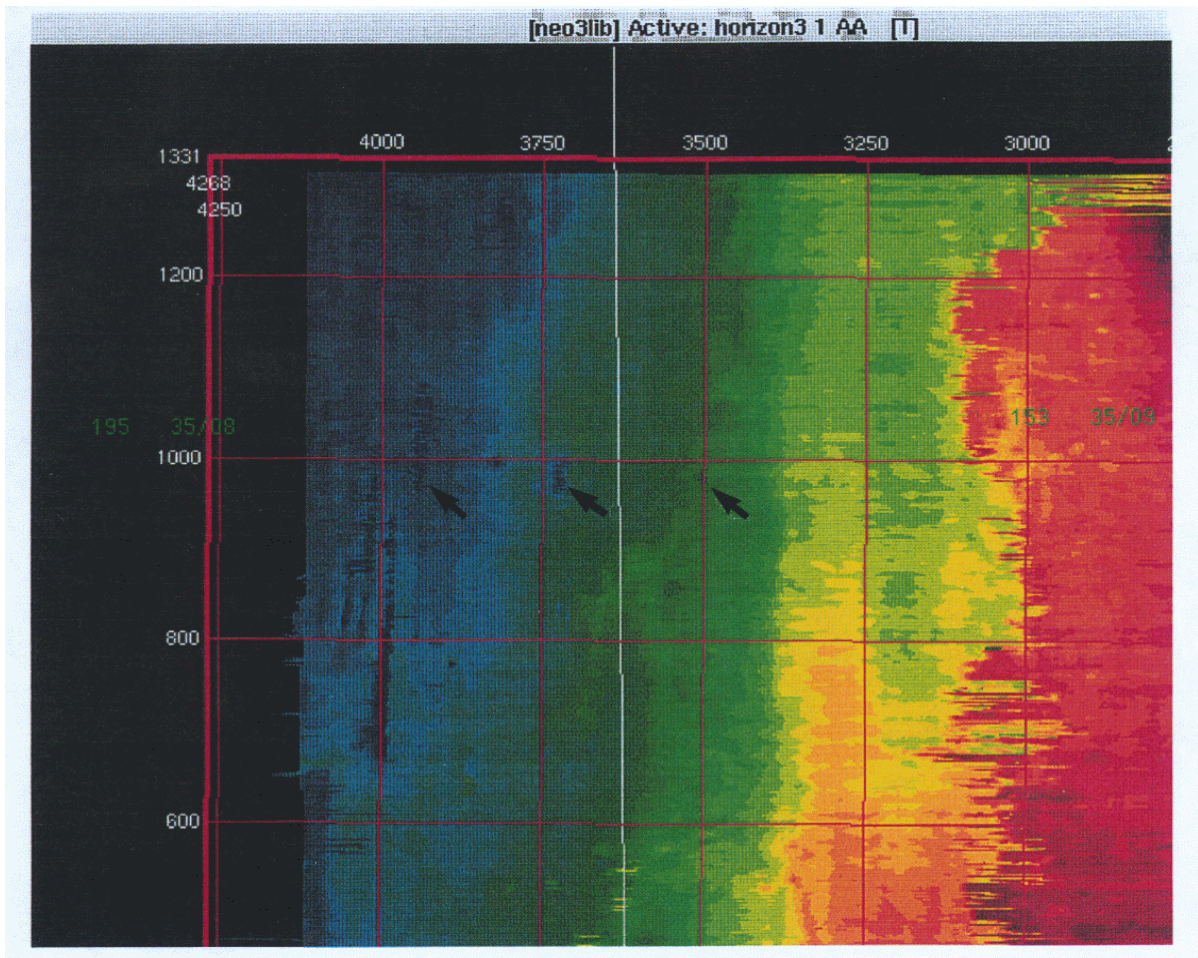
*Fig. 3.3.13.   Map of Horizon 3, NH9202. In the western part (ex. along crossline 4000 be-
tween inline 700 and 900 and at inline 1000/crossline ~3700) some low areas are seen,
probably caused either by erosion or fluid escape. The depressions shown on Fig. 3.3.14 are
marked with arrows.*
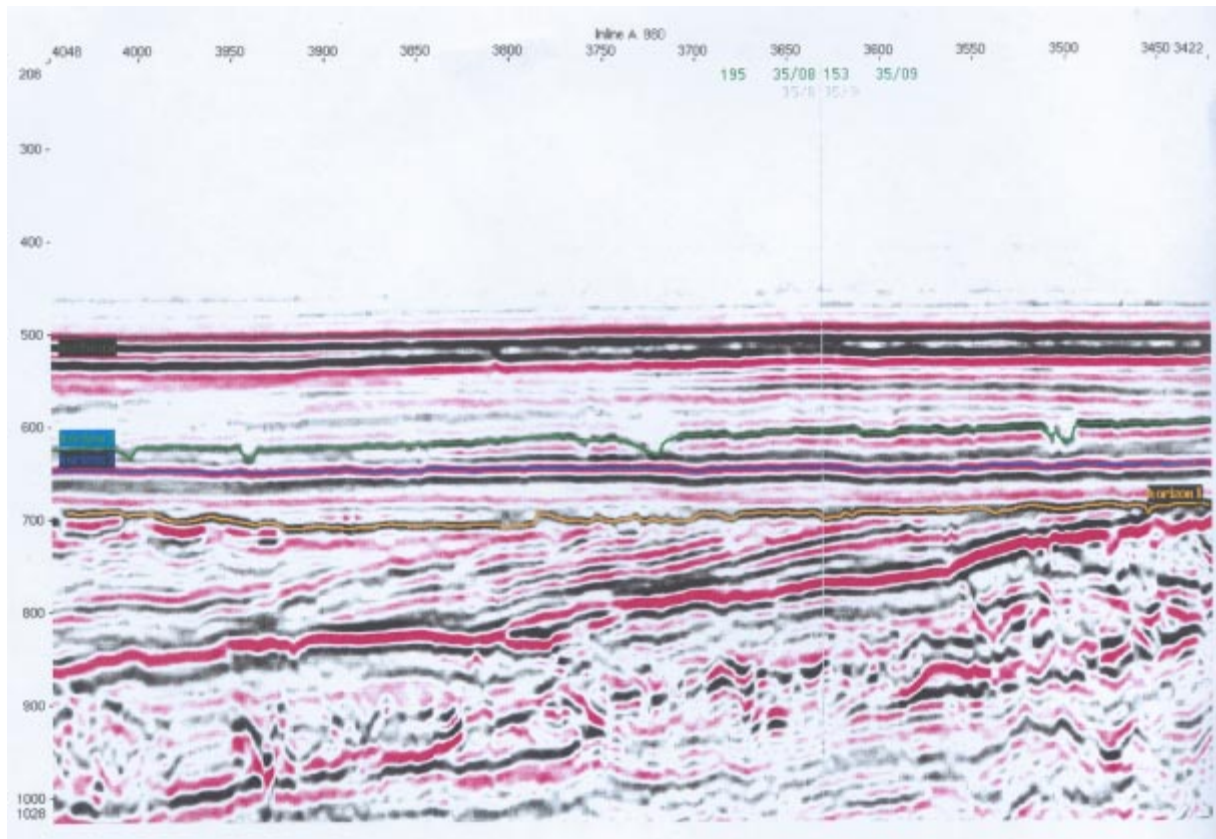
Fig. 3.3.14.   Seismic expressions of the depressions in Horizon 2 shown in Fig. 3.3.13.

Seabed:

A time structure map is shown on Fig. 3.3.15 in addition to Fig. 3.3.6. Occasional ice scouring (plough marks or subglacial scouring) is observed. At approximately sp-3080, a conspicuous north-south lineament is crossing the whole survey. This is a merge effect between NH9202 and a partly overlapping survey from 1989. The effect can also be seen on the seismic example in Fig. 3.3.16.

In the southern three surveys, pockmarks are extremely abundant (Fig. 3.3.17), while they disappear to the north. It is likely that the distribution of pockmarks is related to the gas accumulations in the Troll area.

Relation to deeper structures.

Subtle lineaments were picked on time slices and on the Base Elster map. In the two surveys with more abundant lineaments, the fault pattern of the underlying Tertiary section was interpreted for comparison with the recent. In the SG 9202 survey, an early Cretaceous marker horizon was interpreted to define the fault pattern, while in the northern BPN9401 survey, the Base Tertiary was selected. The fault pattern on these horizons is thought to be representative for the preserved part of the Tertiary section. In Figs. 3.3.18 and 3.3.19, the older fault patterns were derived from the interpreted Cretaceous surface by subtracting a filtered version of the surface from the original interpretation. The Tertiary fault pattern is clearly tectonic in some areas, and NW-SE, E-W and SW-NE trends predominate. Other areas are characterised by hexagonal fault patterns, indicative of dewatering during compaction of the soft sediments.

In the Troll area (survey SG 9202), the Pleistocene lineaments tend to coincide with the Tertiary faults. Possibly, they can also be correlated to clusters of pockmarks (Fig. 3.3.17). In the northern area, there is no simple connection between the older and younger lineaments.

67

Conclusion.

In conclusion, no conclusive observations have been made giving any indication of neotectonic activity that strongly affected the surface in the study area. This indicates that even though the surveys are located in an area of relatively high seismicity, there have been no earthquakes of sufficient magnitude to create easily recognisable surface ruptures comparable to the 5-30 m high fault scarps observed in northern Fennoscandia. There are, however, indications of subtle distortions that could represent fault scarps with heights in the order of 1-3 m, similar to the faults reported by Hovland (1983) discussed above. These subtle faults appear to form a conjugated set with WNW-ESE and WSW-ENE trends.
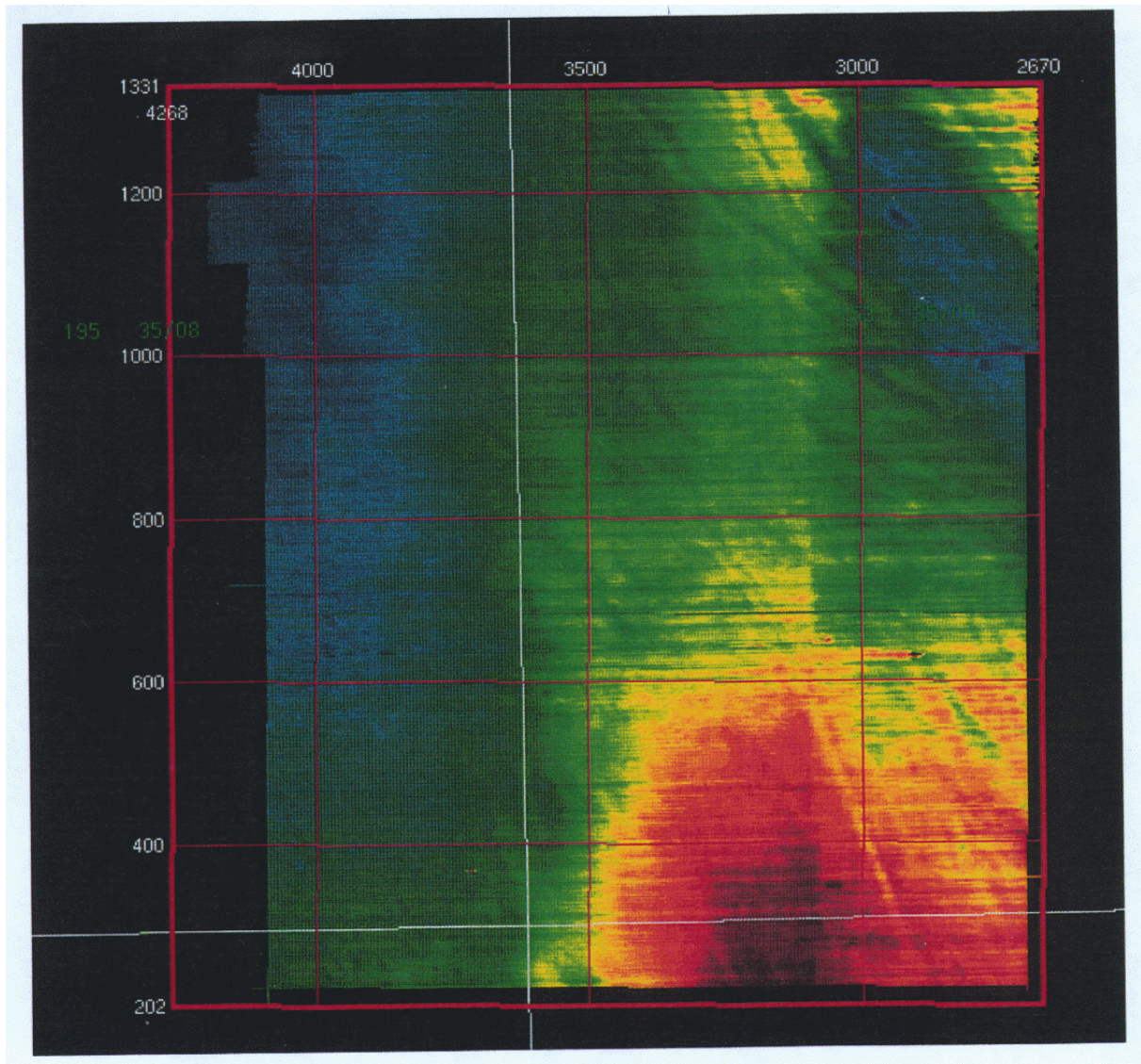
Fig. 3.3.15.   Map of seabed, NH9202. The north south lineament at ~sp 3100 is reported to be a merge effect between the NH9202 survey and an older survey.

68
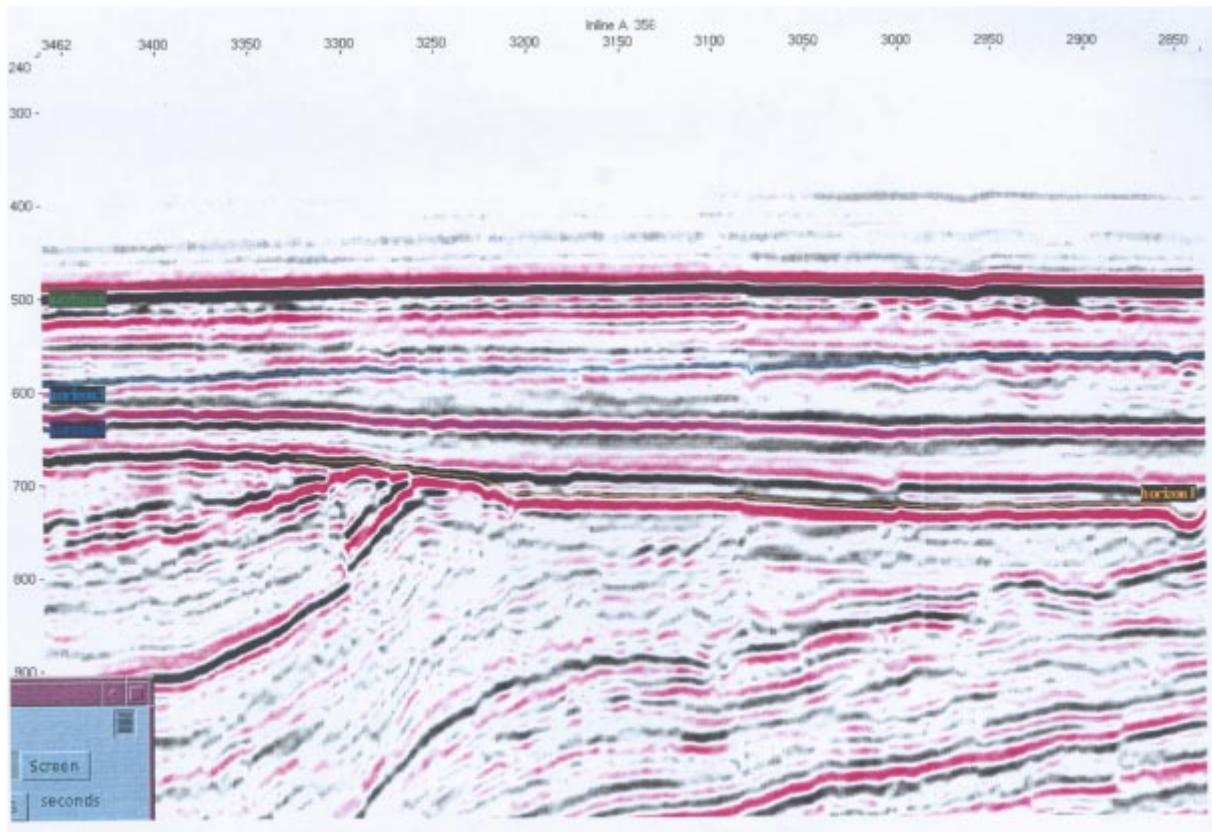
Fig. 3.3.16. Definition of the four interpreted horizons. To the left, the Quaternary erosional ridge is seen. At ~sp3080, the effect of a merge between the NH9202 survey and an older 3D survey from 1989, partly overlapping the NH9202 survey, is seen in the central part of the section.
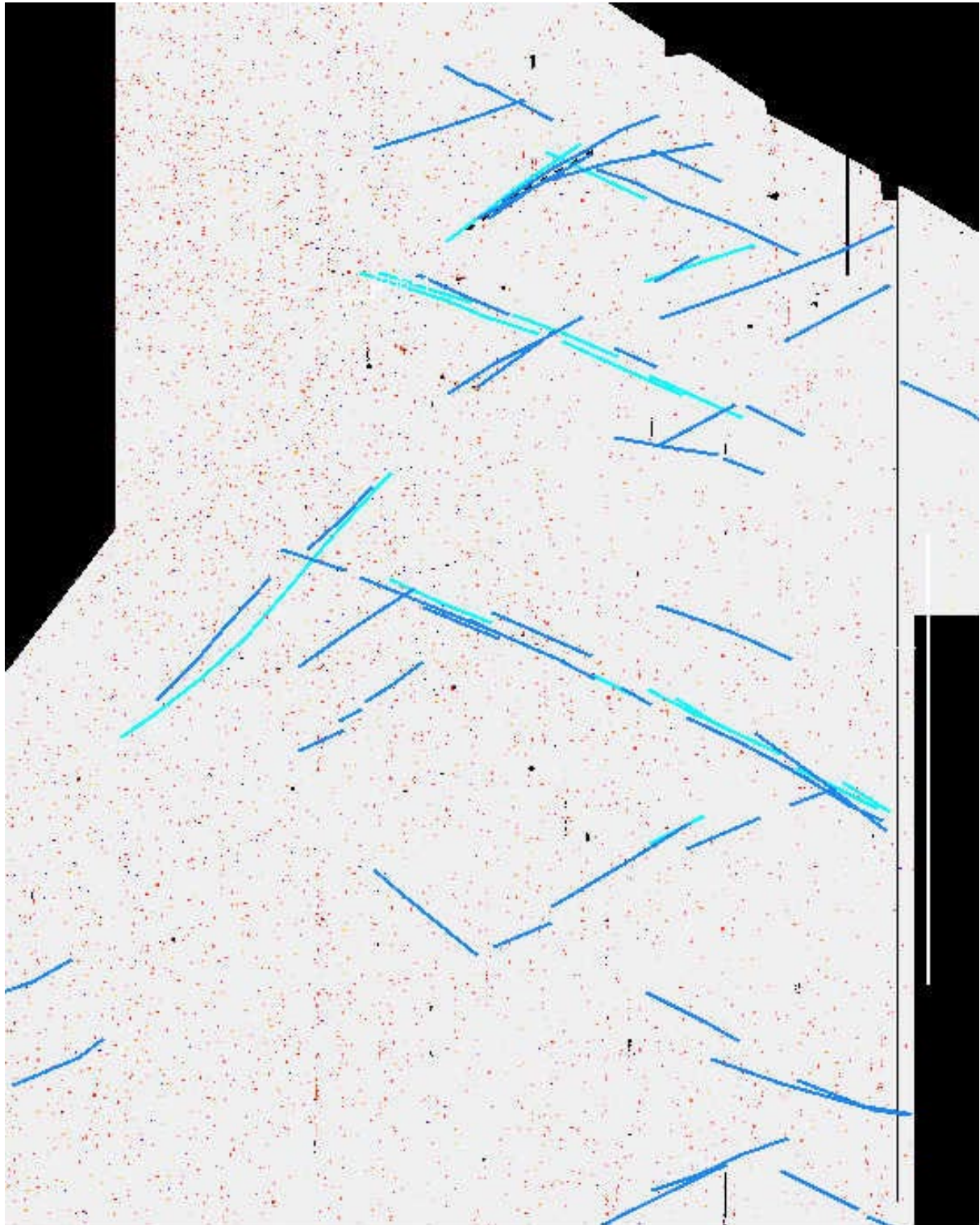
Fig. 3.3.17. Depressions in the sea floor, SG 9202 survey. The small red spots are inter-preted as pockmarks. Some linear features are caused by ice-berg ploughing and by static shifts between seismic lines. The strong concentration of pockmarks in the north-west coin-cides with the large fault shown in Fig. 3.3.19. The Pleistocene lineament in the central part of the map apparently correlates with an increased abundance of pock marks.
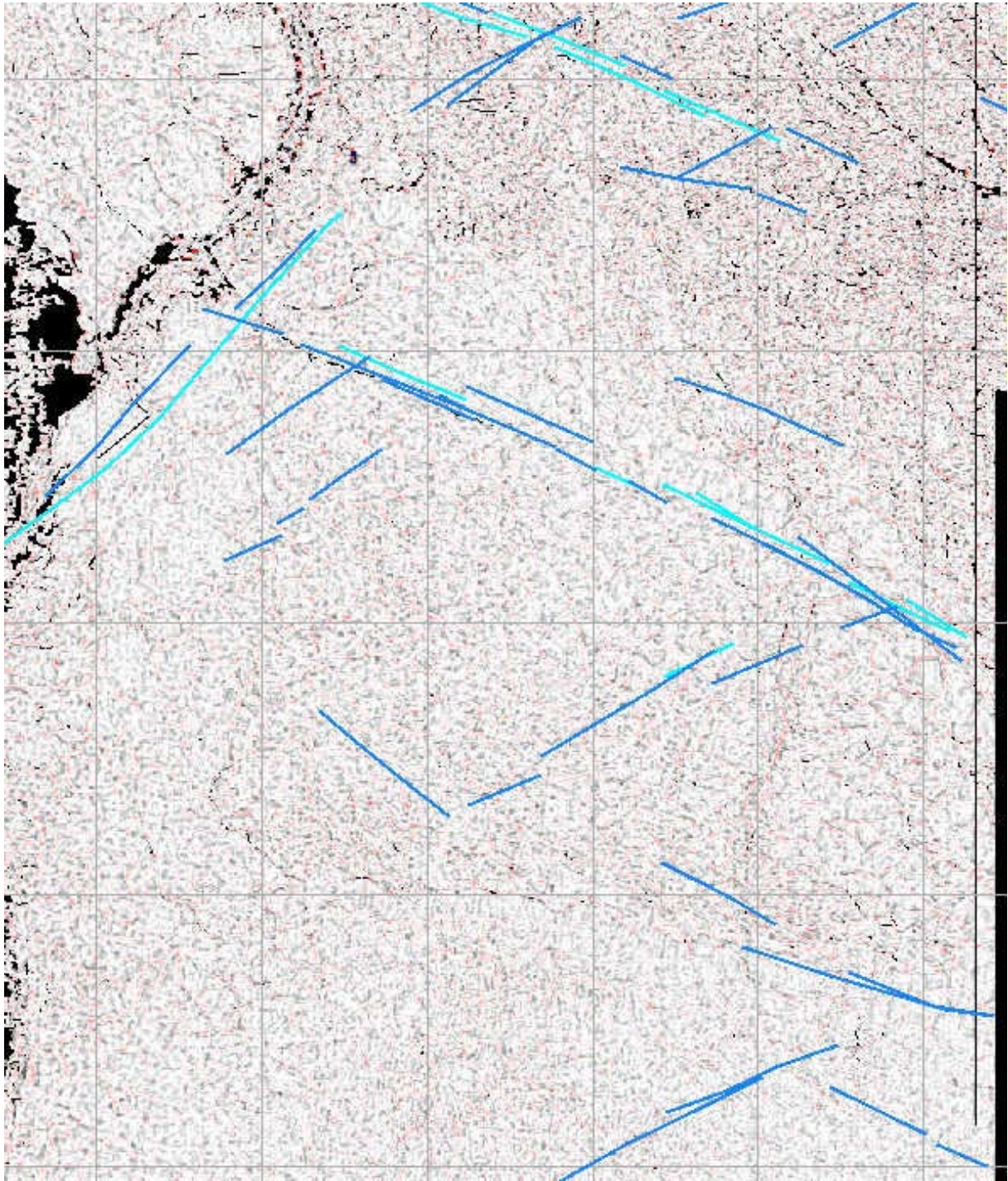
Fig. 3.3.18.   Tertiary fault pattern, BPN 9401 survey. Pleistocene lineaments are shown with blue colours. Note more hexagonal patterns to the west.
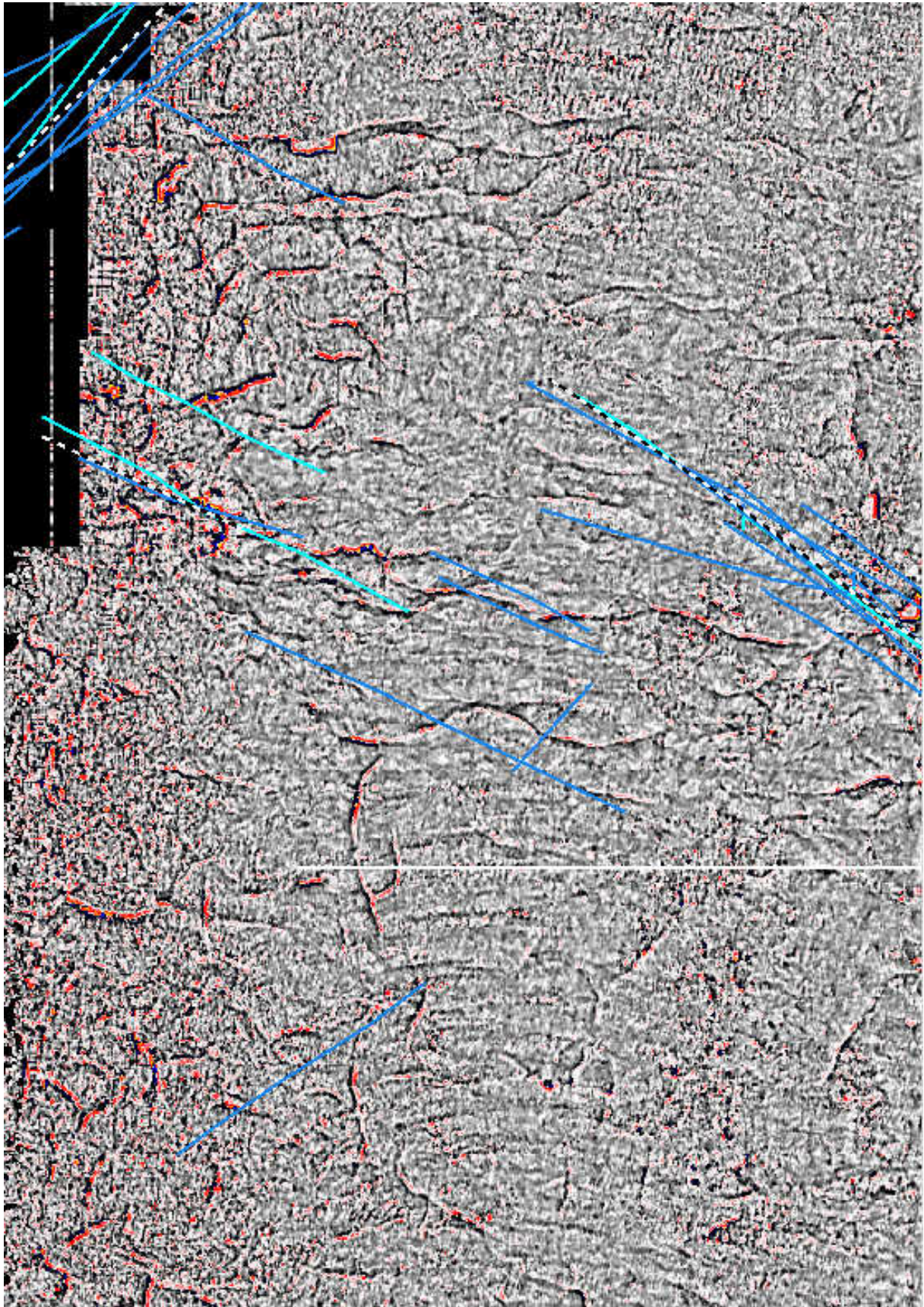
Fig. 3.3.19. Tertiary fault pattern in the central part of SG 9202 survey, Troll East. A large fault in the western part of the map trends NS and NE-SW, minor faults trend WNW-ESE. Hexagonal fault patterns occur throughout. Pleistocene lineaments, shown in blue, coincide with the WNW-ESE trending faults.

3.3.4   Nordland II and VI areas

The Plio-Pleistocene stratigraphy of the area consists of a Late Pliocene – Early Pleistocene prograding, glacially derived unit and a Mid/Late Pleistocene blanketing diamicton (King *et al.* 1987, Henriksen & Vorren 1996 and Eidvin *et al.* 1998). The latter unit is approximately 300 ms thick in the Norne area (ST9203 survey) while these sediments are thin or absent in the Nordland VI area to the north (NH9604 survey).

NH9604

The NH9604 survey is located in the Nordland VI area and covers mainly block 6710/6. In contrast to the northern North Sea and Nordland II areas, the Quaternary cover is thin or absent, and no intra Quaternary horizons were possible to interpret. In addition, the data quality of the upper interval is rather poor, due to hard sea-bottom that causes high amplitudes, low frequency reflections and poses severe multiple problems. The only horizon to be mapped throughout the survey area was therefore the seabed, and even this surface was not straight-forward to interpret by automatic interpretation methods.

The seabed map (Fig. 3.3.20) shows several features that need closer investigation. The most striking is the formation of a large depression in the bedrock surface in the northeastern corner of the 3D survey. This cavity is part of the Vesterdjupet Deep offshore Værøy (one of the two outermost islands within the Lofoten Archipelago). By investigating the seismic data (Fig. 3.3.21), it is clear that this depression has a glacial origin, and not a tectonic.

By compressing the colour table for the map, other features appear more visible (Fig. 3.3.22). First, there is a north-south set of features, which parallels the inline direction. This is believed to be an acquisition or processing effect, and is not given any attention in this report.

Another set of features runs in a northeast - southwest direction. A seismic line across one of these trends (Fig. 3.3.23) shows a gentle ridge on the seafloor, with the amplitude of approximately 10 ms. The ridge happens to coincide with the continuation of a deeper fault. The fault seems to have caused a rupture through the shallow sediment layers, indicating a late movement of the fault. Closer inspection of dip maps and several parallel profiles reveal, however, that the ridge is not parallel to the fault, but has a slightly different direction and is most likely of glacial origin.

Three other indications of postglacial faulting are shown in Figs. 3.3.24-27. Below the glacially eroded trough in the northeast, another fault causing a seabed event can be observed (Fig. 3.3.24). A more careful study of the seismic data does show, however, that these features are related to erosional features at the sea floor and are consequently not effects of tectonic deformation.

In spite of the seafloor multiple problem, the quality of the data is sufficient to exclude the possibility of major neo-tectonic faults. More subtle trends cannot be excluded, as shown on the time slice in Fig. 3.3.28. The timeslice intersects the base Quaternary unconformity in the southwest and a Mesozoic unconformity in the north. A small fault in the section above the Mesozoic unconformity is truncated by the base Quaternary unconformity. A subtle lineament in the continuation of the fault indicates a reactivation in the Pleistocene (arrow).
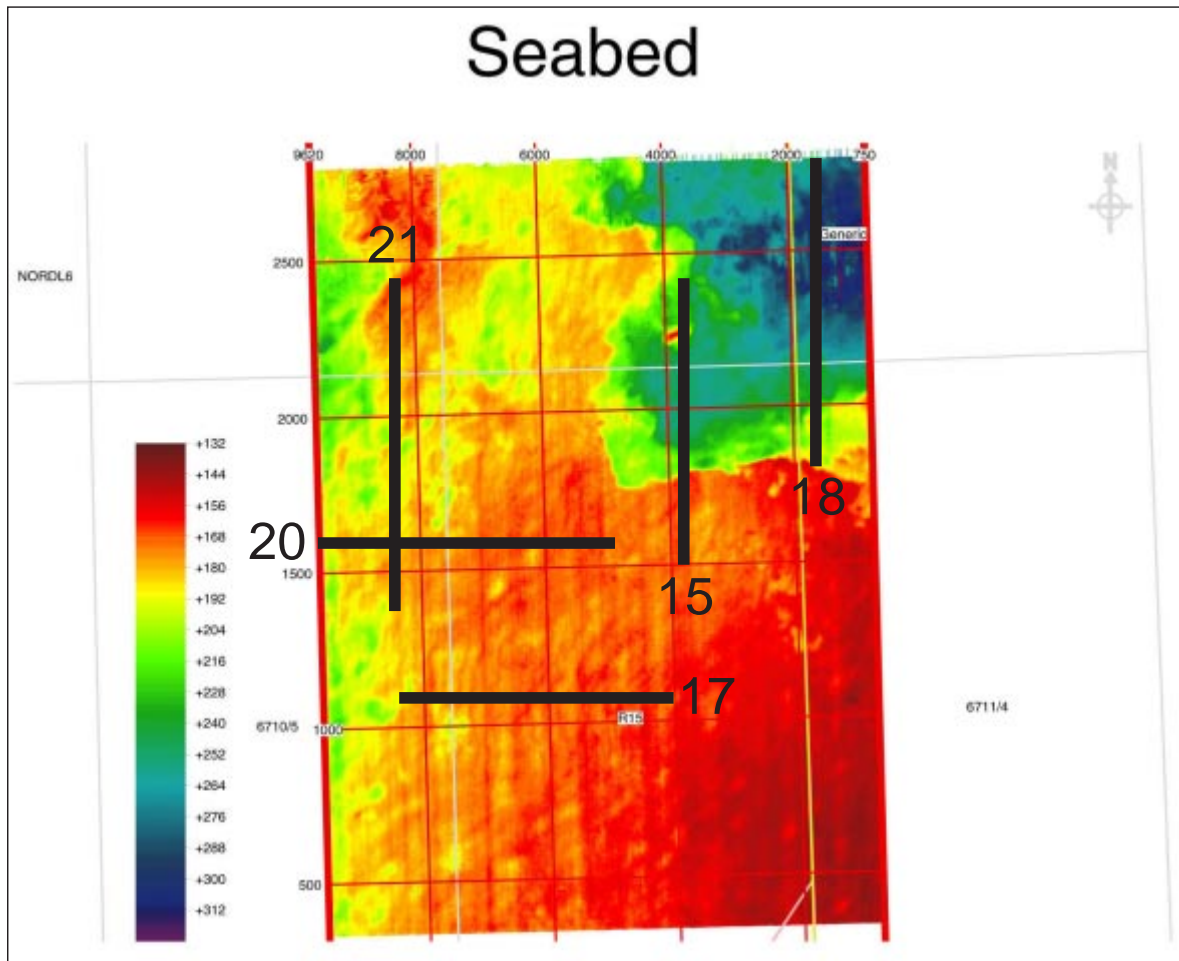
Fig. 3.3.20.   Map of seabed, NH9604, in the Nordland VI area. The glacially eroded sediments appear as a striking depression in the north-eastern corner. Positions of seismic profles shown in the subsequent figures are indicated.
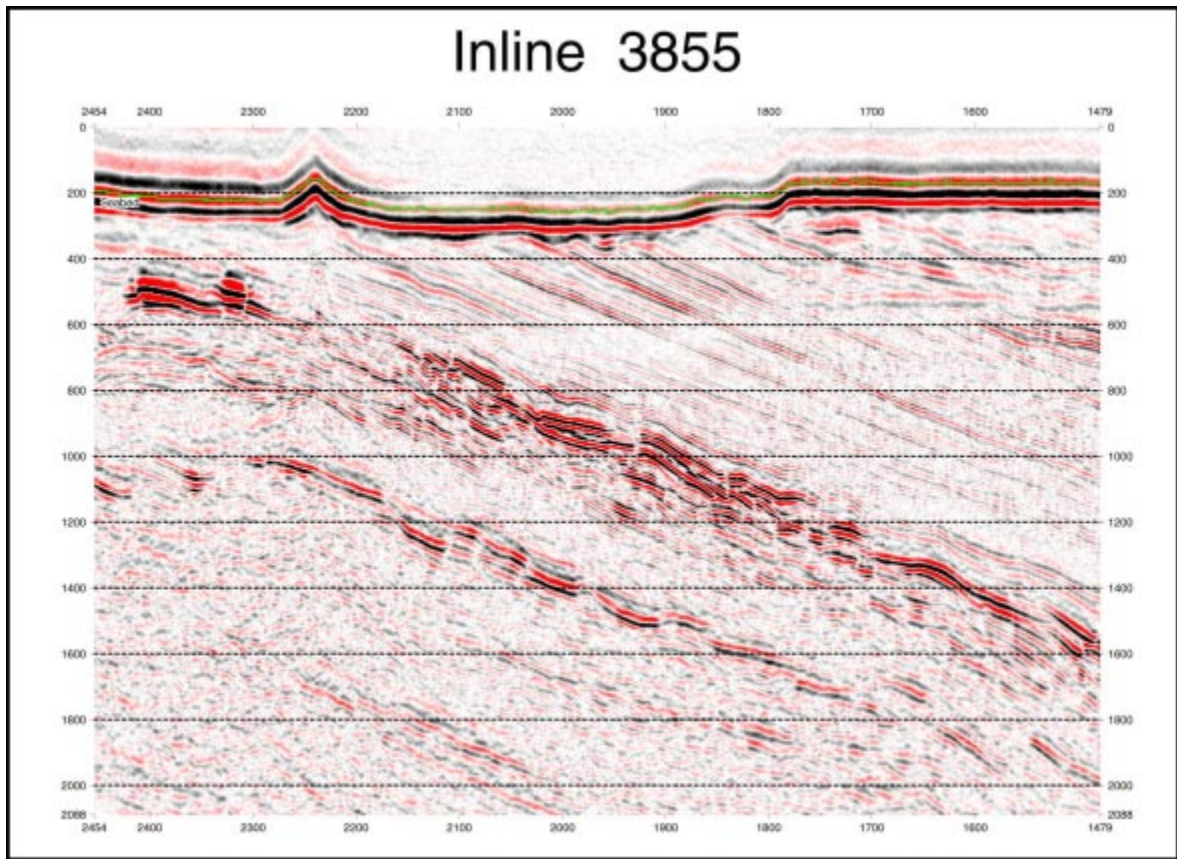
Fig. 3.3.21.   Seismic example of glacial erosion, profile 15 in Fig. 3.3.20. No connection to deeper faulting is observed.

Seabed
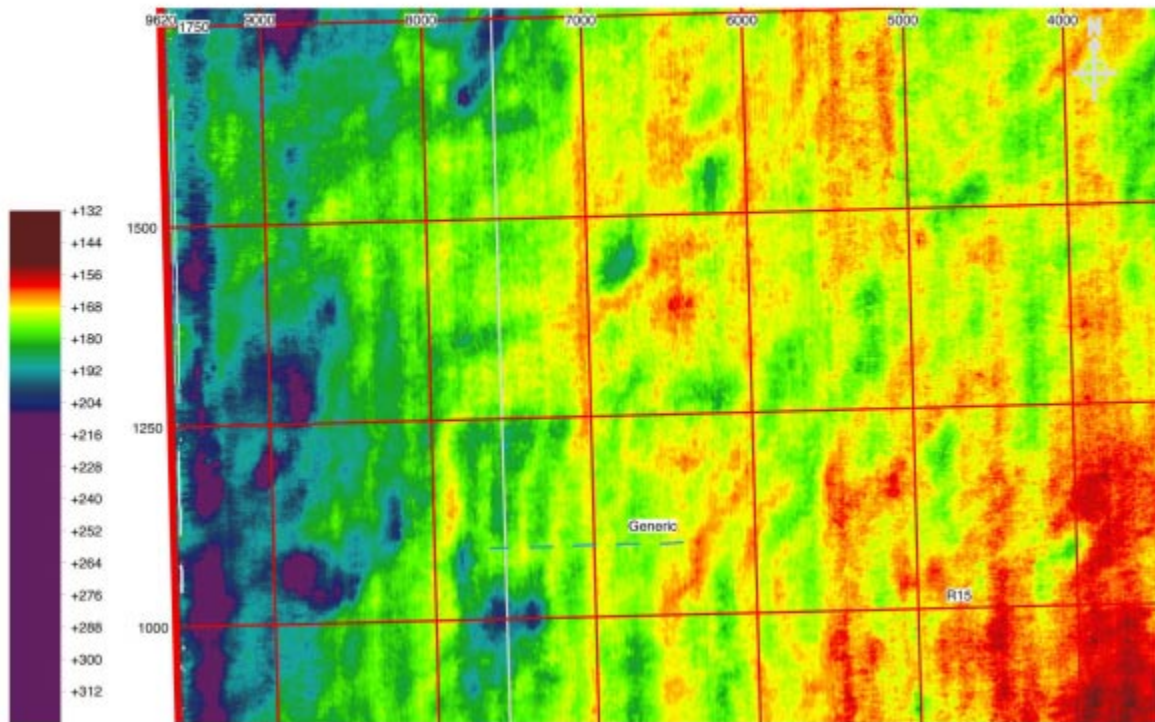
Fig. 3.3.22.   Close-up of the central part of the 3D survey, with compression of the colour table applied, in order to enhance some of the subtle features. Some north - south trends (probably caused by acquisition or processing) and some northeast - southwest trends (of erosional origin) are observed.
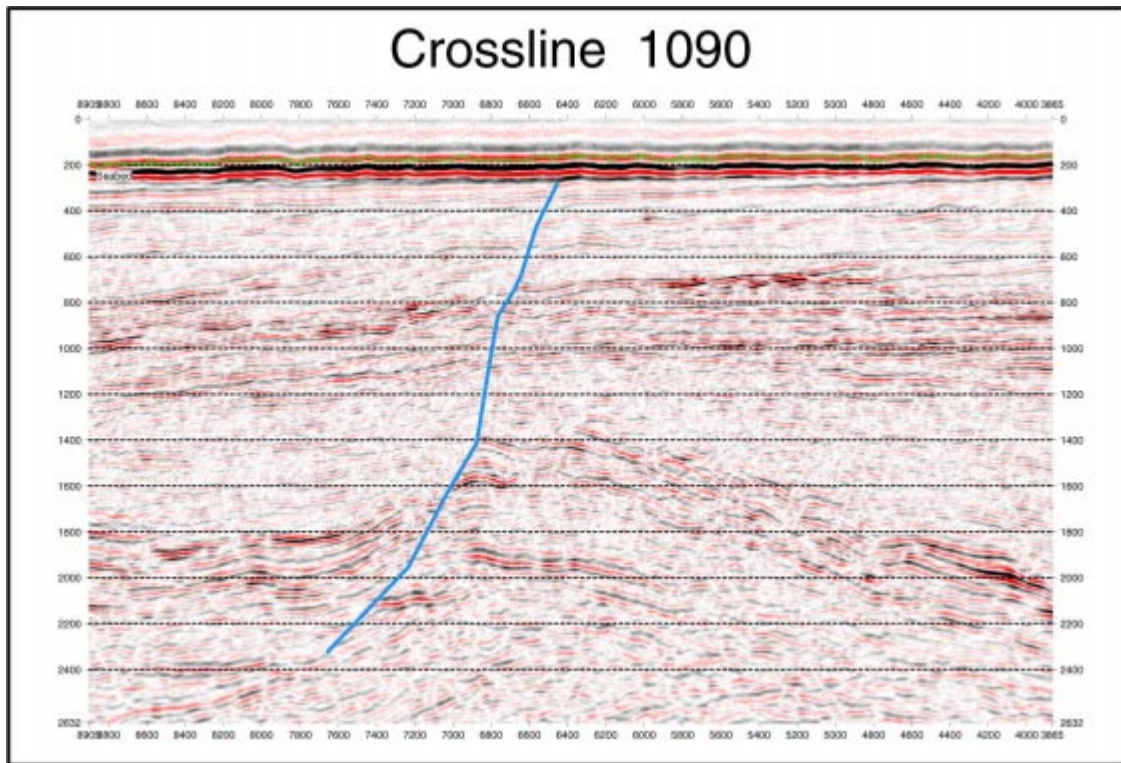
Fig. 3.3.23.   Seismic example of a deeper fault that appear to have a connection to seafloor, profile 17 in Fig. 3.3.20 (position where the 'generic' fault is seen on the map). Closer in- spection of the data has, however, revealed that the ridge is not parallel to the fault and is most likely an effect of glacial erosion.
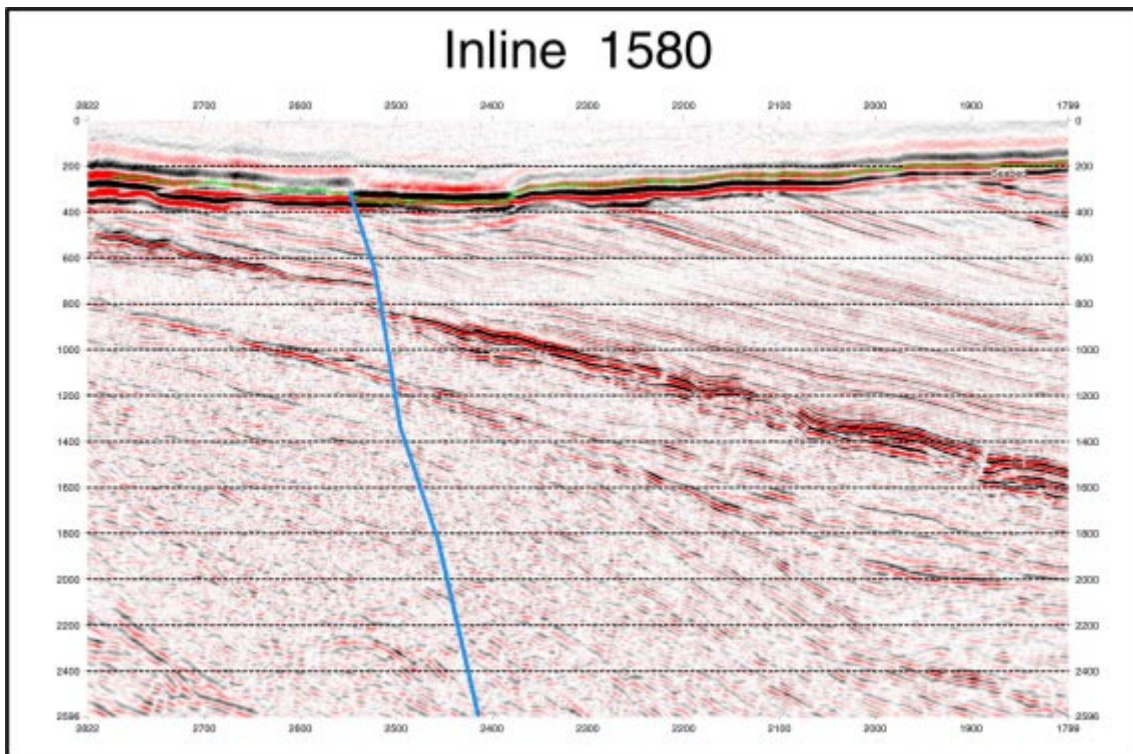
Fig. 3.3.24.   Seismic example from the north-eastern part of the area, profile 18 in Fig. 3.3.20. The fault marked with blue line appears to offset the seafloor. This scarp is, however, most likely an erosional phenomenon and is parallel to the sub-cropping units.
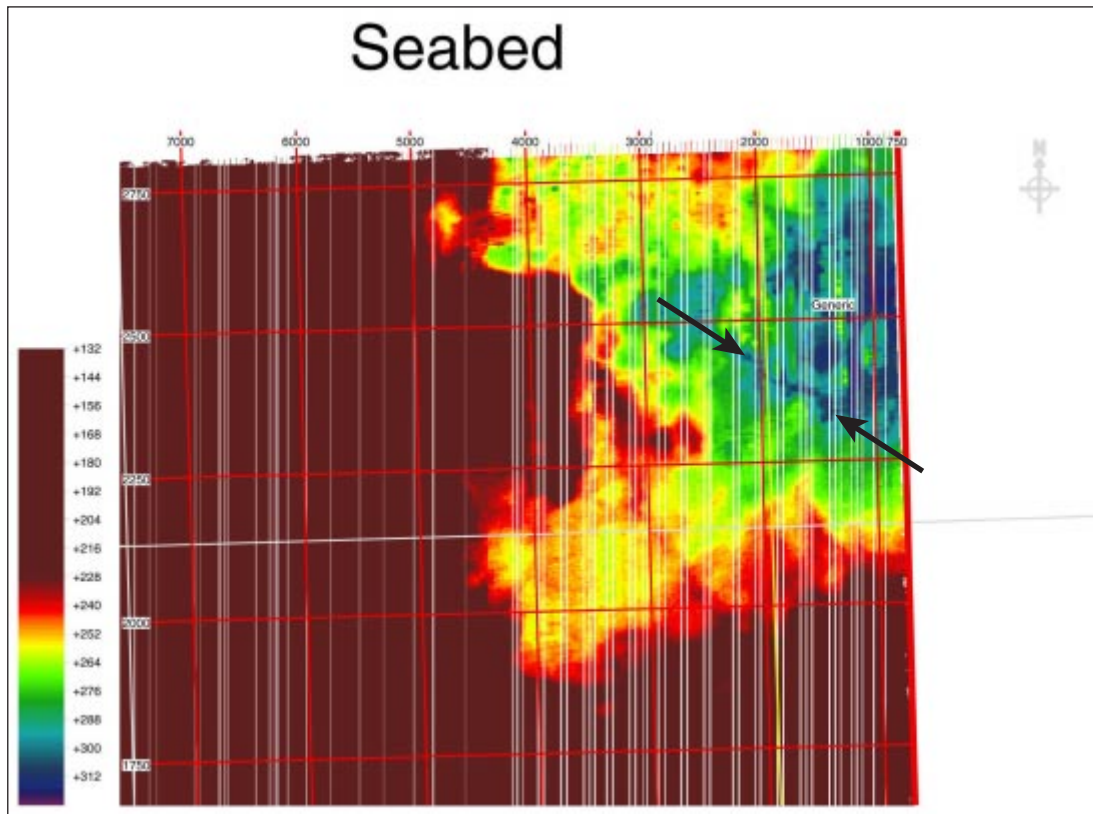
Fig. 3.3.25.   Map close-up from the north-eastern corner of the NH9604 survey, with colour compression applied. A marked lineament (marked with arrows) has been the subject for closer inspection.
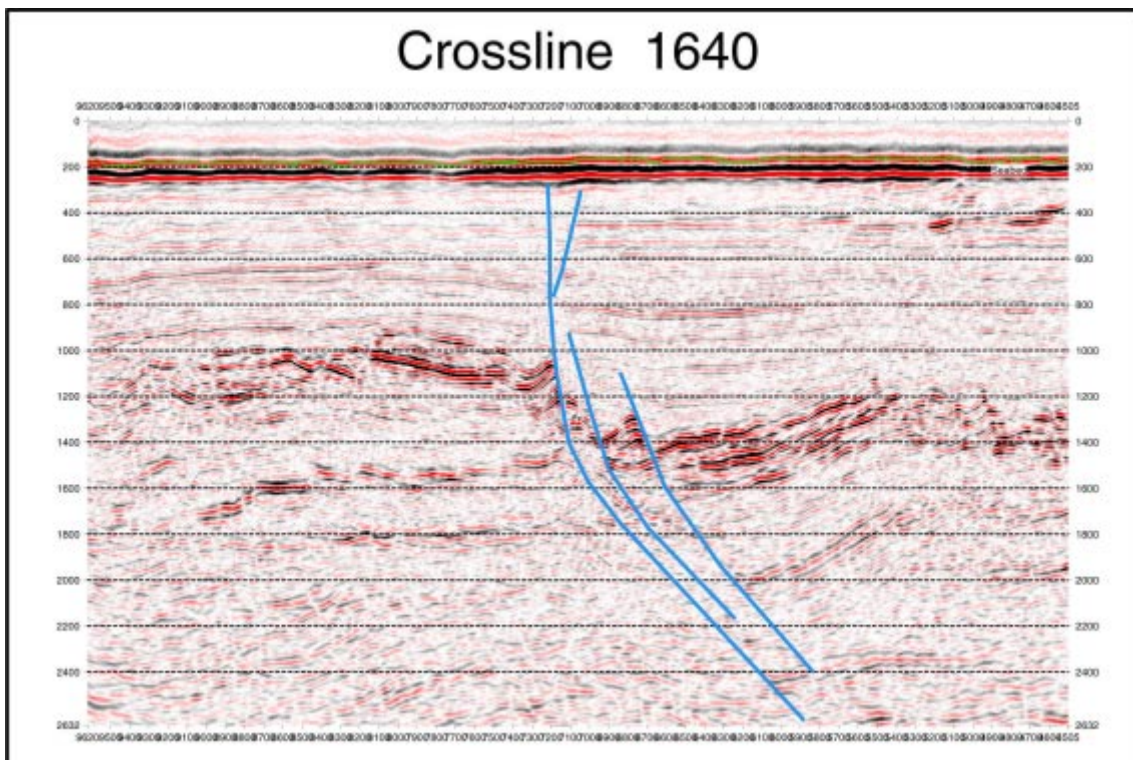
Fig. 3.3.26.   Seismic example of deep fault with possible connection to seafloor, profile 20 in Fig. 3.3.20.

78
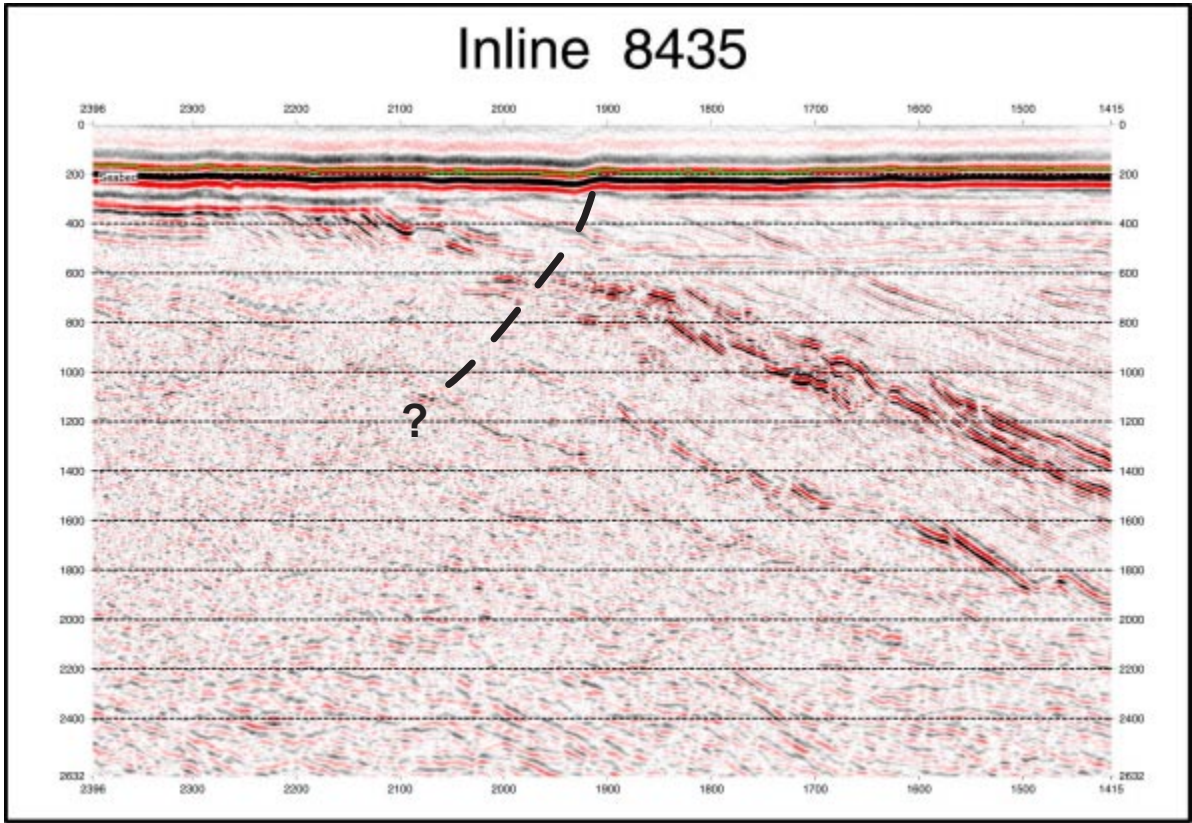
Fig. 3.3.27. Seismic example of seafloor offset, corresponding to a northeast – southwest trend, profile 21 in Fig. 3.3.20. There is, however, no obvious connection to a deeper fault.
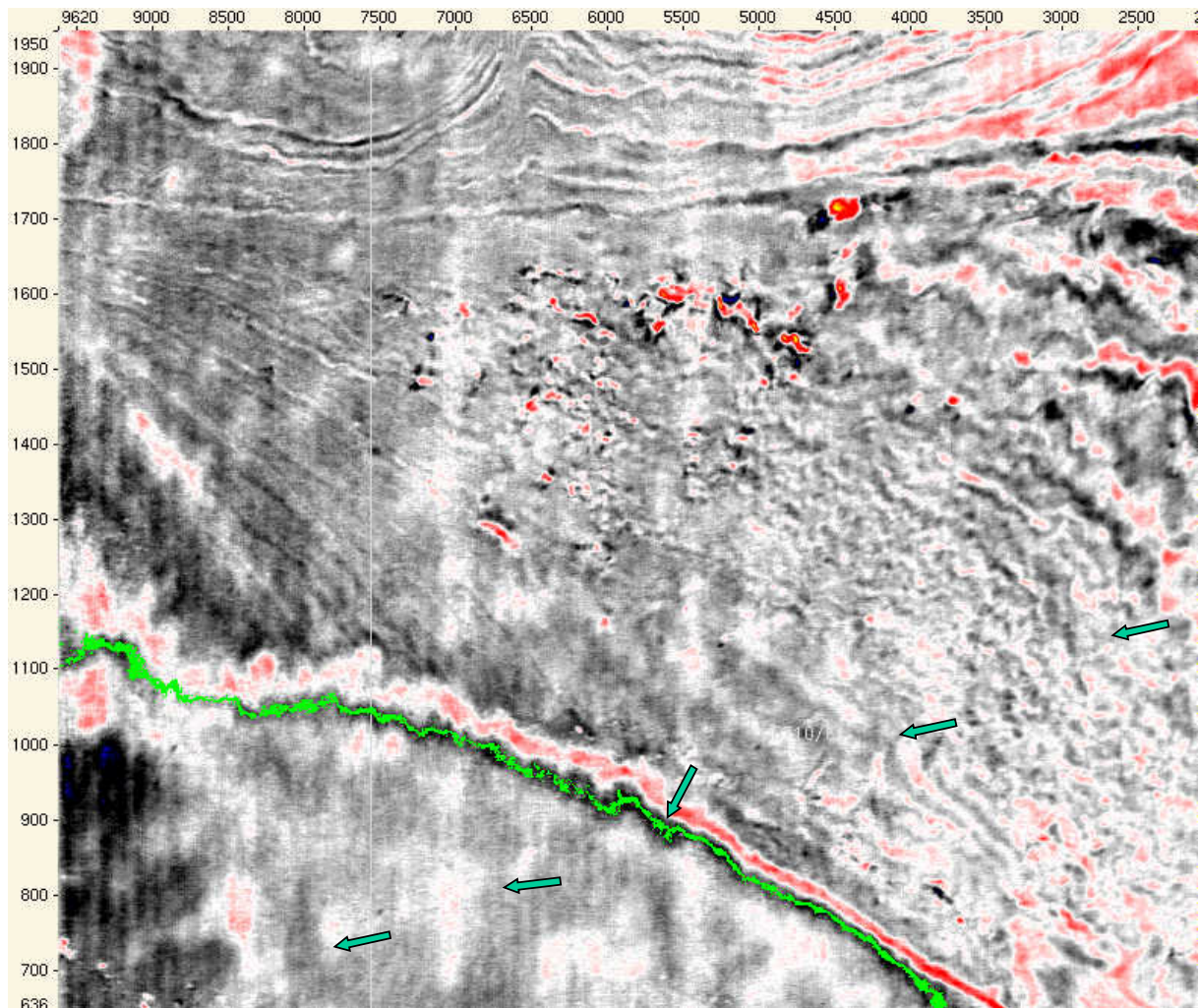
Fig. 3.3.28.   Time slice at 396 ms from the NH9604 survey. A small fault in the pre-Quaternary section continues as a subtle lineament into the Quaternary, as shown by the green arrows.

ST9203

The ST9203 survey covers parts of block 6607/12, 6608/10, 6507/3 and 6508/1 in the Nordland II area and includes the Norne field. Three major units occur in the area (Lower, Middle and Upper Till), which have further been divided by 25 till tongue occurrences (King *et al.* 1987). The till tongues are formed by alternating advancing and retreating glaciers onto the continental shelf and are separated by glaciomarine sediments

Two intra-Quaternary horizons have been mapped within the 3D cube in addition to the sea floor and the base Quaternary. Dip maps of the reflectors are shown in Figs. 3.3.29-33. The lowermost intra-Quaternary reflector (Horizon 2) represents the interface between the Lower and Middle Till of the till tongue stratigraphy by King *et al.* (1987). This reflector represents in more detail the top of till tongue 6. The uppermost Intra-Quaternary reflector (Horizon 3) represents the top of till tongue 12 within the Middle Till.

The sea floor (Horizon 4) is dominated by numerous plough marks. There are multiple directions, but the coast-parallel NE-SW direction dominates. A remnant ice sculptured surface exists to the west with E-W scouring. The base Quaternary reflector has also a prominent E-W pattern of glacial scouring.

The front of till tongue 6 is trending NE-SW through the survey area. The northwestern-most part of Horizon 2 (Fig. 3.3.31) is therefore identical to the base Quaternary reflector (Fig. 3.3.29). An irregular pattern of WNW-ESE trending flutes is dominating the top of till tongue 6. Horizon 3 (top of till tongue 12) is characterised by NW-SE regular trending ridges.

We have been concentrating on checking if linear distortions of the reflectors can be traced through two or more of the interpreted horizons. We conclude that such structures, which could represent tectonic faulting, or flexing have not been found.
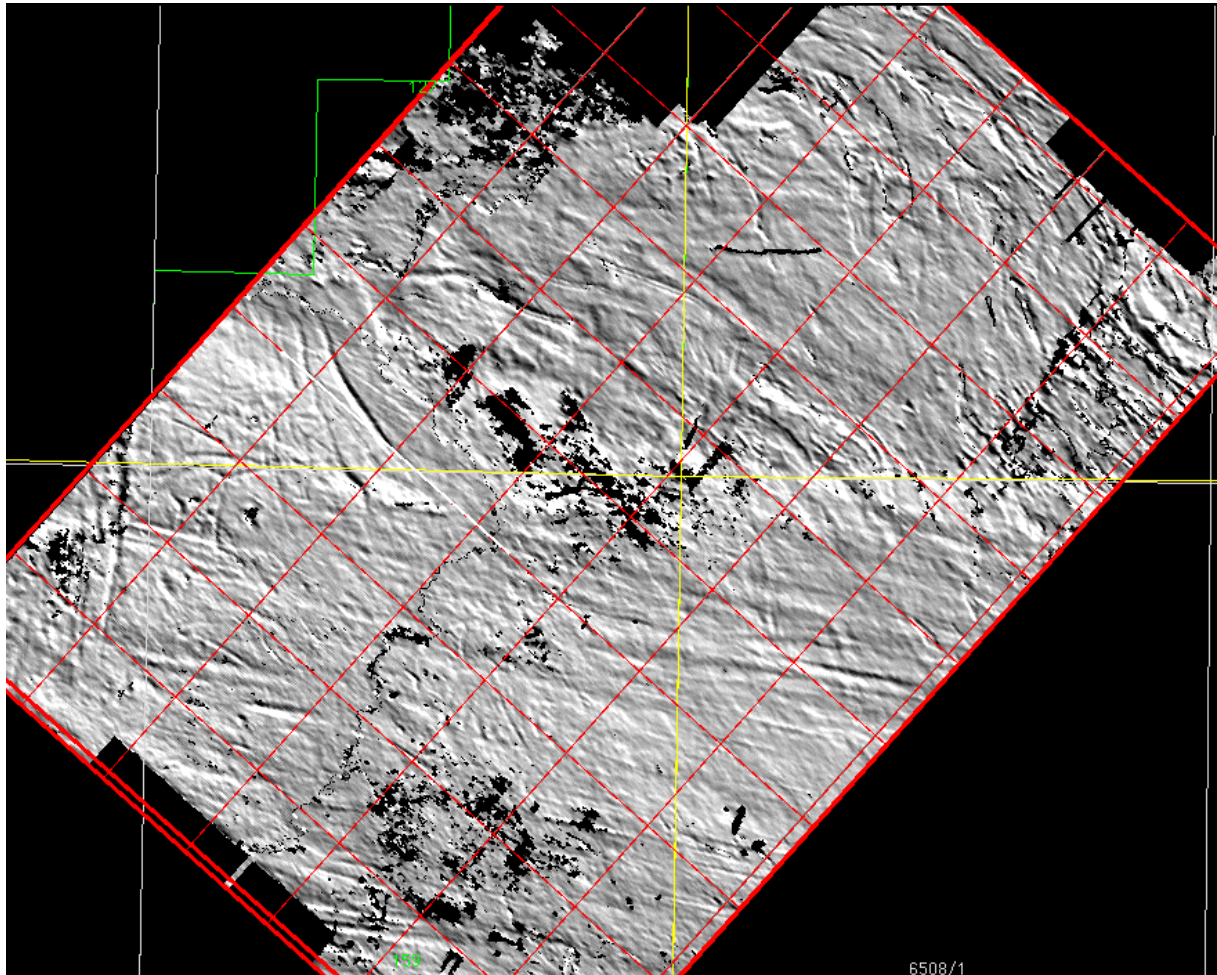
Fig. 3.3.29.   Map of base Quaternary (Horizon 1), ST9203 Norne area. Artificial illumination of dip of surface; light source from north with an inclination of 45□. A 7x7 window is used for calculation of dip. White line shows the location of crossline A 1002 shown in Fig. 3.3.30.
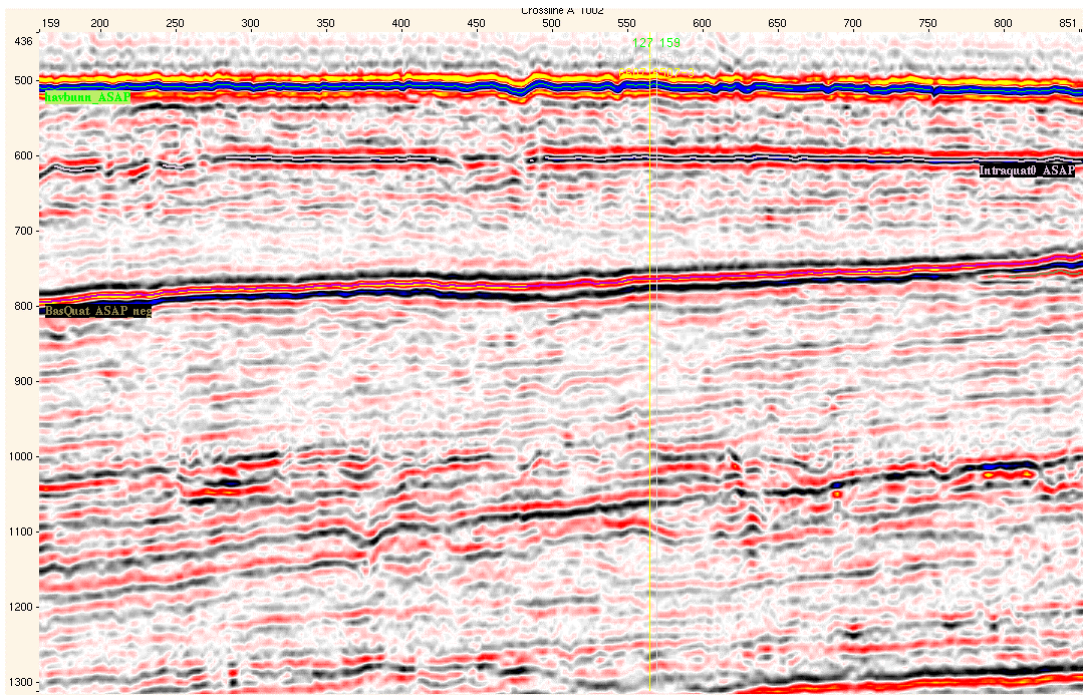
Fig. 3.3.30.   Seismic example showing the Upper and Middle Till (King et al. 1987). The location of the profile is marked with a white line in Fig. 3.3.29. Plough marks from icebergs can be seen at the seafloor.
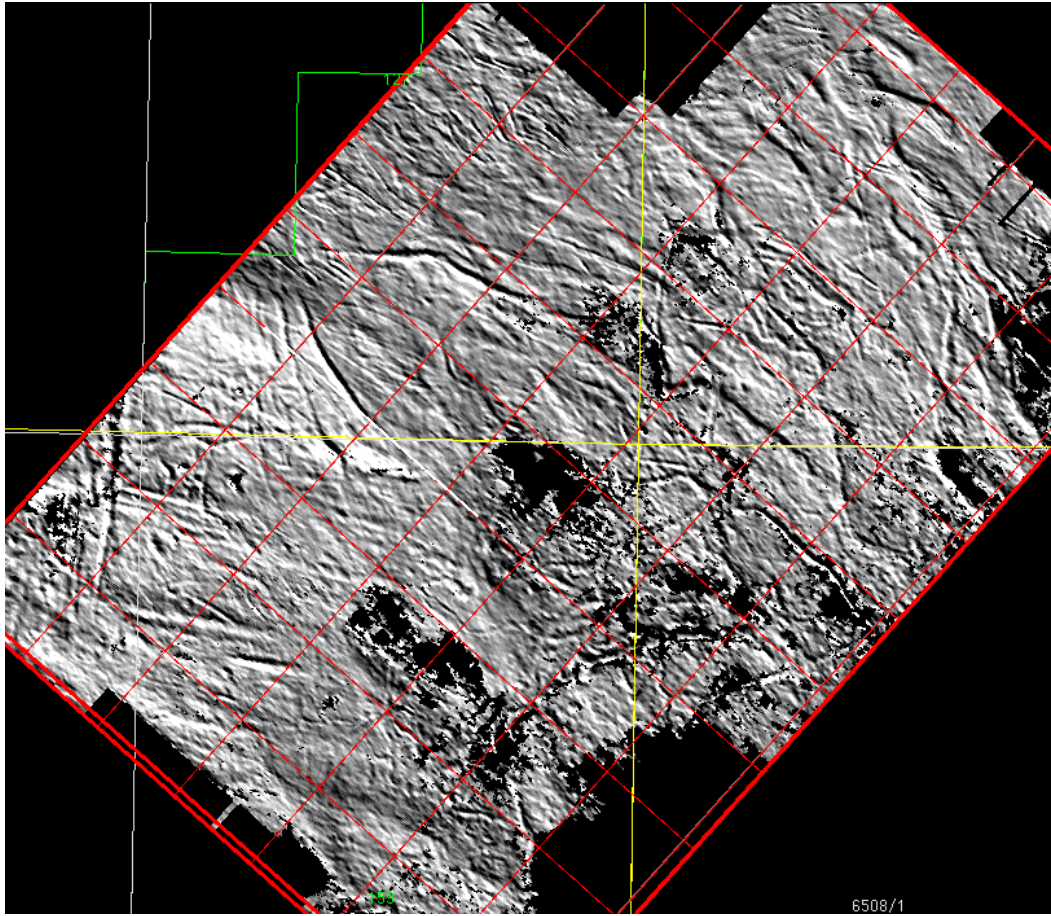
Fig. 3.3.31.   Map of Horizon 2 (top of Lower Till), ST9203 Norne area. Artificial illumination of dip of surface; light source from north with an inclination of 45°. A 7x7 window is used for calculation of dip. White line shows crossline A 1002.
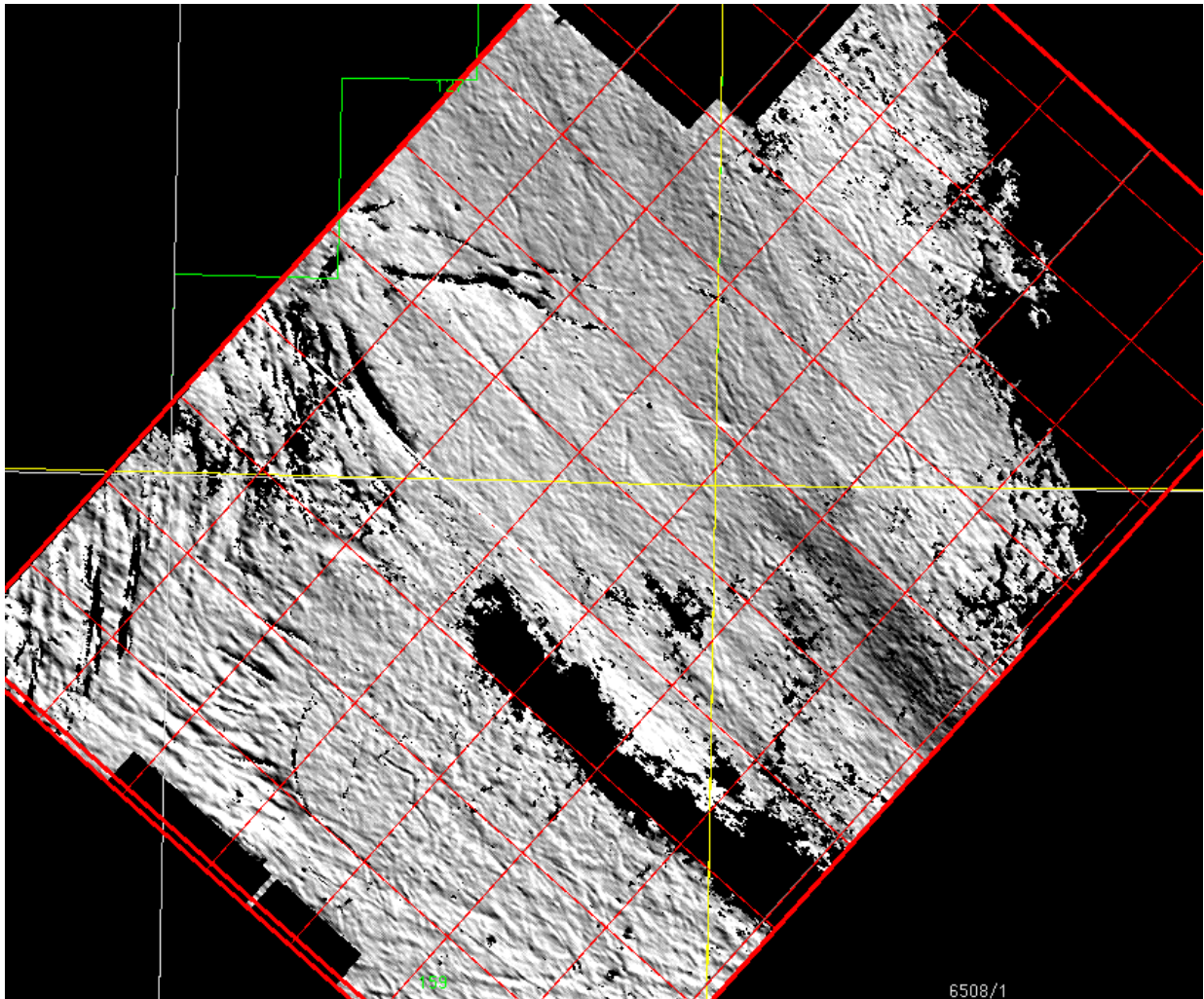
Fig. 3.3.32.   Map of Horizon 3 (top of Middle Till), ST9203 Norne area. Artificial illumination of dip of surface; light source from north with an inclination of 45°. A 7x7 window is used for calculation of dip. White line shows crossline A 1002.
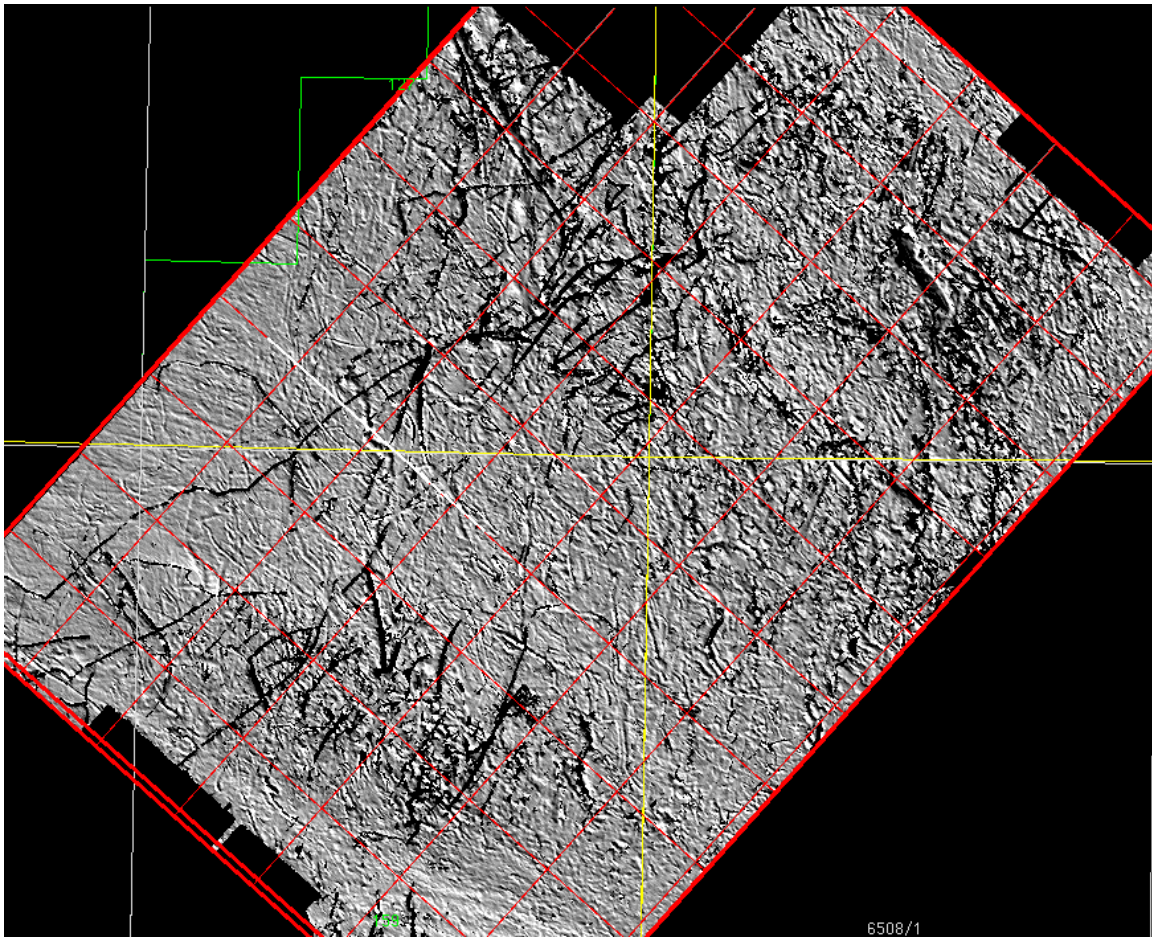
Fig. 3.3.33. Map of seabed, ST9203 Norne area. Artificial illumination of dip of surface; light source from north with an inclination of 60°. A 4x4 window is used for calculation of dip. The black sharp lineaments represent plough marks from icebergs. White line shows crossline A 1002.

3.3.5 Conclusions

Hovland (1983) has previously reported normal faulting in the order of 1-2 metres from high-resolution boomer profiles in the northern North Sea. Subtle distortions of the glaciomarine reflectors from the interpretation of 3D seismic surveys may indicate small scale faulting in the same order (1-3 metres). We have, however, not observed large-scale postglacial faulting (5-30 m offset) similar to the fault-scarps reported from northern Fennoscandia.

The small-scale faults are visible as lineaments on time slices and on the structural maps of the different surfaces. They seem to have consistent trends, and in the Troll area, they are related to underlying faults and possibly to vertical gas migration.

Several distortions of the Quaternary reflectors have been observed on the 3D surveys. Most of them can be attributed, however, to other effects than neotectonic:

1. Plough marks from drifting icebergs (incl. sedimentary draping of underlying plough marks and 'ghosts??' from overlying plough marks)

2. 'Pull-up' effects from overlying till drumlines with increased seismic velocity (e.g. NW-SE lineaments on BPN9401, NH9405 and NH9202)

3. Draping of underlying bedrock escarpments (e.g. sub-cropping units)

4. Static shifts parallel to the seismic lines

5. Inaccurate merging of 3D cubes (e.g. NH9202)

6. Pipelines on the sea floor

3.3.6 References

Bøe, R., 1990: Regionalseismisk undersøkelse i ytre del av Boknafjorden. *NGU Rapport 90.093*, 7 p

Bøe, R., Sørensen, S. & Hovland, M., 1992: The Karmsundet Basin, SW Norway: stratigraphy, structure and neotectonic activity. *Norsk Geologisk Tidsskrift* 72, 281-283.

Dehls, J. & Olesen, O. (eds.) 1998: Neotectonics in Norway, Annual Technical Report 1997. *NGU Report 98.016,* 161 pp.

Desmond Fitzgerald and Associates 1996: INTREPID Geophysical processing and visualisation tools reference manual Vol. 2, *241 pp.*

Fanavoll, S. & Dahle, A., 1990: Earthquake hazard and loads in the Barents Sea. *ESARC Report* 13, SF60.4022.00/01/90 (restricted).

Fanavoll, S. & Dehls, J. 1998: Multibeam echo-sounding data in the Malangen and Lofoten areas. *In:* Dehls, J. & Olesen, O. 1998 (eds.) *Neotectonics in Norway, Annual Technical Report 1997,* NGU Report 98.016, 71-81.

Fenton, C., 1991: *Neotectonics and palaeoseismicity in North West Scotland.* Ph.D. thesis, University of Glasgow Glasgow, 403.

Fenton, C., 1994: Postglacial faulting in eastern Canada. *Geological Survey of Canada, Open file report 2774*, 98 p

Fiedler, A., 1992: *Kenozoisk sedimentasjon i Lofotenbassenget langs vestlige Barentshavmarginen*. Cand. Scient. thesis, University of Oslo Norway, 114.

Geosoft 1994: MAGMAP, 2-D frequency domain filtering. Users manual. 34 pp.

Geosoft, 1997: OASIS montaj, Data processing system for Earth science applications. Version 4.1 User guide. *290 pp.*

Granberg, E., 1992: *A basin modelling study of the Vøring Basin*. Diploma thesis, University of Trondheim, Norway.

Henriksen, S. & Vorren, T.O. 1996: Late Cenozoic sedimentation and uplift history on the mid-Norwegian continental shelf. *Global and Planetary Change 12,* 171-199.

Hovland, M. 1984: Undersøkelse av grunn gass og bunnformer, blokk 25/7 and 24/9. F&U Prosjekt 144. *Internal Statoil Report.* 86 pp.

Hovland, M. 1983: Elongated depressions associated with pockmarks in the western slope of the Norwegian Trench. *Marine Geology 50,* M11-M20.

King, L.H., Rokoengen, K. & Gunleiksrud, T. 1987: Quaternary seismostratigraphy of the Mid Norwegian Shelf, 65° - 67°30'N. – A till tongue stratigraphy. *IKU Publ. 114. Continental Shelf and Petroleum Technology Research Institute A/S,* 58 pp.

Kujansuu, R. 1964: Nuorista sirroksista Lapissa. Summary: Recent faults in Lapland. *Geologi 16,* 30-36.

Lagerbäck, R. 1979: Neotectonic structures in northern Sweden. *Geologiska Föreningen i Stockholm Förhandlingar 100 (1978),* 271-278.

Mokhtari, M., 1991: *Geological model for the Lofoten continental margin.* Dr. Scient. thesis, University of Bergen Norway, 184.

Mokhtari, M. & Pegrum, R. M., 1992: Structure and evolution of the Lofoten continental margin, offshore Norway. *Norsk Geologisk Tidsskrift* 72, 339-355.

Muir Wood, R., 1993: A review of the seismotectonics of Sweden. *Swedish Nuclear Fuel and Waste Management Co. Technical Report 93-13*, 225 p

Muir Wood, R., 1995: Reconstructing the tectonic history of Fennoscandia from its margins: The past 100 million years. *Swedish Nuclear Fuel and Waste Management Co. Technical Report 95-36*, 107 p

Muir Wood, R. & Forsberg, C. F., 1988: Regional crustal movements on the Norwegian continental shelf, ELOCS (Earthquake Loading on the Norwegian Continental Shelf) Report 1-3, *Norwegian Geotechnical Institute, Oslo, NTNF/NORSAR, Kjeller and Principia mechanica Ltd.*, London, 148 p

Olesen, O. 1988: The Stuoragurra Fault, evidence of neotectonics in the Precambrian of Finnmark, northern Norway. *Norsk Geologisk Tidsskrift 68,* 107-118.

Riis, F. 1998: Seismic investigations in the North Sea. *In:* Dehls, J. & Olesen, O. 1998 (eds.) *Neotectonics in Norway, Annual Technical Report 1997,* NGU Report 98.016, 59-70.

Rise, L., Rokoengen, K., Sættem, J. & Bugge, T. 1988: Thickness of Quaternary deposits on the Mid Norwegian Continental Shelf. Scale 1:1000 000. *IKU Publ. 119. Continental Shelf and Petroleum Technology Research Institute A/S, Trondheim.*

Rise, L. & Bøe, R. 1998: Interpretation of seismic data from the Karmsundet Basin. *In:* Dehls, J. & Olesen, O. 1998 (eds.) *Neotectonics in Norway, Annual Technical Report 1997,* NGU Report 98.016, 52-58.

Rokoengen, K. & Sættem, J., 1983: Shallow bedrock geology and Quaternary thickness off northern Helgeland, Vestfjorden and Lofoten. *IKU report P-155/2/83*, 44 p

Rokoengen, K., Rise, L., Bugge, T. & Sættem, J. 1988: Bedrock geology of the Mid Norwegian Continental Shelf. Scale 1:1000 000. *IKU publ. 118. Continental Shelf and Petroleum Technology Research Institute A/S, Trondheim.*

Schlumberger GeoQuest 1998: Geoframe 3.0. Seismic interpretation using Charisma, Training Manual, *321 pp.*

Sejrup, H. P., Aarseth, I., Haflidason, H., Løvlie, R., Bratten, Å., Tjøstheim, G., Forsberg, C. F. & Ellingsen, K. I., 1995: Quaternary of the Norwegian Channel: glaciation history and palaeoceanography. *Norsk Geologisk Tidsskrift* 75, 65-87.

4   1:3 000 000 NEOTECTONIC MAP AND DATABASE (TASK 3)

By John Dehls, NGU

Accompanying this report is a second draft of the neoteconic map of Norway and adjacent areas (Enclosure 1). The main changes since the first draft (accompanying the 1997 Annual Technical Report) are as follows:

- Deletion of some neotectonic faults which are no longer believed to be of tectonic origin.

- Use of a new database of earthquakes from NORSAR.

- Addition of higher resolution bathymetry data for the area around Svalbard and the Barents Sea.

- Changes in layout to reflect the final look of the map.

- Addition of two inset maps. The lower map will contain significant offshore geological features, such as neogene domes, arches and volcanic deposits. The upper map will contain a compilation of in-situ stress data provided by Erik Hicks at NORSAR.

- Changes in the uplift rate contours. These contours reflect new data compiled throughout the year. The exact contours may change in the final map due to choice of gridding method, but the main patterns probably will not change.

As usual, any comments or suggestions for the final map are welcome.

5   GEOLOGY & GEOPHYSICS (TASKS 4 & 9)

5.1   ROCK AVALANCHES, GRAVITATIONAL FAULTING AND ITS POTENTIAL PALAEOSEISMIC CAUSE

By Lars Harald Blikra, NGU

It is known from studies of the effects of historical known earthquakes that many of these earthquakes trigger different types of avalanches, including large rock avalanches (e.g. Keefer 1984; Jibson 1994). The history of rock avalanches could thus be used for palaeoseismic analysis, but this requires detailed mapping of their spatial occurrence and dating of individual events. The review made by Jibson (1994) indicates that large rock avalanches require a minimum earthquake magnitude of about 6.0, and he also concludes that large rock avalanches are the type of avalanche with greatest potential in palaeoseismic studies.

The research on rock avalanches which has been performed in western and northern Norway during the last couple of years could thus be of interest for the NEONOR project. This preliminary report aims to give a brief summary of the results so far, and will propose some further research activities.

5.1.1   Rock avalanches and gravitational faulting in Troms county

Geological studies of rock avalanches in Troms demonstrate a surprisingly high number of events in the Kåfjord and Storfjord areas. Studies from the early seventies also show this pattern (Corner 1972). There are several large-scale gravitational features in this area, characterized by large faults and crevasses. These gravitational features have been observed as far east as Nordreisa, where several portions of the eastern mountain slope have slipped down. Major gravitational faulting has been mapped on Nordnesfjellet, north of Skibotn (Fig. 5.1.1), in an area covering more than 2 km in length. The faults or crevasses are localized on a quite flat plateau and extend up to 400 m from the mountain slope. The most striking observation is that there seems to be a more or less horizontal displacement along the foliation planes. Horizontal displacements of as much as 10 m have been observed here. One of the faults seems to be covered by a small lobate feature that has been interpreted to be a small rock glacier. Fig. 5.1.2 shows another gravitational sliding feature in Manndalen. Part of this fault scarp is also covered by a lobate feature. We need to go back to the Younger Dryas period (11 000 - 10 000 radiocarbon years before present) to find a climate which is cold enough to get active rock glaciers. Part of the gravitational faulting is thus interpreted to have started before 11 000 BP. The size and the large horizontal displacement might indicate that large-scale earthquakes are the most probably trigger mechanism.
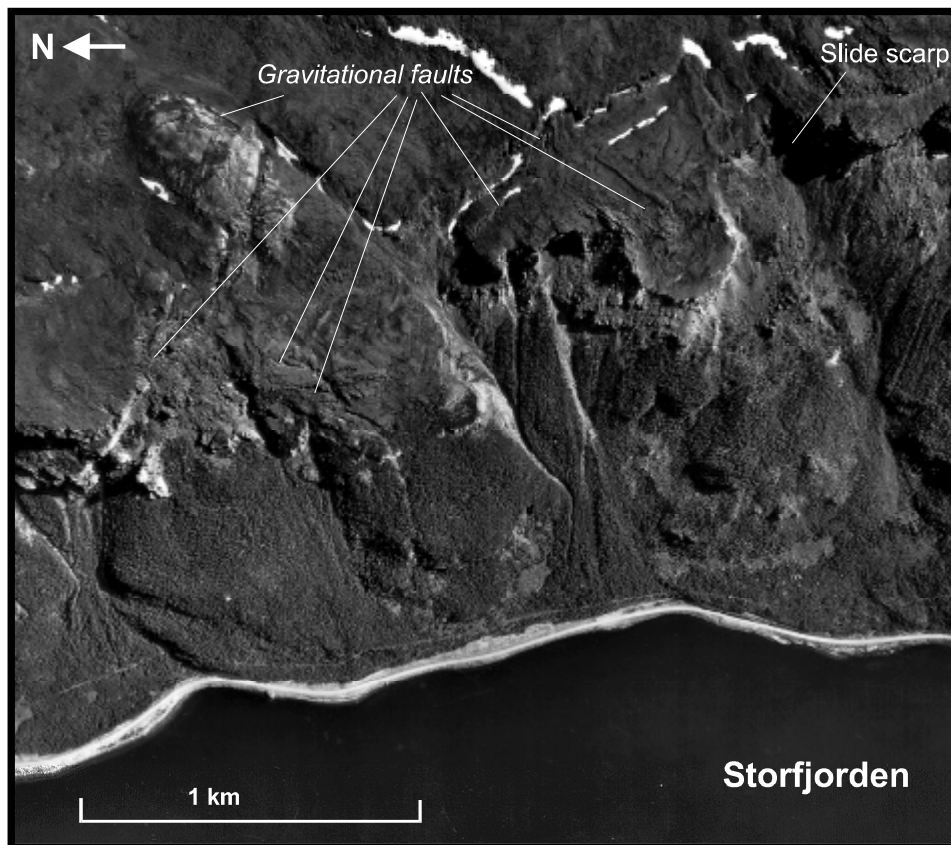
Fig. 5.1.1   Gravitational faults on top of Nordnesfjellet, north of Skibotn in Troms.
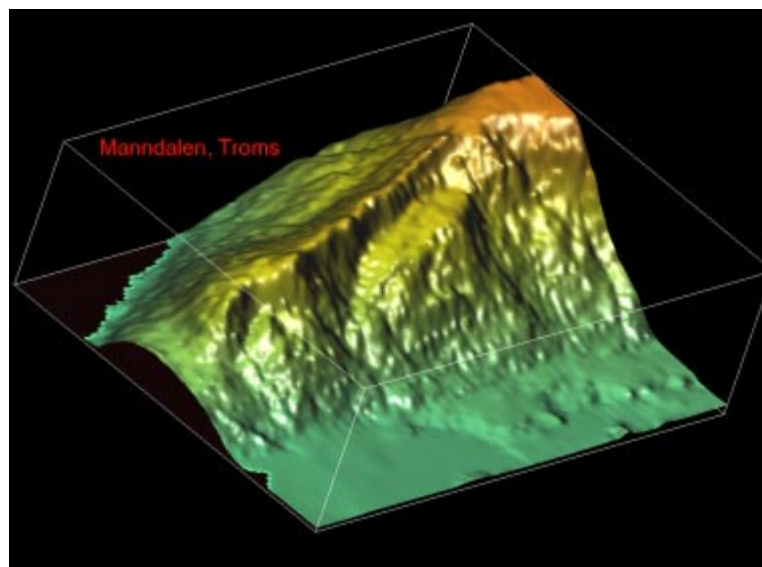
Fig. 5.1.2   Digital 3D model from Manndalen showing a gravitational slide.

Attempts at dating some of the rock-avalanche events have been given priority. Seismic surveys on one avalanche in Sørfjorden, a fjord west of the Lyngen peninsula, indicate that this event occurred shortly after the deglaciation (ca. 10000-9500 years BP). The same conclusion has been made about a rock avalanche studied in Balsfjorden. Three radiocarbon dates on shells that are younger than the avalanche event gave ages between 9500 and 9600 radiocarbon years BP. Mapping of a large rock avalanche close to the Nordmannvik postglacial fault evidenced marine abrasion and formation of beach terraces on high altitudes, demonstrating

that the event occurred shortly after the deglaciation. Geophysical investigations have been performed on these deposits in order to map the relation between blocky rock-avalanche deposits and the marine sediments. A large bedrock collapse west of Salangen formed huge blocky rock-avalanche deposits. Road cuts through this avalanche exposed marine sediments with mollusc-shells on relatively high altitudes. Two dates from the shells show that the avalanche were older than 9900 radiocarbon years BP and older than ca. 10300 BP). Another rock avalanche further west on Andørja was dated to be older than 9500 radiocarbon years BP. The preliminary conclusions of this study indicate that the rock avalanches in Troms are concentrated to specific zones, and they seem to be old, formed shortly after the deglaciation. This might imply that there were major earthquakes in the period 10000 to 9500 years BP, which can possibly be correlated with the postglacial faulting in Nordmannvikdalen.

5.1.2 Rock avalanches and gravitational faulting in Møre & Romsdal

A project focusing on mapping large rock avalanches and evaluating their potential hazard has been going on in Møre & Romsdal since 1996 (Blikra & Anda 1997; Anda & Blikra 1998). The project has produced a map showing the distribution of large rock avalanches in this county (Fig. 5.1.3). The distribution map shows that such avalanches are common in the region, with more than 100 localities. The avalanches seem to be grouped into certain regions, with concentrations in some of the well-defined NNW-SSE oriented valleys and fjords. Tafjorden and Romsdalen represent two such areas, with Romsdalen containing more than 10 rock-avalanche deposits. We know, so far, little about the causes of the concentrations of these rock avalanches. Postglacial tectonic may be important. The concentrations of events in Romsdalen might be correlated with a 500-700 m high regional escarpment of the land surface. This large-scale geomorphic feature indicates a distinct "fault zone" associated with the Cenozoic uplift in Norway (Anda 1995).
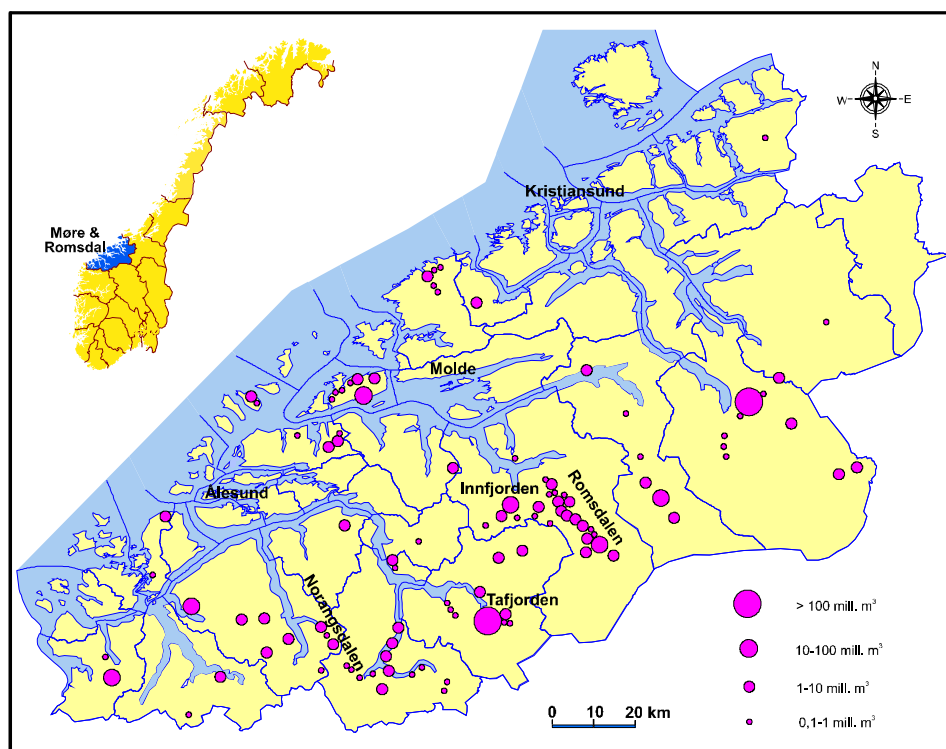
Fig. 5.1.3   Registration map of rock avalanches from the Møre & Romsdal county (Blikra & Anda 1997).

90

Some of the rock-avalanche events have been radiocarbon dated by sampling organic material found under the deposits (palaeosoils). A minimum age can be found for some of them by relating the deposits to older sea-level stands. Several of the large rock avalanches has given surprisingly young ages, the youngest date in Romsdalen gave an age of 1500 years BP. It has been commonly accepted that most rock avalanches formed shortly after the deglaciation, but the present studies have demonstrated that many of them were generated during the last 5000 years.

Several areas of major gravitational faulting and sliding have been observed in Møre & Romsdal. One of the largest is localised on Børa, a mountain plateau on the western side of Romsdalen (Fig. 5.1.4), covering a more than 2 km by 200 m large area. The faults are characterised by more than 20 m deep crevasses and horizontal displacements of more than 20 m. Some of them can be followed for more than 1.5 km in length. Some of the faults appear to be active and information from local inhabitants supports this. Large gravitational faulting has also been mapped at Oppstadhornet in the Midsund area (see description in Robinson et al. 1997) and at Storhornet in Vanylven County.

Fig. 5.1.4   Gravitational faults on Børa, western side of Romsdalen.

5.1.3   Palaeoseismic cause?

It is too early in the project to conclude that palaeoseismic is the cause for some of the trends and regional differences in the distribution of large rock avalanches and gravitational faulting. However, the so far consistency in the age of some of the rock avalanches and the gravitational faulting or sliding features in the Troms area strongly indicate a palaeoseismic cause. If this is correct there seems to have been major earthquakes in the order of 6.0 or more during two periods, one before 11 000 and one between 10.000 and 9500 radiocarbon years BP. The

last of these periods could be related to the postglacial faulting in Nordmanvikdalen in Kåfjord. This is strongly supported by the unexpected high numbers of rock avalanches in this region. No conclusion has been drawn about the possible link to palaeoseismicity in the Møre & Romsdal region. Since many of the rock-avalanche events in this region are much younger, they can not be related to the active processes during the Younger Dryas period. There is a need for more detailed studies in order of dating individual events.

5.1.4 Further research activities

There will be a need for a more systematic registration of areas affected by gravitational faulting. This will be important both for the NEONOR project and for evaluating hazard and risk zones. Detailed mapping and studies of some of the largest gravitational-fault systems will be given priority. An understanding of their structural and tectonic evolution will be essential in order of being able to do slope-stability analyses. Jibson (1994) concluded that the most direct way to assess the relative likelihood of seismic versus aseismic triggering of an individual landslide is to apply methods of static and dynamic slope-stability analysis. The main question will be: Do we need an earthquake to get these gravitational fault systems? There are plans for doing detailed studies in two areas in 1999; one in Romsdalen in Møre & Romsdal (Fig. 5.1.4) and one on Nordnesfjellet in Troms (Fig. 5.1.1). Detailed digital topographic data will be constructed from these localities.

In addition to the registration or mapping of individual events, a series of detailed dating studies should be done. The registration should be done in areas were the NEONOR project indicates that postglacial tectonics have been active.

The mapping and registration of large rock avalanches and gravitational faulting should have been performed in an early stage in order of focusing the search for possibly neotectonic features. Their distribution pattern and age in some areas indicate that they might be controlled by postglacial earthquakes.

5.1.5 References

Anda, E. 1995. Romsdalen og Romsdalsfjorden. Hovedtrekkene i landskapet. *In* Sanden, J., *ed.. Romsdalen, natur og kultur*. Romsdalsmuseet, årbok 1995, 14-34.

Anda, E. & Blikra, L.H, 1988.: Rock-avalanche hazard in Møre & Romsdal, western Norway. *Norwegian Geotechnical Institute Publikasjon 203*, 53-57.

Blikra L. H. and Anda, E. 1997. Large rock avalanches in Møre og Romsdal, western Norway. (Extended abstract). *Nor. Geol. Unders, Bull. 433*, 44-45.

Corner, G. 1972: Rockslides in North Norway, Norway. Unpublished report Tromsø museum, 10 pp.

Jibson, R.W. 1994: Using landslides for Paleoseismic analysis. In McCalpin (ed.): *Paleoseismology*. International geophysics series 62, 397-438. Academic press.

Keefer, D.K. 1984: Landslides caused by earthquakes. *Geological Society of America Bulletin* 95, 406-421.

Robinson, P., Tveten, E. & Blikra L. H. 1997. A post-glacial failure at Oppstadhornet, Oterøya, Møre og Romsdal: a potential major rock avalanche. (Extended abstract). *Nor. Geol. Unders, Bull. 433*, 46-47.

5.2 LATE QUATERNARY FAULTING AND PALEOSEISMICITY IN FINNMARK, NORTHERN NORWAY.

By Lars Olsen, John Dehls and Odleiv Olesen, NGU

Traces of confirmed or inferred neotectonic (Late Quaternary) movements in Finnmark have been reported since more than a decade ago. These traces include both a recent groundwater outburst after an earthquake in Masi in 1997 (Fig. 5.2.1; Olesen & Dehls 1998), older postglacial traces as till avalanches, possibly initiated from earthquakes (Olsen unpubl., 1989) and the 80 km long Stuoragurra Fault (Figs. 5.2.1 & 5.2.2; Olesen 1988, Muir Wood 1989, Olesen et al. 1992a, b, Roberts et al. 1997).

The interpretation of the character and age of the Stuoragurra Fault has been based, up to 1998, mainly on airphoto-interpretation and geophysics. The fault cuts an esker to the northeast of Masi and other glaciofluvial deposits to the northeast of Iesjavri. This indicates a late-glacial or younger age for the fault. In August 1998, we excavated the overburden in two 25 metre long trenches across this fault at Fidnajohka (Figs. 5.2.3-5; section 1; 69°16′58.3′′N, 23°27′33.9′′E; WGS 84), midway between Masi and Kautokeino in Finnmark. In this way, we were able to see, for the first time, deformational structures in the loose deposits covering the fault escarpment. These deformational structures establish that the major fault movement occurred during or after the last deglaciation in this area (some 9,300 14 C-years BP?), and that the fault escarpment was produced in probably *one* major reverse fault-step. The fault movement has obviously not occurred as a series of minor events, with numerous small steps that together appear as a major fault escarpment, such as has been recorded in several active fault zones of the world (A. Sylvester, pers. comm. 1998).

As parts of the fault escarpment appear with two distinct steps in the slope, it has been speculated that this may indicate that the fault developed as a result of two distinct tectonic events, separated in time. However, the deformation structures observed in the excavated sections do not support this hypothesis. All deformational structures seen may be explained as a result of one major fault event, and the bump in the slope profile represents simply the crest of a pressure ridge located in the head of the major fold structure.

In excavation no. 1 at Fidnajohka, the vertical fault height is c. 7.2 m in the southern trench wall, which corresponds well with the c. 7.0 - 7.5 m height of the fault escarpment as it appears on the ground surface. The reference level in the deformed overburden is the c. 3°-sloping boundary between a basal till and the overlying deglaciation material, consisting of glaciofluvial sediments, with diamict zones included. The boundary zone appears to be mainly undeformed, with nearly the same dip in the easternmost and westernmost parts of the trench.

The length and vertical one-step displacement of the Stuoragurra Fault indicate that this structure was a result of a tectonic event with an associated earthquake of magnitude c. 7.4. This is based on a comparison with analogous data from recent active fault zones (cf. Wells & Coppersmith, 1994). Bungum & Lindholm (1996) estimated the magnitude of the accompanying earthquake to the Stuoragurra Fault to be 7.7 on the assumption that it was created by one single event.

The length and vertical one-step displacement of the Stuoragurra Fault indicate that this structure was a result of a tectonic event with an associated earthquake of strength c. 7.4. This is based on a comparison with analogous data from recent active fault zones (cf. Wells & Coppersmith, 1994).

Whereas the nose of the up-thrown hanging block of bedrock was well exposed in the middle of the studied area, it was exposed below 3 m of overburden in the trench in the upper part of the escarpment (Fig. 5.2.6). The hanging wall has a dip of 55°, which confirms previous estimates of the dip of the fault plane, based on drilling and ground geophysics (Olesen et al. 1992b). The loose deposits have been bulldozed and folded during the fault process. Abundance of liquefaction structures and other deformations, such as convolutions (Fig. 5.2.7), diapirism, squeezing, injections etc., are recorded in the sections.

Fig. 5.2.1.   Late Quaternary faults in northern Fennoscandia. The area covering the Stuoragurra Fault (Fig. 5.2.2) is framed. 1 – Masi, recent earthquake. 2, 3 – Till avalanches, possibly earthquake initiated. Mainly after Olesen et al. (1992a).
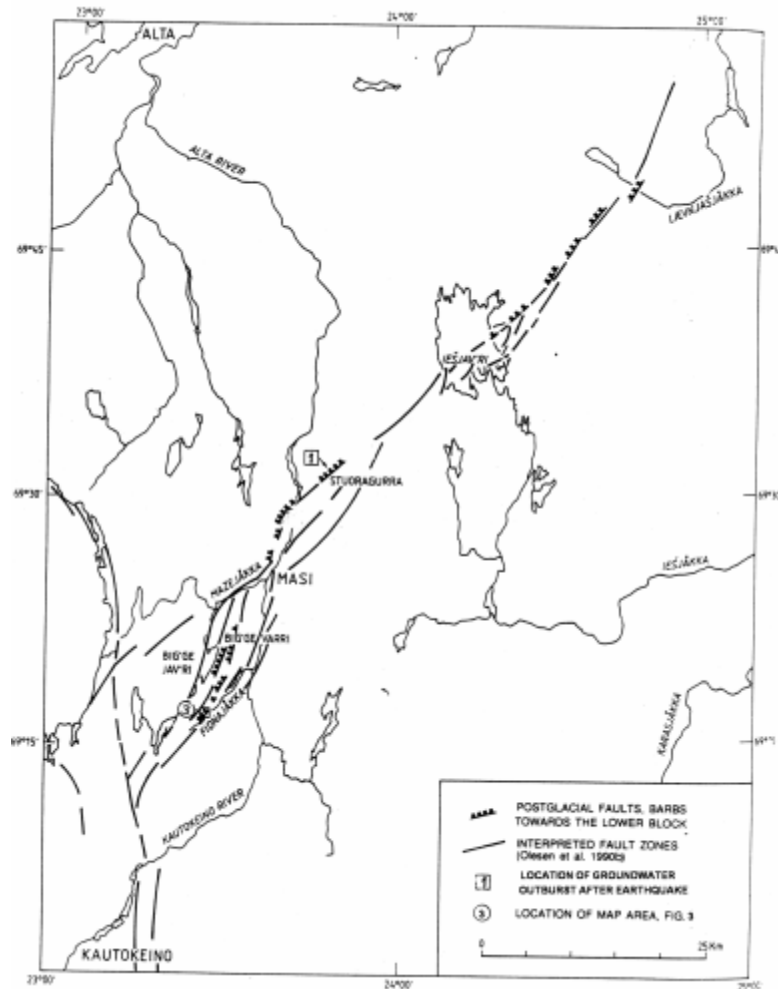
Fig. 5.2.2.   Postglacial faults on Finnmarksvidda, including the Stuoragurra Fault. After Olesen et al. (1992a).

A sub-horizontal unit of gravel and sand may include remnants of the previous soil (Fig. 5.2.5), which therefore may be buried in the fault escarpment. The sand facies of this horizon includes organic-bearing material that may represent either such a buried soil or secondary input of dissolved or particulate organic matter through groundwater transportation. This is not yet fully evaluated. However, in any case the fault-derived deformation of the sediments appears to have moved out from the fault zone towards the northwest with the possible buried soil as a décollement plane.

Some of the most striking deformation structures observed in the lower part of the main section are injections of clast-supported gravel of the local bedrock lithology. These gravely injections which start at the hanging wall - sediment interface, wedge out towards the west (Figs. 5.2.5 & 5.2.9), but may be followed at least to the lower break of the escarpment, i.e. 12-14 m from the fault. Analyses of roundness and lithology of the gravels support strongly our interpretation of a tectonic origin of these wedges (Figs. 5.2.8 & 5.2.9). The sharp-edged and almost 100% - Masi Quartzite derived lithology of the gravels in the injections indicate a distinctly different genesis compared to the pebbles and cobbles in the other, mainly glacially derived sediments in this area. We interpret the sharp-edged gravel injections simply to be injections of *fault breccia* (e.g. Carver & McCalpin, 1996).

95
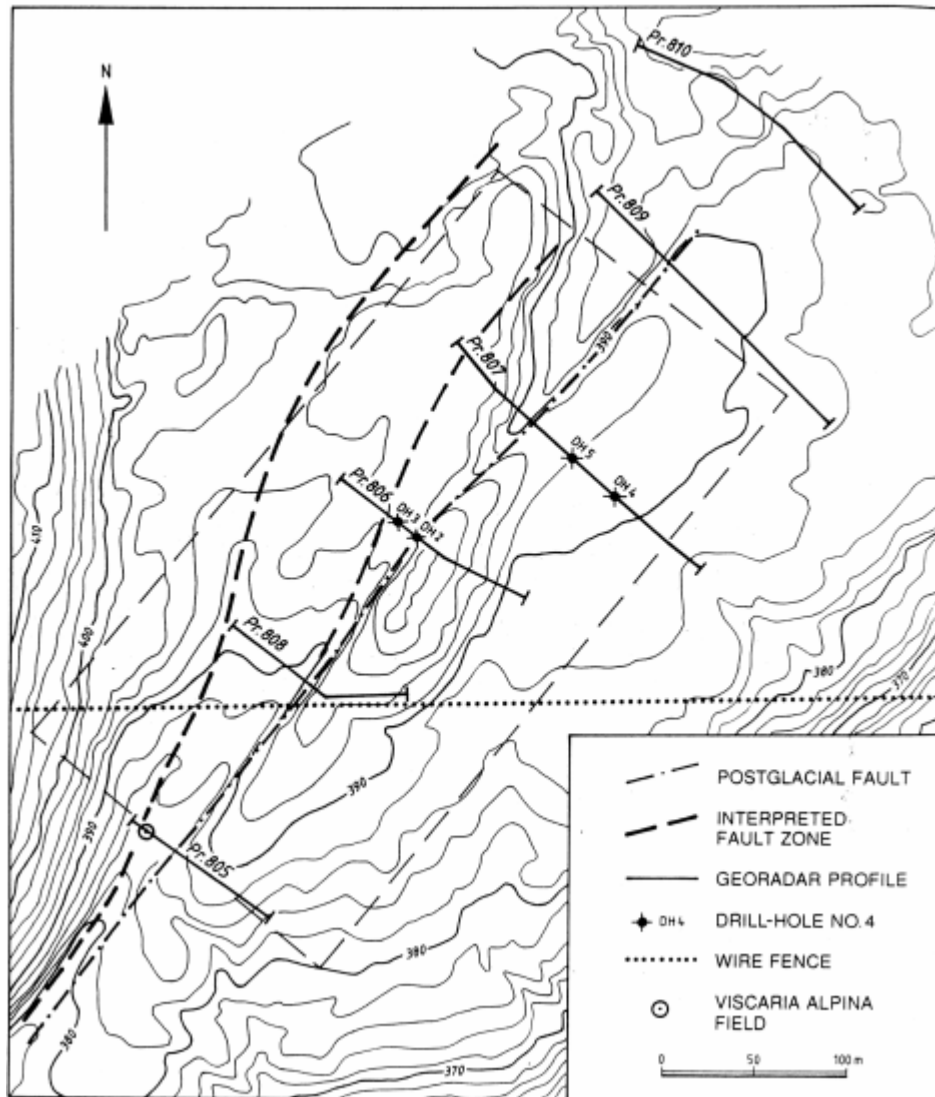
Fig. 5.2.3.   Detailed topographic map from the Fidnajohka area. After Olesen et al. (1992a). The survey area (Fig. 5.2.4) is indicated by the frame.

5.2.1   Summary

Traces of confirmed or inferred Late Quaternary seismic events in Finnmark are summarized as follows:

1. Recent groundwater outburst occurred after earthquake in Masi 1997 (Olesen & Dehls 1998).

2. Postglacial till avalanches possibly initiated by earthquakes are reported from Suvcagan-varri and Bæivasgieddi (Olsen unpubl., 1989). The accurate ages of these are not known.

3. Excavations across the Stuoragurra Fault last year revealed structures which indicate that this fault is indeed a reverse fault, and movement along it occurred most likely in one step with a vertical displacement of c. 7.2 m at Fidnajohka. The length and vertical displace-ment of the fault indicate an associated earthquake of size 7.4, based on a comparison with analogous data from recent active fault zones of the world (cf. Wells & Coppersmith, 1994). The precise age of this tectonic event is not known, however the structures and stratigraphy of the overburden show that the fault developed either during the very last

part of the last deglaciation of Finnmarksvidda, i.e. c. 9,300 14C-yr BP, or shortly after that - possibly after a short phase of pedogenesis.
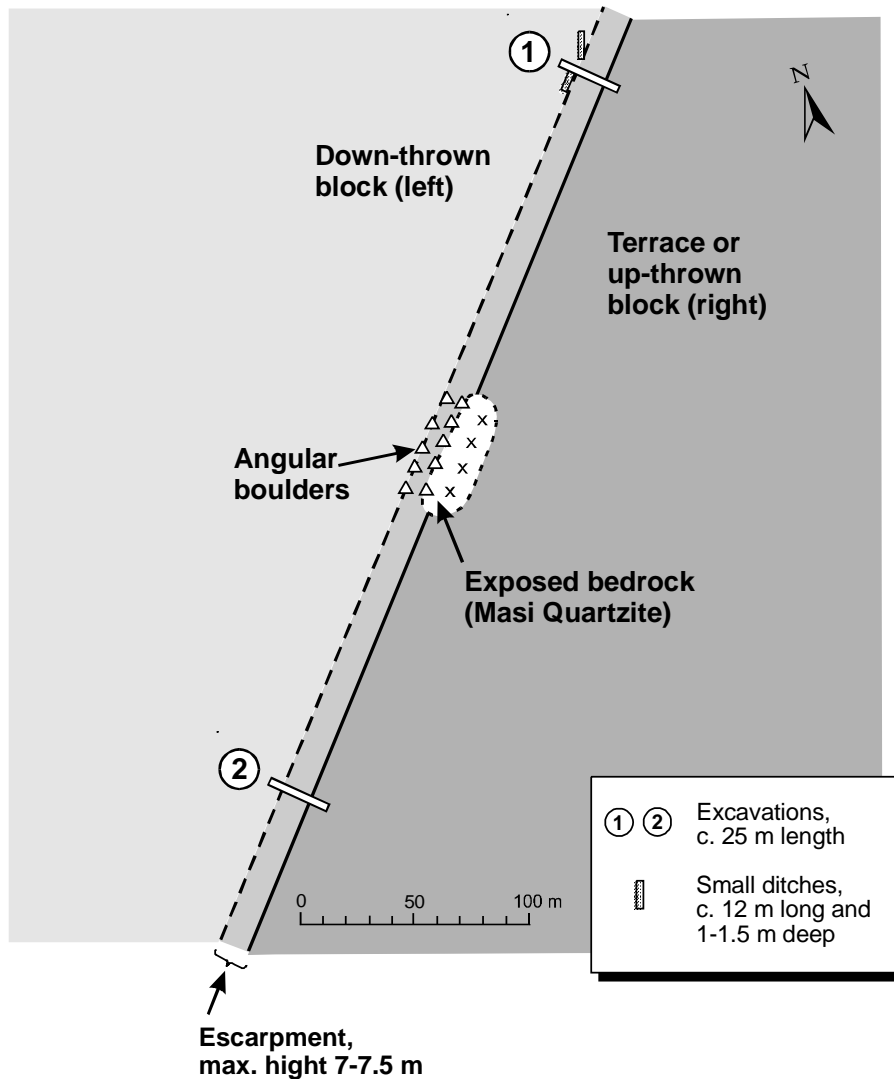
Fig. 5.2.4.   Simplified map of the survey area with excavations at Fidnajohka.
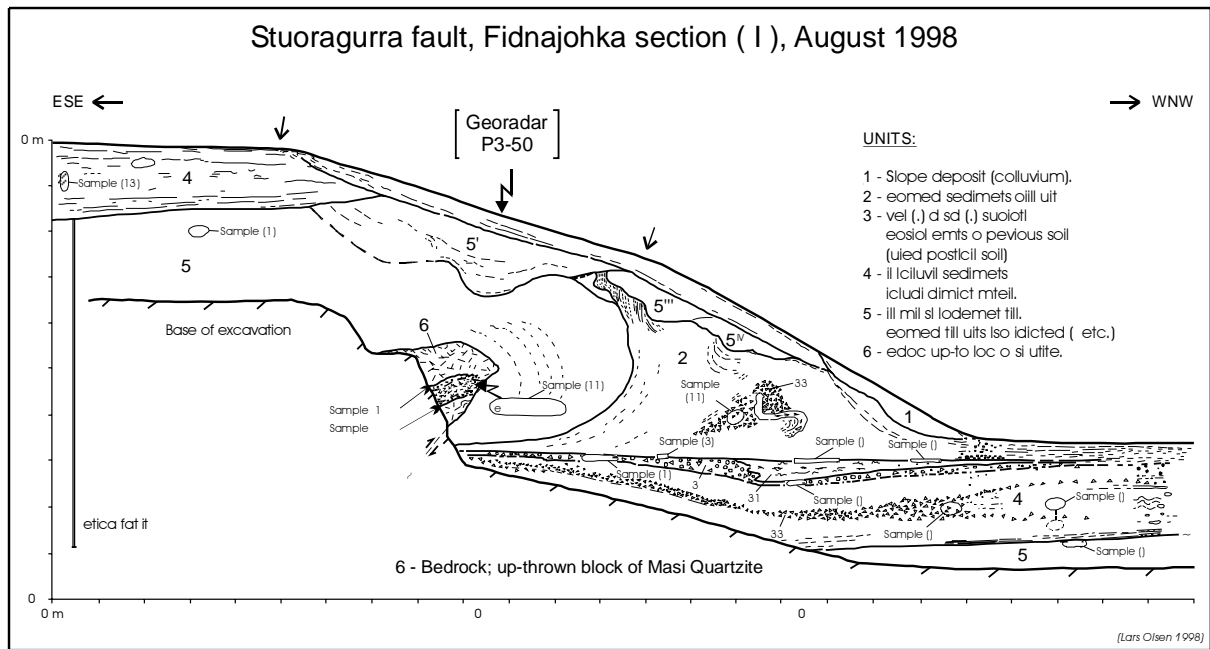
Fig. 5.2.5. Outline of the main section (I) in excavation 1 at Fidnajohka. The orientation of the section is normal to the fault. The nose of the up-thrown block of bedrock (6) is buried by deformed basal till (5E) and glaciofluvial gravel and sand (2, 3 & 4), with colluvial slope deposits (1) on top.

Fig. 5.2.6. Photograph of the trench (excavation 1) across the Stuoragurra Fault at Fidnajohka, with the bedrock nose of the up-thrown block and the deformed overburden visible.

98
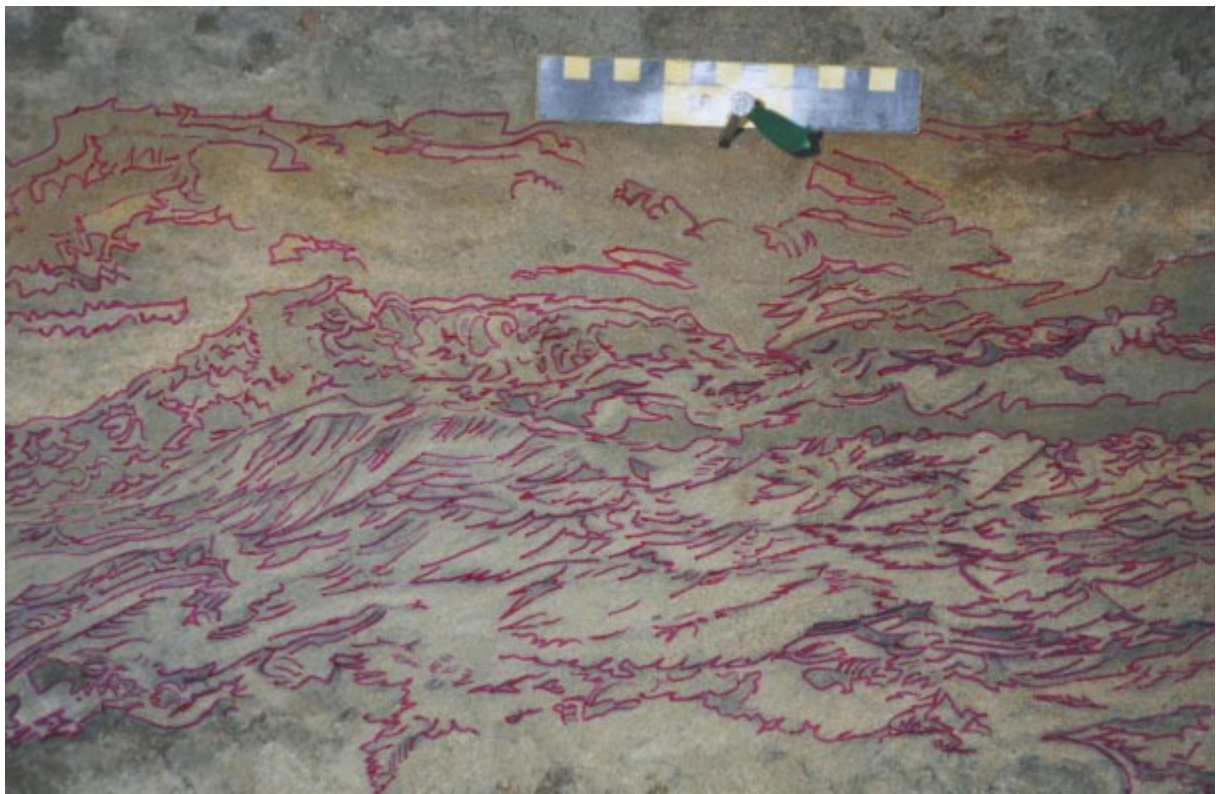
Fig. 5.2.7.   Photographs of convolutions and other disturbances in the sediments in the main section from excavation 1 at Fidnajohka. See also Fig. 5.2.5

I (0m)

II (m)

61%

1%

%

1%

A A

A A

o oer n
    ure

    ure

III (m)

I (m)

%

1%

%

1%

A A

A A

A A

Well rounded (4)

ounded ()

unulr ()

nulr ()

nulr reded
unulr derounded

(m)

I (0m)

%

1%

%

1%

A A

A A

m

0
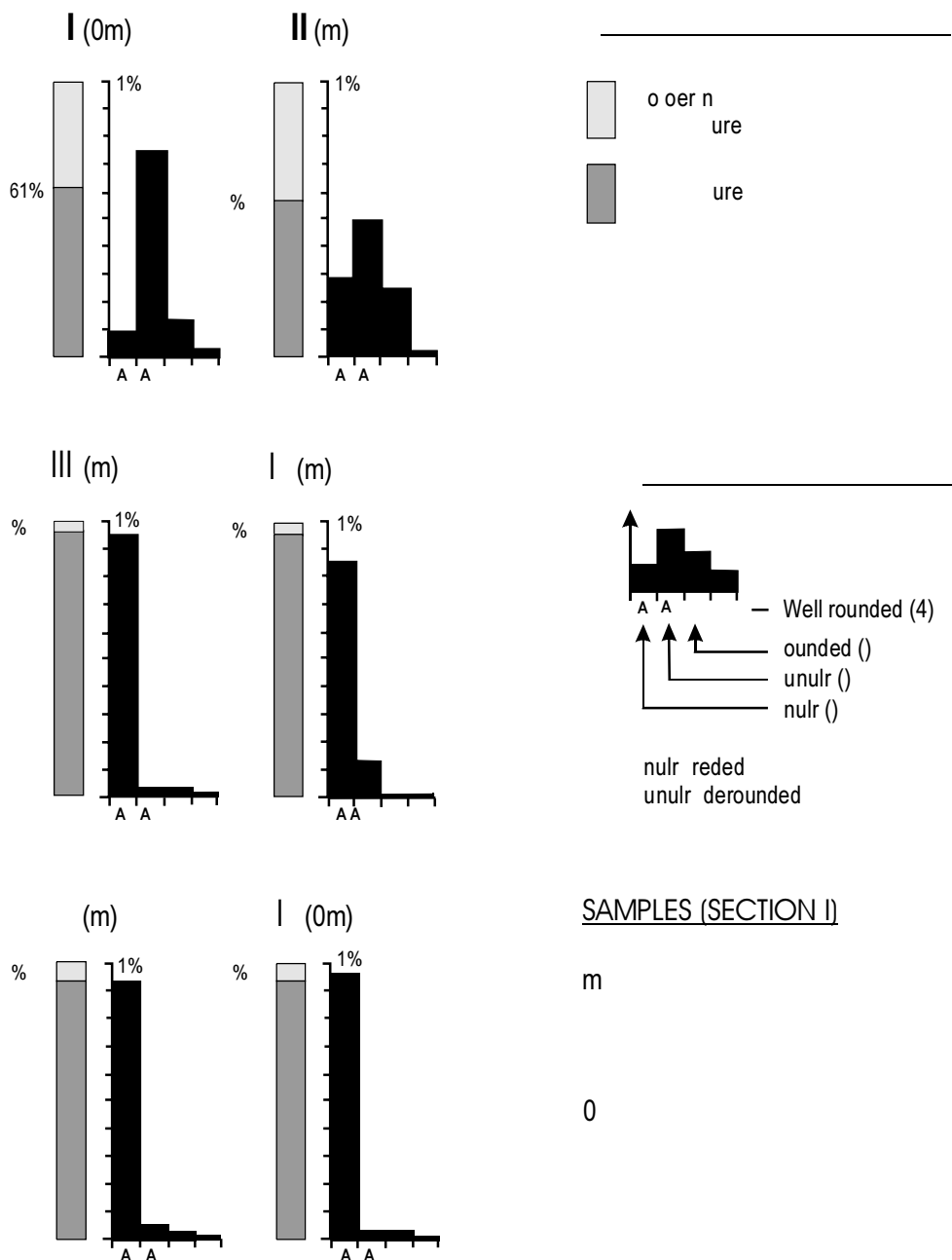
Fig. 5.2.8.   Petrography (rock types) and roundness of gravels from the diamict zones in the glacifluvial material (I and II) and from gravel injections produced by the fault process, occurring in wedges an unregular clast-supported lenses (III, IV, V & VI).
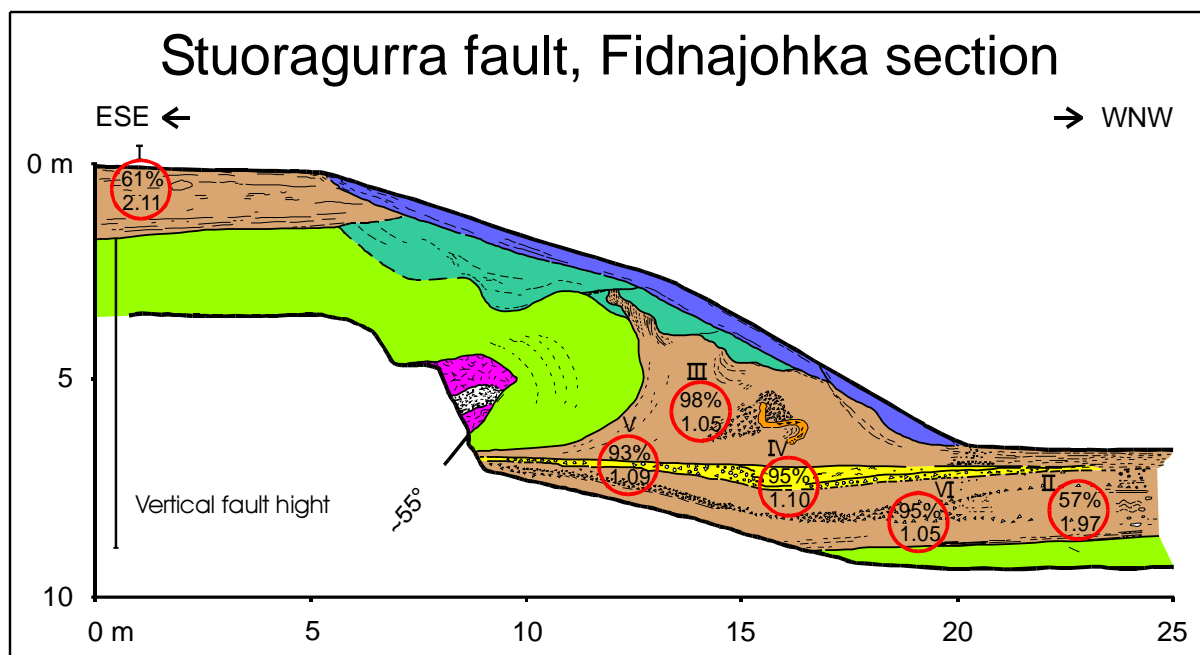
Fig. 5.2.9.   Data from Fig. 5.2.8 plotted according to sample position in the main section at Fidnajohka. The content of Masi Quartzite (%) and the roundness index are indicated. The roundness index may vary between 1 (100% sharpedged) and 4 (100% well rounded), but is here either close to 1, for the gravel injections, or c. 2 for the glacigenic diamict zones included in the glacifluvial sediments.

5.2.2   References

Bungum, H. & Lindholm, C. 1998: Seismo- and neotectonics in Finnmark, Kola Peninsula and the southern Barents Sea. Part 2: Seismological analysis and seismotectonics. *Tectonophysics*, 270, 15-28.

Carver, G.A. & McCalpin, J.P. 1996: Paleoseismology of Compressional Tectonic Environments. In McCalpin, J.P. (ed.): Paleoseismology. Academic Press, Inc., 183-270.

Muir Wood, R., 1989a: Extraordinary deglaciation reverse faulting in northern Fennoscandia. In Gregersen, S. & Basham, P. W. (ed.), Earthquakes at North-Atlantic passive margins: neotectonics and postglacial rebound. Kluwer Academic Publishers, Dordrecht, The Netherlands, 141-173.

Olesen, O., 1988: The Stuoragurra Fault; evidence of neotectonics in the Precambrian of Finnmark, northern Norway. Norsk Geologisk Tidsskrift 68(2), 107-118.

Olesen, O., Henkel, H., Lile, O. B., Mauring, E., Rønning, J. S. & Torsvik, T. H., 1992a: Neotectonics in the Precambrian of Finnmark, northern Norway. Norsk Geologisk Tidsskrift 72, 301-306.

Olesen, O., Henkel, H., Lile, O. B., Mauring, E. & Ronning, J. S., 1992b: Geophysical investigations of the Stuoragurra postglacial fault, Finnmark, northern Norway. Journal of Applied Geophysics 29(2), 95-118.

Olesen, O. & Dehls, J. 1998: Neotectonic phenomena in northern Norway. In: Dehls, J. & Olesen, O. 1998 (eds.): Neotectonics in Norway, Annual Technical Report 1997, NGU Report 98.016, 3-30.

Olsen, L., 1989: Bæivašgied'di 2033 III, kvartærgeologisk kart - M 1:50 000. Geological Survey of Norway.

Roberts, D., Olesen, O. & Karpuz, M. R., 1997: Seismo- and neotectonics in Finnmark, Kola Peninsula and the southern Barents Sea; Part 1, Geological and neotectonic framework. Tectonophysics 270(1-2), 1-13.

Wells, D.L. & Coppersmith, K.J. 1994: Empirical relationships among magnitude, rupture length, rupture area, and surface displacement. Bull. Seismol. Soc. Am. 84, 974-1002.

5.3 REVERSE-SLIP OFFSETS AND AXIAL FRACTURES IN ROAD-CUT BOREHOLES FROM FINNMARK: NEOTECTONIC STRESS ORIENTATION INDICATORS

By David Roberts, NGU

Summary: Reverse-slip offsets of road-cut drillholes, and axial fractures developed in the walls of many such holes, have been recorded from areas in the Porsangerfjord and Laksefjord districts of Finnmark. Displacement vectors of the offset boreholes indicate movement towards 120-136º in the Laksefjord Nappe. At the base of the Kalak Nappe and in the Gaissa Nappe in western Porsanger, reverse-slip offset is directed almost due east. Observations of the extensional axial fractures, which are considered to have developed normal to the least principal in situ stress, σ_3, at the time of blasting, support a c. ESE-WNW orientation of S_{Hmax} at or close to the surface in these parts of Finnmark.

5.3.1 Introduction

Following the NEONOR meeting and excursion in Alta in August '98, three days were spent examining drillholes (boreholes) in road-cuts over a wide area extending from western Porsangerfjord to eastern Laksefjord in north-central Finnmark county, with the purpose of registering possible reverse-slip displacements in the boreholes as well as recording the occurrence and trends of axial fractures in these anthropogenic features. Such structures – recent reverse-slip offsets and axial fractures – are important in neotectonic research in that they can provide valuable information on the regional and local stress fields in the uppermost crust, providing that there is a measure of consistency in the recorded data in any one particular area.

In addition to the work in the Porsangerfjord-Laksefjord district, one day was spent further east, on Varanger Peninsula, searching for similar structural features, observing strandlines for possible fault displacements, and also sampling certain rock-types for isotopic dating. During the course of other work in another NGU project, in the counties of Nord- and Sør-Trøndelag, Central Norway, an offset borehole was also observed in the Roan district of the Fosen Peninsula. This is mentioned briefly, and illustrated, towards the end of this report.

5.3.2 Regional geology

The features described in this report, with the one exception from Roan, are all in metasedimentary rocks of the Caledonian fold belt. In terms of established Caledonide tectonostratigraphy (Roberts & Gee 1985), the examined boreholes are in rocks of the Lower and Middle Allochthons, namely the Gaissa (Lower), and the Laksefjord and Kalak (Middle) Nappe Complexes (Fig. 5.3.1). Details of the internal lithostratigraphies and structural histories of these nappes are contained in e.g. Chapman et al.(1985), Gayer et al. (1985, 1987) and Roberts (1985).
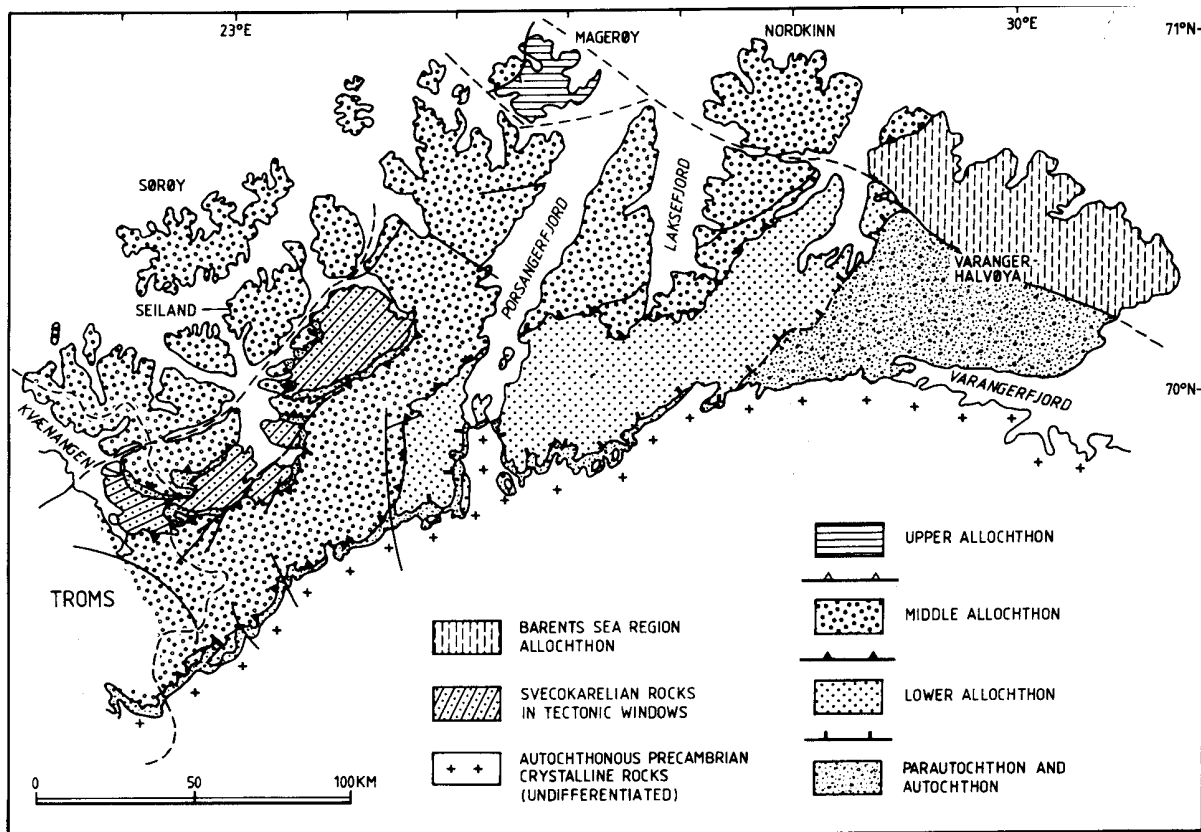
Fig. 5.3.1.   Principal divisions of the tectonostratigraphy of the Caledonides in Finnmark (from Roberts 1985). The Kalak and Laksefjord Nappe Complexes are part of the Middle Allochthon, while the Gaissa Nappe Complex forms most of the Lower Allochthon in this part of Norway.

5.3.3   The studied areas

In this brief inverstigation, the two main areas chosen for a closer examination of road-cut boreholes are in western *Porsangerfjord* and the southeastern parts of *Laksefjord*. Road-cuts along the western parts of Porsangerfjord are mainly in amphibolite-facies, multilayered psammites and pelites of the Kalak Nappe Complex. Road sections in upper anchizone to lower greenschist-facies sandstones, mudstones and dolomites of the subjacent Gaissa Nappe Complex were also examined.

In the Laksefjord district, road sections south of Lebesby in greenschist-facies phyllites of the Laksefjord Nappe Complex had earlier provided evidence of contemporary, thrust-fault displacement of one particular borehole (Roberts 1991). This locality was visited with the purpose of reexamining the offset to see if further displacement had occurred; and at the same time to take a closer look at the drillholes in this and neighbouring road-cuts. In this same district, the disused slate quarries at Friarfjord, innermost Laksefjord, were also judged to be potential sources of borehole structural data which may have a bearing on the regional in situ stress situation. Consequently, the boreholes exposed in the several faces of these quarries were investigated.

5.3.4   The Laksefjord area

The road-cut between Lebesby and Skogvika (Fig. 5.3.2) with the documented example of reverse-slip displacement of a borehole (Roberts 1991) was a primary target here. On reex-

amination, the displaced borehole (first and last observed in 1989), in phyllites of the Friar-fjord Formation (Fig. 5.3.3), did not appear to show any further detectable offset along the displacement surface. The reverse-slip vector here is towards c.118°. Careful examination of other boreholes along the discontinuous road-cuts in this same general area north of Skogvika (Fig. 5.3.2) did, however, reveal two further cases of reverse-slip offset, one of which is shown in Fig. 5.3.4. In these cases, the offsets are along two different reverse-fault surfaces, both of which are broadly parallel to that reported earlier, i.e. along the NW-dipping, axial-plane cleavage of Caledonian folds. The recorded slip vectors are 124° and 136° (Fig. 5.3.5a).
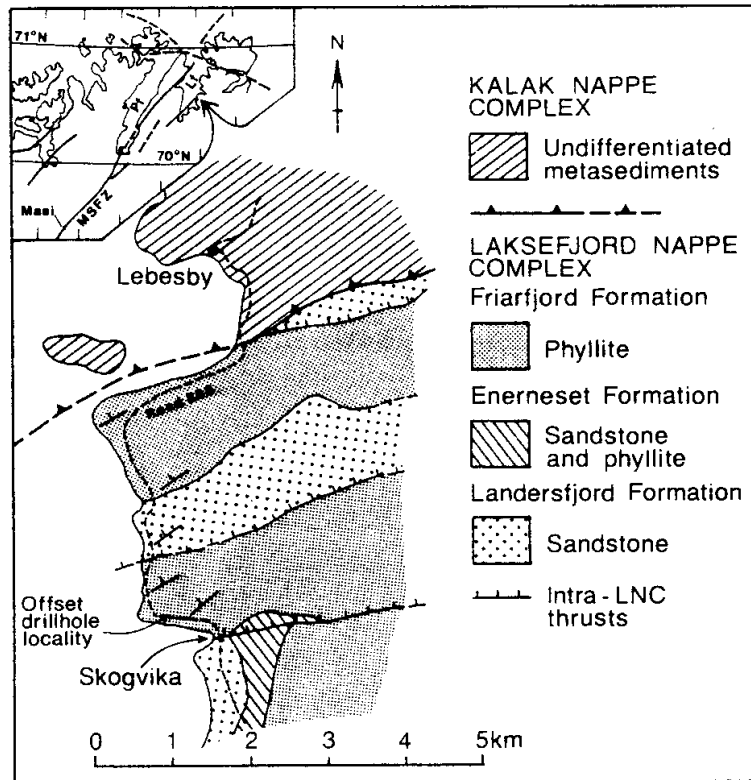
Fig. 5.3.2. Simplified geological map of the Lebesby-Skogvika area, southeast Laksefjord, showing the location of the offset drillhole (from Roberts 1991).

Fig. 5.3.3. (Left) *The offset borehole previously documented in Roberts (1991), in phyllites of the Friarfjord Formation; from Skogsvika, near Lebesby, Laksefjord, looking north-northeast. Bedding depicted by silty layers dips steeply to the left (northwest). The reverse-slip displacement of the drillhole occurred along a Caledonian slaty cleavage. Locality – 1:50, 000 map-sheet 'Lebesby' 2136 II, 3-NOR edition, grid-ref. MU0045 2270.*

Fig. 5.3.4. (Right) *Another borehole offset from a road-cut close to that in Fig. 5.3.3, in Friarfjord Formation phyllites with siltstone layers; looking northeast. Grid-ref. MU0000 2275.*

In a few of the boreholes along this same road section, *axial fractures* were observed along their walls (Fig. 5.3.6). The approximate orientations of these very narrow, near-vertical fractures could be measured by inserting the thin blade of a pocket-knife into the crack and thus record its trend. Axial fractures of this type, first oberved conjointly by John Adams and Sebastian Bell in Canada in the early 1990's and described by Bell & Eisbacher (1996), are considered to be coeval with the blasting operations. They are interpreted by these authors as gas pressure-induced extensional fractures that formed instantaneously when the charges in the drillholes were fired. In this way, they are believed to have propagated parallel to S_{Hmax} (maximum principal horizontal stress, essentially σ_1) in the plane of the two largest principal stresses, σ_1 and σ_2 (Fig. 5.3.7). The possibility that axial fractures may be present in the Lak-

sefjord boreholes was first suggested to the author by Sebastian Bell (pers. comm. 1997) in an e-mail discussion of the offset borehole (Roberts 1991) near Lebesby.
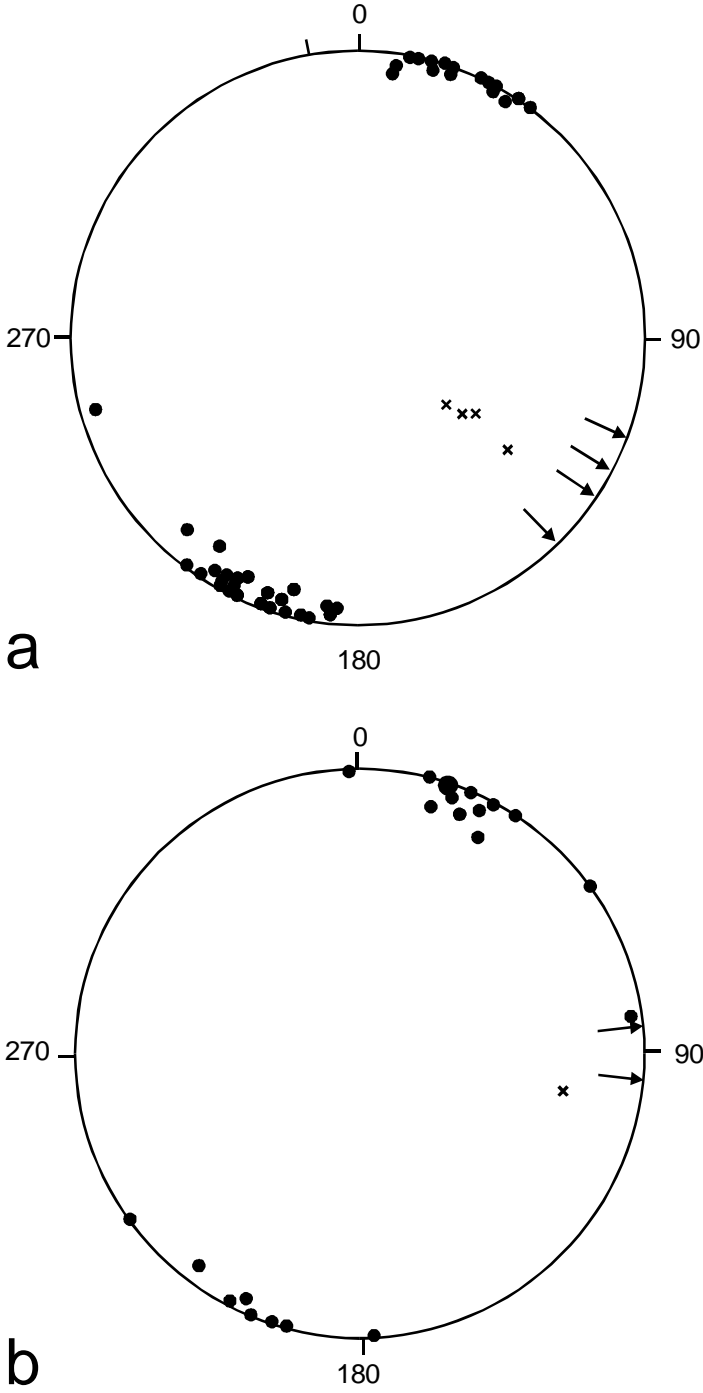
Fig. 5.3.5.   Structural data from boreholes from southeastern Laksefjord and western Por-sangerfjord. Equal area, lower hemisphere. (a) Lebesby-Skogsvika road sections and Friar-fjord slate quarries, Laksefjord Nappe Complex. (b) Road sections north and south of Older-fjord, Russenes, Kolvik bay, and south of Kolvik, Kalak and Gaissa Nappe Complexes. Dots – poles to axial fractures: crosses – poles to reverse-slip faults displacing boreholes: arrows – hanging-wall reverse-slip displacement vectors.

*Fig. 5.3.6.   Axial fracture in a borehole wall at Skogvika, Laksefjord, in Friarfjord For-
mation phyllites with silstone layers; looking northwest. Indications of borehole offset can be
seen to the right of the pencil (hanging-wall coming 'up', out of the picture).*
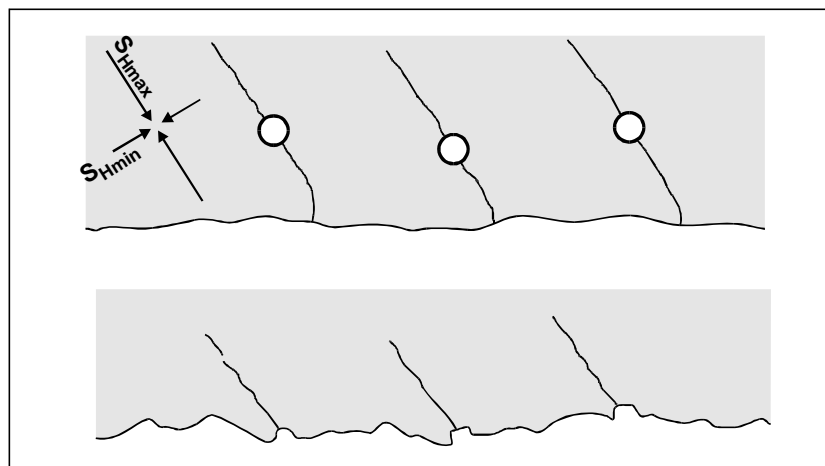
*Fig. 5.3.7.   Sketches showing the inferred origin of axial fractures in the walls of vertical
or near-vertical boreholes at the time of blasting; modified from Bell & Eisbacher (1996).
Upper sketch: Vertical view of the rock body at the time of blasting, showing gas pressure-
induced fractures parallel to S_{Hmax}. Lower sketch: Vertical view of the new rock face after
blasting and removal of the rock mass.*

Measurements of the few, convincing axial fractures at these localities showed that they trend at about 120º-300º (Fig. 5.3.5a), which is more or less parallel to the borehole displacement vector. Since the reverse-faulting affecting three of the boreholes accords with a regional maximum horizontal compressive stress trending between NW-SE and WNW-ESE (Roberts 1991), then the axial fractures do, in fact, fit quite readily with an interpretation as extensional fractures which developed by a sudden release of accumulated strain energy. This also fits quite well with the actual occurrence and distribution of axial fractures in what now remains of the borehole walls. In these road-cuts, which are aligned broadly parallel to the borehole offset trend, i.e. roughly WNW-ESE, prominent axial fractures are almost entirely absent from the borehole walls. Conversely, where the road cuts obliquely through the phyllites or even normal to the displacement vector, then the extensional axial fractures are easier to detect.

A visit to the old slate quarries at Friarfjord proved particularly rewarding. Here, only one convincing example of an offset drillhole was found in the main quarry, the displacement directed towards c. 110º (Fig. 5.3.5a). Along this same c. NW-SE-trending quarry wall, axial fractures were noticeably absent. However, examination of steep to near-vertical boreholes in steep quarry faces aligned c. NE-SW revealed a comparative abundance of well developed axial fractures (Fig. 5.3.8). Almost every borehole wall carries discernible axial fractures, though some are more continuous than others. Measurements of the axial fractures showed a clear clustering around a WNW-ESE trend (Fig. 5.3.5a), which parallels the displacement vector of the one recorded borehole offset in these quarries. Thus, an interpretation of these fractures as extensional fractures relating to the local, and regional, stress regime seems perfectly reasonable. In this case, even if no single borehole offset had been detected, the abundance and consistency of trend of the axial fractures would have provided a fairly reliable indicator of the orientation of S_{Hmax}, i.e. c. WNW-ESE.

5.3.5 The western Porsangerfjord area

Road-cuts through rocks of the Kalak Nappe Complex provided comparatively meagre neo-tectonic stress orientation data from a study of available boreholes in selected areas. Along the south side of Olderfjorden, southeast of Russenes, where the E6 road runs almost E-W, neither borehole offsets nor axial fractures were found. The absence of axial fractures on the concave borehole walls here is perhaps not too surprising as the general trend of the road-cuts is broadly parallel to that of the postulated maximum principal horizontal stress.

Some few kilometres north of Russenes, however, where there are several long road-cuts trending roughly NNE-SSW, steep to vertical axial fractures were observed and measured in a few of the borehole walls. Their general trend is WNW-ESE (Fig. 5.3.5b).

Farther south along western Porsangerfjord, near Kolvik, a road-cut in mylonites at the base of the Kalak Nappe Complex exposes a curviplanar reverse-fault which displaces a borehole by 6-8 mm. The displacement vector is here towards 096º. Only one other, reverse-slip, borehole displacement was observed in this western Porsangerfjord area, in thin-bedded siltstones and shales of the Gaissa Nappe Complex. In this particular case, the bedding-parallel offset is c. 1.5 cm and is directed towards 085º (Fig. 5.3.5b). Along road-cuts in the same Gaissa lithologies in this same general area, axial fractures (Fig. 5.3.9) show a WNW-ESE to almost E-W trend, which is in accord with the local borehole displacement vector.

Fig. 5.3.8. (Left)   Well developed axial fracture in a borehole in slates of the Friarfjord Formation, Laksefjord Nappe Complex, from the roofing slate quarries at Friarfjord, close to the old quay. 1:50,000 map-sheet 'Adamsfjord' 2135 I, 3-NOR edition, grid-ref. MU9695 1810. This particular quarry face trends N-S, and the photo is taken looking due west.

Fig. 5.3.9. (Right)   Axial fracture in a borehole in thin-bedded shales, siltstones and sand-stones of the Stabbursdal Formation, Gaissa Nappe Complex, western Porsangerfjord. Looking west-northwest. Locality – 1:50,000 map-sheet 'Lakselv' 2035 III, 3-NOR edition, grid-ref. MT2320 9380.

5.3.6   Concluding remarks

The observations made in the road-cuts in all three nappe complexes are quite similar in terms of the trends of the axial fractures in boreholes, as well as in the displacement vectors along minor faults which offset the near-vertical boreholes in a reverse-slip sense (Fig. 5.3.5). Axial fractures show fairly consistent c. WNW-ESE trends throughout the Porsangerfjord-Laksefjord region from nappe to nappe. Accepting that these features are extensional fractures that developed normal to the least principal in situ stress, σ_3, and propagated parallel to S_{Hmax} at the time of blasting, then they provide a reasonably reliable indicator of neotectonic stress orientations at or close to the surface in these parts of Finnmark.

By and large, the displacement vectors of the reverse-offset boreholes also corroborate this general stress regime, especially in the phyllites and slates of the Laksefjord Nappe where the

hanging-wall blocks are displaced towards 120º-136º. In the two examples from the Gaissa Nappe and mylonites at the base of the Kalak, however, the displacement vectors are almost due east. Whether or not this difference is kinematically meaningful is impossible to say at this stage in view of the sparsity of the data. Nevertheless, there is a possibility that the present-day S_{Hmax} in western parts of the metamorphic allochthon in Finnmark may be orientated rather more E-W than in areas farther east where a WNW-ESE trend obtains.

Farther south in Finnmark, the post-glacial Stuoragurra Fault trends NE-SW and carries evidence of NW-directed reverse-slip displacement (Olesen 1988, Olesen et al. 1992, Roberts et al. 1997), including quite recent movement (details may be found in other parts of this multi-author NEONOR project report). In that area at least, S_{Hmax} is orientated approximately NW-SE, confirmed by focal mechanism solutions for five earthquakes recorded along or close to the Stuoragurra Fault (Bungum & Lindholm 1997) (Fig. 5.3.10). Earthquake mechanisms in northern Sweden also show a comparable NW-SE trend for present-day horizontal crustal compression (Slunga 1989).
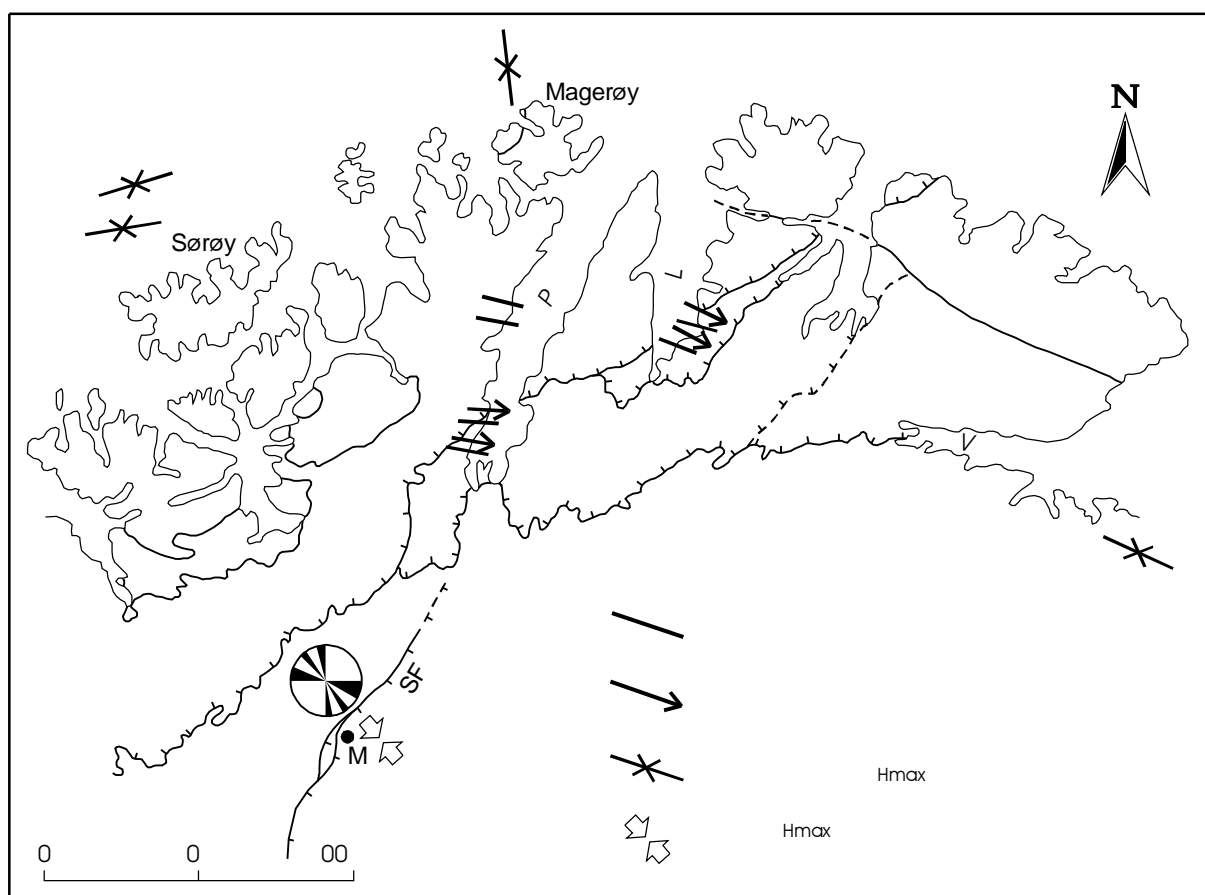
Fig. 5.3.10.   Contemporary horizontal compressive stress data from Finnmark. The break-out data are from the World Stress Map compiled by Zoback et al. (1989). The data from the Stuoragurra Fault, near Masi, including the rose diagram of S_{Hmax} derived from 5 fault-plane solutions, are from Bungum & Lindholm (1997).

A recent attempt at determining the principal stresses in the vicinity of the Stuoragurra Fault using the hydraulic fracturing method was not successful, due to the presence of intensive fracturing in the Masi quartzite at the test localities (Jóhannsson, this report). Twenty-four test sections in three 50 m-deep boreholes were measured, but no satisfactory results were obtained. The fracture pattern in the quartzite is dominated by near-vertical, c. E-W-striking

joints, and it is possible that this trend may approximate to that of the current S_{Hmax} in this district (Jóhannsson 1998).

Taking Finnmark and northern Norway as a whole, the current maximum horizontal compressive stress operative at upper crustal levels does, however, appear to be showing some variations in trend from area to area (Fig. 5.3.10). More stress data are required, however, before a more meaningful picture of in situ stress distribution can be obtained for this part of Norway. Current stress pattern data available from this region are insufficient to allow more than generalisations to be made (Myrvang 1988, Stephansson 1988), but the regional σ_1 does appear to trend broadly NW-SE to WNW-ESE (Fig. 5.3.10).

5.3.7 *An addendum from Trøndelag*

During the course of fieldwork in the Roan district of the Fosen Peninsula, Sør-Trøndelag, Central Norway in July this year, as part of another NGU project, an offset borehole displaced in a reverse-slip sense was observed in quartz-monzonitic granulite gneisses of Proterozoic age. The offset, of some 3.5-4 cm, is directed towards c. 295° on an east-dipping (008°/28°) fault surface (Fig. 5.3.11). Other parallel, E-dipping, fault surfaces along this particular road-cut show similar but smaller, reverse-slip borehole displacements. Although these few data alone are not definitive, they do point to a local S_{Hmax} trending c. WNW-ESE. A closer inspection of road-cut drillholes in this area seems warranted.

Fig. 5.3.11.   Offset borehole in granulite gneisses, south of Beskelandsfjorden, Roan, Fosen Peninsula, Sør-Trøndelag; looking south. Locality – 1:50,000 map-sheet 'Roan' 1623 III, 3-NOR edition, grid-ref. NS6075 1815.

5.3.8 References

Bell, J.S. & Eisbacher, G.H. 1996: Neotectonic stress orientation indicators in southwestern British Columbia. *Geological Survey of Canada, Current Research 1996-A,* 143-154.

Bungum, H. & Lindholm, C. 1997: Seismo- and neotectonics in Finnmark, Kola and the southern Barents Sea, Part 2: Seismological analysis and seismotectonics. *Tectonophysics 270,* 15-28.

Chapman, T.J., Gayer, R.A. & Williams, G.D. 1985: Structural cross-sections through the Finnmark Caledonides and timing of the Finnmarkian event. *In* Gee, D.G. & Sturt, B.A. (eds.) *The Caledonide orogen – Scandinavia and related areas.* John Wiley & Sons, Chichester, 593-609.

Gayer, R.A., Hayes, S.J. & Rice, A.H.N. 1985: The structural development of the Kalak Nappe Complex of eastern and central Porsangerhalvøya, Finnmark, Norway. *Norges geologiske undersøkelse Bulletin 400,* 67-87.

Gayer, R.A., Rice, A.H.N., Roberts, D., Townsend, C. & Welbon, A. 1987: Restoration of the Caledonian Baltoscandian margin from balanced cross-sections: the problem of excess continental crust. *Transactions of the Royal Society of Edinburgh: Earth Sciences 78,* 197-217.

Myrvang, A. 1988: Rock stress measurements in Norway: recent results and interpretations. *Report, Workshop on Nordic rock stress data. SINTEF, Trondheim, 10 October 1988, 5 pp.*

Olesen, O. 1988: The Stuoragurra Fault, evidence of neotectonics in the Precambrian of Finnmark, northern Norway. *Norsk Geologisk Tidsskrift 68,* 107-118.

Olesen, O., Henkel, H., Lile, O.B., Mauring, E., Rønning, J.S. & Torsvik, T.H. 1992: Neotectonics in the Precambrian of Finnmark, northern Norway. *Norsk Geologisk Tidsskrift 72,* 301-306.

Roberts, D. 1985: The Caledonian fold belt in Finnmark: a synopsis. *Norges geologiske undersøkelse Bulletin 403,* 161-177.

Roberts, D. 1991: A contemporaneous small-scale thrust-fault near Lebesby, Finnmark. *Norsk Geologisk Tidsskrift 71,* 117-120.

Roberts, D. & Gee, D.G. 1985: An introduction to the structure of the Scandinavian Caledonides. *In* Gee, D.G. & Sturt, B.A. (eds.) *The Caledonide orogen – Scandinavia and related areas.* John Wiley & Sons, Chichester, 55-68.

Roberts, D., Olesen, O. & Karpuz, M.R. 1997: Seismo- and neotectonics in Finnmark, Kola Peninsula and the southern Barents Sea. Part 1: Geological and neotectonic framework. *Tectonophysics 270,* 1-13.

Slunga, R. 1989: Earthquake mechanisms in northern Sweden, October 1987- April 1988. *Svensk Kärnbränslehandtering AB, Technical Report 89-28,* 165 pp.

Stephansson, O. 1988: Ridge push and glacial rebound as rock stress generators in Fennoscandia. *Bulletin of the Geological Institution of the University of Uppsala 14,* 39-48.

Zoback, M.L. et al. (29 co-authors) 1989: Global patterns of tectonic stress. *Nature 341,* 291-298.

5.4 GROUND-PENETRATING RADAR PROFILES ACROSS POSTGLACIAL FAULTS AT KÅFJORD (TROMS), MASI (FINNMARK) AND SODANKYLÄ, FINLAND

By Eirik Mauring, Jan Steinar Rønning and John Dehls, NGU

5.4.1 Introduction

Ground-penetrating radar (GPR) measurements have been carried out across presumed postglacial faults at Kåfjord (Troms) and Masi (Finnmark) in Northern Norway and at Sodankylä, Finland.

The purpose of the measurements was to map the subsurface extension of the faults, and to clarify whether the Nordmannsvik fault (Kåfjord) is a gravitational induced fault or a true tectonic post-glacial fault. The measurements were carried out by Jan Steinar Rønning in the period of 08.08-19.08-1998. Processing was carried out by Eirik Mauring. Interpretation of GPR records was done by Eirik Mauring, Jan Steinar Rønning and John Dehls.

5.4.2 Instrumentation and data acquisition

GPR measurements were carried out along one profile at Kåfjord and five profiles at Masi and Sodankylä. At the two latter locations, common mid-point (CMP) records were obtained for velocity analysis and depth conversion of the GPR records. Measurements were carried out using pulseEKKO IV GPR system (manufactured by Sensors & Software Inc., Canada). Transmitter frequency and voltage were 50 MHz and 1000 V respectively. The antennae separation was 1 m and the sample interval was 1.6 ns (nanoseconds). Profile information and additional acquisition parameters are listed in Table 5.4.1.

Table 5.4.1.   Profile information and acquisition parameters.

Location	Profile #	Profile length (m)	Step size (m)	Recording time (ns)	Stacks
Kåfjord	4	914	0.5	1500	16
Masi	1	170	0.5	800	32
Masi	2	75	0.5	1000	16
Masi	2b	75	0.5	1000	16
Masi	3	100	0.5	1000	32
Masi	3b	100	0.5	1000	32
Sodankylä (Step 0.5)	1	150	0.5	700	32
Sodankylä (Step 0.2)	1	150	0.2	700	32
Sodankylä (Step 0.5)	2	300	0.5	700	32
Sodankylä (Step 0.2)	2	250	0.2	700	32
Sodankylä (Step 0.5)	3	300	0.5	700	32
Sodankylä (Step 0.1)	3	50	0.1	500	64
Sodankylä	4	225	0.5	600	32
Sodankylä	5	160	0.5	600	32

5.4.3 Processing

CMP measurements were carried out for velocity analysis at Masi and Sodankylä. At both locations, the correct CMP stacking velocity seems to be c. 0.10 m/ns. Hence, a velocity of 0.10 m/ns was selected for depth conversion at both localities.

After data acquisition, some GPR records were terrain corrected. Terrain variations were corrected for using elevation information from comments on the GPR records. During plotting, an exponential gain function was applied to the data to compensate for spherical divergence and attenuation losses. In addition, 5-point stacking along traces was applied to reduce high-frequency noise.

5.4.4 Results

Some of the profiles give no information on faulting activity, and these profiles are not described in the text. However, digital data from these profiles are available from NGU.

Kåfjord

One of the objectives of the investigations at Kåfjord is to try to determine whether the Nordmannsvik fault is a gravitational induced fault or a true tectonic postglacial fault. Varnes et al. (1989) suggests that gravity induced sliding is most likely to occur when the elevation difference is greater than 300 m. At Kåfjord, the slope of the terrain is 10-12°, and the elevation difference between the fault scarp and the valley bottom is 150-200 m. Thus, gravitational sliding seems less likely, but still has to be considered. Earlier GPR investigations (Mauring et al., 1997, Dehls & Olesen, 1998) outlined a dipping reflector that was interpreted as a postglacial fault. Although less likely, the fault could represent gravitational sliding as mentioned above. A fault resulting from gravitational sliding should have a gentler dip towards the valley bottom.

An additional GPR profile extending down to the valley bottom was recorded as part of the investigations of 1998. The suggested location for this profile was along a creek to the east of the earlier profiles (Fig. 5.4.1), giving a shorter distance down to bedrock, thus increasing the penetration into bedrock. It turned out to be difficult to make a traverse along the creek due to rough terrain and abundance of boulders. The profile was placed close to the creek (Fig. 5.4.1). Most reflectors in the record (not presented here) represent structures in the overburden with very little penetration into bedrock. Hence, the record gives no information about structures in the bedrock, and the problem of whether the fault represents gravity induced sliding or tectonic activity still remains unresolved.
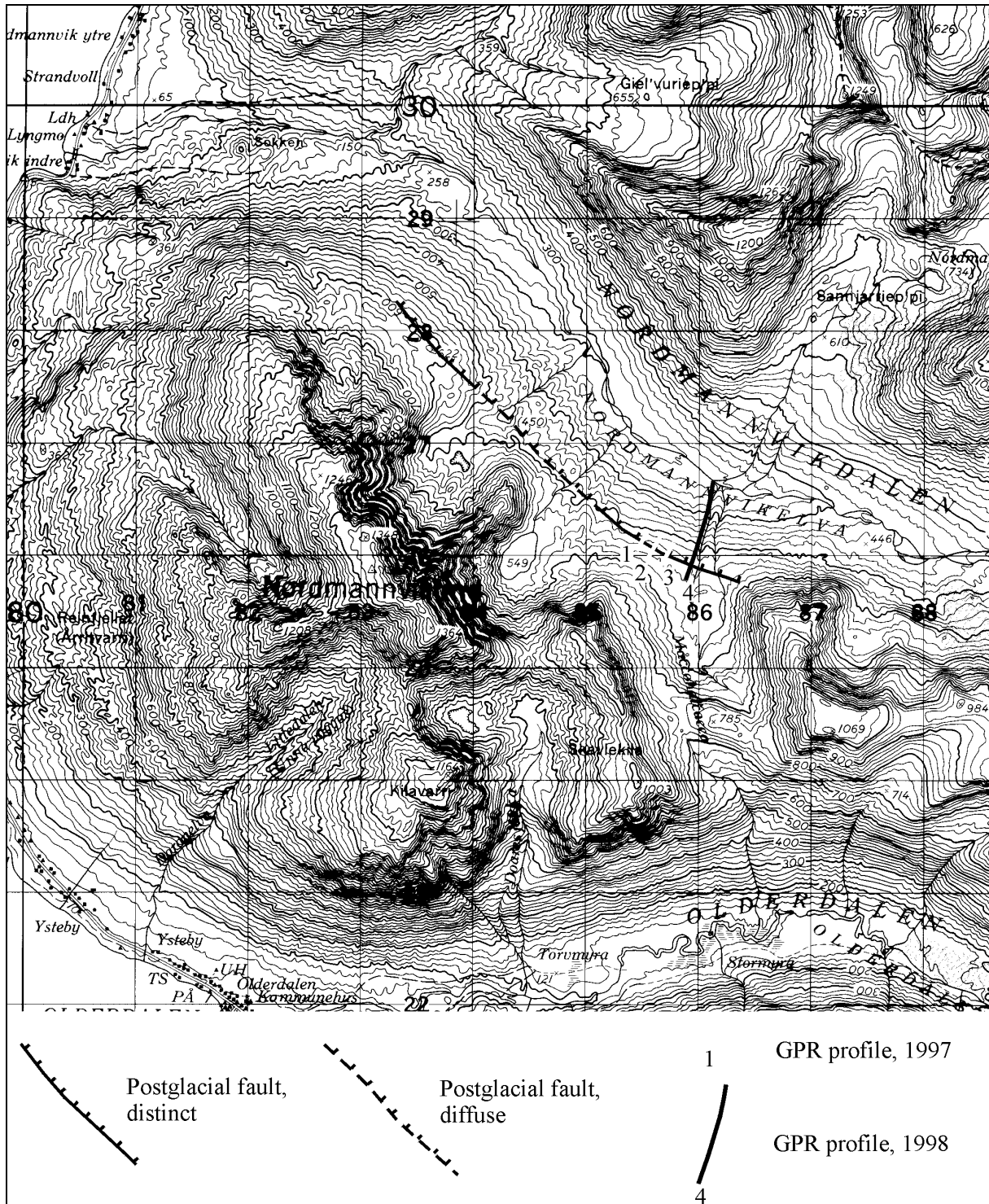
Fig. 5.4.1.   Map of the investigated area at Nordmannvikdalen, Kåfjord (scale 1:50 000).

Masi

This area has been subject to previous extensive geophysical investigations (Olesen et al., 1990 & 1992, Mauring et al., 1997, Dehls & Olesen, 1998). The presence of a postglacial fault is evident in this area. The fault is named the Stuoragurra fault which can be traced in a SW-NE direction for 80 kilometers. The fault is reverse. Previous GPR measurements along profile 807 (Figs. 5.4.2 and 5.4.3) delineated fractures running subparallel to the postglacial fault at c. 30°. Additional GPR measurements close to this profile have been carried out in 1998. Not all profiles are described in this report.
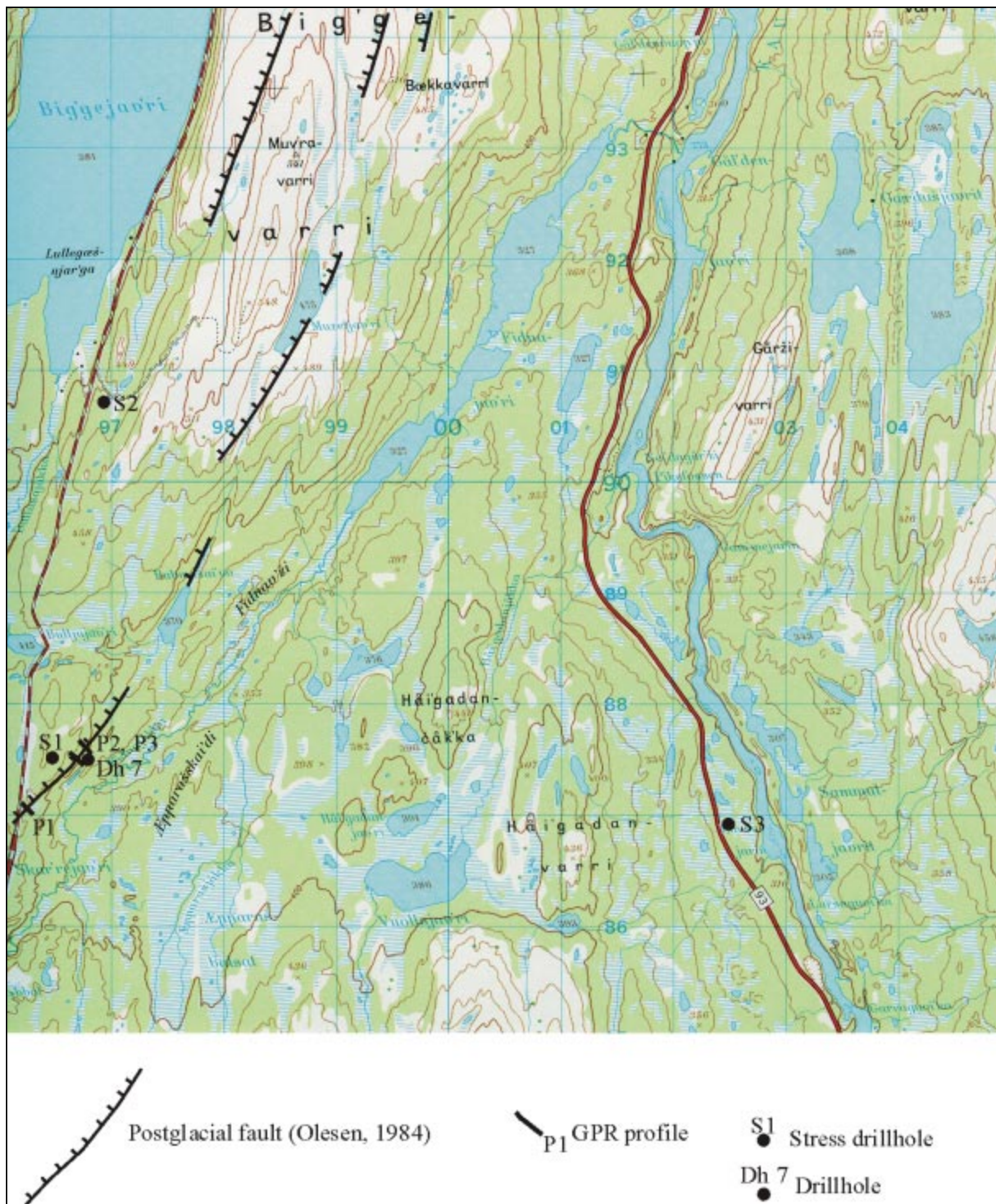
Fig. 5.4.2.   Map showing the location of the investigated area at Masi (Scale 1:50 000).
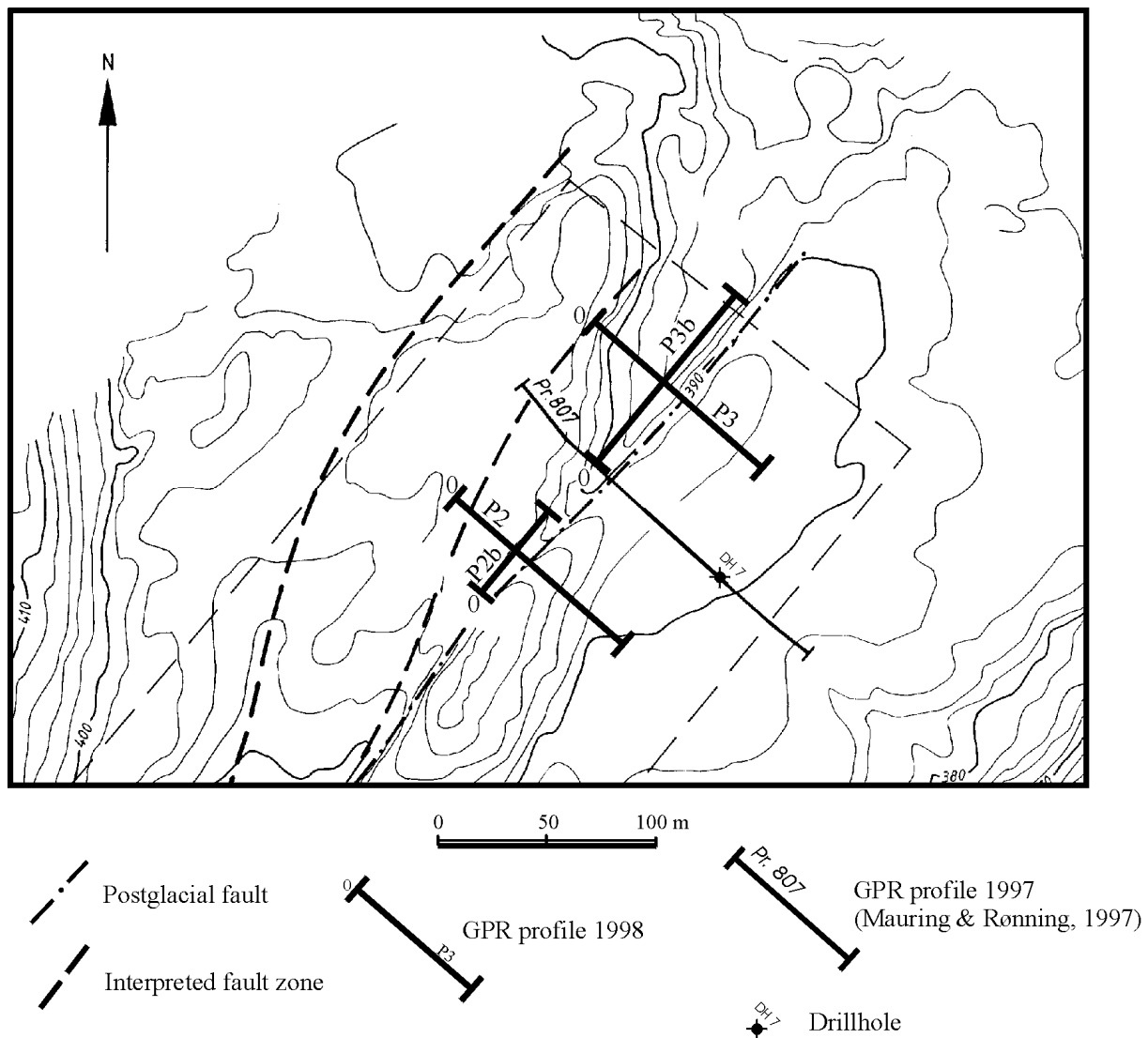
Fig. 5.4.3.   Detailed location map from Masi.

P1

The location of the profile is shown on Fig. 5.4.2. The record shows no evidence of postglacial faulting and is not presented here.

P2

The location of the profile is shown on Fig. 5.4.3. The record is shown in Fig. 5.4.4, with the interpretation in the right part of the figure. The bedrock can easily be identified as a distinct reflector along most of the profile. A vertical offset consistent with faulting is indicated between positions 32 and 42. The offset is in the order of 5 m. Dipping structures that are possibly related to reverse faulting have been interpreted.

P3

A dipping structure possibly related to reverse faulting can be seen on the record between positions 55 and 70 (Fig. 5.4.5). The bedrock is represented as a very prominent reflector between positions 50 and 100. Several probe drillings have been carried out between positions 20 and 55. These mostly gave information on depth to bedrock which has been used in the interpretation of the GPR record shown in the right part of Fig. 5.4.5. Depth to bedrock is in the order of 5 m between positions 0 and 40. The probe drillings show that the overburden mainly consists of very coarse material (sand/gravel, coarse till). Drillhole 6 shows a depth to solid bedrock of c. 13 m,

while the GPR record shows the presumed bedrock reflector at a depth of 5-6 m where the material has been characterised as till in the probe drilling log. Rather than till, it is probably heavily fractured or weathered bedrock. In the area of faulting (40-55), the bedrock probably has a vertical displacement of 6-7 m according to the GPR record.
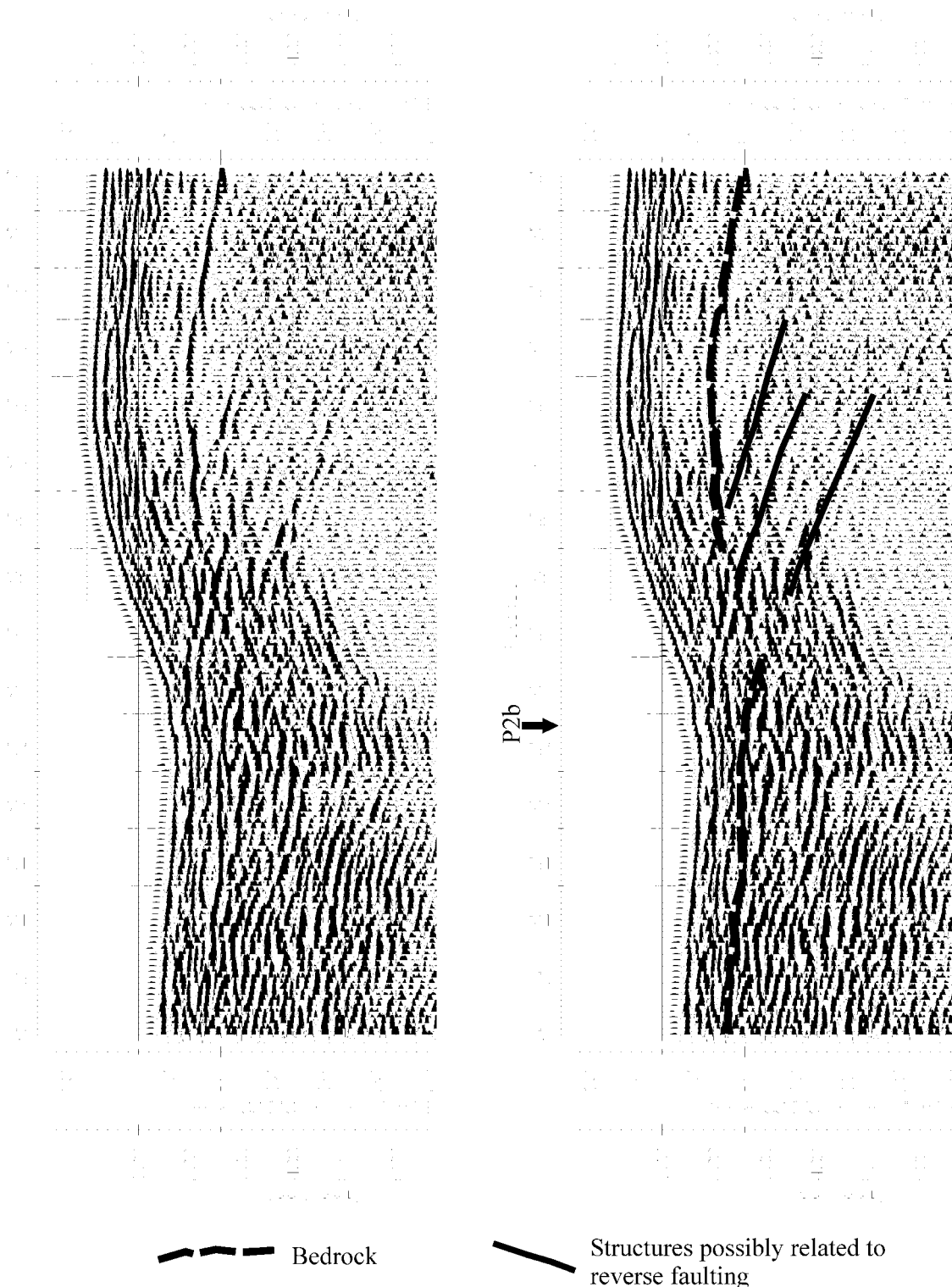
Fig. 5.4.4.   GPR record P2 from Masi. Right part shows interpretation.

5
⇩ Probe drilling   Bedrock   Structure possibly related to reverse faulting
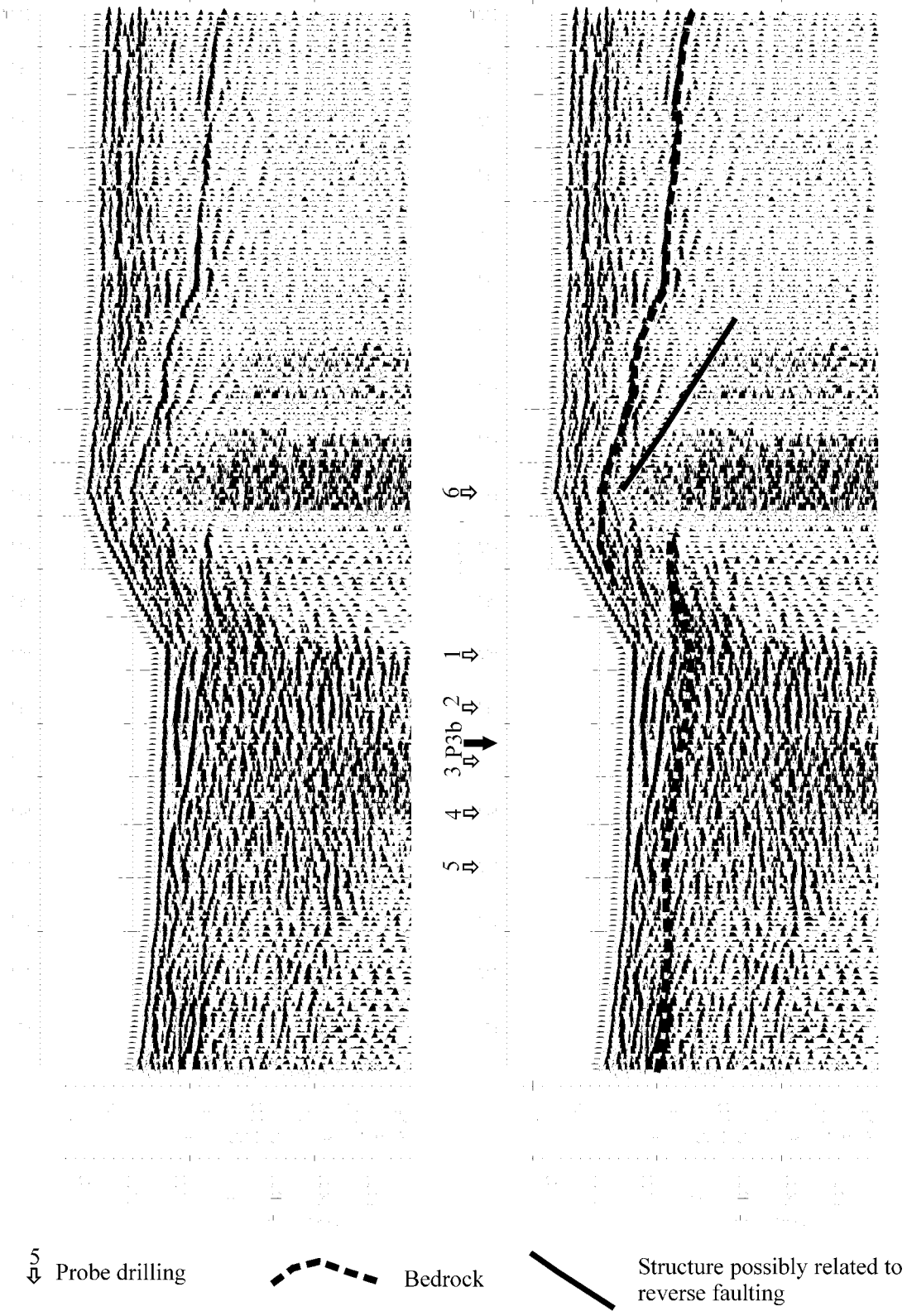
Fig. 5.4.5.   GPR record P3 from Masi. Right part shows interpretation.

Sodankylä

GPR measurements have been carried out across the Vaalajärvi fault zone, which is located c. 22 km west of Sodankylä in northern Finland (Fig. 5.4.6). The structure within the area is character-

ised as a postglacial fault, which has surface expressions in terms of ridges and depressions. Several GPR profiles traverse the presumed postglacial fault (see Fig. 5.4.6). Only one profile (P4) shows features indicating normal faulting (see Fig. 5.4.7). These features are dipping reflectors, where several have a surface expression as vertical offsets. Structures between positions 60 and 135 and positions 160-200 are dipping in opposite directions. Structures within the latter area are probably secondary collapse features.
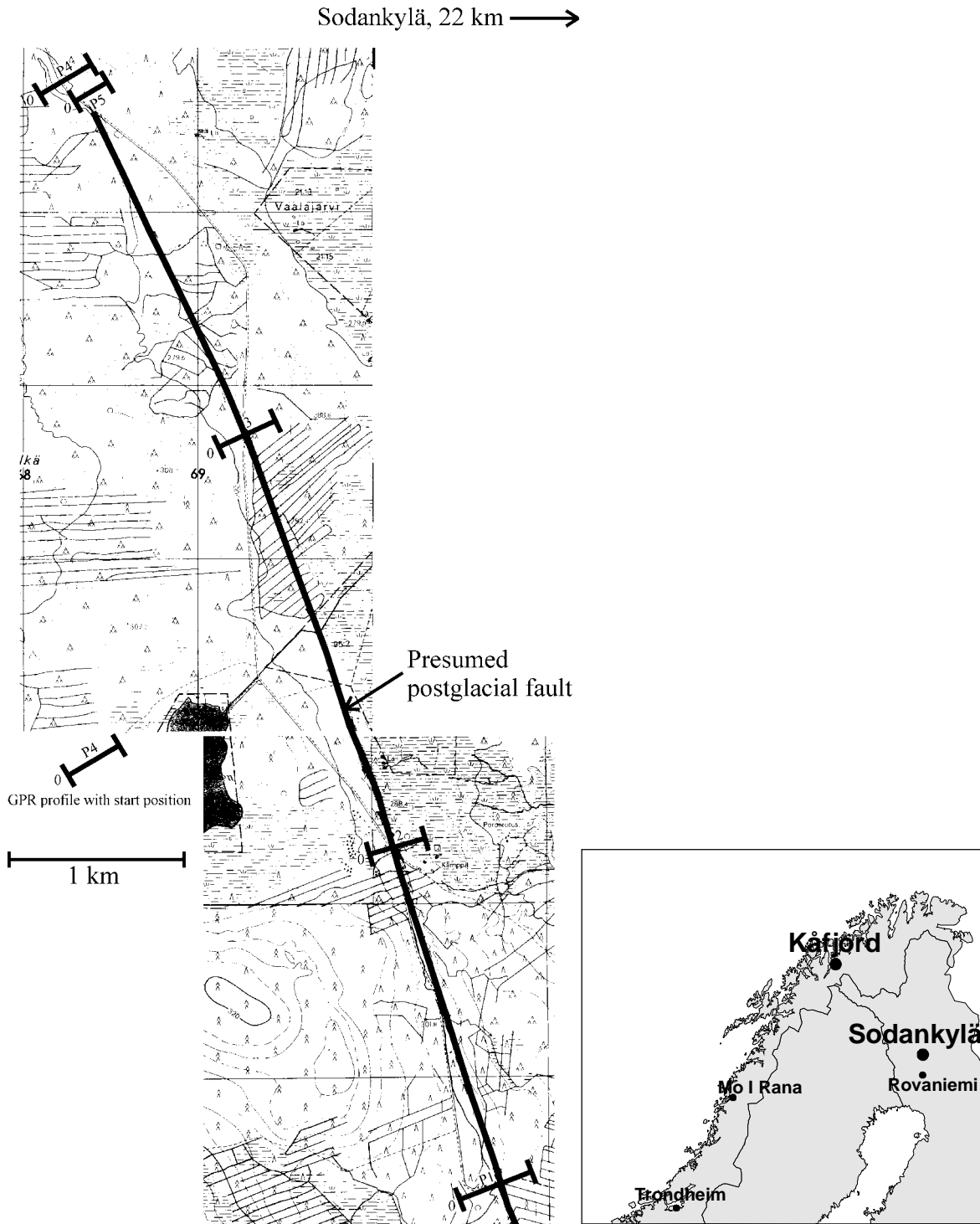
Fig. 5.4.6.   Map of the surveyed area at Sodankylä, Finland.
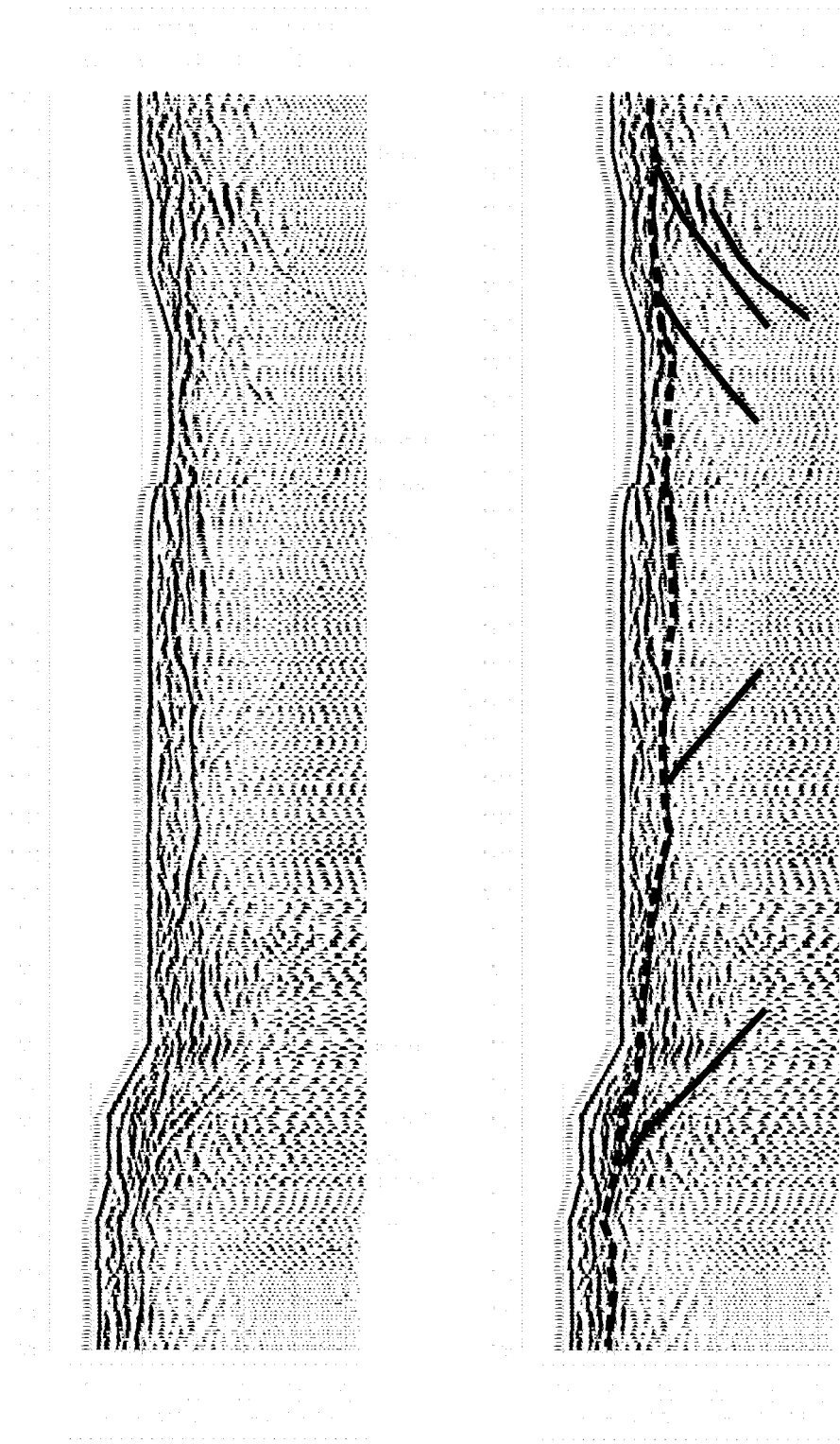
Structures possibly connected to normal faulting

Bedrock

Fig. 5.4.7. *GPR record P4 from Sodankylä, Finland. Right part shows interpretation.*

5.4.5 Conclusions

GPR measurements have been carried out across presumed postglacial faults at Kåfjord (Troms), Masi (Finnmark) and Sodankylä (Finland). The purpose of the measurements was to map the subsurface extension of the faults, and to clarify whether the Nordmannsvik fault (Kåfjord) is a gravitational induced fault or a true tectonic, postglacial fault.

At Kåfjord, previous GPR measurements indicated a structure dipping 45-50° towards the north-east that may represent either tectonic faulting (listric) or gravitational induced faulting. To try to resolve this ambiguity, an additional profile has been measured along a creek down to the valley bottom in the north-eastern direction to see if the structure would reach towards the surface at the valley bottom. This would be in favour of gravitational induced faulting. The record did not show structures within bedrock, so the question of whether the fault is tectonic or gravitational induced is still unresolved.

At Masi, a postglacial, reverse fault has been subject to previous extensive investigations. Two more profiles crossing the fault have been measured. Both profiles show records with structures related to faulting and possible bedrock displacement of 5-7 m across the fault.

At Sodankylä in Finland, one GPR record shows structures related to normal faulting and associated collapse features. Several structures have associated vertical topographic offsets.

5.4.6 References

Dehls, J. & Olesen, O. 1998: Neotectonics in Norway. Annual Technical Report 1997. *NGU Report 98.016.*

Mauring, E, Olesen, O, Rønning, J.S. & Tønnesen, J.F. 1997: Ground-penetrating radar profiles across postglacial faults at Kåfjord, Troms and Fidnajohka, Finnmark. *NGU Report 97.174.*

Olesen, O., Henkel, H., Lile, O.B., Mauring, E. & Rønning, J.S. 1992: Geophysical investigations of the Stuoragurra postglacial fault, Finnmark, northern Norway. *Journ. Applied Geophysics 29,* 95-118.

Olesen, O., Henkel, H., Lile, O.B., Mauring, E. & Rønning, J.S. 1992: Geophysical investigations of the Stuoragurra postglacial fault, Finnmark, northern Norway. *Journ. Applied Geophysics 29, 95-118.*

Varnes, D.J., Radbruch-Hall, D.H. & Savage, W.Z. 1989: Topographic and structural conditions in areas of gravitational spreading of ridges in the Western United States. *U.S. Geological Survey professional paper 1496.*

5.5 RESISTIVITY MEASUREMENTS IN DRILLHOLES AT MASI, FINNMARK

By Eirik Mauring and Jan Steinar Rønning, NGU

5.5.1 Introduction

In one drillhole (Dh7), resistivity measurements were carried out in order to extrapolate the sub-surface position of the postglacial fault and related fractures based on resisitivity characteristics. Additional resistivity measurements were carried out in holes originally drilled for stress measurements. The location of the drillholes are shown on Fig. 5.5.2. The measurements were done by Jan Steinar Rønning in the period of 14.08-17.08-1998. Interpretation was carried out by Eirik Mauring and Jan Steinar Rønning.

5.5.2 Instrumentation and data acquisition

Resistivity measurements were carried out using the SASLOG 300 borehole equipment with a Terrameter recording instrument, both manufactured by ABEM, Sweden. A sketch of the SASLOG 300 logging probe is shown in Fig. 5.5.1.
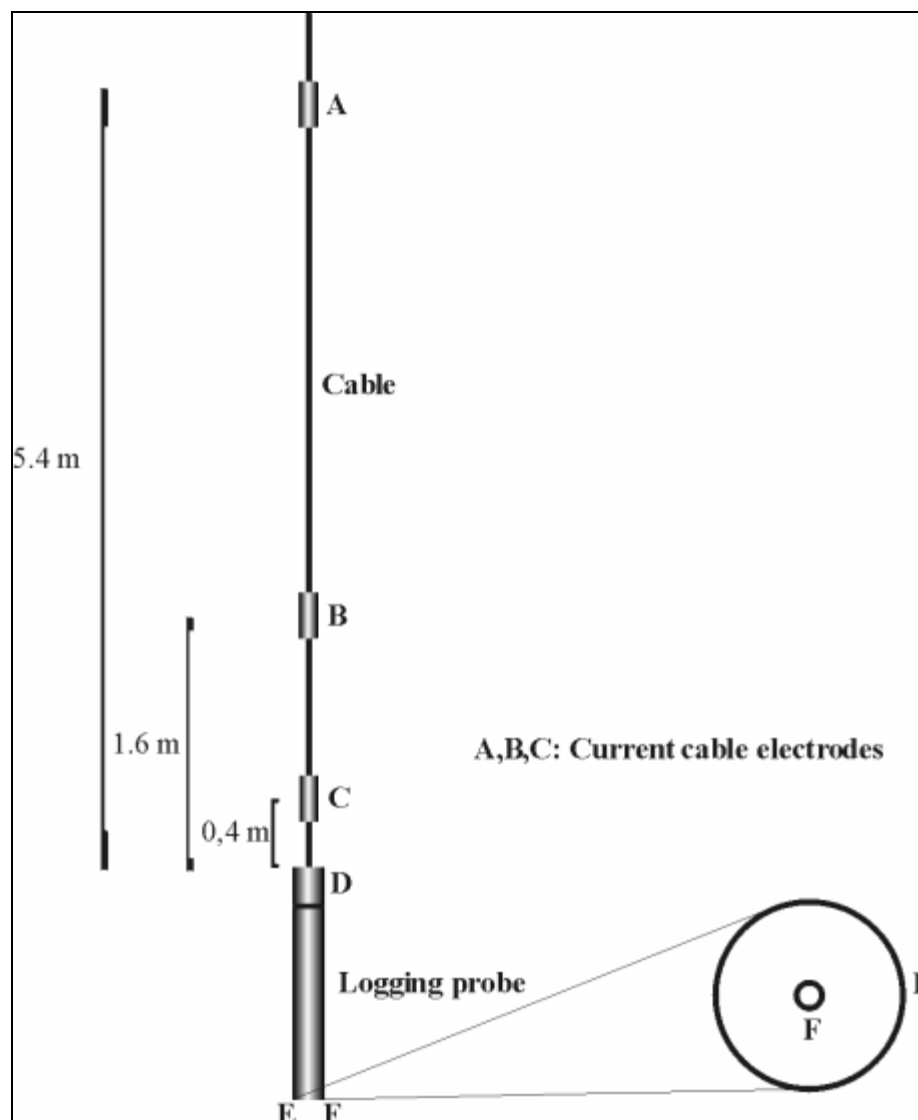
Fig. 5.5.1.   Components of the SASLOG 300 logging probe.

The SASLOG 300 measures formation resistivity with three different configurations which are described below. In addition, SASLOG 300 can record self potential (SP), temperature and fluid resistivity.

'Short normal' (SN) resistivity measurements use a pole-pole configuration with D (see Fig. 5.5.1) as the pole current electrode. The other current electrode is placed on the surface at 'infinity'. The voltage is measured between the ring electrode E and a surface electrode at 'infinity'.

'Long normal' (LN) is also a pole-pole configuration where the current is injected via cable electrode B while the potential is measured at the ring electrode E. Since the distance between the potential and current electrodes are larger than for the SN configuration, resistivity values are representative for a larger bulk of rock since much of the current penetrates deeper into the drillhole walls.

The 'long lateral' (LL) setup is a pole-dipole configuration with the current electrode at A and the potential electrodes at C and E. Resistivity values are representative for even larger volumes of rock than the two former configurations. The configuration is less sensitive to small variations in resistivity than the SN and LN configurations.

For the fluid resistivity (FR) configuration, current is injected via the ring electrode E and surface electrode at 'infinity', while the potential is measured between D and F.

Data sampling was done in 0.5 m downhole intervals, except for temperatures which were sampled at 1 m intervals. Acquisition parameters are listed in Table 5.5.2.

Table 5.5.1.   Drillhole data acquisition parameters.

Drillhole	Depth (m)	Current (mA)	SN	LN	LL	FR	T
Dh7	31.5-90.5	5	X	X	X	X	X
S1	23-50	5	X	X	X	-	-
S2	21-50.5	5	X	X	X	X	X
S3	2-51	5	X	X	X	X	X

X: Measured parameter

-: Not measured parameter

5.5.3   Results

Dh7

The position of the drillhole is shown in Figs. 5.5.2 and 5.5.3. This drillhole penetrates the postglacial fault at depth. Measurements were carried out shortly after the well was blown dry, and then letting water seap back into the well with no subsequent pumping. Graphs of the measured parameters are shown in Fig. 5.5.2 together with qualitative descriptions noted during drilling (termed 'drill log' in Fig. 5.5.9). From the resistivity log, three major low resistivity zones can be seen at depths of 37-43, 53-63 and 73-75 m. The resistivity values are in the order of 1000-2000 ohmm at these depths, indicating fracturing. An extrapolation of a possible fracture on GPR record 807 (Mauring et al. 1998) seems to coincide with the low resistivity zone at 37-43 m depth. The low resistivity zone at 53-63 m may coincide with the actual fault plane. Indeed, fault gauge material is indicated at 61-63 m depth as soft rock. A fractured hanging wall block (53-61 m) is a common phenomenon in this area. In addition to fractures noted during drilling, fractures (probably small) are indicated on the logs at depths of 51, 78 and 88 m. Both the temperature and the

fluid resistivity logs show only small anomalies, indicating that the variations in the values for SN, LN and LL are due to fracturing (increased porosity).

MASI, SASLOG drillhole measurements, drillhole 7
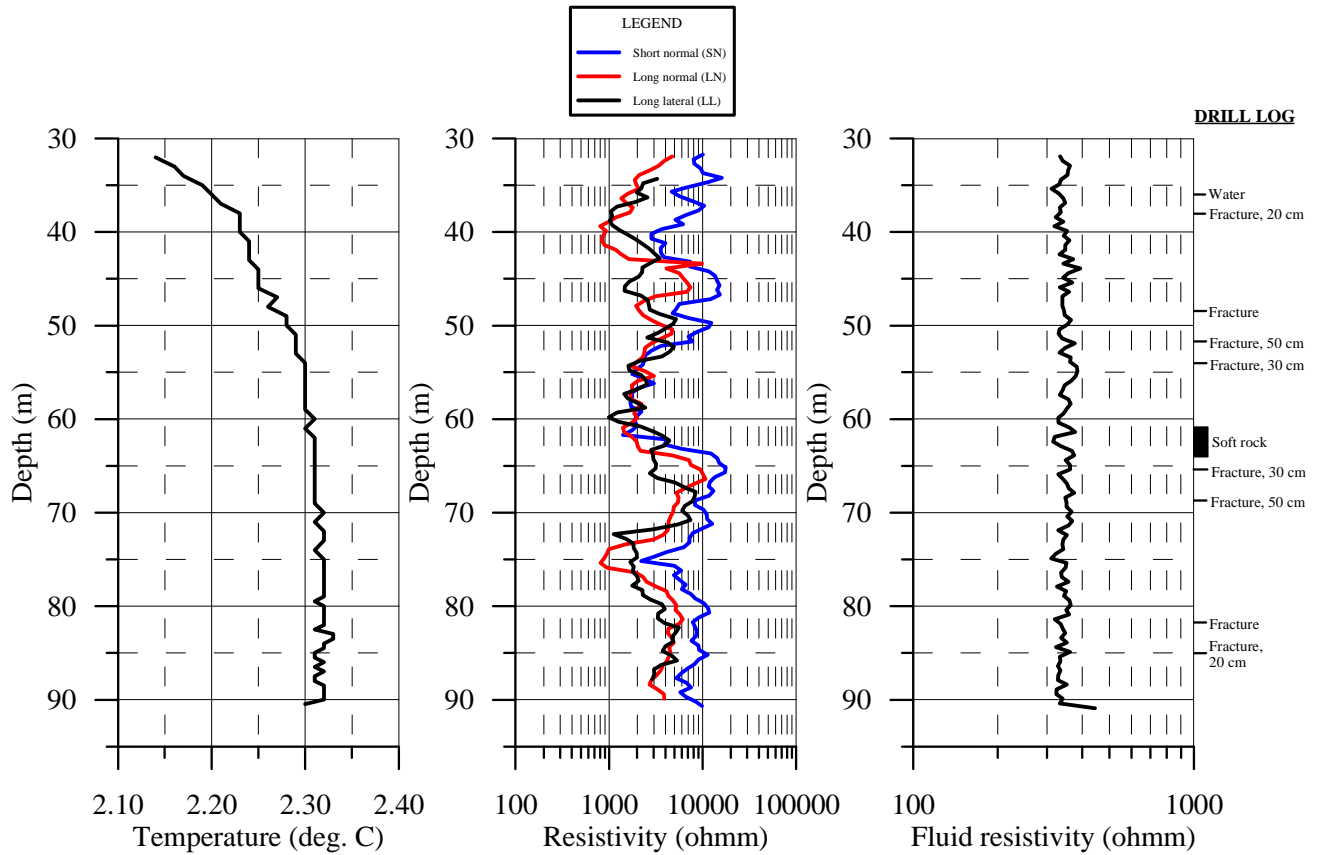
Fig. 5.5.2.   Graphs of recorded parameters from drillhole 7.

Stress drillhole 1-3 (S1-S3)

As mentioned earlier, these holes were drilled for carrying out stress measurements. These measurements failed probably due to brittle and fractured bedrock. The position of the drillholes are shown in Fig. 5.5.2.

<u>S1</u>

Fractures encountered during drilling are clearly seen as low resisitivity zones on Fig. 5.5.10. The LL values are most representative of the bulk resisitvity of the bedrock, since the current penetrates a larger rock volume than the LN and SN configurations. The resistivity values for LL are mostly in the order of 2000-3000 ohmm which are considered low for this type of bedrock (quartzite), thus indicating a fracturing of the rock. The zones of highest resistivity values were selected for hydraulic fracturing. This failed, probably due to small fracturing partly indicated by the SN log (c. ½ fracture per meter).
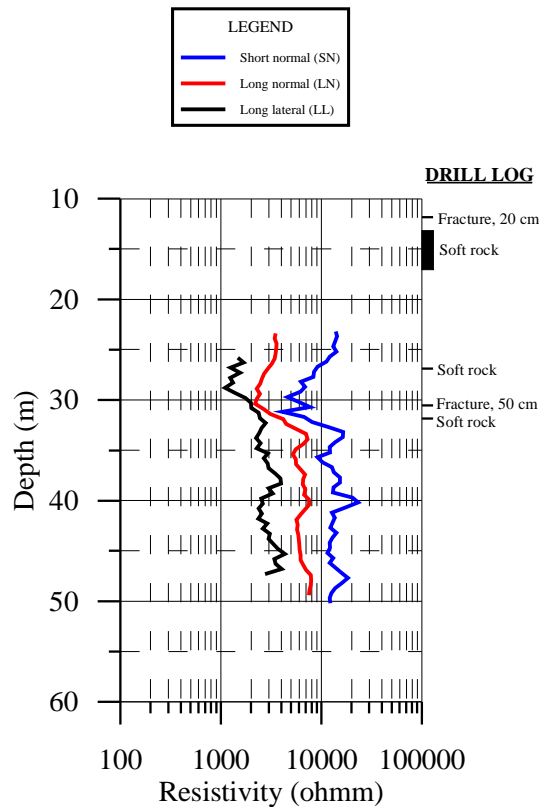
Fig. 5.5.3.   Graphs of recorded parameters from stresshole 1.

S2

The resistivity values stay fairly constant and low down to a depth of c. 35 m (see Fig. 5.5.11). From 35 m, there is a general linear increase in the resistivity values, indicating a lesser degree of fracturing from 35 m depth. From this depth, resistivity values are still irregular, indicating fracturing. The resistivity values down to 35 m are in the order of 200-1000 ohmm, indicating extensive fracturing, explaining the problems with stress measurements. Although no drill log is available from this hole, prominent fractures can be depicted at depths of 35, 47 and 49 m. A severe drop in fluid resisitivity between 46 and 50 m is also causing the SN to drop in the same area.
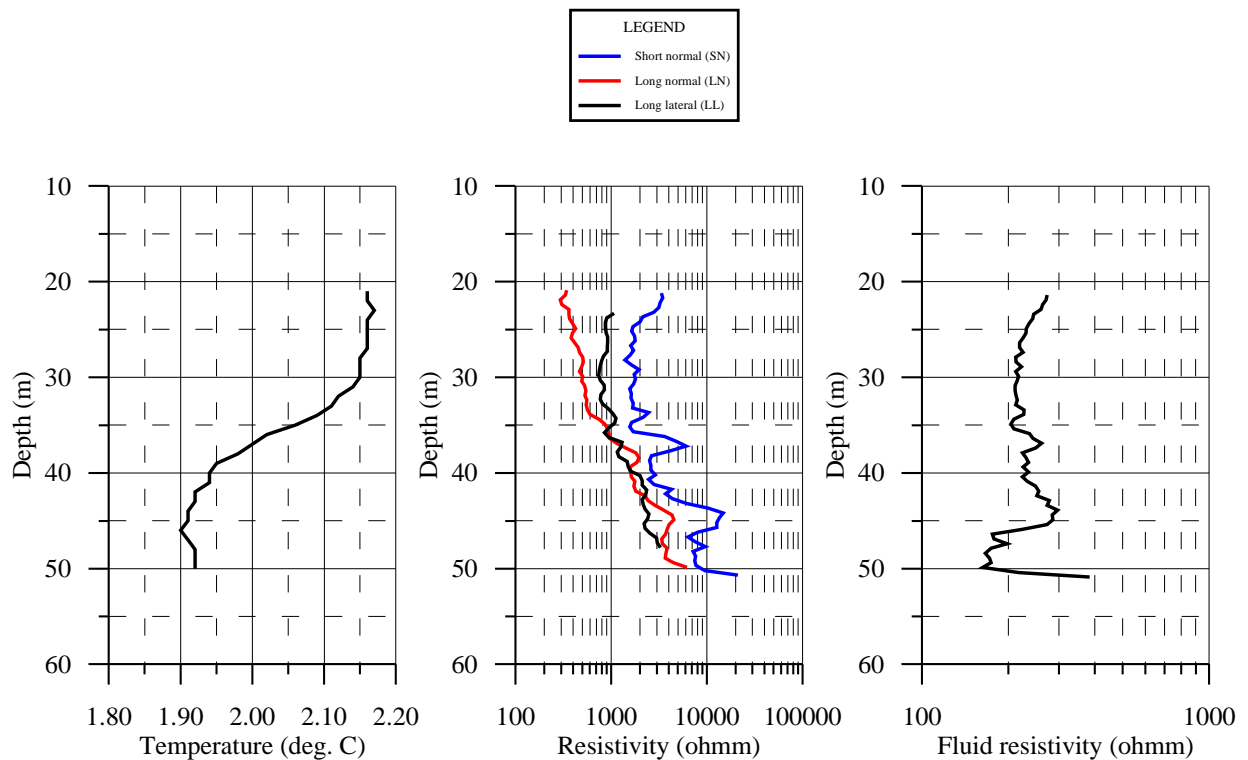
Fig. 5.5.4.   Graphs of recorded parameters from stresshole 2.

S3

This drillhole was placed at a greater distance from the postglacial fault (see Figs. 5.5.2 and 5.5.12). The resisitvity values are relatively high; on the order of 10000 to 30000 ohmm. This normally represents bedrock with relatively few fractures. Thus, this area is probably not affected by the tectonic processes related to the Stuoragurra fault. A few resistivity lows correspond to fractures encountered during drilling (at depths of 8, 14 and 24 m). Possible fractures not noted during drilling occur at depths of 18, 21, 26, 29, 34, 40, 42 and 45 m. Even though the drillhole shows overall high resistivity values, suggesting solid bedrock, measurements of stress were precluded also at this location, probably due to micro-fracturing as noted above.
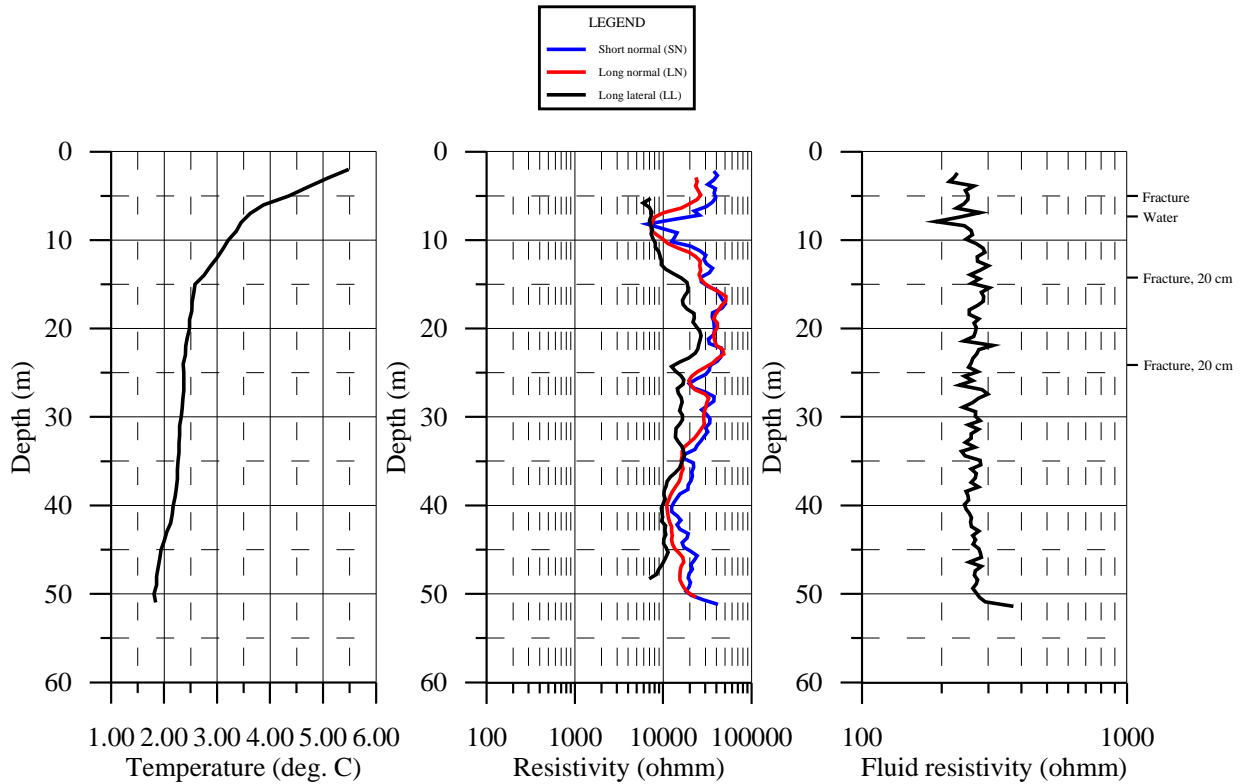
Fig. 5.5.5. *Graphs of recorded parameters from stresshole 3.*

5.5.4 Conclusions

Resistivity measurements have been carried out in four drillholes near the Stuoragurra postglacial fault. One of these was drilled to map the subsurface extent of the fault. The three others were drilled for measurements of bedrock stress. Resistivity measurements were done to give additional information on fracturing/faulting and the overall resistivity values for the bedrock in the area.

The drillhole to the east of the fault suggests its position at a depth (along the drillhole) of c. 60 m, which is in agreement with a linear extrapolation of the known subsurface location of the fault. The stress drillholes generally show low resistivity values, indicating extensive fracturing, precluding measurements of rock stress.

5.6 ROCK STRESS DETERMINATION AT FINNMARK, NORTHERN NORWAY

By Ægir Jóhannsson, SINTEF Civil and Environmental Engineering

5.6.1 Introduction

In connection with geophysical investigations of the Stuoragurra postglacial fault, Finnmark, northern Norway, SINTEF Civil and Environmental Engineering, department of Rock and Mineral Engineering was engaged to carry out rock stress measurements in the vicinity of the fault. The measurements were carried out in the period August 14 - 19, 1998.

5.6.2 Work performed

The work was performed according to test procedures given in Appendix A, with the exception that there was no supply of electricity and water at the boreholes locations.

Three boreholes were intended for testing. The location of the boreholes; 01, 02 and 03, is shown on the map in Appendix B. The holes were all vertical and 50 m deep with diameter of 76 mm (3"). The original program was to carry out tests in three sections in each hole, but due to bad rock quality, resulting in leakage in the test sections, a total of 24 sections were tested in the holes. Each test section is 1 m long and the distance between each section is at least 1.5 m.

5.6.3 Results

Curves that show water pressure and flow as a function of time for each test section are given in Appendix C. Table 3.1 lists the results from the tests. The table shows the depth of each test section, the fracture initiation pressure, P_f, or breakdown pressure (1. cycle) (in this case this is the jacking pressure), fracture reopening pressure, P_r (2. cycle) and instantaneous shut-in pressure, P_s. Measuring of the orientation of fractures was not actual.

As observed, in majority of the tests, only the first cycle of three was performed. This is due to the fact that jacking occurred in 1. cycle in almost every test section, which makes the 2nd and 3rd cycle worthless.

Hole 01

A total of six test sections were tested in this hole. The jacking pressure in the first cycle varies from 26 to 88 bars. Two sections were tested with three test cycles but the reopening pressure in those cases is not readable because the water pressure increases gradually with the water flow. In one case it seems to be around 5 bar. The shut in pressure varies from 8 to 23 bars. In section nr 02 the breakdown pressure is around 88 bar and the shut in pressure from 11 to 17 bar. In between tests the pressure sank down to zero in a short time. This indicates an open water passage in the rock and will result in direct relationship between water-pressure and water-flow in cycle 2 and 3.

Hole 02

A total of six test sections were tested in hole 02. The jacking pressure in the first cycle varies from 17 to 79 bars. The reopening pressure in newer readable and the shut in pressure varies from 8 to 27 bars.

Hole 03

A total of eleven test sections were tested in hole 03. The jacking pressure in the first cycle varies from 7 to 132 bars. The reopening pressure varies between 3 and 6 bar. The shut in pressure varies from 9 to 90 bars. From resistance logging of the test hole, which was done before the hydraulic tests started, some changes in the rock mass characteristics were registered in the depth of about 24 m. This was confirmed by the hydraulic tests, which gave higher jacking and shut in pressure in

the area above 24 m. The results from tests in this area, as in the rest of the test hole, indicate an open water passage from the test sections which results in direct relationship between the water-pressure and the water-flow. This can be seen on the pressure-time diagram for section 21.8 - 22.6 m in Appendix C. In this section the water-flow in cycle 2 was reduced to see if it influenced the water pressure, and as can be seen the water pressure drops with the water flow.

Table 3.1 *Hydraulic fracturing test results, Masi, Finnmark.*

Hole nr.	Section nr.	Depth [m]	Breakdown pressure P_f [bar]	Reopening pressure P_r [bar]		Shut in pressure P_{isi} [bar]		
				2. cycle	3. cycle	1. cycle	2. cycle	3. cycle
01	01	46.7-47.5	72	-	-	23	-	-
01	02	44.1-44.9	88	*	5	11	17	16
01	03	39.6-40.4	46	*	*	10	11	8
01	04	37.6-38.4	48	-	-	8	-	-
01	05	36.1-36.9	*	-	-	*	-	-
01	06	24.1-24.9	26	-	-	9	-	-
02	01	46.4-47.2	17	*	-	8	16	-
02	02	44.4-45.2	71	*	-	10	15	-
02	03	42.9-43.7	25	-	-	*	-	-
02	04	41.4-42.2	79	*	*	17	17	17
02	05	38.8-39.6	56	-	-	27	-	-
02	06	36.6-37.4	53	-	-	11	-	-
03	01	48.4-49.2	31	-	-	12	-	-
03	02	46.6-47.4	81	-	-	37	-	-
03	03	45.7-46.5	87	6	-	53	50	-
03	04	42.1-42.9	41	-	-	2	-	-
03	05	35.6-36.4	*	-	-	23	-	-
03	06	32.6-33.4	83	-	-	14	-	-
03	07	29.6-30.4	68	-	-	14	-	-
03	08	21.8-22.6	123	*	*	11	8	9
03	09	23.8-24.6	116	4	4	76	80	72
03	10	25.7-26.5	7	-	-	*	-	-
03	11	20.1-20.9	132	3	4	88	80	90

* Not readable from the results.

5.6.4 Conclusions

Because of the bad condition of the rock mass in the test holes, it is difficult to draw any conclusions from the results. In order to obtain good results, a hydraulic fracture has to be initiated in intact rock on the borehole wall in the test section. This crack has then to be reopened in the following two cycles. If the hydraulic pressure opens an existing crack in the rock mass, so-called hydraulic jacking of the crack will occur. Hydraulic jacking of existing cracks occurred in all sections of the three boreholes that were tested in Masi, giving no results to be able to calculate the minimum and maximum stresses together with their orientation, as well as the tensile stregth of the rock mass.

For further studies it is crucial that the location of the test holes is chosen correctly to increase the chance of good results from the tests. An experienced rock engineer with knowledge of the hydraulic fracturing method should visit the potential sites well befor the testing period.

In this case the quarzite rock mass is highly fractured, and from experience it is then likely that the general horizontal stress level is low.

5.6.5 Addendum: General evaluation of the stress situation in the Stuoragarra fault region.

The hydraulic fracturing measurements were not successful due to the fractured quartzite rock at the measuring sites.

Appendix D shows the situation at the testhole 3. It will be seen that the quartzite is distinctly fractured both on a larger and smaller scale. This makes it virtually impossible to obtain a borehole length about 1 m without visible fractures, which is the minimum requirement in connection with hydraulic fracturing in a 3″ hole.

The fracture pattern is totally dominated by prominent, nearly vertical, approximately E - W striking fractures. Experience from many locations in Norway show that the major principal horizontal stress tend to be parallel with a dominating fracture pattern of this type, i.e. σ_{H1} in this case could then be oriented E - W.

Previous overcoring measurements at about 100 m depth in the Bidjovagge (30 km from the fault) and Bjørnevann mines in Finnmark (See Appendix E, from Myrvang (1993)) have shown that the major and intermediate principal stresses are both horizontal, with magnitudes in the order 15 - 17 MPa and 12 - 13 MPa respectively, while the minor, vertical principal stress in accordance with gravity is approximately 3 MPa. The major principal stress is oriented approximately N - S, which is in accordance with directions derived from focal mechanism studies in Finnmark and the Barents Sea. However, σ_{H1} and σ_{H2} are in practical terms rather equal in magnitude, which means they may easily interchange in direction, and thus fit with the assumed σ_{H1} at the measuring site 3.

The stress pattern found in the two mines is the pattern necessary to give a reverse or thrust fault situation according to the Mohr - Coulomb failure criterion (see f. i. Jaeger & Cook , (1976)), i.e. the major and intermediate principal stresses are horizontal, and the minor principal is vertical.

5.6.6 References

Myrvang, A. (1993): Rock stress and rock stress problems in Norway. *Comprehensive Rock Engineering, vol. 3*. Pergamon Press, London

J.C. Jaeger and N.G.W. Cook (1976): *Fundamentals of Rock Mechanics.* Chapman & Hall, London.

5.6.7 Appendix A: Field Measurements - Method Statements

Hydraulic Fracturing

The selected method used for the hydraulic fracturing is adopted from the International Society for Rock Mechanics (ISRM): Suggested Methods for Rock Stress Determination.

Apparatus

Drilling equipment

Any drilling equipment capable of producing a stable hole to the required test depth may be used. The hole diameter should suit the available packer equipment or vice versa. The drilling equipment should also be capable of obtaining core samples in the vicinity of the test sections in order to examine discontinuity orientations and characteristics.

Packer equipment

A system to isolate a test section of borehole is required. Inflatable packers, through which a water flow pipe runs, are used to seal the hole, enabling a test section to be pressurised. Double packer systems (straddle packer), which isolate a part of the hole, are generally used, but a single packer which isolates the base of a hole, also may be considered. Gas expansion is used to set the packers and seal the test interval. The initial packer setting pressure depends on the packer type. If the interval pressure approaches the packer pressure, the packer pressure should be increased to a level sufficient to prevent leakage bypassing the packers. The packers are separated by spacers, and a minimum length five times the borehole diameter is commonly recommended. Fig. 1 presents schematic representation of (a) hydrofracturing tool and (b) impression packer.
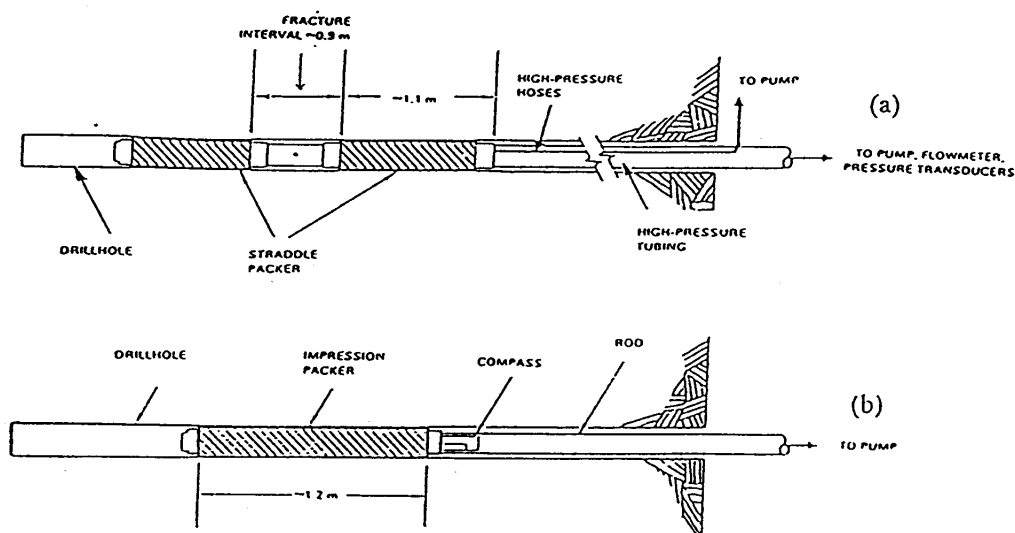
Fig. 1. Schematic representation of (a) hydrofracturing tool and (b) impression packer.

Injection equipment

A high-pressure pumping system is used, capable of maintaining a constant flow over the range of pressures expected during the test. The pumping system should have sufficient capacity to initiate hydrofracture. Sufficient supply rods, tubing and hose are needed for the required depth of meas-

urement. These are usually used to put the packer in to the borehole. Water and electricity supply to the borehole location is provided by the client.

Measuring equipment

Pressure transducers for measurement of fluid and packer pressures are located at the surface. A flow metre located on surface is used for recording fluid flow with time. Pressure and flow are continuously recorded during the testing using analogue electrical devices connected to a data acquisition system run on a portable computer.

Procedure

Drilling and packer insertion

Choice of hole diameter and size of hydraulic fracturing equipment is based on equipment available. Final choice of test zone length and depth is based upon the fracture characteristics of recovered cores, or readings from water loss measurements if available. Prior to testing, the borehole must be carefully flushed to remove debris and ensure clear passage for the packer assembly. The packer assembly is inserted to the predetermined depth, the depth is recorded, and the packers are inflated to a pressure sufficient to seal against the applied fluid pressure.

Testing

The pressure in the test interval is increased slowly to ensure minimal pressure losses in the tubing (especially in very deep holes). No standard pressurisation rate or flow rate exists, however, a common range of pressurisation rates is about 0.1-2.0 MPa/sec. The packer pressure is initially set well below the anticipated breakdown pressure, and the packer pressure is then increased at the same rate as the injection pressure. This procedure reduces the possibility of fracture initiation caused by the packer pressure.

The test interval pressure is recorded against time. Fracturing will occur if the induced tensile stress reaches the borehole rupture strength. If the test section is cut by any rock joint, jacking may occur. Evidence of failure may be obtained from the pressure/time curve. The borehole fluid pressure at the moment of borehole rupture is termed the "fracture initiation pressure" (P_f), or breakdown pressure. After injecting a volume sufficient to propagate a fracture length equal to about three times the borehole diameter, injection is stopped and the hydraulic system is sealed or "shut in" yielding the "instantaneous shut-in pressure (P_s).

A normal procedure consists of one breakdown cycle as a minimum, to obtain P_f and P_s. Additional depressurisation cycles may be used to determine the "fracture reopening pressure" (P_r) and repeated measurements of the shut-in pressure (P_s). When requested by the client, up to three repressurisation cycles are used to verify the measurement at each test section and identify the mode of failure (i.e., fracturing or jacking).

The packer is then deflated and moved to a new position, or the equipment is removed from the borehole.

A hole inspection is carried out to observe and record hydrofracture positions and orientation. This test is carried out by using a special impression packer. This packer is coated with soft rubber giving an imprint of the fracture zone.

The test may fail if the specific test section is crossed by open joints of high conductivity that prevent pressure build-up, or the borehole is block with rock debries or equipment stuck in the borehole.

5.6.8 Appendix B: Location of test holes

5.6.9 Appendix C: Pressure and water flow curves

138

Hydraulic fracturing, Mási, Finnmark
Hole 03, depth 35.8 - 36.4 m

Hydraulic fracturing, Mási, Finnmark
Hole 03, depth 38.8 - 39.4 m
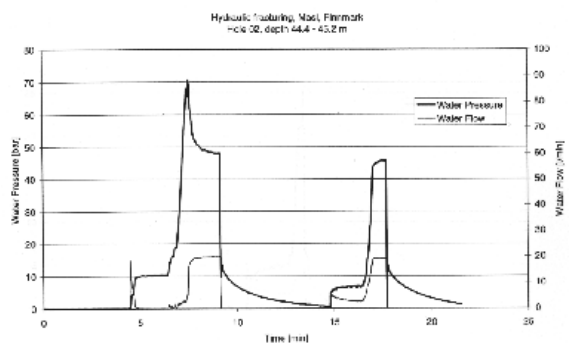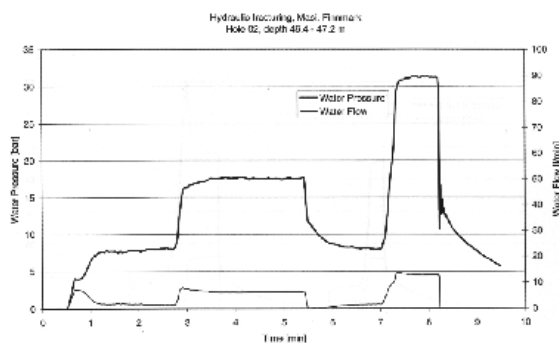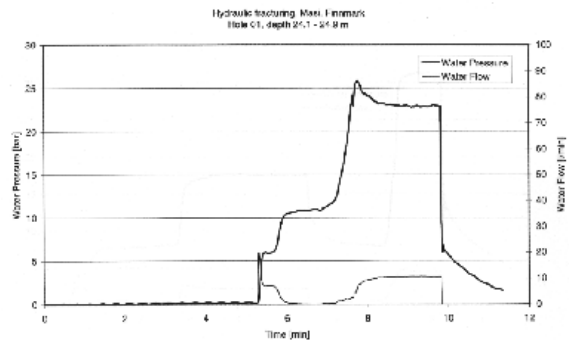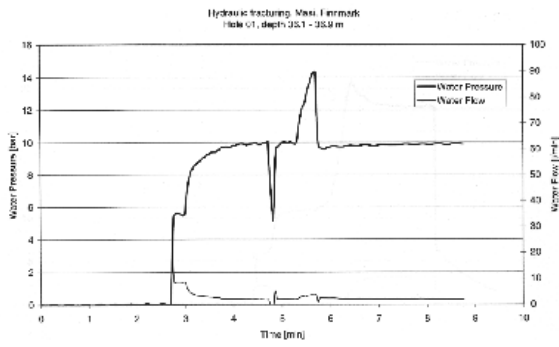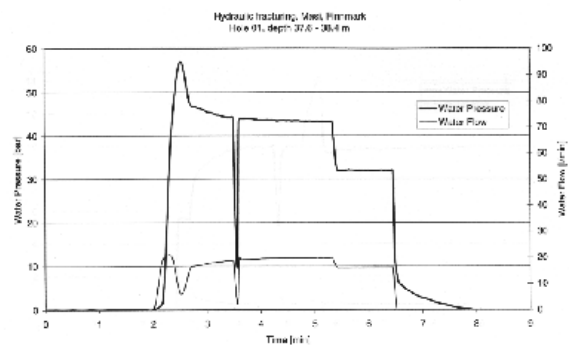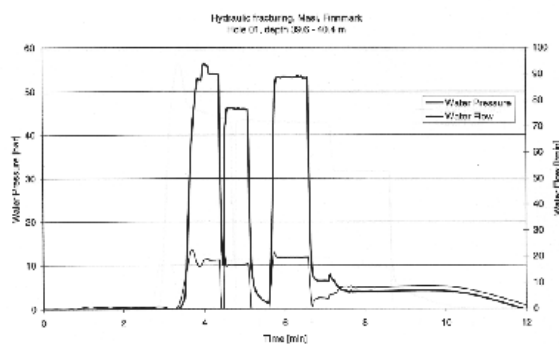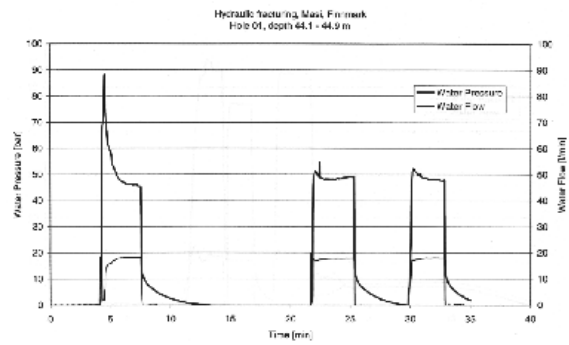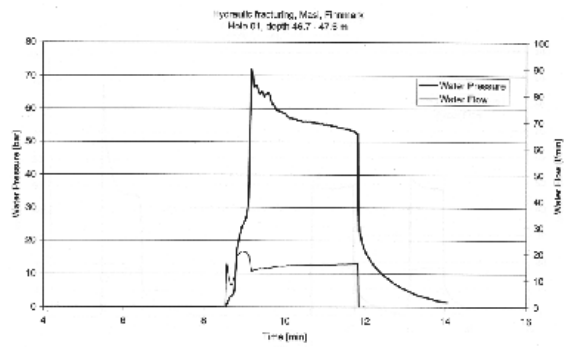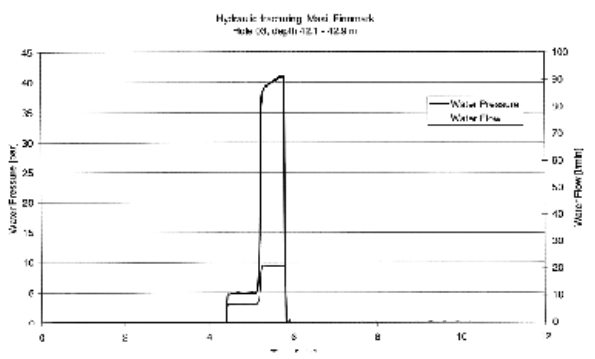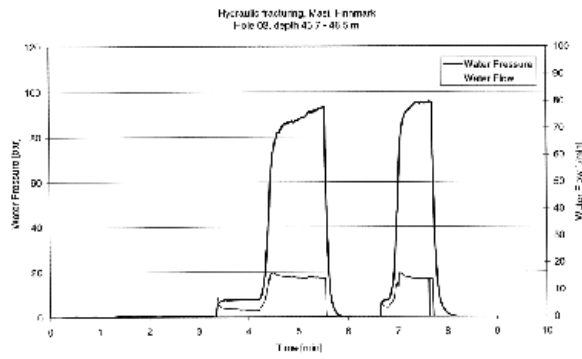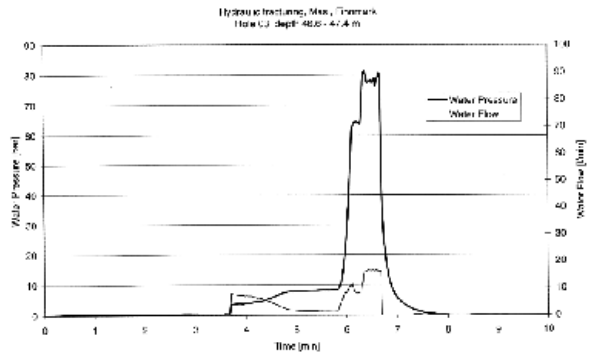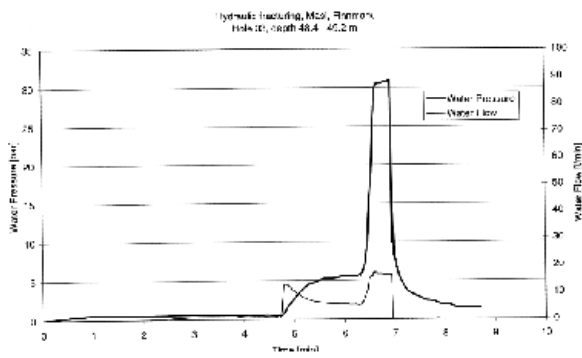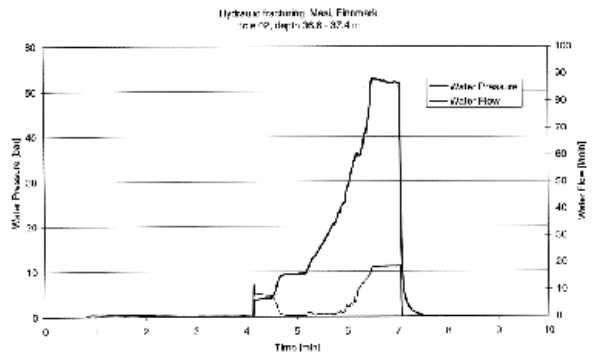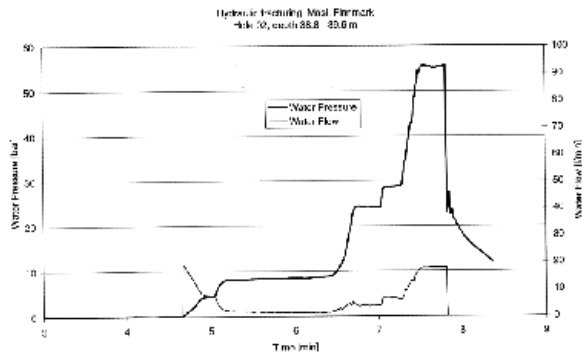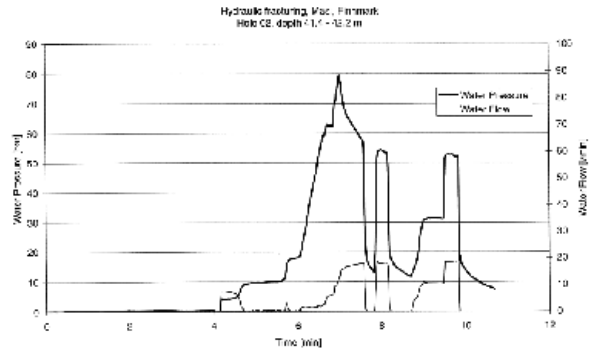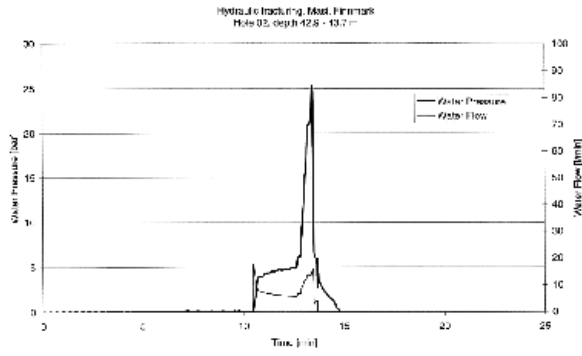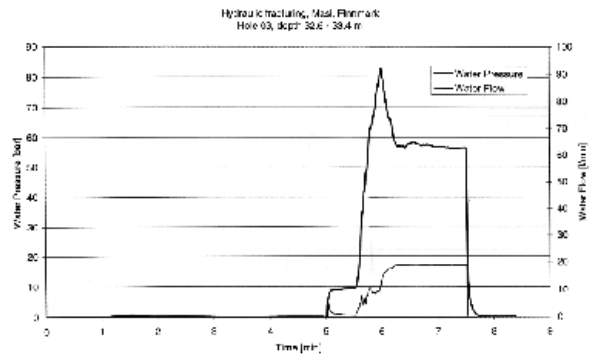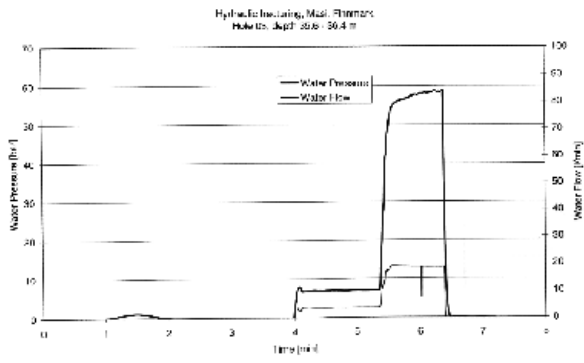
5.6.10 Appendix D:

Masi Finnmark

Dominating fracture pattern

Strike/dip [º]: 265/88 to 270/90
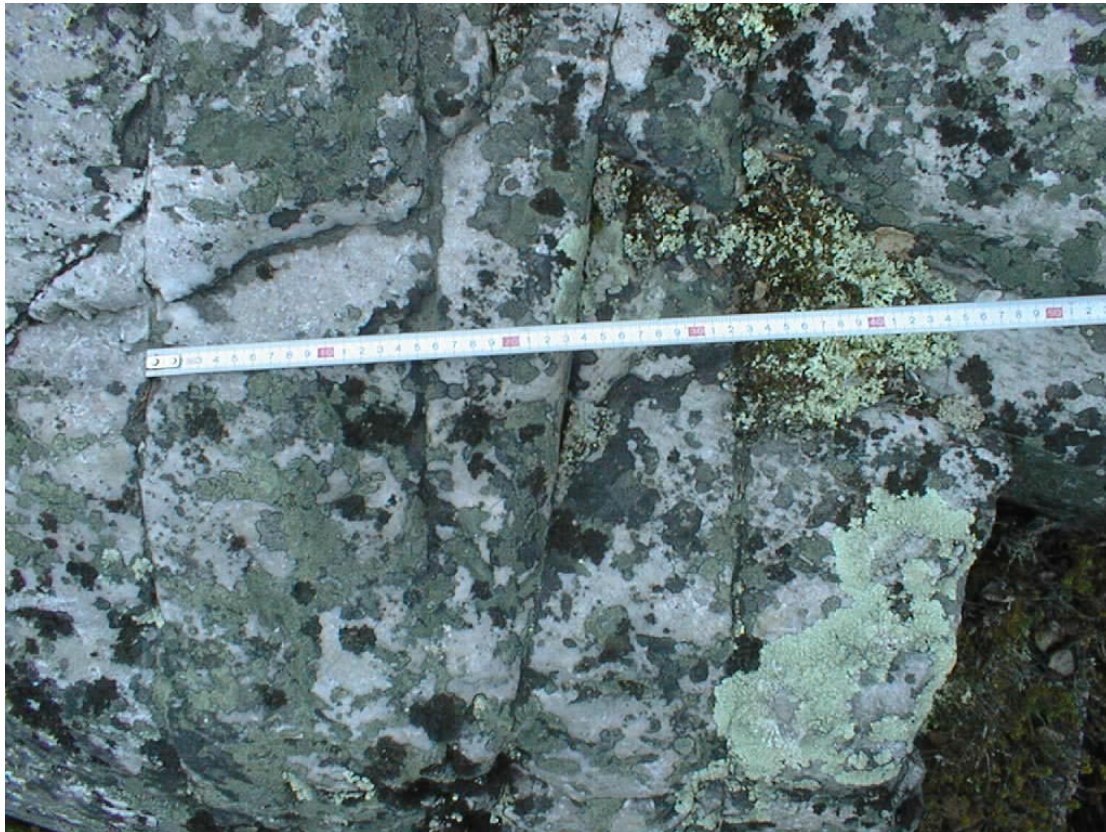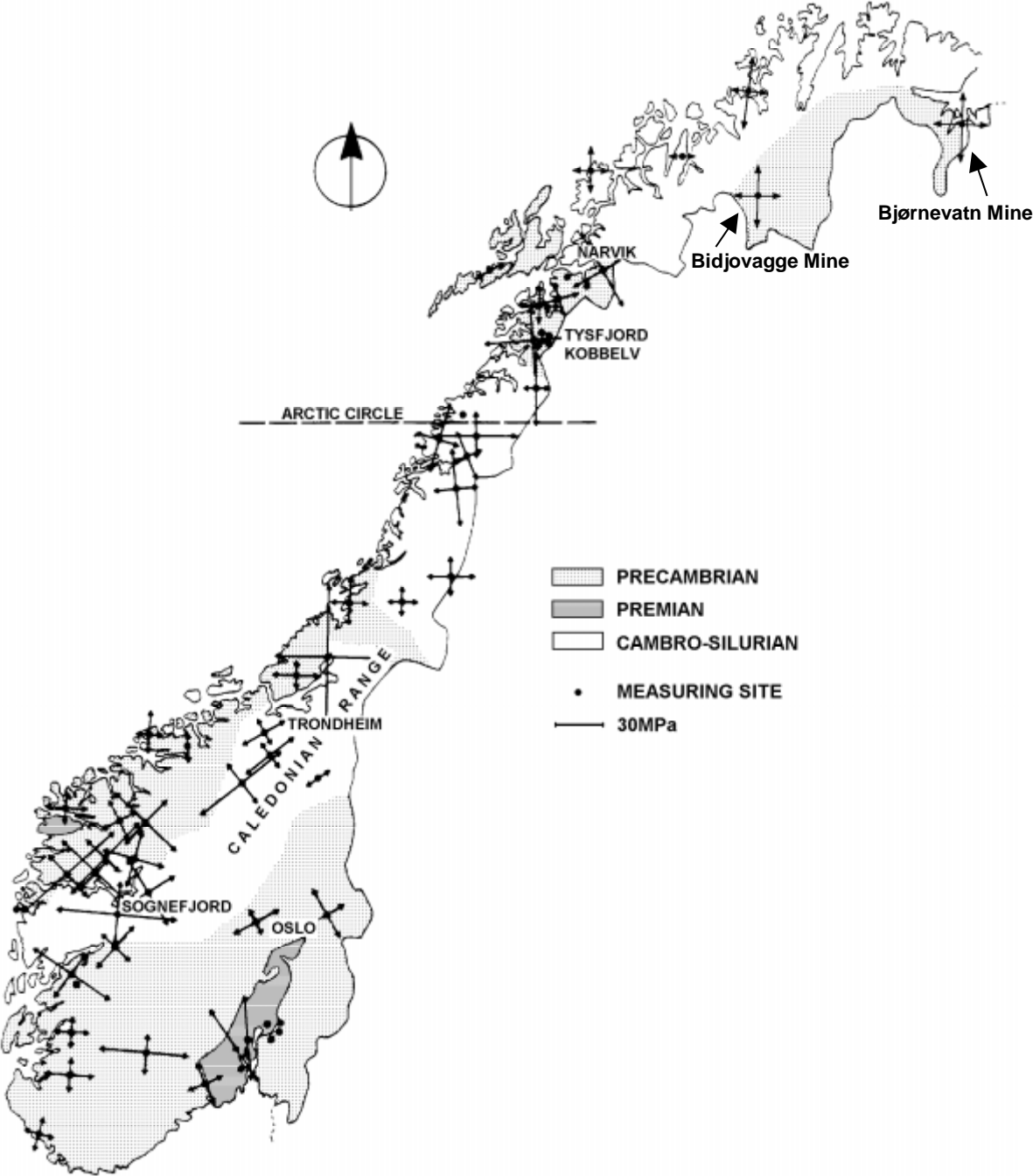
Simplified geological map of Norway with horizontal stresses plotted

5.7 GROUNDWATER STUDIES IN THE STUORAGURRA FAULT

By Tidemann Klemetsrud and Bernt Olav Hilmo, NGU

5.7.1 Introduction

A 90-m deep percussion drilling well was located in the hanging wall block of the Stuoragurra Fault in the Fidnajåkka area. The well has a diameter of 5.5" and reaches a depth of 90 m (along the inclined line).

The thickness of the Quaternary overburden is approximately 9 m. Geological and geophysical borehole data indicated several zones of fracturing.

Short-time pumping tests were carried out using a submersable pump with a capacity of c. 17 m^3/hour. Because the well was blocked at a depth of c. 41.5 m, the pump could not reach deeper down in the well. The ground water surface before the test pumping was at a depth of 31.5 m. The test pumping was carried out in two intervals, each of 90 minutes duration with 7 minutes between the intervals. The break between the two pumping periods was caused by a power failure.

5.7.2 Results

The pumping results from the two intervals were identical. The groundwater yield of 16.8 m^3/hour (maximum pump capacity) caused a 0.5 m lowering of the water surface in the well. This lowering stabilised after 7 minutes. This borehole yield is among the highest ever measured in hard rock aquifers in Norway. The average yield for borehole in crystalline rocks in Norway is about 0.4 m^3/hour.

Field measurements after 30 minutes of pumping within interval 1:

- Q = 16.8 m^3/hour
- T = 3.3 °C
- Oxygen = 3.3 mg/l
- Conductivity = 2.43 mS/m
- Groundwater level = 32 m

Repeated analysis after additional 1 hour showed the same results. Additional analysis of CO_2 showed c. 100 mg/l.

The water level increased to initial level during 4 minutes after the pumping halted. Repetition of the pumping started 7 minutes after termination of the first pumping. Repeated field measurements after 30 and 90 minutes showed the same results as in interval 1. Water that was filled on a bottle and shaken showed numerous bubbles, which most likely was caused by the high CO_2-content. When opening the bottle, a weak puff could be heard - a little weaker than from opening a bottle of CO_2-containing mineral water.

5.7.3 Conclusions

It is necessary to continue the test pumping for a longer period of time to estimate the groundwater yield. The pump that was applied during the test is the largest available for a 5.5" diameter well.

A sample of the water was analysed for physical-chemical parameters at the NGU laboratory. The analysis results are shown in Table 5.7.1. The water has an almost neutral pH-value and has low ion-content due to the bedrock composition (quartzite within the Masi Formation). This poor buffered rock type is resistant to weathering. A low groundwater temperature (3.3ºC) compared to air- and surface water-temperature and a relatively high Si-content (4.4 mg/l) indicate that the groundwater has a quite long residence time in the bedrock.

All measured parameters except nitrite (NO2) fulfil the requirements of drinking water. The high nitrite content may indicate pollution from animal manures, but more analysis (including bacteriological analysis) are needed to reach a more reliable conclusion.

The groundwater has a relatively high content of copper and zinc, which most likely originate from sulphide-mineralizations along the Stuoragurra Fault or adjacent fracture zones. During water sampling there was a smell of H_2S which is oxidized to SO_4 before lab analysis. The relative high content of CO_2 may originate from destruction of organic material and a low carbonate content in the bedrock. Low oxygen content in the groundwater supports this theory.

A more detailed evaluation of the groundwater chemistry is possible after test pumping during a longer time period with accompanying sampling and/or sampling at different levels in the well.

Table 5.7.1.   Geochemical analysis of water from the Fidnajåkka well.

Brønn-nr/sted		Storevann		
Dato		**17.08.98**		
Brønntype		**Fjellbrønn**		
Prøvedyp	**m**	**41**		
Brønndimensjon	**mm**	**140**		
X-koordinat	**Sone: 32**			
Y-koordinat	**Sone: 32**			
Fysisk/kjemisk			Veiledende	Største tillatte
Surhetsgrad,	**pH**	**7.17**	**7.5-8.5**	**6.5-8.5**[2]
Ledningsevne,	**mS/m**	2.43 2.47	**< 400**	
Temperatur	**°C**	**3.3**	**< 12**	**25**
Alkalitet	**mmol/l**	**0.17**	**0.6-1.0**[2]	
Fargetall	**mg Pt/l**	**3.2**	**< 1**	**20**
Turbiditet	**F.T.U**	**0.27**	**< 0.4**	**4**
Oppløst oksygen	**mg O₂/l**	**3.3**	**> ca 9**	
Fritt karbondiok-	**mg CO₂/l**	**100**	**< 5**[2]	
Redoks.potensial,	**E_h**			
Anioner				
Fluorid	**mg F/l**	**< 0.05**		**1.5**
Klorid	**mg Cl/l**	**0.78**	**< 25**	
Nitritt	**mg NO₂/l**	**0.18**		**0.16**
Brom	**mg Br/l**	**< 0.1**		
Nitrat	**mg NO₃/l**	**1.46**		**50**
Fosfat	**mg PO₄/l**	**< 0.5**		
Sulfat	**mg SO₄/l**	**1.95**	**< 25**	**100**
Sum anioner+alkalitet	*meq/l*	*0.25*		
Kationer				
Silisium	**mg Si/l**	**4.44**		

Aluminium	**mg Al/l**	**0.032**	**< 0.05**	**0.2**
Jern	**mg Fe/l**	**0.025**	**< 0.05**	**0.2**
Magnesium	**mg Mg/l**	**0.58**		**20**
Kalsium	**mg Ca/l**	**1.86**	**15-25[2]**	
Natrium	**mg Na/l**	**1.50**	**< 20**	**150**
Kalium	**mg K/l**	**0.92**	**< 10**	**12**
Mangan	**mg Mn/l**	**0.002**	**< 0.02**	**0.05**
Kobber	**mg Cu/l**	**0.019**	**< 0.1**	**0.3**
Sink	**mg Zn/l**	**0.028**	**< 0.1**	**0.3**
Bly	**mg Pb/l**	**< 0.05**		**0.02**
Nikkel	**mg Ni/l**	**< 0.02**		**0.05**
Kadmium	**mg Cd/l**	**< 0.005**		**0.005**
Krom	**mg Cr/l**	**< 0.01**		**0.05**
Sølv	**mg Ag/l**	**< 0.01**		**0.01**
Sum kationer[3]	*meq/l*	*0.23*		
Ionebalanseavvik[4]	*%*	*-4*		

5.8 FIELD STUDIES AND ANALYSIS OF A DIGITAL ELEVATION MODEL AT KÅFJORD.

By John Dehls, NGU

5.8.1 Introduction

The Nordmannsvika postglacial fault (Fig. 5.8.1) was described in the 1997 Annual Technical Report (Olesen & Dehls, 1998). The fault was first described by Tolgensbakk & Sollid (1988). It is a normal fault, with an escarpment of up to 1 metre height. Ground penetrating radar (GPR) profiles made during the summer of 1997 revealed a pair of prominent reflectors in the bedrock, dipping about 45º-50º to the northeast (Mauring *et al.,* 1998). One of the reflectors, when extrapolated to the surface, coincided with the surface scarp of the fault.

The reflector could be seen in three parallel GPR profiles. In two of the profiles, it dipped 45º-50º. However, in the third profile, it had a more shallow dip, indicating a possible gravitational origin. It was decided to follow up in 1998 with more GPR profiles, as well as field mapping. The results of the new GPR work are presented in this report (Mauring *et al.,* section 5.4). The results of the field studies are presented below.

Fig. 5.8.1.   The Nordmannsvika postglacial fault seen from the northwest.

5.8.2 Field Studies

The main purpose of the field studies was twofold. First, to rule out the possibility of the scarp being the top of a gravitational slump. Second, to rule out the possibility that the parallel reflectors visible in the GPR profiles were bedding or foliation planes.

146

Evidence for gravitational slumping

If the scarp in Nordmannsvikdalen represented the head of a gravitational slump feature, we would expect to see several things. First, the scarp should be somewhat arcuate in shape. This is not the case. The curvature seen in map view is due to the topography (see below). Second, we should see some sort of accomadation structures along the sides. The western end of the scarp terminates against a large rock flow. Due to the large size of the blocks, it is impossible to determine the relative ages of the two features. It is possible that the rock flow conceals the original side of a slump, however there is no evidence pointing towards this. The eastern end of the scarp terminates agains the edge of a mountain (Fig. 5.8.2). Here, there is clearly no evidence for slumping. Third, we should see the foot of the slump along the valley floor. Although there are numerous small terraces between the scarp and the valley floor, there is no feature that could be interpreted as the toe of a slump.

Fig. 5.8.2.   The easternmost end of the Nordmannsvika fault terminates against the side of a mountain. The rubbly nature of the mountain side makes it impossible to determine if the fault continues, and if so, in which direction.

Regional bedding and foliation

Measurements of bedding and foliation throughout Nordmannsvikdalen showed that both surfaces dip to the southwest. This is the opposite direction to the reflectors seen in the GPR profiles. The fault scarp is cut by two stream beds near the eastern end. Within the bedrock exposed in these stream beds, the bedding and foliation surfaces are quite variable. In places, they dip towards the northeast (Fig. 5.8.3), but they are highly folded (Fig. 5.8.4) and generally dip to the southwest. The dipping reflectors seen in the GPR profiles must represent discrete fracture/fault surfaces.

Fig. 5.8.3.   Foliation and bedding surfaces are subparallel, and dip shallowly towards the northeast in places.

Fig. 5.8.4.   Bedding and foliation are strongly folded along the stream beds that cut the Nordmannsvika fault.

5.8.3 Digital Elevation Model

The fault scarp in Nordmannsvikdalen runs over two gentle hills and is cut by two stream beds. It was thought that a digital elevation model (DEM) would allow us to estimate the dip of the fault by standard geometrical techniques. A dem, and accompanying orthophote, were produced by Fjellanger Widerøe A/S (Fig. 5.8.5). One metre elevation contours were supplied in vector format, as well as lake edges, stream paths and cliff edges. A model was built within Arc/Info, which was then used to produce a grid with a one metre cell size.
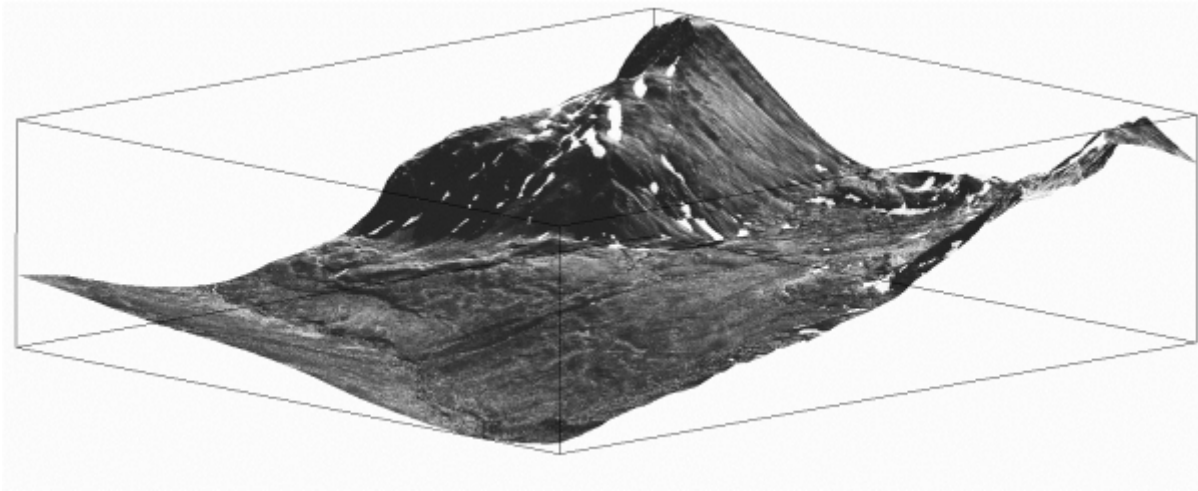
Fig. 5.8.5.   Orthophoto draped over a DEM of the area around the Nordmannsvika fault. View is from the northwest. Sides of the box are 2500 metres.

The traces of both the bottom and the top of the fault scarp were digitized. The x, y, and z values of the DEM along the traces were then used to fit an optimum plane through the points. A least-squares algorithm was used. The resulting plane has a dip of 28º to the northeast (Fig. 5.8.6). This is obviously much shallower than the reflectors seen in the GPR. However, this can be explained by the different mechanical properties of the overburden, in which we have done our analysis, and the bedrock. If the overburden is lying upon a planar bedrock surface, and the local relief is due to variations in overburden thickness, then this 3D analysis only reflects the orientation of the dip within that overburden. The fault plane cannot continue upwards through the overburden at the same steep angle at which it cuts the bedrock, and thus the analysis does not contradict the results of the GPR studies. However, if the surface relief reflect the bedrock relief, and there is a layer of overburden with constant thickness, then this argument cannot be applied, and we must find another explanation for the apparent contradiction.
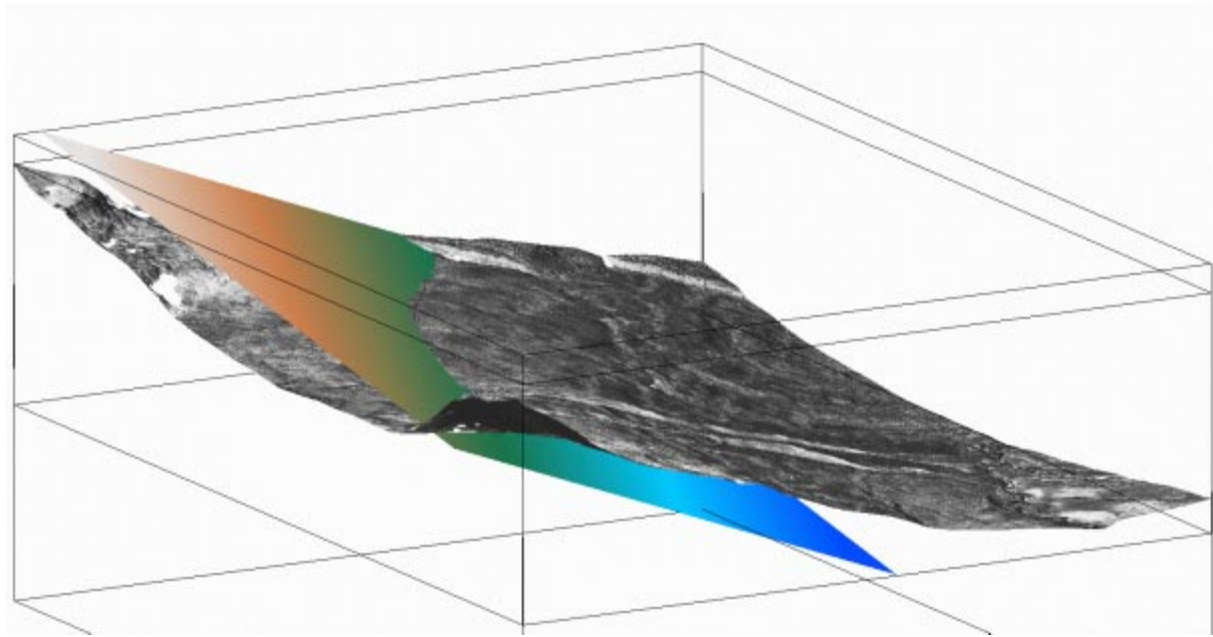
Fig. 5.8.6.   The best-fit plane through the trace of the fault scarp dips 28º to the northeast. View is from the southeast.

5.8.4   Conclusions

Detailed field mapping, GPR imaging and terrain analysis rule out the possibility that the Nordmannsvika fault is a gravitational fault. In the absence of a gravitational explanation for the origin of the fault, we propose that the fault is a tectonically driven normal fault, probably formed shortly after the last deglaciation of northern Norway.

5.8.5   References

Mauring, E., Olesen, O., Rønning, J.S. & Tønnesen, J.F., 1998: Ground-penetrating radar profiles across postglacial faults at Kåfjord, Troms and Fidnajohka, Finnmark. *In:* Dehls, J. & Olesen, O. (eds.): Neotectonics in Norway, Annual Technical Report 1997. NGU Report 98.016, 161 pp.

Olesen, O. & Dehls, J.: Neotectonic phenomena in northern Norway. *In*: Dehls, J. & Olesen, O. 1998 (eds.) Neotectonics in Norway, Annual Technical Report 1997, NGU Report 98.016, 3-30.

Sollid, J. L. & Tolgensbakk, J., 1988: Kåfjord, kvartærgeologi of geomorfologi 1:50 000, 1634 II. Geografisk institutt, Universitetet I Oslo.

6 GEODESY (TASKS 5, 6 & 7)

6.1 NORWEGIAN MAPPING AUTHORITY: REPORT FOR 1998

By Lars Bockmann, Statens Kartverk

6.1.1 General

GPS measurements at Masi and Bremanger have so far been completed only once, and therefore no information is yet available concerning significant deformations. Indications of deformations will only begin to emerge once additional observations and computations are completed in 1999. Meanwhile, the reduction of the GPS observations at Bremanger are not yet complete, and no results are therefore included in this report.

The following is a brief review of the 1998 season fieldwork and the reductions that have so far been performed.

6.1.2 Fieldwork

The Norwegian Mapping Authority's primary levelling network passes through Ølen in Sunnhordland, and was first observed in 1965. Routine relevelling in 1988 showed an abnormal height difference at bench mark B36N0063. Additional bench marks were therefore emplaced in stable bedrock each side of and as close as possible to the suspect bench mark. At the same time, plans for a further relevelling were made.

During the period 9 to 12 November 1998, 2600 metres of high precision two-way levelling was performed in Ølen between bench marks B36N0064 and B36N0062. The observations were carried out using a Zeiss DiNi 11 digital level together with 3 metre calibrated invar levelling staves. Conditions were still, partly rainy, and with temperatures between 2º and 6º Celsius.

6.1.3 Computations

GPS Observations at Masi

The standard Ashtech reduction software was used throughout for computing the observed vectors, which were subsequently adjusted in a horizontal network by means of the Norwegian Mapping Authority's program "GUNDA". A total of 49 vectors, all observed more than 4 times over a period of at least four hours, were included in the network adjustment. The standard errors for the horizontal components resulting from the adjustment were approximately 1 mm, while in the vertical they were in the region of 3 mm. First indications are that the observations reveal horizontal and vertical deformations of 3 mm per year and 9 mm per year respectively. These values, however, can only be confirmed by further observations in 1999, assuming that observational errors can be avoided so that there is consistency from year to year.

The two shortest vectors, between respectively NM01 and NM02, and NM05 and NM06, were also reduced and computed separately. These two vectors cross directly over the fault, and have the following values:

| NM01 to NM02: | 175.549 | m | ± | 0.001 |
| NM05 to NM06: | 767.810 m ± 0.003 | | | |

The above results, however, appear somewhat indecisive, and it is open to question whether an interval of only two years between observations is in fact too short to be able to properly identify the deformations that are suspected.

6.1.4 Classical Observations - Yrkje and Ølen

Fig. 6.1.1 is an overview showing Yrkje and the other sites involved in the Neonor project.
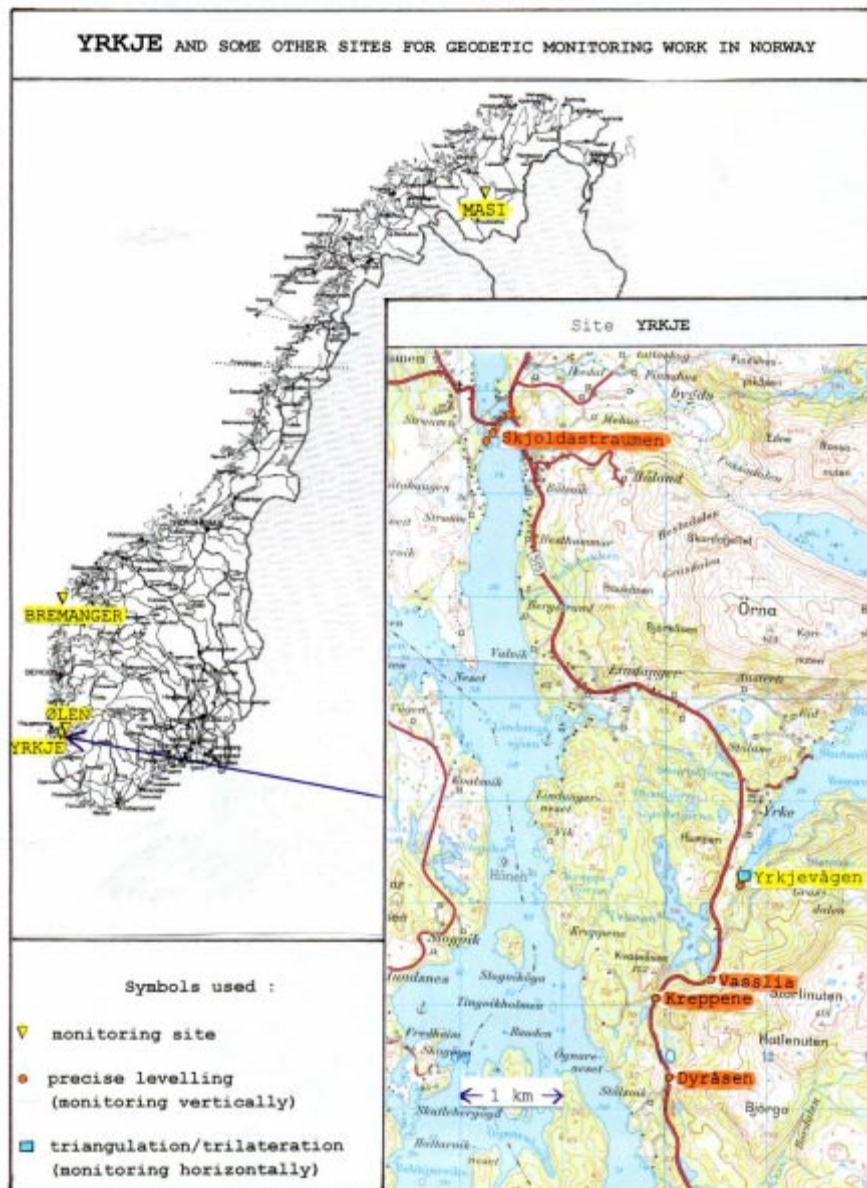
Fig. 6.1.1.   Horizontal Monitoring at Yrkjevågen

The computations are in hand, using a number of different and independent programs for network adjustment. So far, these are producing differing results which need to be examined further. Final results are expected early in 1999. The apparent co-ordinate shifts for all points are less than 0.2 mm per year.

Vertical Monitoring at Yrkje

Seven levelling lines were observed during 1997 over assumed faults. Six of these levellings showed no significant height changes with respect to earlier observations. A significant height change is, however, apparent on the seventh levelling line, at Skjoldstraumen Bridge, although this needs to be confirmed by further observations.

Vertical Monitoring at Ølen

Bench mark B36N0063 appeared to have moved vertically by 16 mm in the period from 1965 to 1988. The most recent relevelling in 1998 showed a further movement of 7 mm. Careful examination of the area around the bench mark now indicates that it was emplaced in an unstable block or slab of rock. Similar vertical movements were not found at the extra bench marks that were established in 1988, and this serves to further confirm that the suspect bench mark was originally founded at an unstable location.

Fig. 6.1.2 is a diagram showing the apparent elevation changes at Ølen 1965-1988-1988
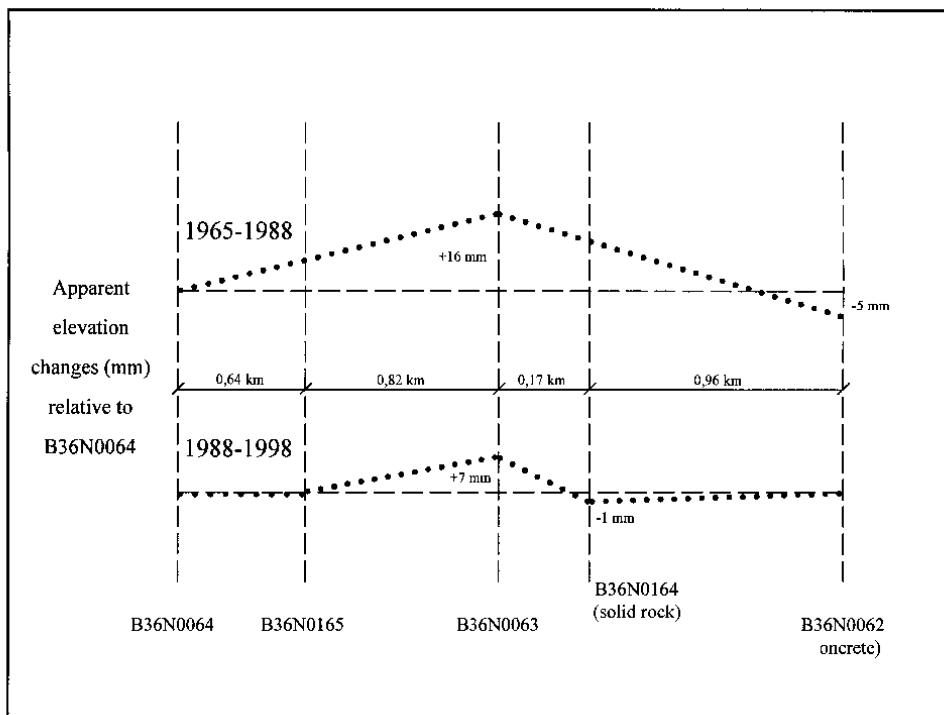
Fig. 6.1.2.   Apparent elevation changes at Ølen 1965-1988-1988

6.2   EVALUATION OF REPEATED LEVELINGS ACROSS THE STUORAGURRA FAULT, FINNMARK, NORWAY, 1987 TO 1996

Arthur G. Sylvester, University of California, Santa Barbara

Abstract

An analysis was made of four repeated levelings of a small array of bench marks across the Stuoragurra fault near Masi in Finnmark between 1987 and 1996 to determine if they are sufficiently reliable to allow conclusions about a 2.3 mm of observed vertical displacement across the fault between 1987 and 1991. Each of the data sets lacks some essential information necessary for a critical evaluation of the quality of the leveling, including the standards used and their calibration, and the atmospheric conditions under which the surveys were done. The critical shot across the fault is nearly 90 m, a distance that is extremely difficult to survey accurately with an optical level of the type that was used and by conventional leveling procedures. A modified procedure was used, but without assurance that the data can be taken at face value. These factors may contribute to standard errors that equal or exceed the observed displacement. Therefore, the data and conclusions about the height change should be taken with a healthy dose of skepticism before the apparent behavior of the fault during the observation period is ascribed to a tectonic cause.

6.2.1   Introduction

Several fault scarps have been found in northern Scandinavia that are thought to be post- or late-glacial in age (e.g., Lagerbäck, 1990) and, therefore, active or potentially active. Some of the faults are as long as 150 km, strike NNE-SSW, and have vertical separations up to about 30 m. They are thought to have formed by reactivation of ancient faults due to a combination of Holocene, post-glacial, isostatic rebound of the Fennoscandian crust following retreat and melting of the extensive Pleistocene ice cap (Muir Wood, 1993), together with plate tectonic stresses associated with sea floor spreading and "ridge push" in the Norwegian-Greenland Sea (Olesen et al., 1992a; 1992b; Bungum and Lindholm, 1996).

One of these faults, the Stuoragurra fault in northern Norway, is 80 km long (Fig. 6.2.1), strikes NNE-SSW, dips steeply SE, and has a scarp 7.5 m high in the vicinity of Masi (Olesen, 1988). Small earthquakes, including a M4 earthquake near Masi on 21 January 1996, have been recorded within a 30 km-wide zone parallel to the fault, giving reason to conclude that the fault may be active. In addition, a preliminary analysis of four repeated levelings over nine years at one locality across the fault near Masi indicated that the fault's footwall subsided 2.3 ± 0.8 mm relative to the hanging wall in between 1987 and 1991 (Skjøthaug, 1991; Dehls and Olesen, 1998a, p. 8; 1998b, p. 26).
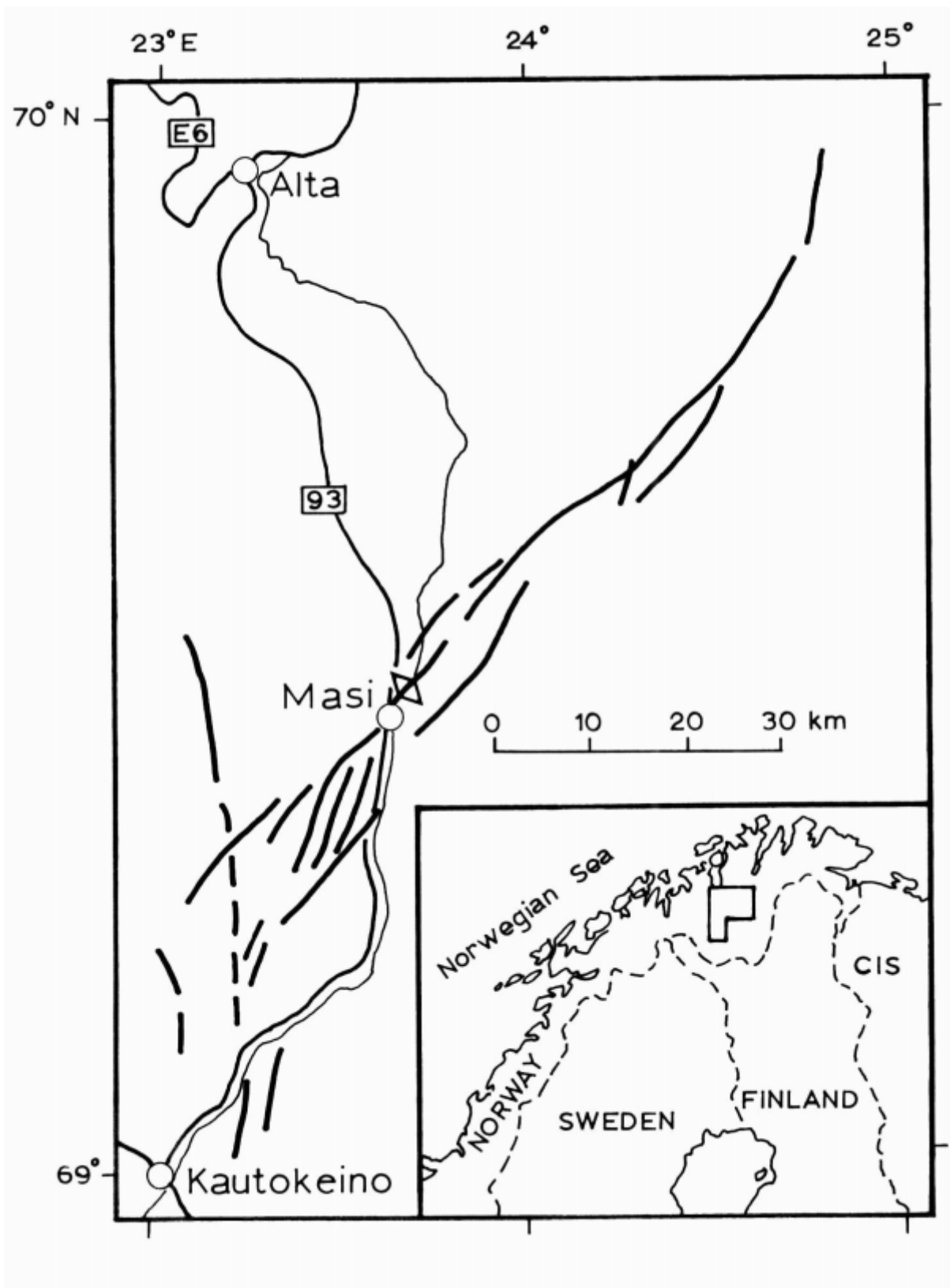
Fig. 6.2.1. Location map of Stuoragurra fault zone in western Finnmark, Norway, relative to Alta, Masi, and Kautokeino. Leveling array is indicated by diamond across fault strand northwest of Masi. Inset depicts location of map in northern Scandinavia.

It is of considerable interest to determine if the apparent height changes across the fault could be tectonic, perhaps as aseismic creep, because it would imply that other related post-

155

glacial faults in Fennoscandia may also slip by creep. That would be significant indeed, because fault creep is a rare phenomenon limited to only a few, major strike-slip faults in the world, and even fewer instances of vertical fault creep have been documented or even suggested (cf. Sylvester, 1995).

6.2.2 The Leveling Array

The Masi leveling line of four bench marks was established across the Stuoragurra fault near Masi in Finnmark, by Statens kartverk in 1987 to search for and monitor possible active vertical displacement at a single site along the 80 km length of the presumably active fault (Skjøthaug, 1991). Initially the line was 206 m-long and consisted of two pairs of permanent bench marks in bedrock, one pair on each side of the fault (Fig. 6.2.2). A swamp about 90 m wide separates the bench mark pairs. The two bench marks in each pair are about 50 m apart on each bedrock outcrop. Two additional permanent bench marks were set in 1997 for GPS measurements, one in bedrock, the other in a very heavy block of stone, and each on opposite sides of the fault, so that three bench marks are now on each side of the fault.
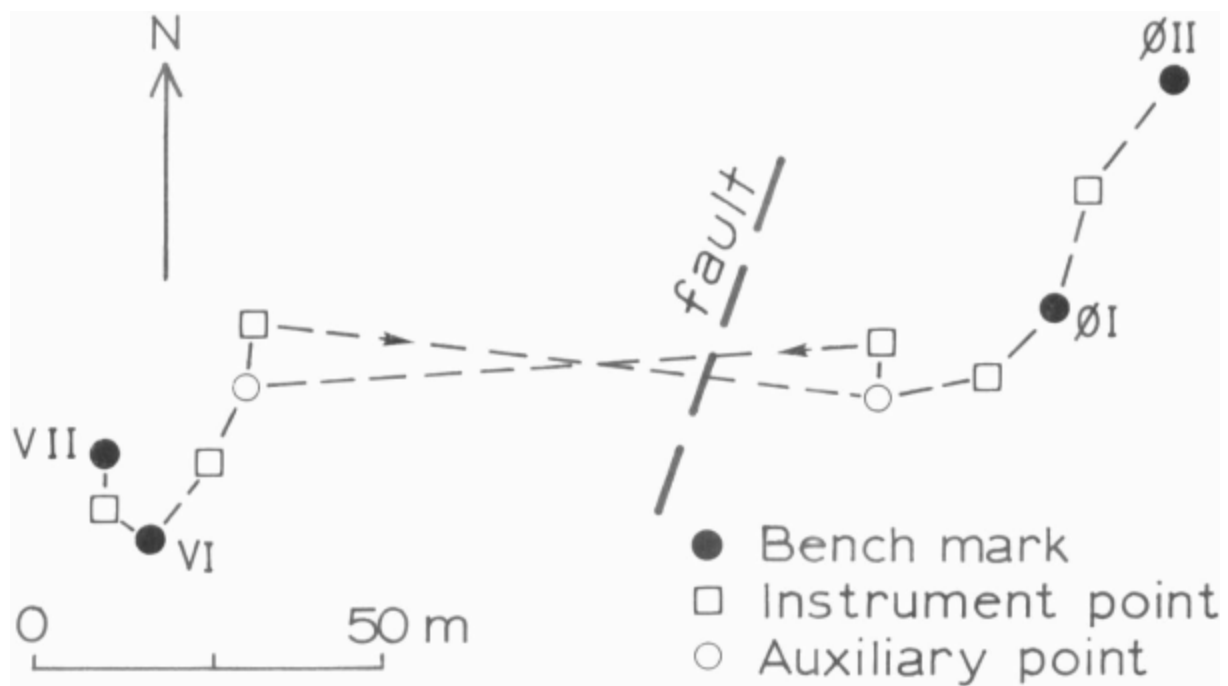
Fig. 6.2.2.   Arrangement of bench marks in Masi leveling array across Stuoragurra fault. Note that fore- and backsights across fault are nearly 90 m.

Results

The Masi leveling array has been surveyed four times by Statens kartverk: 1987, 1990, 1991, and 1996. The observed height differences across the fault, relative to 1987 and to bench mark ØI, increase from 1 mm in 1990, to 2.3 mm in 1991 (Fig. 6.2.3; Table 6.2.1). No change was observed between 1991 and 1996.

Table 6.2.1.   Results of the leveling at Masi.

	9/19/87	8/27/90	8/19, 8/20/1991	7/13/96
Instrument	N3#173660	N3#183178	N3#183178	N3#183178
Rods	Wild#3665A/B*	Zeiss#55283, 55284*	Wild#1788A/B	Wild#1788A/B
Method	double run, modified	double run, modified	double run, modified	double run, modified
	across swamp*	across swamp*	across swamp*	across swamp*
Weather	unknown	unknown	unknown	overcast
Height difference VI-ØI*	3.8599 m	3.8612 m	3.8622 m	3.8620 m
ΔHeight ØI to VI, since 1987*	-	+1.3 mm	+2.3 mm	+2.1 mm
Misclosure (mm)*	0.4†	0.7†	0.9#	0.3°
Misclosure (mm)† (this study)	-0.35	-0.54	-0.8	-2.95
Survey order (this study)	tectonic first	first	first	low
ppm (this study)	1.35	2.08	4.124	11.35
Rod Calibration	Regular checks at	Lantmäteriver-ket and	at Statens kartverk*	
Peg test	no	yes	yes	yes
Instrument adjustment	no record	none in field	none in field	none in field
Umbrella	probably not*	probably not*	probably not*	no
Comments	none	none	none	mygg!!
Observer	Tåsåsen*	Tåsåsen, Skjøthaug*	Tåsåsen, Skjøthaug*	Sundsby

*written communication, Leif Grimstveit, 15 Feb. 1999

†calculated as difference between fore and back runs between bench marks.

#calculated by Statens kartverk as difference between leveling results on two different days

°computed by Statens kartverk as sum of misclosures in two triangles
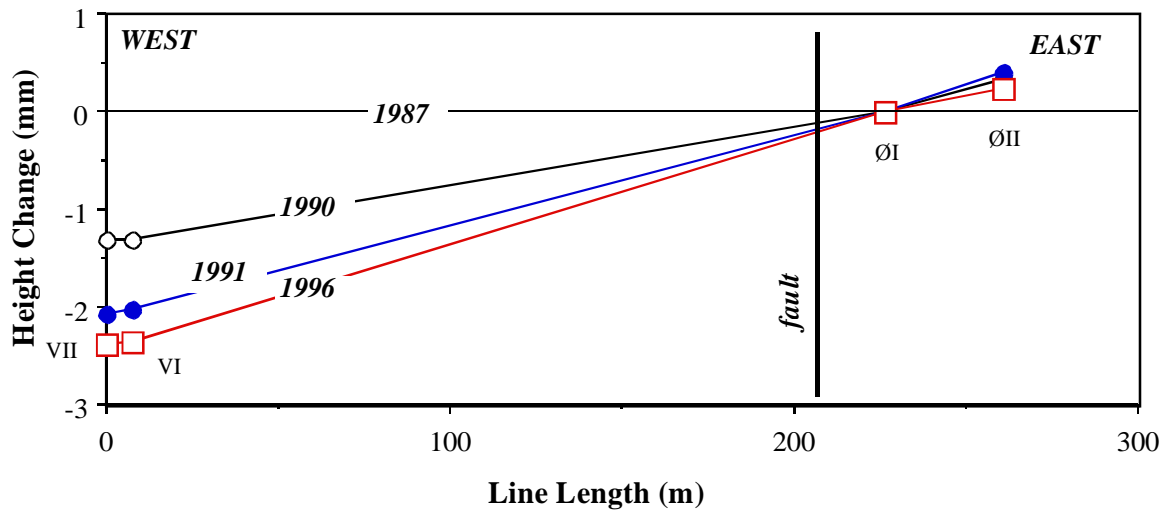
Fig. 6.2.3.   Height changes of bench marks in leveling array across Stuoragurra fault near Masi, 1987 to 1996. Bench mark Ø1 arbitrarily held fixed. Conventional error bars would fall outside the diagram.

6.2.3   Evaluation Of The Array And Surveying Procedure

The 90 m sight across the swamp precludes a straightforward backsight/foresight leveling procedure by standard optical methods to determine the height changes across the swamp. The 1990 and 1991 surveys used a pair of temporary bench marks to shorten the sighting distance across the swamp. The temporary bench marks were placed differently in each survey. The two additional bench marks were set in 1997 as part of a regional GPS-line, and they provide an additional fixed point on each side of the fault for future surveys. Even so, the minimum distance between the closest bench marks across the swamp is about 85 m.

When the sightings were made across the swamp, the foresight was 85-90 m, but the backsight was only about 10 m in most instances. Assuming the instrument is in perfect adjustment (including focusing), collimation and parallax errors should not occur even with such a sight length imbalance, but refraction error may be very significant over the 90 m. To mitigate refraction errors, first-order leveling procedures specify that shot lengths be kept under 25 m (Federal Geodetic Commission, 1984). It is difficult, moreover, to read a leveling rod accurately at 90 m with the standards used in the Masi surveys (Table 6.2.1), especially when and if the atmospheric conditions are poor, including when shimmer or misty weather prevail, as they did in 1991 and 1996, respectively, and as they usually do over vegetation in warm weather (Castle et al., 1994)

To overcome these difficulties, Statens kartverk resorted to a modified procedure making paired setups over a short time interval, according to the following assumptions (Grimstveit, written commun., 1999):

1) The instrumental error does not change between the two setups;

2) The atmospheric conditions remain unchanged between the setups; and

158

3) The paths of the sight lines are circular arcs, or could be considered as such for the purposes of this project.

The following procedures were used in each of the surveys (Grimstveit, written commun, 1999):

1987: The leveling was made directly between bench marks, without establishing temporary ones. Standard procedure was used except for crossing the swamp. The paired levelings for this critical shot were made only once, so that a good estimate for the elevation difference was determined, but the misclosure check was not as strong as it should have been. Still, the misclosure is small.

1990: One temporary bench mark was set on each side of the swamp. The levelings (fore and back) between these marks were made twice, on the same day, using the same procedure as 1987. Four comparable one-way elevation differences were thus obtained. Three of them agreed well. The fourth differed about 2 mm and was not used in the analysis, nor was the paired, opposite-directed, leveling result.

1991: A pair of temporary bench marks was set differently from those used in 1990. Two levels were used simultaneously to level across the swamp on each of two consecutive days to obviate assumption 2 mentioned above. The misclosure check was stronger than those in 1987 and 1990, considering the difference between result day 1 and result day 2 as the misclosure across the swamp.

1996: Two additional permanent bench marks were established, however (probably?), not in bedrock. They may be considered as stable during the epoch of leveling, as were the preliminary bench marks during the epochs 1990 and 1991. Complete leveling VI-ØI was made on each of two days, using different leveling paths. Each of the triangles VI-VIII-ØIII and ØIII-ØII-ØI gives a misclosure check, and the leveling measurements were adjusted as a network, instead of simply meaning fore and back levelings.

6.2.4   Standards

The same level and rod pair were used only in the 1991 and 1996 surveys (Table 1). The field notes lack any information about the standards used in 1987, but according to Leif Grimstveit (written commun. 1999), Wild rods #3665A/B were used (Table 1). Field tests were performed before each survey, judging from the field notes, except 1987 to determine whether or not the instrument was in adjustment. The leveling rods were calibrated by comparing them with "normalmeter" no. 11915, last certified in 1968 (Sundsby, written commun., 1998). In the beginning of the 1990s, that "normalmeter" was also calibrated by the Lantmäteriverket in Sweden (Sundsby, written commun., 1998), but information does not seem to be available about how and how often the rod comparisons were made, or if the rods used in the Masi leveling were compared with the "normalmeter". We also don't know how the cali-

brations of the "normalmeter" compared between 1968 and the 1990s. This critical information is not ordinarily provided for every leveling in general. Typically all that is known is similar to what Grimstveit (written commun., 1999) stated for the rods used in the Masi surveys: "Our rods for precise leveling are checked regularly at Lantmäteriverket, Sweden, as well as at Statens kartverk in the periods between. Errors have been found to be 0.03 mm/m, or less. As the leveled elevation difference in Masi is 3.85 m, we consider this scale error as far from critical." I concur, but the calibration data are still of critical interest. Irregularities in the calibration process at the U.S. Navy's west coast calibration laboratory have been known to introduce significant errors when the data are adjusted for apparent rod errors.

In summary, documentation is lacking about the adjustment or calibration history of the instruments or rods beyond Grimstveit's statements, unless it is in Statens kartverk records that were unavailable to me at the time this report was written. Without calibration data, it is entirely permissible to assert that the observed height differences among the Masi array bench marks between 1987 and 1996 can be attributed entirely to rod errors and instrument misadjustments, although I suspect this is unlikely.

6.2.5 Survey Conditions

Neither the field notes nor Statens kartverk have information about the weather and atmospheric conditions for the 1987 and 1990 surveys, and there is no indication whether the instrument was shaded in any of the surveys. The Wild N3 level is known to perform less than optimally in direct sunlight and when unprotected from the wind. The field notes indicate that it was a humid, overcast day for the 1996 survey and that the observer was plagued by mosquitoes. The field notes also say that it began to rain immediately after the 1996 survey was completed, so the humidity must have been high during that survey. Shimmer plagues optical sightings with surveying instruments especially over shots as long as 90 m. Shimmer is prevalent in long shots across vegetation, in hot weather, and when the air is calm and humid. All of these conditions may combine to yield systematic errors that are difficult or impossible to recognize or correct confidently, especially at the degree of precision required for tectonic studies (Castle et al., 1994).

6.2.6 Survey Quality

The quality of each of the Masi surveys may be determined conventionally from the uncorrected field observations by calculating the misclosure, the allowable misclosure, and the precision of each survey, wherein "misclosure" is the height difference between the fore- and back-runs. Acceptable misclosure equals $\underline{s}L^{1/2}$ where L is the one way distance in km, and $\underline{s}$ is one standard deviation per kilometer (Federal Geodetic Commission, 1984). For "tectonic first order" standards, $\underline{s}$ must be less than 1 mm. The allowable misclosure so calculated for 260 m-long Masi array is 0.44 mm.

Only the 1987 survey qualifies for the designation "tectonic first order" with a misclosure of -0.35 mm calculated in the conventional way for a conventional survey; the 1990 and 1991 surveys are first order (-0.54 and -0.80, respectively); the 1996 survey had a misclosure of -2.95 mm which the Federal Geodetic Commission would designate as "low order" work (Table 6.2.1). More revealing than the misclosure and survey order is the ratio of the misclosure to the length of the survey array, given as ppm in Table 6.2.1. These are the values that one would to assign uncertainty ("error bars") in a graph of height differences from year to year (Table 6.2.1). Clearly the uncertainty with even the best survey (1.8 ppm in 1987) is almost as great as the observed height change (2 mm) from 1987 to 1996 (Fig. 6.2.3). The uncertainties with the 1990 and 1991 surveys are even greater, and the 15 ppm uncertainty in 1996 is simply unacceptable in any case.

6.2.7 Summary

The swamp between bedrock outcrops that straddle the Stuoragurra fault near Masi presents nearly insurmountable problems for completing a leveling survey having the necessary precision to allow determination of tectonic displacements that may be as small as 1 mm/yr. Statens kartverk recognized these problems and so surveyed the array by a modified procedure and calculated the misclosure also in a modified way with better results (Table 1).

The necessary and sufficient information is lacking, however, to determine how comparable each survey was with one another in terms of the standards used, the accuracy of the standards, and the weather and atmospheric conditions of the first two surveys. The kind and size of errors inherent with major differences in atmospheric conditions, refraction over long shot lengths, shimmer, unshaded levels, and miscalibrated leveling rods all may combine to yield results with large misclosures as large as those in these four surveys.

I believe Statens kartverk did the best job of surveying it could under the circumstances, but I remain skeptical that such a small height change, 2.3 ± 0.8 mm, can be stated so confidently, given the difficulties of the 90 m shot, the lack of information about the atmospheric conditions, and the lack of documentation about the rod calibrations. I would be very hesitant to compare the results of such disparate surveys at the level of precision required to distinguish confidently vertical displacements as small as 1 mm from year to year . I am particularly dubious of the 1996 survey and I maintain that it should not be included in any data set used to draw tectonic conclusions about vertical displacement across the Stuoragurra fault during the period 1987 to 1996, although vertical displacement is not claimed to have occurred between 1991 and 1996. It is possible that the 2.3 mm in a year's time is real, because such displacement rates have been measured over many years on faults in tectonically active areas elsewhere in the world. In the case of the Stuoragurra fault, however, many more surveys over a much longer period of time will be needed to confirm convincingly that this fault has the tendency or capability to cause such displacements.

Interseismic fault creep is a rare phenomenon, having been observed only along strike-slip faults chiefly belonging to the San Andreas fault system in California (eg., Sylvester, 1995). Therefore, great caution must be exercised in the evaluation of horizontal or vertical changes among benchmarks in successive surveys before concluding that those changes have tectonic causes, especially fault creep. In the majority of instances, the changes have nontectonic causes, especially subsidence related to poroelastic stressing and consequent induced seismicity in areas of pumping of subsurface fluids (Segall, et al., 1994; Segall and Fitzgerald, 1998), and possibly even related to rainfall and atmospheric pressure changes (e.g., Dal Moro and Zadro, 1998). Before causal conclusions can be reached, however, the primary data must be scrutinized carefully and thoroughly to exclude erroneous contributions from from unstable bench marks, from systematic, random, and procedural errors in each individual survey, as well as between and among repeated surveys.

6.2.8   Recommendation

Future resurveys of this array should be done, but they should be done either with digital instrumentation or by surveying a longer route on firm ground around the swamp. Unfortunately the ground around the swamp is hardly more stable or firm than the swamp itself and a longer route will introduce additional uncertainty. No optical instrument is currently available that can perform a conventional leveling survey with a direct shot of 90 m and still achieve tectonic first order requirements routinely. The Leica NA2000 digital level can barely do so to second order standards over that distance; the Leica NA3000 digital level yields first order results only over distances less than 60 m (Sylvester, 1996; Arabatzi, et al., 1993; Leica Heerbrugg AG, 1990). The uncertainties in vertical measurements associated with GPS are still too large ($\pm$ 5 mm) to consider GPS as a viable alternative to some kind of optical or infra-red ranging technique over time periods of 10 years or less at the presumed displacement rate of 1 mm/yr. A field procedure should be devised for the NA2000 or equivalent level using multiple combinations of repeating sightings that will yield statistically meaningful data.

Future resurveys should be compared only with the 1987 survey, because it is the only one having the requisite precision to qualify as "tectonic first order". The others, especially the 1996 survey, are unusable for height changes across the array of 3-4 mm because of their low precision.

6.2.9   Acknowledgments

6.2.10 References

Arabatzi, O., G. Mavrellis, and D. Stathas, 1993. Testing the digital level Wild NA-2000 in laboratory and field conditions. *Survey Reviews 32*, 99-108.

Bungum, H., and C. Lindholm, 1996. Seismo- and neotectonics in Finnmark, Kola and the southern Barents Sea, part 2: Seismological analysis and seismotectonics. *Tectonophysics 270* , 15-28.

Castle, R. O., R. K. Mark, and R. H. Shaw, 1994. An empirical assessment of refraction error in leveling as a function of survey order and environment. U.S. Geological Survey Bulletin 2114, 50 p.

Dal Moro, G., and M. Zadro, 1998. Subsurface deformations induced by rainfall and atmospheric pressure: Tilt/strain measurements in the NE-Italy seismic area. *Earth and Planetary Science Letters 164*, 193-203.

Dehls, J., and O. Olesen, 1998a. Neotectonics in Norway. *Norges Geologiske Undersøkelse* Report, 98.016, 149 pp.

Dehls, J., and O. Olesen, 1998b. Neotectonics in Norway. Unpub. project meeting report and field excursion guide, 48 p.

Federal Geodetic Commission, 1984. *Standards and specifications for geodetic control networks*, National Geodetic Survey, Rockville, MD, 31 p.

Lagerbäck, R., 1990. Late Quaternary faulting and paleoseismicity in northern Fennoscandia, with particular reference to the Lansjärv area, northern Sweden. *Geologiska Föreningens i Stockholm Förhandlingar 112*, 333-354.

Leica Heerbrugg AG, 1990. Wild NA3000 Specifications.

Muir Wood, R., 1993. A review of seismotectonics of Sweden. Technical Report 93-13, Svensk Kärnbränslehantering, 225 p.

Olesen, O., 1988. The Stuoragurra fault, evidence of neotectonics in the Precambrian of Finnmark, northern Norway. *Norsk Geologist Tidsskrift 68*, 107-118.

Olesen, O., H. Henkel, O. B. Lile, E. Mauring, J. S. Rønning, and T. H. Torsvik, 1992a. Neotectonics in the Precambrian of Finnmark, northern Norway. *Norsk Geologisk Tidsskrift 72*, 301-306.

Olesen, O., H. Henkel, O. B. Lile, E. Mauring, and J. S. Rønning, 1992b. Geophysical investigations of the Stuoragurra postglacial fault, Finnmark, northern Norway. *Journal of Applied Geophysics 29*, 95-118.

Segall, P., J-R. Grasso, and Antony Mossop, 1994. Poroelastic stressing and induced seismicity near the Lacq gas field, southwestern France. *Journal of Geophysical Research 99*, 15, 423-15, 438.

Segall, P., and S. D. Fitzgerald, 1998. A note on induced stress changes in hydrocarbon and geothermal reservoirs. *Tectonophysics 289*, 117-128.

Skjøthaug, p. 1991. Rapport fra nivellement over Stuoragurraforkastningen 1991. Statens kartverk (Norwegian Mapping Authority), unpub. report, 2 pp.

Sylvester, A. G., 1995. Nearfield vertical displacement in the creeping segment of the San Andreas fault, central California, 1975 to 1994. *Tectonophysics 247*, 25-47.

Sylvester, A. G., 1996. Snake River, Wyoming, crossing with the Leica NA-3000 digital level. *Survey Reviews 33*, 383-388.

7   SEISMICITY (TASK 10)

7.1   SEISMIC INSTALLATIONS IN RANA AND BREMANGER

By Erik Hicks & Conrad Lindholm, NORSAR

7.1.1   Summary

The seismic network installed in June 1997 in the Rana area was originally planned to be de-mobilized during 1998, but a continued presence was considered beneficial in light of the ex-cellent results from the first year of operation. It was possible to maintain a network of four stations at minimal cost by installing a remote data acquisition system at the central station.

A six-station network was installed in the Bremanger area in September/October 1998 by NORSAR, using a similar remote data acquisition system to Rana. This has reduced the sub-stantial transmission costs of the first year to next to nothing. There has been some hardware problems with the modem in Bremanger, which are currently being addressed.

7.1.2   Technical installations

There are currently two networks operated under the NEONOR project, the reduced network in the Ranafjord area, now consisting of four stations (Fig. 7.1.1), and a six-station network in the Bremanger/Nordfjord area in Western Norway (Fig. 7.1.2). Both networks are based on the Seislog remote data acquisition system from the Institute of Solid Earth Physics (IFJF) at the University of Bergen (available free of charge). This is the same system used to operate the national Norwegian seismic network.
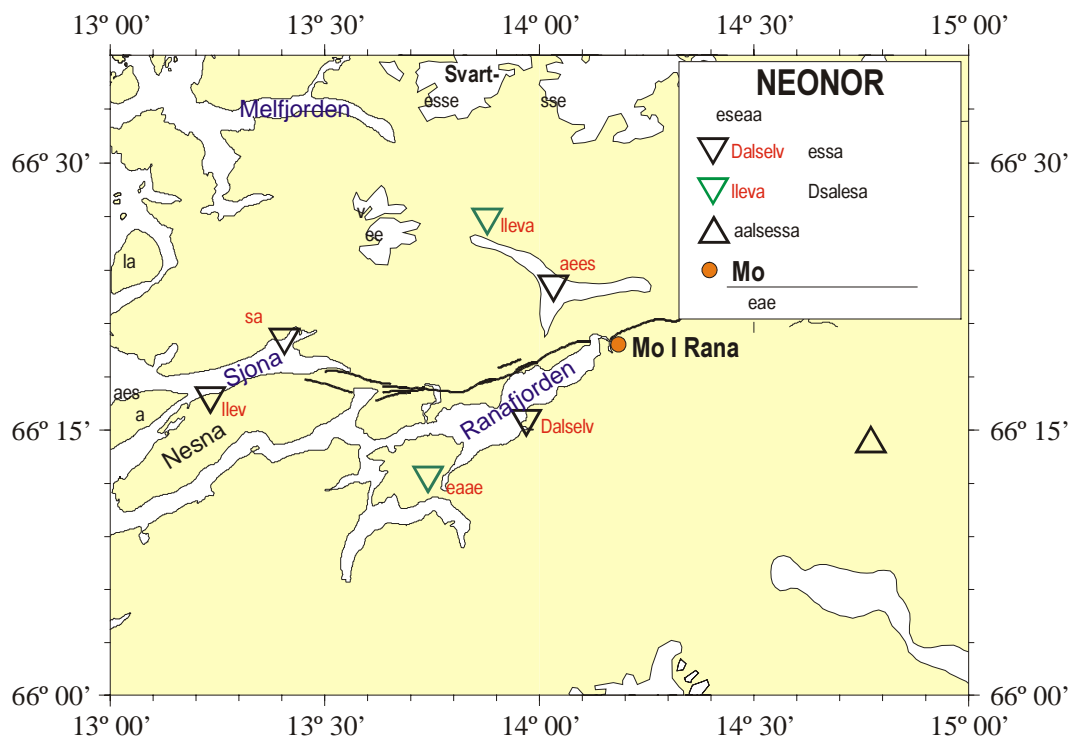
Fig. 7.1.1.   The revised network in the Rana area (black inverted triangles), The disman-tled stations are shown by the green inverted triangles.

165

The system runs on standard Intel PC´s, using the QNX unix operating system. The PCs used by NEONOR are old 486 machines that were donated by NORSAR and upgraded to AMD K6-2 processors and 2.5 GB hard disks. Data transmission to NORSAR is via modem (Rana) or ISDN (Bremanger), programs for automated data transfer are also available from IFJF.

The PCs have a diskloop containing 10 days of continuous data, in addition to space for a minimum of around 5,000 events.

Fig. 7.1.3 shows the receiver mast for the central station and Fig. 7.1.4 shows the installation of the discriminators, PC and modem for the Bremanger network.
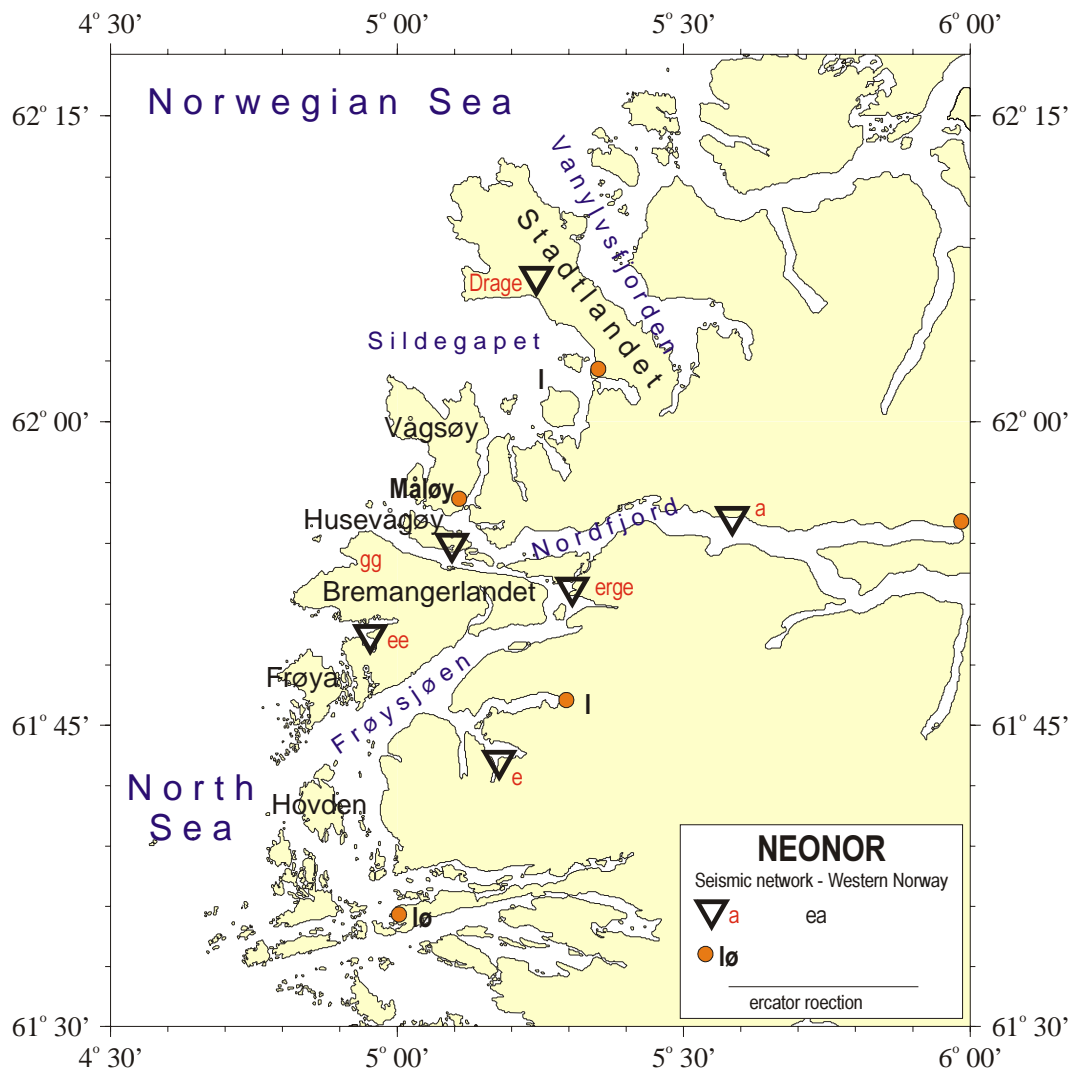
Fig. 7.1.2.   The new seismic network in the Bremanger area (inverted triangles).

Field work, Rana

The removal of two stations and installation of the remote data acquisition system was performed during three working days in the week of September 14-18 by Erik Hicks and Kjell Arne Løken (NORSAR). Removal of the two stations Vettahaugen (N1R1) and Lillevand (N1R4) was straightforward. The house owner at the central station was very helpful and forthcoming in allowing the installation of the PC and modem in a closet in the basement, and installation of wires for the telephone line, GPS clock and data. The discriminators and digitizer remain in their previous location in a freestanding garage, with a serial cable transmitting data to the Seislog system.

Since the station on Vettahaugen (N1R1) was no longer available as a repeater for the radio signals from Nordsjona (N1R3) it was necessary to increase the height of the transmitter mast in order to transmit a satisfactory signal to the central station. This was the only technical problem encountered. The PC and modem were configured before departure to Mo i Rana, so there were no delays during installation.

Installation and field work, Bremanger

The installation of the new network in Bremanger was performed during two weeks from September 28 to October 9, by Erik Hicks and Kjell Arne Løken (NORSAR). The original plan using the Telenor/Norkring installation on Steinfjellet, Bremangerlandet as a central station had to be changed, as Norkring wanted a very high rent for the installation, and also placed inconvenient limitations on access to the site. This reduced the value of the previous trip made in June 1998 by Erik Hicks, but with thorough preparation and the help of friendly locals this did not hamper work to any noticeable degree.

Two days were spent finding suitable locations and testing radio transmission and the only viable point found for a central station was at Tytingvågen on Husevågøy just south of Måløy. This point has the receiver mast (Fig. 7.1.3) on the summit of a 75 m high hill, so around 150-200 m of cable was required for power and data. The discriminators, digitizer, power supply, PC and modem were installed in an uninhabited house at the foot of the hill (Fig. 7.1.4). The installation of the central station took around four days in all, including burial of the data cables to the receiver mast.

The other stations generally needed around 4-5 hours of work to install, unlike the Rana station the seismometers in the Bremanger network were installed directly on bedrock, saving much time compared to the cement foundation used in Rana. The masts used were also of a different type, which were bolted directly to the bedrock (Fig. 7.1.5). However, transportation between the stations was slow due to ferries and often narrow and winding roads.

The northernmost station presented some problems in finding a location, as localities that had accessible bedrock had no access to electricity and vice versa. It was finally decided to attempt a solar powered station above Drage on Stadtlandet (Fig. 7.1.6). A somewhat sheltered location was found, and the station has survived the first autumn storms. The station has around 350 Ah of battery capacity, which should be enough to maintain operation for several months without sunlight, however there might be a short period in which the batteries are depleted around Christmas.

Fig. 7.1.3.   The receiver mast at the central station, Bremanger.

Fig. 7.1.4.   The data acquisition system, Bremanger.

Fig. 7.1.5.   Drilling the foundation for one of the masts.

The weather was good throughout most of the two-week period, with quiet and sunny conditions most days, meaning no time was lost due to weather considerations. Fig. 7.1.7 shows the view from the Leirgulen station east of Bremangerlandet, looking towards the central station on Husevågøy.

The finished network as shown in Fig. 7.1.2 has an aperture of around 35 km in the east-west direction, and 45 km north-south. This should be sufficient to provide much improved locations in the northern parts of the North Sea.

During the first weeks after the installations the network was plagued with intermittent problems on all channels thought to be caused by a faulty power supply, noise on the Myklebust station, and finally the modem malfunctioning. Maintenance work was therefore carried out by Erik Hicks in the first week of November. It turned out that the problems at the central station were related to water entering the amplifier box on the receiver mast, thereby shorting out power to all receivers. Two of the receivers were also dead; it is currently unsure if this is related to the same problem or if it is lightning related. The dead receivers meant several transmitters also had to be replaced, as redundant receivers for all frequencies were not available. The frequencies used between Myklebust (N2B2), Løvikneset (N2B3) and the central station were also exchanged, reducing the observed noise from the Myklebust station to a minimum.

Unfortunately, the new modem failed only a few days after the completion of this field work, and we were unable to determine the cause of this. It appeared that the data acquisition was running, so it was decided to order an ISDN line and install a router, as this was thought to be a more stable solution. The ISDN line was installed February 1., after a delay of several weeks due to delivery problems at Telenor. Erik Hicks traveled to Bremanger the same day to install the router and retrieve data for the period November '98 to January '99. Unfortunately, both power supplies for GPS clock and digitizer/receivers had been destroyed around the middle of January, most likely in a thunderstorm. Replacements were not available locally, so a new trip will be carried out as soon as possible. The possibility of installing some kind of lightning protection is also being examined.

7.1.3   Data analysis

The Seislog system detects events by continuously monitoring the value of the short term average over long term average for bandpass filtered data for each station (Utheim & Havskov, 1997). The short term and long term time windows, as well as filter parameters and trigger/detrigger thresholds are adjustable via remote login through the modem/internet, so fine tuning is possible after installation. A minimum number of station triggers within a set time limit is considered an event detection, and a detection is entered into the detection database and data are saved to disk.

The detections and data are downloaded into a temporary database at NORSAR, where the data can be evaluated, and the event discarded or copied to the NEONOR database for analysis. This is all done from within the Seisan program package (Havskov, 1997), also from IFJF. Data samples for the two networks are shown in Fig. 7.1.8 and 7.1.9.

Fig. 7.1.6.   The solar powered station at Drage (N2B4) on Stadtlandet. The batteries are in the large box by the mast. The seismometer is under the green cover barely visible just left of K.A.Løken.

Fig. 7.1.7.   View westwards from the Leirgulen (N2B6) station toward the central station at Tytingvågen.
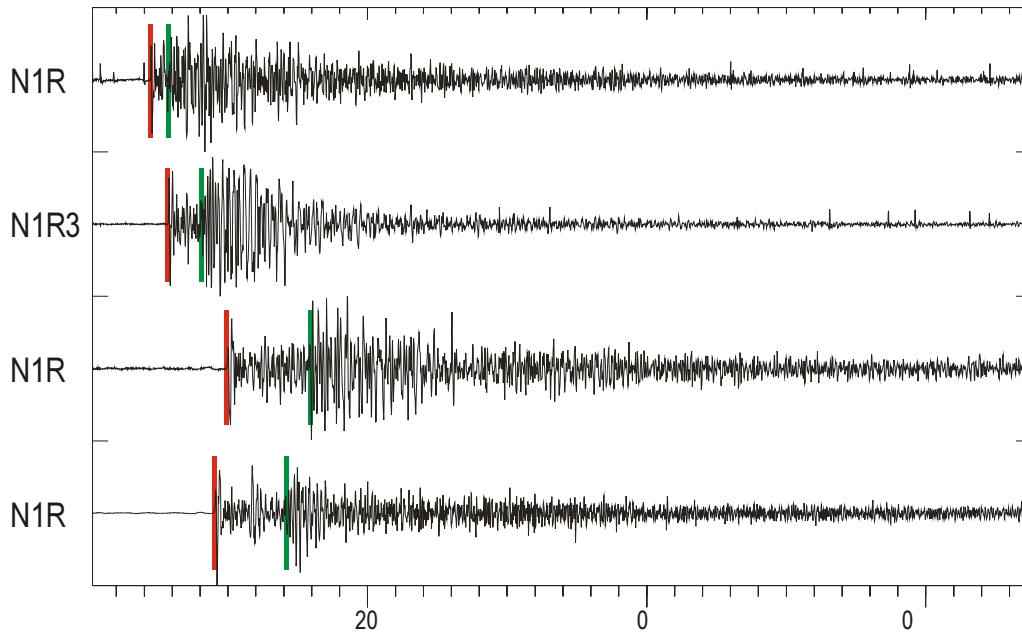
Fig. 7.1.8.   Data sample from the current Rana network. The earthquake was located by Handnesøya at a depth of around 2-4 km, and had a magnitude of M_L 2.5. P-phase (compression) arrivals are marked by red lines. S-phase (transverse) arrivals are marked by green lines.
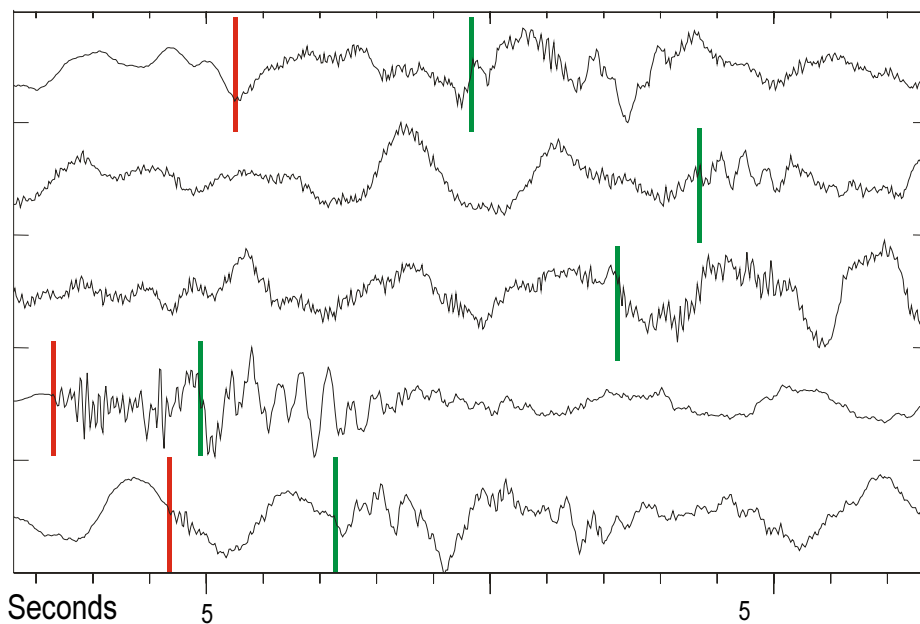
Fig. 7.1.9.   Sample event from the Bremanger network, Note that station no. 4 (Drage) was not yet operational. The event is most likely a surface quarry blast, and has an equivalent magnitude around M_L 1.7. P- and S-phase arrivals are shown in red and green respectively.

7.1.4   System response

Since the sensors, amplifiers, gain and filter settings and digitizers are identical for all stations in both Mo i Rana and Bremanger, the same system response can be used. System response is calculated from sensor, filter and digitizer parameters, thus including all factors of influence

on the signal. The Seisan program package includes a program for calculating system response, and creates a parameter file used directly by other Seisan programs during analysis, to calculate ground motion from the signal. This is necessary for calculation of magnitudes and synthetic waveform modelling. A system displacement response curve is shown in Fig. 7.1.10.
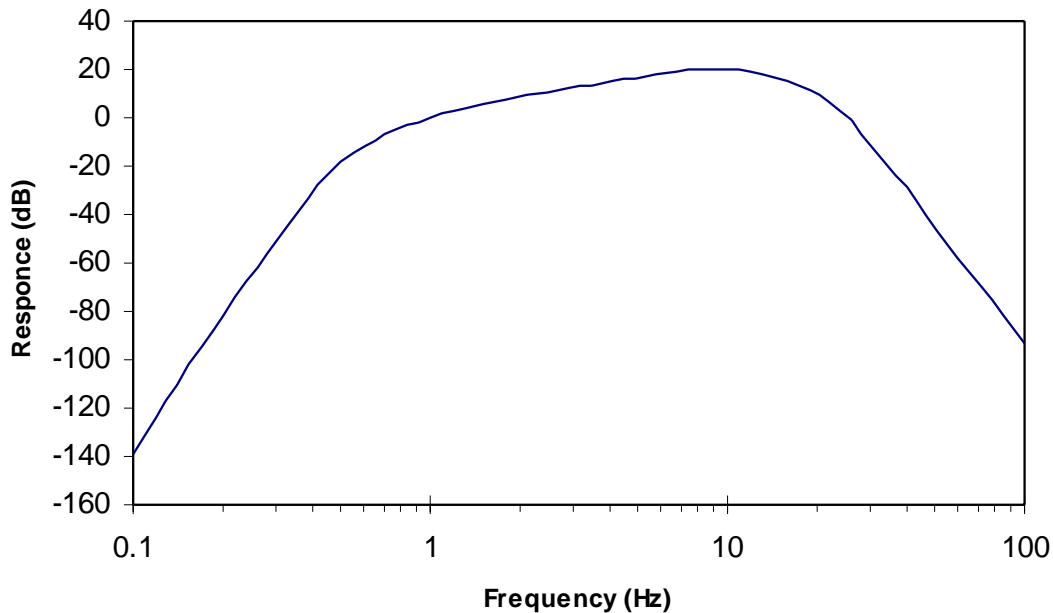
Fig. 7.1.10.   System displacement response for the NEONOR seismic stations.

7.1.5   References

Havskov, J., (1997): *The Seisan earthquake analysis software*, Institute of Solid Earth Physics, University of Bergen, 236 pp.

Utheim, T. & J. Havskov, (1997): *The Seislog data acquisition system*, Institute of Solid Earth Physics, University of Bergen, 101 pp.

7.1.6 Appendix A – Revised technical information, Mo I Rana

This document contains current technical information concerning the NEONOR seismic network in Mo i Rana. Last changes to the newtork were during file work September 14-18, 1998.

Station no. 1 (N1R1) - Vettahaugen
Dismantled September 1998.

Station no. 2 (N1R2) - Lillevik (Nesna)
Latitude: 66º 16' 53.4" N
Longitude: 13º 14' 00.3" E
Height above MSL: 61 m
Contact: Kristian Lillevik, Tel.: 75057544
Gain: 60 dB
Highpass filter: 0.2 Hz
Lowpass filter: 12.5 Hz
VCO freq.:   1360 Hz
Receiver freq.:   N/A
Transmitter freq.:   441.725 MHz to station no. 3 (N1R3) – Nordsjona

Station no. 3 (N1R3) - Nordsjona
Latitude: 66º 20' 14.0" N
Longitude: 13º 24' 22.6" E
Height above MSL: 68 m
Contact: Harry A. Nilsen, Tel.: 75163263
Gain: 60 dB
Highpass filter: 0.2 Hz
Lowpass filter: 12.5 Hz
VCO freq.:   1700 Hz
Receiver freq.:   441.725 MHz from station no. 2 (N1R2) - Lillevik (Nesna)
Transmitter freq.:   173.900 MHz to central point (N1R6) – Dalselv

Station no. 4 (N1R4) - Lillevand
Dismantled September 1998.

Station no. 5 (N1R5) - Hammernes
Latitude: 66º 23' 12.8" N
Longitude: 14º 01' 58.2" E
Height above MSL: 62 m
Contact: Hans Leiramo, Tel.: 75169568
Gain: 60 dB
Highpass filter: 0.2 Hz
Lowpass filter: 12.5 Hz
VCO freq.:   2720 Hz
Receiver freq.:   N/A
Transmitter freq.:   174.000 MHz to central point (N1R6) – Dalselv

Station no. 6 (N1R6) - Dalselv (central point)

Latitude:	66º 15' 39.6'' N
Longitude:	13º 58' 11.0'' E
Height above MSL:	85 m
Contact:	Olaf M. Hansen, Tel.: 75164540
Gain:	60 dB
Highpass filter:	0.2 Hz
Lowpass filter:	12.5 Hz
VCO freq.:	N/A
Receiver freq.:	173.900 MHz from station no. 3 (N1R3) - Nordsjona
	174.000 MHz from station no. 5 (N1R5) - Hammernes
Transmitter freq.:	N/A
Discriminators:	Teledyne Geotech model 46.12
Digitizer:	Nanometrics RD6
Timing system:	Garmin GPS-35
Acquisition system:	Seislog PC. 300 Mhz AMD K6-2 proc., 64 MB ram
Disk capacity:	Diskloop: 850 MB = 10 days continous. Detections: 1500 MB
Modem:	Ericsson Semafor 2314C 14400 bit/s

All stations:

Seismometer type:	Teledyne Geotech S-13
Amplifier:	Teledyne Geotech model 42.50
VCO:	Teledyne Geotech model 46.22

7.1.7   Appendix B - Technical information, Bremanger

This list contains current technical information concerning the NEONOR seismic network in Bremanger. Last changes to the network were during field work Febuary 1-2, 1998.

Station no. 1 (N2B1) - Tytingvågen (central point)

Latitude:	61° 53' 59.8" N
Longitude:	5° 05' 46.5" E
Height above MSL:	75 m
Contact:	Selmar Nordbø, Tel.: 57851664
Gain:	60 dB
Highpass filter:	0.2 Hz
Lowpass filter:	12.5 Hz
VCO freq.:	N/A
Receiver freq.:	173.900 MHz from Løvikneset (N2B3)
	142.300 MHz from Drage (N2B4)
	174.000 MHz from Haus (N2B5)
	441.650 MHz from Leirgulen (N2B6)
Transmitter freq.:	N/A
Discriminators:	Teledyne Geotech model 46.12
Digitizer:	Nanometrics RD6
Timing system:	Garmin GPS-35
Acquisition system:	Seislog PC. 300 Mhz AMD K6-2 proc., 32 MB ram
Disk capacity:	Diskloop: 850 MB (10 days), detections: 1500 MB
Router:	Cisco 770 Series

Station no. 2 (N2B2) - Myklebust

Latitude:	61° 43' 16.1" N
Longitude:	5° 10' 39.5" E
Height above MSL:	25 m
Contact:	Roald Vedvik, Tel.: 57795604
Gain:	60 dB
Highpass filter:	0.2 Hz
Lowpass filter:	12.5 Hz
VCO freq.:	1360 Hz
Receiver freq.:	N/A
Transmitter freq.:	142.000 MHz to station no. 3 (N2B3) – Løvikneset

Station no. 3 (N2B3) - Løvikneset

Latitude:	61° 49' 30.1" N
Longitude:	4° 57' 11.6" E
Height above MSL:	10 m
Contact:	Rolf Eikeset, Tel.: 57791535
Gain:	60 dB
Highpass filter:	0.2 Hz
Lowpass filter:	12.5 Hz
VCO freq.:	2040 Hz
Receiver freq.:	142.000 MHz from station no. 2 (N1R2) - Myklebust
Transmitter freq.:	173.900 MHz to central point (N2B1) - Tytingvågen

Station no. 4 (N2B4) - Drage

Latitude:	62º 07" 07.8' N
Longitude:	5º 14" 35.5' E
Height above MSL:	110 m
Contact:	Harry Tunheim, Tel.: 57857375
Gain:	60 dB
Highpass filter:	0.2 Hz
Lowpass filter:	12.5 Hz
VCO freq.:	1700 Hz
Receiver freq.:	N/A
Transmitter freq.:	142.300 MHz to central point (N2B1) – Tytingvågen

Station no. 5 (N2B5) - Haus

Latitude:	61º 55" 20.6' N
Longitude:	5º 14" 35.5' E
Height above MSL:	30 m
Contact:	Klarens Manseth, Tel.: 57863135
Gain:	60 dB
Highpass filter:	0.2 Hz
Lowpass filter:	12.5 Hz
VCO freq.:	2720 Hz
Receiver freq.:	N/A
Transmitter freq.:	174.000 MHz to central point (N2B1) – Tytingvågen

Station no. 6 (N2B6) - Leirgulen

Latitude:	61º 51' 49.4" N
Longitude:	5º 18' 21.3" E
Height above MSL:	30 m
Contact:	Ragnar Kolseth, Tel.: 57794208
Gain:	60 dB
Highpass filter:	0.2 Hz
Lowpass filter:	12.5 Hz
VCO freq.:	2380 Hz
Receiver freq.:	N/A
Transmitter freq.:	441.650 to central point (N2B1) – Tytingvågen

All stations:

Seismometer type:	Teledyne Geotech S-13
Amplifier:	Teledyne Geotech model 42.50
VCO:	Teledyne Geotech model 46.22

7.2 SEISMIC ACTIVITY IN THE RANA AND BREMANGER AREAS

By Erik Hicks, Hilmar Bungum & Conrad Lindholm, NORSAR

7.2.1 Introduction

During a total of 18 months operation (July 1997 – January 1999), the seismic network in the Ranafjord area has been used to detect and locate almost 400 seismic events, of which around 300 are local earthquakes. A large number of these earthquakes are located in four groups in the western parts of the network. All four groups have very similar NNW-ESE trends in epicenter locations, and all are have shallow foci (2-12 km). The magnitude range is between M_L 0.1 and 2.8. Earthquake focal mechanism solutions show a local stress field that has the principal horizontal compressive stress oriented subparallel to the coastline and the continental margin, implying that the stress tensor has been inverted 90° with regard to the regional ridge push dominated stress field.

The Bremanger network has experienced a number of technical problems since its installation in October 1998, problems which are still not fully resolved. This is further documented in Section 7.1.2. However, some data are available from November 1998 to January 1999. These data have been analyzed, and locations compared to locations from the University of Bergen, based on data from the national Norwegian network. Data from nearby stations within this network can be included in the NEONOR solutions through cooperation with the University of Bergen, improving the range and accuracy of the hypocenter locations determined by the NEONOR network.

7.2.2 Results, Rana

As of February 1, 1999, a total of almost 400 seismic events have been located by the network. Around 60 of these are within distances of 50 and 200 km from the network, and are outside the main area of interest. A total of 50 events have been classified as probable local explosions, and therefore removed from the maps. These explosions mainly originate from a talc mine, a few km northwest of Mo i Rana, and from Storforshei Gruber around 40 km east of Mo i Rana.

This leaves approximately 280 probable local earthquakes from the beginning of July 1997 to the end of January 1999, with 180 since December 1, 1997. Fig. 7.2.1 shows a map of the earthquakes around the Ranafjord area.

Event locations

There are four major groups of earthquake epicenters visible in Fig. 7.2.1, all of which lie in the western part of the network, and all have similar NW-SE trending distributions of epicenter locations. All locations shown on a 1:250.000 map of the Rana area (Enclosure 6).

- The group located under the eastern part of the Sjona fjord is described in the annual technical report for 1997 (Dehls & Olesen, 1998), and has had only sporadic activity since then.

- The group in the western part of the Sjona fjord occurred mainly in November and December 1997, so there are a few new events in this group, combined there are about 20 earthquakes in total.

- The group further north, just onshore of the Aldra island north of the Sjona fjord was mainly active in January and February 1998, although there was some sporadic activity here also in 1997. A total of around 15 earthquakes make up this group, including the largest earthquake within the network, with a magnitude of M_L 2.8. Hypocenter depths in this group are around 10-12 km.

- The fourth group consists of around 50 earthquakes that occurred close to Handnesøya in October and December 1998. The largest earthquake in this group had a magnitude of M_L 2.7, and several of the quakes were felt and heard by local inhabitants as banging/cracking noises. This implies a very shallow hypocenter depth, in the order of only a few kilometers.

The remaining local epicenters are fairly well scattered, with some of the largest ones being located under the Rana fjord on the south side of the Nesna peninsula. There was also a fairly large (M_L 2.8) earthquake around 10 km southwest of Bleikvassli Gruber, this is the only significant activity observed south of the network.

Focal mechanisms and derived crustal stress

A total of four new focal mechanism solutions have been determined using waveform modeling, bringing the total to nine. All solutions are listed in Table 7.2.1 (one composite- and eight individual solutions).

The focal mechanisms are plotted with associated maximum horizontal compressive stress directions in Fig. 7.2.2, along with in-situ stress measurements from the IBS-DNM project (Fejerskov et al., 1996).

Table 7.2.1. Earthquake focal mechanism solutions determined using data from the NEO-NOR seismic network. The composite solution is determined by first motion polarities only, the other eight are determined by first motion polarities combined with full waveform modelling. P-trn, P-plng, T-trn and T-plng are the trend and plunge for the P (compression) and T (tension) axis respectively.

Date	Lat.	Lon.	Depth	Mag.	P-trn	P-plng	T-trn	T-plng
Comp.1	66.31	13.32	5 km	N/A	167	48	270	11
97.11.21	66.41	13.22	7 km	2.3	208	29	302	7
97.11.25	66.52	12.40	11 km	2.7	77	29	343	7
97.11.28	66.32	13.14	11 km	1.7	74	58	299	23
97.11.28	66.32	13.15	11 km	1.7	74	58	299	23
97.12.26	66.33	13.11	11 km	1.8	176	1	268	67
98.01.08	66.37	13.13	13 km	2.2	27	33	284	19
98.02.09	66.39	13.10	11 km	2.8	351	22	257	11
98.03.09	65.85	13.53	7 km	2.8	118	13	228	57
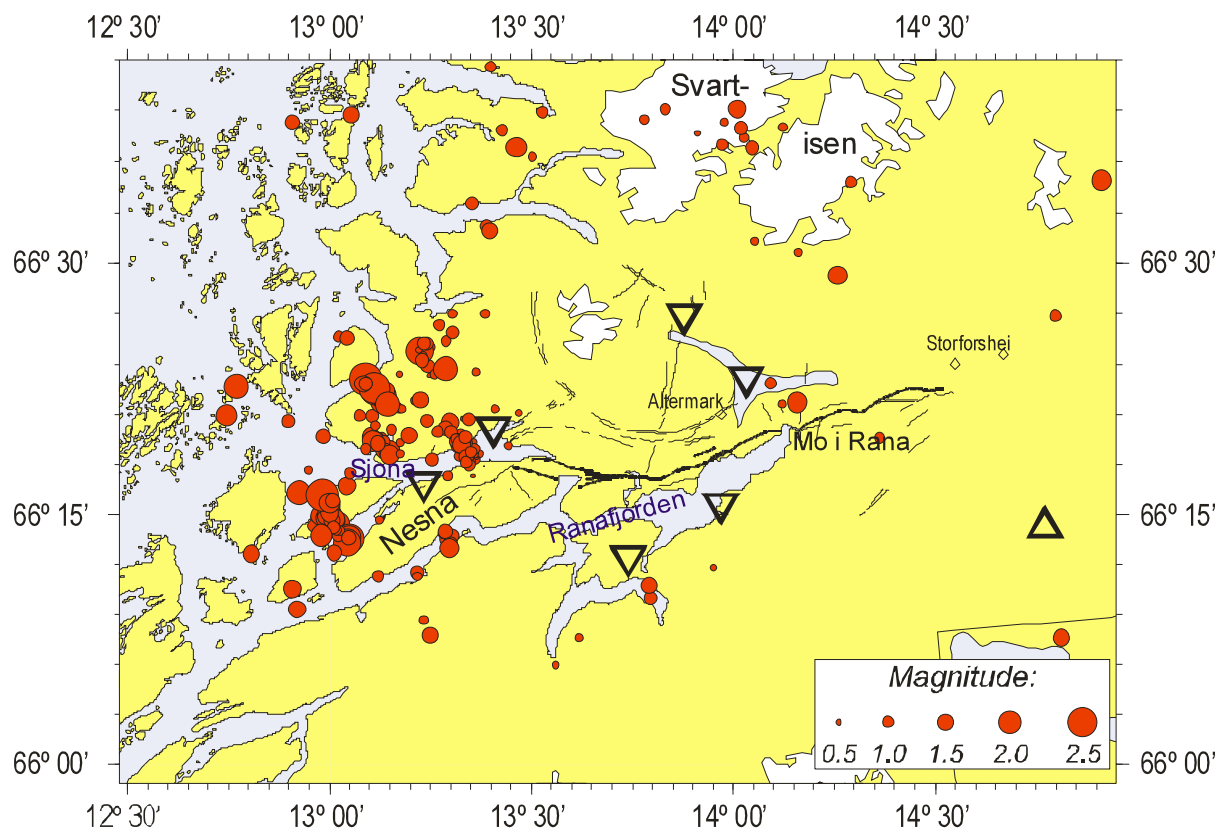
Fig. 7.2.1.   Earthquakes located by the NEONOR seismic network in Rana between July 1997 and January 1999. The Båsmoen fault is shown by the solid black line.
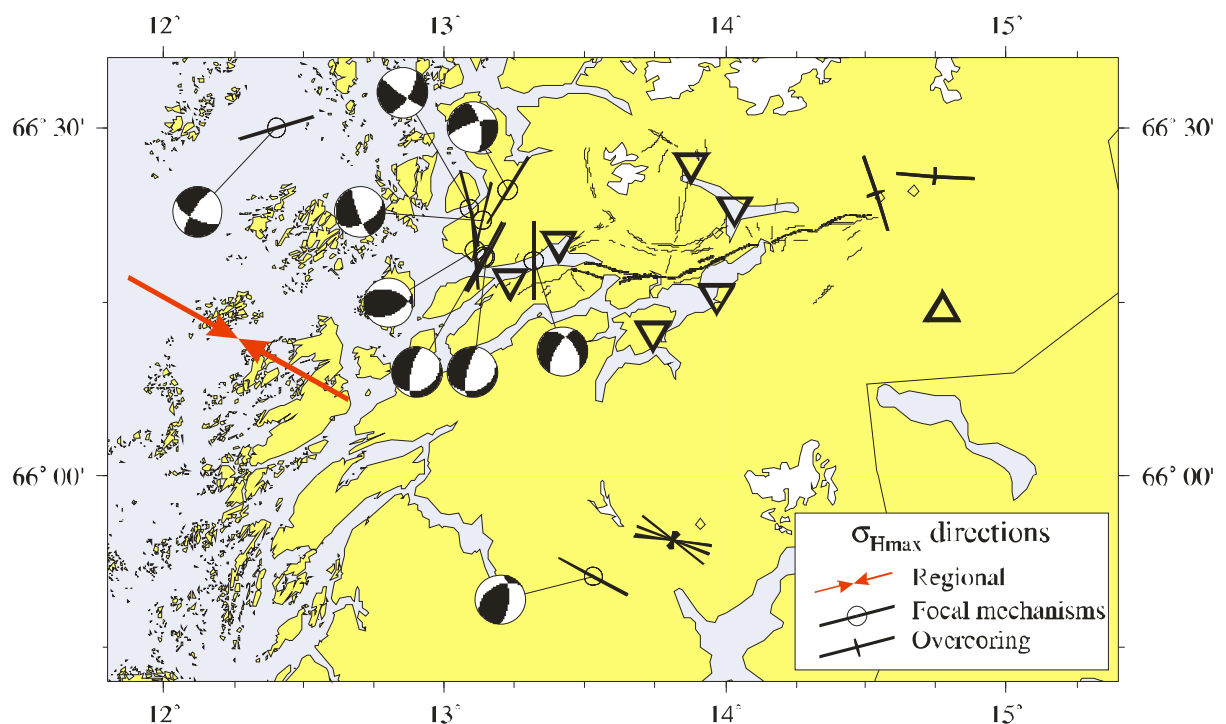
Fig. 7.2.2.   Focal mechanisms and corresponding σHmax directions. Overcoring measurements are also shown. The main regional compressive stress direction (Hicks, 1996) is shown by the large red arrow.

All of the new focal mechanism solutions since the 1997 annual report were determined by waveform modeling (using Herrmann's code, Havskov, 1997), using the first motion polarities to constrain possible solutions. All seven focal mechanism solutions within the network (four old and three new) show a rotation with regard to the regional stress field, while the focal mechanism for the earthquake further west has a maximum horizontal compressive stress direction that is closer to the regional trend. The M_L 2.8 earthquake further south has a compressive stress direction that complies more or less exactly with the regional stress field.

Magnitude and depth distributions

The magnitude distribution plot shown in Fig. 7.2.3 indicates that the detection threshold is around magnitudes (M_L) of 0.9. The detection threshold in the active areas near the Sjona fjord is most likely unchanged by the removal of two stations in October (further described in Section 7.1.2), due to the fact that the two closest stations have been retained. The effect on location precision should be similarly small.
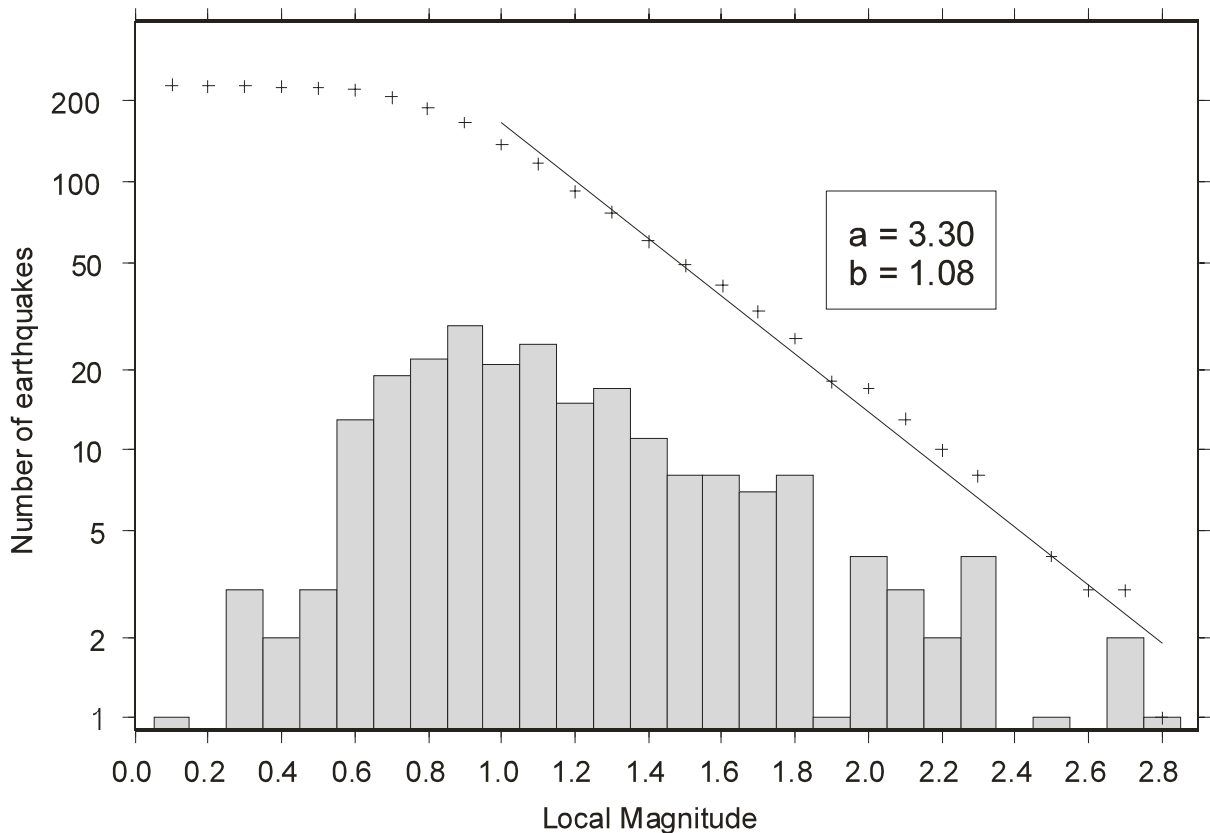
Fig. 7.2.3.   Magnitude distribution for the earthquakes in the Ranafjord area determined by the NEONOR network (probable explosions removed). Note that the threshold of detection drops sharply below magnitudes around M_L 0.9. Crosses represent the cumulative number of earthquakes. The activity rate is defined using the magnitude range M_L 1.0 to 2.8.

A fundamental scaling relationship for earthquakes says that for a given region over a given period of time, the relation between number of earthquakes N of magnitude equal to or greater than M is given by:

$$\log N = a - bM$$

180

The a and b values have been estimated from the available date from the NEONOR network, giving values of a=3.30 and b=1.08. This gives a return period of 10.5 years for earthquakes of magnitude M_L 4 or larger, 126 years for M_L 5 and just over 1500 years for M_L 6. Although M_L is not properly defined at the level of magnitude 6, it still gives a ballpark indication of the activity level in this area.

Fig. 7.2.4 shows a plot of the depth distribution within the network. The activity observed to the north and west of the Sjona fjord appears to have somewhat less shallow foci, with depths around 8-12 km. The approx. 50 earthquakes comprising the group by Handnesøya had hypocenter location depths around 7-9 km, but the witness reports of loud cracking and banging noises in conjunction with the earthquakes implies a shallower depth. These events have therefore been placed in the 3-5 km bin in Fig. 7.2.4. This illustrates the uncertainty in the depth determination of earthquake hypocenters, although a local network may provide epicenter locations within a few km, the hypocenter depths may still have errors of 5 km.

It should be noted that most of the depths observed (2-6 km) are very shallow compared to what is generally the case in Norway (5-30 km), and the slightly deeper earthquakes to the western and north of the Sjona fjord (8-12 km) would also be considered shallow in this sense. Shallow seismic activity appears not to be atypical for coastal areas in northern Norway where earthquake swarms have been studied, such as in Meløy (Bungum et al., 1979) and in Steigen (Atakan et al., 1994).
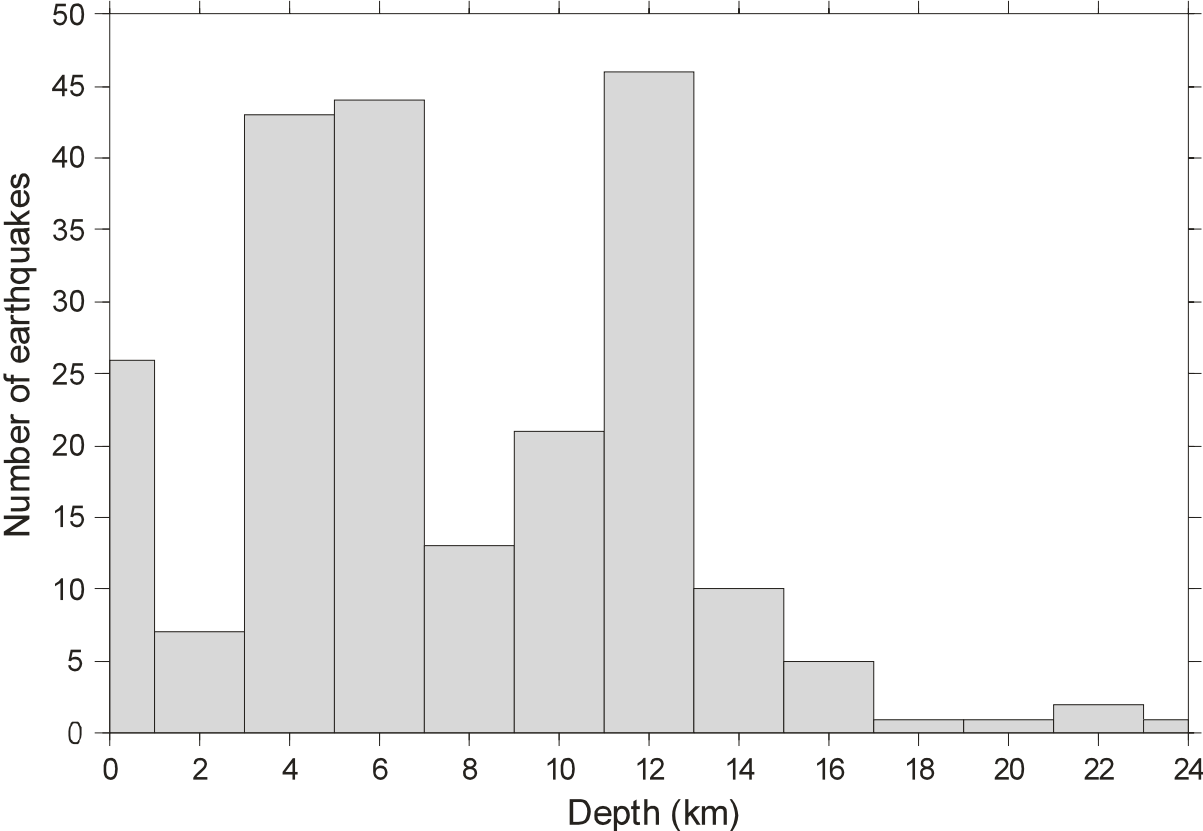
Fig. 7.2.4.   Depth distribution of the earthquakes within the network (probable explosions removed).

Comparison of historic and recent seismicity

A 1:250.000 map of current and historic seismicity in the Rana area has been compiled (Enclosure 6), also including new focal mechanism solutions and stress directions, and reports of felt effects from the 1819 earthquake (Muir Wood, 1989). Note that much of the activity is located in the western part of the Ranafjord area for the instrumental data 1980 to 1997. A number of large historic earthquakes (pre 1980), including the 1819 event, have locations in an area just north of Mo i Rana. However, the location uncertainty for most of these earthquakes are on the order of 30-50 km, and some of these errors could also be systematic (biased). However, it is notable that the Rana area has been, and still is, an area of elevated seismic activity. The fact that the new microearthquake data do not appear to be connected to the Båsmoen fault does not, however, exclude that possibility for some of the historic data. It is also uncertain if the large 1819 earthquake can be linked to any of the structures as today's activity is observed on, even though the reported felt effects were in the same areas.
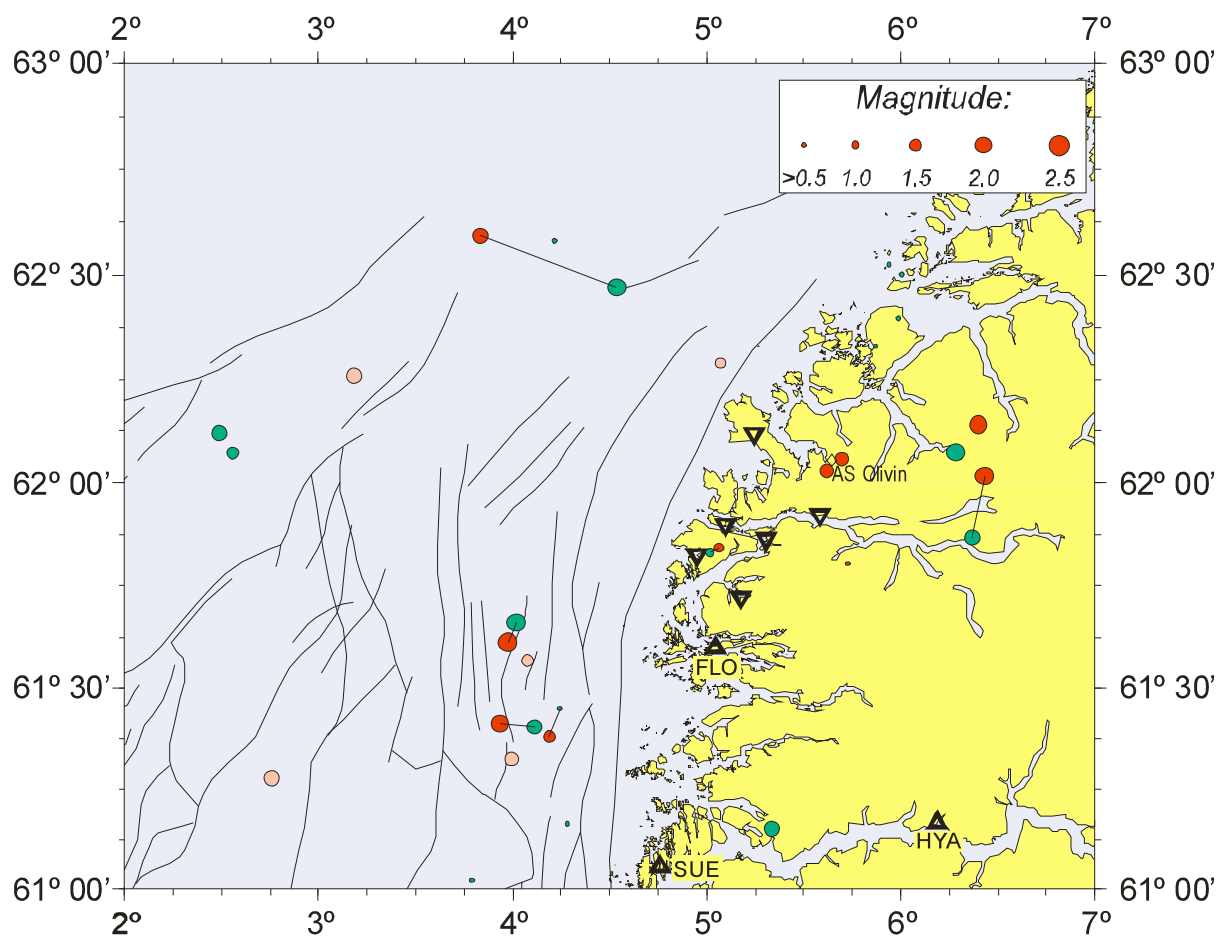
Fig. 7.2.5.   Events located by the NEONOR network in Bremanger in November and December 1998 (red) and January 1999 (pink). Events located by the national network in November and December are shown in green. Lines link the two locations for the same event. Inverted triangles represent the NEONOR stations, triangles represent stations that are part of the national Norwegian network.

7.2.3   Results, Bremanger

From the beginning of November 1998 to the middle of January 1999, 17 seismic events were located in the vicinity (within ~ 200 km) of the network. The two northernmost stations were

having problems most of this period, so the detection threshold and location accuracy are somewhat reduced. Two of the events appear to be explosions, from the locations it is probable that they originate form AS Olivin, a large open-pit quarry east of Stadtlandet. The other 15 appear to be earthquakes, with magnitudes mainly in the M_L 1.0 to 2.3 range. An additional 7 earthquakes at greater distances (up to 600 km) were also located, although these are of less interest in the present context.

Six of the located events in November and December 1998 were also located by the national Norwegian seismic network, which has also reported five fairly small earthquakes which the NEONOR network did not detect. This may be due to intermittent noise problems, possibly due to adverse weather, combined with the fact that two of the stations were not operating. The events are shown in Fig. 7.2.5, with stations are plotted as inverted triangles. The three nearby stations Florø (FLO), Sulen (SUE) and Høyanger (HYA) are part of the national Norwegian seismic network, shown by triangles. Earlier seismicity (1980-1998) is shown in Fig. 7.2.6 with the same map boundaries for comparison reasons. It appears that the earthquakes southwest of the network are located in the active area visible in Fig. 7.2.6.
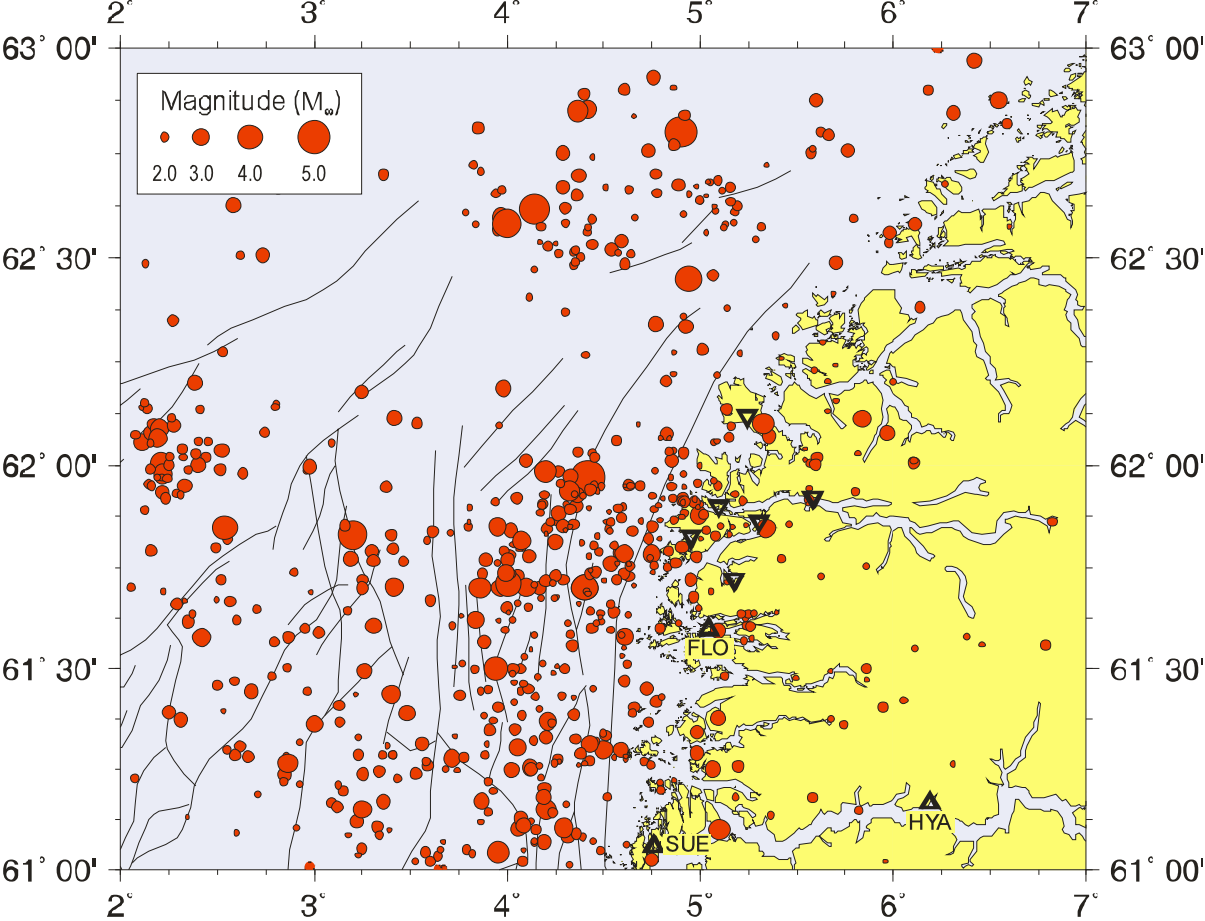
Fig. 7.2.6.   Earthquakes from 1980 to 1998 from the NORSAR catalog, moment magnitudes (M_ω) greater than 1.5.

183

7.2.4   Conclusions

Rana

The Rana area has long been known as one of the seismically most active regions in Norway (e.g., Byrkjeland, 1996). This fact in combination with the existence of the potential postglacial Båsmoen fault does implicate some form of connection, and thus warrant closer examination.

The study confirms the area as being seismically active, as the network has identified of the order of several hundred earthquakes within a limited area, with magnitudes up to M_L 2.8. This is very high for onshore Baltic shield areas.

Local stress sources certainly play an important role in controlling the seismic activity in the Rana area, as evidenced by the 90° inversion of the principal horizontal compression stress direction with regard to the regional stress field, which is commonly accepted to be related to the first order source of stress from the ridge push force (Bungum et al., 1991; Hicks, 1996). The majority of the earthquakes used to determine the regional stress field in mid Norway are located on the margin, (Byrkjeland, 1996; Hicks 1996), so it may be inferred that seismic activity is to a large degree controlled by local second and third order sources of stress (density inhomogenities, flexural stresses, topographic loads, geological features, etc.) rather than first order (plate motion related) effects, as also indicated both by the Meløy (Bungum et al., 1979) and the Steigen earthquake sequences (Atakan et al., 1994). Byrkjeland et al. (1998) point in this respect to a possible correlation between topography and earthquakes on a larger scale along the Trøndelag and Nordland coastal areas, as the coastal areas adjacent to the most elevated provinces also have the highest levels of seismic activity.

The consistency of the NNW-SSE lineations observed in the four main groups of earthquakes in the western parts of the network is remarkable, although the geological connection is at present uncertain, and should receive further attention both from a seismological and geological viewpoint.

Bremanger

Although the Bremanger network has so far been plagued by technical problems, the data obtained show that there is a good potential. When the power supplies are replaced and the weather calms later in the spring and summer, we expect much improved data for this area.

The few located events show that the observed activity from the last 20 years is continuing today, implying that high-quality data for fairly large events should be available within a year of operation. Even with its reduced capacity due to only four operational stations, most locations comply very well with the solutions found by the national Norwegian network operated by the University of Bergen. Once the network is operating fully, and including arrival time data from the nearby Florø (FLO), Sulen (SUE) and Høyanger (HYA) stations, a substantial improvement in location accuracy is expected for the northeastern parts of the North Sea.

7.2.5   References

Atakan K., C. D. Lindholm and J. Havskov (1994): Earthquake swarm in Steigen northern Norway: an unusual example of intraplate seismicity. *Terra Nova*, 6, 180-194.

Bungum, H., A. Alsaker, L.B. Kvamme and R.A. Hansen (1991): Seismicity and seismotec-

tonics of Norway and surrounding continental shelf areas. *J. Geophys. Res.*, 96, 2249-2265.

Bungum, H., B.K. Hokland, E.S. Husebye and F. Ringdal (1979): An exceptional intraplate earthquake sequence in Meløy, Northern Norway. *Nature*, 280, 32-35.

Byrkjeland, U. (1996): *Seismotectonics of the Norwegian Continental Margin, 62º-71ºN*. Cand. Scient thesis in applied geophysics, University of Oslo, Norway, 146 pp.

Byrkjeland, U., H. Bungum & O. Eldholm (1998): Seismotectonics of the Norwegian continental margin. Submitted to JGR, Nov. '98.

Dehls, J.F. and Olesen, O. (1998): *Neotectoncs in Norway, Annual Technical Report 1997*, NGU Report 98.016, 149 pp.

Fejerskov, M., C.D. Lindholm, H. Bungum, A. Myrvang, R.K. Bratli and B.T. Larsen (1996): *Crustal stress in Norway and adjacent offshore regions*, Final report for the IBS-DNM project, Topic 1.3 "Regional stress field".

Havskov, J., (1997): *The Seisan earthquake analysis software*, Institute of Solid Earth Physics, University of Bergen, 236 pp.

Havskov, J., L.B. Kvamme, R.A. Hansen, H. Bungum and C.D. Lindholm (1992): The northern Norway seismic network: Design, operation and results. *Bull. Seism. Soc. Am.*, 82, 481-496.

Hicks, E. C. (1996): *Crustal stresses in Norway and surrounding areas as derived from earthquake focal mechanisms and in-situ stress measurements*. Cand. Scient thesis in applied geophysics, University of Oslo, Norway, 163 pp.

Olesen, O., S. Gjelle, H. Henkel, T.A. Karlsen, L. Olsen and T. Skogseth (1994*): Neotectonics in the Ranafjorden area, northern Norway*. NGU Report No. 94.073, 33 pp.

Muir Wood, R. (1989): The Scandinavian earthquakes of 22 December 1759 and 31 August 1819. *Disasters*, 12, 223-236.

8   MODELLING (TASK 11)

8.1   NEONOR COMBINED INTERPRETATION; 'SEISMIC PUMPING' OF HYDROCARBONS AND GROUNDWATER

By Odleiv Olesen (NGU) & Fridtjof Riis(NPD)

8.1.1   Introduction

The concept of 'seismic pumping' was suggested by Sibson *et al.* (1975) on the basis of out-pourings of warm groundwater along fault traces following some magnitude 5-7 earthquakes. The mechanism has gained wide acceptance among ore geologists to explain the textures of hydrothermal vein deposits associated with ancient faults. Muir Wood & King (1993) found further support for this pumping mechanism to explain observed crustal fluid flow. The hydrological changes that follow earthquakes were found to depend on the mode of faulting (Fig. 8.1.1). The most significant response is found to accompany major normal fault earthquakes. Increases in spring and river discharges peak a few days after the earthquake, and typically, excess flow is sustained for a period of 6-12 months. In contrast, hydrological changes, accompanying pure reverse fault earthquakes are either undetected or indicate lowering of well levels and spring flows.
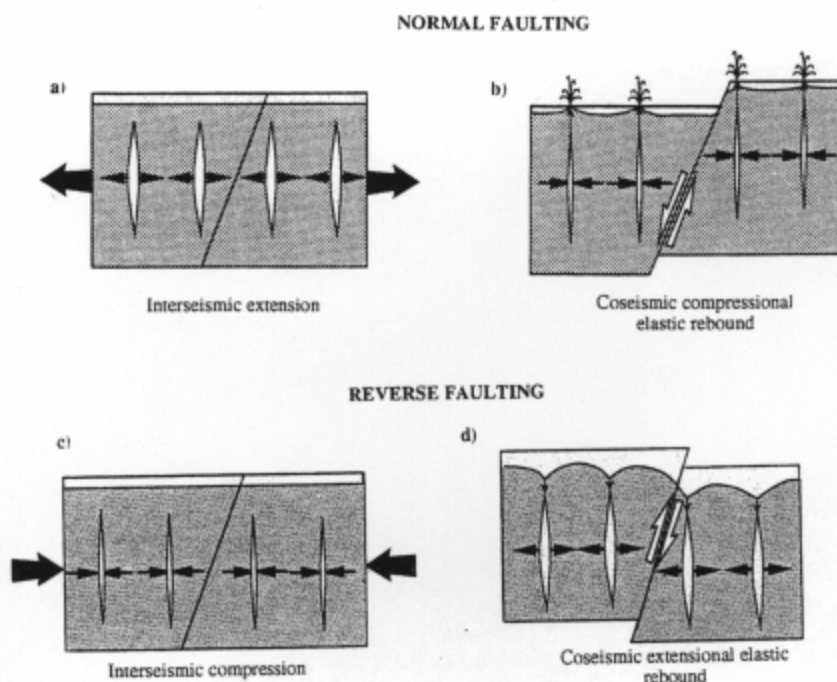
Fig. 8.1.1.   Simplified model for the accumulation and coseismic release of strain in extensional and compressional tectonic environment. (a) For extensional faulting, the interseismic period is associated with crack opening and increase of effective porosity. (b) At the time of the earthquake, cracks close and water is expelled. (c) For compressional faulting, the interseismic period is associated with crack closure and the expulsion of water. (d) At the time of the earthquake, cracks will open and water will be drawn in. Both mechanisms will contribute to an increased groundwater and hydrocarbon migration. From Muir Wood & King (1993).

186

Sibson *et al.* (1975) and Muir Wood & King (1993) suggested that the quantities of fluid involved in the seismic pumping process are such (0.01-0.60 km^3 ~ 60-360 million barrels) that the mechanism may substantially assist the migration of hydrocarbon fluids in tectonically active areas. Muir Wood & King (1993) concluded from modelling of seismic and geodetic data that crustal volume strain to a depth of at least 5 km and laterally to a distance of 50-100 km is involved in this tectonically induced fluid flow.

The recent recognition that the Lapland postglacial faults most likely were formed during single events shortly after the last deglaciation (Lagerbäck, 1990, 1992; Olsen *et al.,* this report) is of importance in this context. These faults were created during earthquakes with magnitude ranging between 7.0 and 8.1 (Bungum & Lindholm, 1996). Mörner & Trøften (1993) have, based on varve studies, concluded that southern Sweden may have suffered at least three major seismic event immediately after or coinciding with the deglaciation at approximately 10.000 BP.

There is no reason to believe that the last glaciation was different from the seven other major glaciations (Fig. 8.1.2) during the last 600.000 years. The Weichsel and Saale glaciations consist of several subglaciations and it is also likely that each of the three Saale and the Elster glaciations are also made up of several sub-glaciations. All of these earlier glaciations are, however, known and understood much more poorly than the last one.
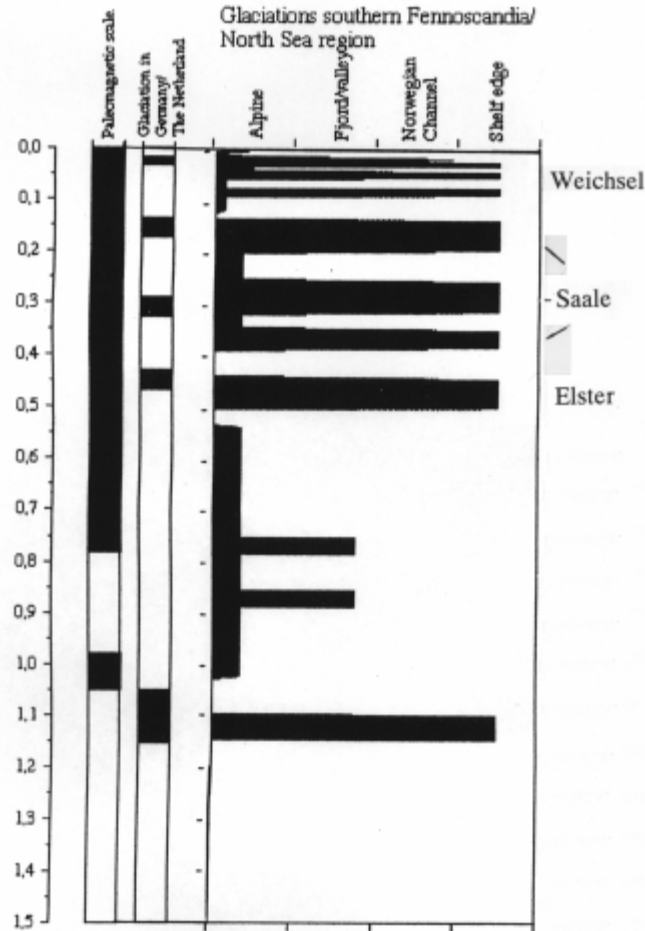
Fig. 8.1.2.   Glaciation curve for southern Fennoscandia through the last 1.5 m.y. The Weichsel and Saale glaciations consist of several subglaciations and it is likely that each of the three Saale and the Elster glaciations are also made up of several sub-glaciations. From Sejrup et al. *(in press).*

Johnston (1987) has provided a theoretical basis for the postglacial pulse of seismic strain release. Starting from the evidence that the crusts beneath the Antarctica and Greenland continental-scale ice sheets are virtually aseismic, he demonstrated a mechanism for the suppression of fault failure for as long as the ice sheet exists at or near its maximum thickness. The accumulation of tectonic strain energy beneath large ice-sheets for 10,000 years or more can consequently provide the energy source and explanation for the large-scale, late-glacial faulting in Fennoscandia. This theory implies that the large-scale earthquakes occurred in areas with coinciding cyclic formation of ice-sheets during Late Pleistocene and preglacial fault failure (that may also represent areas with postglacial and present seismicity).

We will within the NEONOR project investigate the potential connection between seismicity and migration of hydrocarbon and groundwater in bedrock. The present account is a first phase of this task. We have compiled previously reported earthquake triggering of gas seepage and included hydrological observations in three of the areas with observed neotectonic phenomena in Norway: Masi, Kåfjord and Rana.

8.1.2 Triggering of gas seepage by earthquakes

Hovland & Judd (1988) documented several locations where earthquakes are known to have triggered gas seepage, e.g. at the Malibu Point on the coast of California, USA (Clifton *et al.* 1971 and Nardin & Henyey, 1978). Gas bubbles 0.5-2.0 cm across appeared from small craters (40 cm across and 10-15 cm deep) at the sea surface at the time of a magnitude 6.6 earthquake (9 February 1971) at San Fernando some 50 km to the south-east. Scuba divers observed that the seepage continued for at least one more day. The craters were arranged in a linear zone 12 m wide and 120 m long, aligned parallel to a geological structure.

Field & Jennings (1987) reported formation of pockmarks following the magnitude 7 earthquake occurring off the Klamath River delta in northern California (8 November, 1980). This area had been covered by side-scan sonar profiling before the earthquake and was surveyed again afterwards. A series of ridges, mounds, pockmarks and gas vents had been formed. The released gas might have been in part thermogenic in origin.

Hasiotis *et al.* (1996) have also reported similar phenomena in the Patras Gulf in Greece after a magnitude 5.4 earthquake in 1993. A majority of the pockmarks in the area were venting gas bubbles for a few days after the earthquake. During the 24 hour period prior to the earthquake the bottom water temperature increased anomalously indicating that huge quantities of hot gas were intermittently emitted through the pockmarks. During earthquakes in 1817 and 1882 in the same area, gas bubbles were reported to appear on the sea surface and the seawater became hot enough to burn the hands of the fishermen during the 1817 event.

Pecore & Fader (1990) observed that eyed pockmarks and plumose structures in the Passamaquoddy Bay, New Brunswick, Canada were oriented parallel to nearby known faults on land. They suggested that the release of gas might have occurred concomitant with active faulting.

Earthquakes in the North Sea are relatively weak and also quite deep, and there is a general agreement that these events are of no significance to the formation of the numerous pockmarks in the area (Hovland & Judd 1988). Seismicity maps for Norway (Enclosure 1, this report; Bungum *et al.* 1991) show on the other hand that there is, relatively, an increased earthquake activity in the Central Graben, in the Viking Graben and at the Halten Terrace areas that make up the known petroleum provinces in Norway. Olesen *et al.* (this report) reported indications of a spatial correlation between young faults, occurrence of pockmarks and areas with increased seismicity in the Troll area.

8.1.3 Hydrogeological phenomena in the Masi, Kåfjord and Rana areas

Several groundwater springs occur along the Stuoragurra Fault, and drilling through the fault has revealed high ground water yield (Olesen *et al.* 1992a,b, Klemetsrud & Hilmo, this report). In the Fidnajåkka area a spring occurs 20 metres to the west of the escarpment. Nothing but the flower Viscaria Alpina and some moss grow in a 25 m long and 3-5 m wide field downstream from the spring revealing that the ground water has a quite high content of heavy metals. Chemical analysis of three soil samples show copper content of 0.36, 0.50 and 1.34%. Induced polarisation (IP) measurements in the area show, however, that the sulphide content

in the bedrock along the fault is very low (unpublished NGU data). Analysis of the ground water from the fault show a high content of Cu and Zn (Klementsrud & Hilmo, this report). Similar springs with Viscaria Alpina fields have been observed along the postglacial faults in Sweden (Lagerbäck, 1979).

Large amounts of water poured out of the escarpment some time between the 21 January 1996 earthquake (magnitude 4.0) and August of that year (Olesen & Dehls, 1998). The Norwegian Water Resources and Energy Administration (NVE) in Narvik (R. Sværd, pers. comm., 1998) has provided river flow data for the period 1989-1997 from the Iesjåkka River, which drains the area where the M 4 earthquake occurred. The gauge is located in Jergul, 20 km to the west of Karasjok. The water level was reduced by 15-20 % during the first weeks after the earthquake and stayed low during the months of February, March and April till the snow melting started in the middle of May (Dehls & Olesen, 1998b). These data are, however, hampered with uncertainties since they are not corrected for changing ice conditions during the winter. Reduced water flow after large reverse fault earthquakes has also been reported from Alaska and Japan (Muir Wood & King, 1993). Normal fault earthquakes, on the other hand, cause increased water flow (Fig. 8.1.1). The fault plane mechanism from the 1996 earthquake shows that it is a reverse fault earthquake (Bungum & Lindholm 1996).

Following the interpretations of Muir Wood (1989a) and Lagerbäck (1990) several magnitude 7-8 earthquakes were associated with the formation of the postglacial faults within the Lapland Province. If such large earthquakes occurred after each of the numerous glaciations during the Pleistocene, and if the seismic pumping models by Sibson *et al.* (1975) and Muir Wood & King (1993) are valid, this may have implications for both the occurrence of ground water on land and hydrocarbons offshore.

Olsen *et al.* (this report) concluded from trenching of the Stuoragurra Fault that fault breccia had been injected from the fault zone and more than 12-14 m horizontally into the lower part of the glacial overburden. It is reasonable to assume that the fault breccia must be mixed with high pressure ground water to reach this transportation length in the consolidated till.

Hovland & Judd (1988) reported the occurrence of several pockmarks at the sea floor in the Lyngenfjord. Most of the locations are situated along the NW extension of the Nordmannvikdalen postglacial fault and the nearest pockmark is located only 5-6 km from the fault. The pockmarks have been attributed to either groundwater from a hydraulic head caused by nearby high mountains with lakes, streams and glaciers, or to substantial volumes of biogenic gas generated by the decomposition of organic matter in the fjord sediments. It is possible that an earthquake associated with the formation of the postglacial Nordmannvikdalen Fault has triggered the release of groundwater or gas. Blikra (this report) has also found an anomalously high concentration of rock avalanches along the Lyngenfjord that could also be an effect of the same earthquake.

Helzen (1834) and Muir Wood (1989b) described the hydrological effects of the magnitude 5.8-6.2 earthquake in 1819 in the outer Ranafjord area: 'many streams were disturbed as though they had been mixed with milk, such that the water, smelling strongly of sulphur, re-

mained undrinkable, even for animals, for three days'. At Saltdal (150 km to the north of the Rana area) the water emerging from two small springs at the foot of a mountain, 'became whitened with clay although there was no such material along the stream-banks' (Sommer-feldt, 1827; Muir Wood, 1989b).

8.1.4 Concluding remarks

The Stuoragurra Fault has been studied by percussion drilling (Olesen *et al.*, 1990) and ground water was encountered at a depth of 35 m (2 m above the main fault zone). After penetration of the fault gouges at a depth of 37 m the ground water was drained but appeared again at a depth of 40 m. The fault gouges consequently caused a 'hanging' ground water surface above the main fault zone. We conclude that the fault gouges in the Stuoragurra Fault have sealing properties, even if the more than 10 m wide fault-zone is totally fractured and water-bearing at larger depths.

There is increasing evidence in Scandinavia for a major seismic pulse accompanying each of the deglaciations following the multiple major glaciation cycles during the last 600.000 years. It is possible that the interaction of the contraction and dilation of fissures associated with the seismic cycles may create conditions that assist in concentrating hydrocarbons from their source rocks and pumping them to potential reservoir formations and/or leakage from these reservoirs.

8.1.5 References

Bungum, H., Alaskar, A., Kvamme, L. B. & Hansen, R. A., 1991: Seismicity and seismotectonics of Norway and surrounding continental shelf areas. *Journal of Geophysical Research* 96, 2249-2265.

Bungum, H. & Lindholm, C., 1996: Seismo- and neotectonics in Finnmark, Kola Peninsula and the southern Barents Sea. Part 2: Seismological analysis and seismotectonics. *Tectonophysics* 270, 15-28.

Clifton, H.E., Greene, H.G., Moor, G.W. & Phillips, R.L., 1971: Methane seep off Malibu Point following San Fernando earthquake. *U.S. Geological Survey Professional Paper 733,* 112-116.

Dehls, J. & Olesen, O., 1998b: Excursion guide to the Stuoragurra and Nordmannvikdalen postglacial faults in Masi, Finnmark and Kåfjord, Troms. *NGU Report 98.070,* 31 pp.

Field, M.E. & Jennings, A.E., 1987: Seafloor gas seeps triggered by a northern California earthquake. *Marine Geology 77,* 39-51.

Hasiotis, T., Papatheotorou, G., Kastanos, N. & Ferentinos, G., 1996: A pockmark field in the Patras Gulf (Greece) and its activation during the 14/7/93 seismic event. *Marine Geology 130,* 333-344.

Heltzen, I. A., 1834: Ranens Beskrivelse, *Rana Museums og Historielag*, Mo i Rana, 290 p

Hovland, M. & Judd, A.G., 1988: *Seabed pockmarks and seepages.* Graham & Trotman, London, 293 pp.

Johnston, A.C., 1987: Suppression of earthquakes by large continental ice sheets. *Nature 330,* 467-469.

Lagerbäck, R., 1979: Neotectonic structures in northern Sweden. *Geologiska Föreningens i Stockholm Förhandlingar, 100 (1978),* 271-278.

Lagerbäck, R., 1990: Late Quaternary faulting and paleoseismicity in northern Fennoscandia, with particular reference to the Lansjärv area, northern Sweden. *Geol. Fören. Stockh. Förh.* 112, 333-354.

Lagerbäck, R., 1992: Dating of Late Quaternary faulting in northern Sweden. *Journal of the Geological Society of London* 149, 285-291.

Muir Wood, R., 1989b: The Scandinavian Earthquakes of 22 December 1759 and 31 August 1819. *Disasters* 12, 223-236.

Muir Wood, R. & King, G.C.P., 1993: Hydrological signatures of earthquake strain. *Journ. Geophys. Research 98,* 22,035-22,068.

Mörner, N.-A. & Trøften, P.-E. 1993: Palaeoseismotectonics in glaciated cratonal Sweden. *Zeitschrift für Geomorphologie N.F. Suppl.-Bd. 94,* 107-117.

Nardin , T.R. & Henyey, T.L., 1978: Pliocene-Pleistocene diastrophism of Santa Monica and San Pedro Shelves, California central borderland. *American Association of Petroleum Geologists Bulletin 62,* 247-272.

Olesen, O., Henkel, H., Lile, O.B., Mauring, E. & Rønning, J.S., 1990: Detailed geophysical investigations of the Stuoragurra postglacial fault, Finnmark, northern Norway. *NGU Rapport 90.160,* 24 s.

Olesen, O., Henkel, H., Lile, O. B., Mauring, E., Rønning, J. S. & Torsvik, T. H., 1992a: Neotectonics in the Precambrian of Finnmark, northern Norway. *Norsk Geologisk Tidsskrift 72,* 301-306.

Olesen, O., Henkel, H., Lile, O. B., Mauring, E. & Ronning, J. S., 1992b: Geophysical investigations of the Stuoragurra postglacial fault, Finnmark, northern Norway. *Journal of Applied Geophysics 29,* 95-118.

Olesen, O. & Dehls, J., 1998: Neotectonic phenomena in northern Norway. In: Dehls, J. & Olesen, O. 1998 (eds.): Neotectonics in Norway, Annual Technical Report 1997, NGU Report 98.016, 3-30.

Pecore, S.S. & Fader, B.J., 1990: Surficial geology, pockmarks, and associated neotectonic features of Passamaquoddy Bay, New Brunswick, Canada. *Geological Survey of Canada Open-File Report 2213,* 45 pp.

Sejrup, H.P., Larsen, E., Landvik, J., King, E., Haflidason, H. & Nesje, A. in press: Quaternary glaciations of southern Fennoscandia; evidences from the south-western Norway and the northern North Sea region. *Quaternary Science Reviews.*

Sibson, R.H., Moore, J. McM. & Rankin, A.H., 1975: Seismic pumping – a hydrotermal fluid transport mechanism. *Journal Geological Society of London 131,* 653-659.

Sommerfeldt, S.C., 1827: Fysisk – økonomisk beskrivelse over Saltdalen i Nordlanderne. *Kongelige Norske Videnskaber Selskabs Skrifter, Trondheim 19/ii,* 27 pp

9 ACKNOWLEDGEMENTS

10 APPENDIX 1: NEONOR STATUS REPORT, 1998

By Odleiv Olesen, NGU

Report of the main activities second half of 1998 and plans for first half of 1999

The NEONOR activities in 1998 have generally followed the lines of the NEONOR Project Document. There have been some delays in the interpretations of the 3D seismic data but this work will now be reported in the NEONOR 1998 Technical Report. Studies of the Øygarden Fault Zone and ground water occurrence in the postglacial Stuoragurra Fault, which were both suggested by the sponsors at the 1997 NEONOR Project Meeting, have been given high priority.

1) Classification and quality assessment of reported neotectonic phenomena

An evaluation of neotectonic claims in Hjeltefjorden has been carried out. The work has been reported and is included in the Annual Technical Report for 1998. Seismic profiles from the Hjeltefjorden area are provided from NGI/Geoteam and Norsk Hydro. Postglacial faulting has been proposed at the bottom of this fjord. We visited the premises of Statoil in November to study multibeam echo-sounding data from the same area. The survey was carried out in 1996 for the planning of a pipeline between Sture/Kollsnes and Mongstad. The data set was only presented as contour maps when we first visited Statoil in 1997. This time, shaded relief maps had been prepared. Subtle structures on the sea floor could therefore be studied in detail. Unfortunately, the data of the most interesting area were muted due to military restrictions. Because of the high height/length ratio (0.01-0.02) of the fault scarp, we have, however, concluded that the apparent offset of the seismic reflectors is most likely due to changing current regime and deposition regime in Hjeltefjorden. Most of the known surface scarps of neotectonic faults in northern Fennoscandia and elsewhere have a height/length ratio of 0.001-0.0001 (see Table 1).

The locations of two reported neotectonic phenomena in southern Norway were visited for closer geological and geomorphological examination in 1998. Field work in northern Gudbrandsdalen has shown that the proposed postglacial faults by Werenskiold (1931) can be related to erosion (plucking) along steeply dipping fracture zones (Gnedden between Otta and Kvam) and gravity-induced sliding (Rudihø between Lalm and Heidal).

Reported locations with potential neotectonic phenomena in Norway have been classified into five groups:

(1) Neotectonic faults (e.g. Stuoragurra and Nordmannvikdalen faults)

(2) Gravitationally induced faults (e.g. Beiarn, Vassdalsfjellet, Rudihø, Ringja and Ulvegrovane)

(3) Erosional along older zones of weakness (e.g. Skipskjølen, Nordreisa, Skjomen, Austerdalsisen, Gnedden and Lygre)

(4) Overburden draping of underlying bedrock features (e.g Gæssagielas)

(5) Stress release features (e.g. Lebesbye, Kobbelv and Ødegården)

The present status of well documented (grade A) neotectonic faults of postglacial age in Fennoscandia is:

*Table 1. Summary of properties of the documented postglacial faults within the Lapland province. * From Bungum & Lindholm, 1996.*

Fault	Country	Length	Max. scarp height	Height length ratio	Trend	Type	Moment magnitude*	Comment	Reference
Suasselkä Fault	Finland	48 km	5 m	0.0001	NE-SW	reverse	7.4		Kujansuu 1964
Pasmajärvi-Venejärvi Fault	Finland	15 km	12 m	0.0008	NE-SW	reverse		two separate sections	Kujansuu 1964
Vaalajärvi Fault	Finland	6 km	2 m	0.0003	NW-SE	??			Kujansuu 1964
Pärve Fault	Sweden	150 km	13 m	0.0001	NE-SW	reverse	8.1		Lundquist & Lagerbäck 1976
Lainio-Suijavaara Fault	Sweden	55 km	30 m	0.0005	NE-SW	reverse	8.0		Lagerbäck 1979
Merasjärvi Fault	Sweden	9 km	18 m	0.002	NE-SW	reverse		secondary fault to the Pärve Fault	Lagerbäck 1979
Pirttimys Fault	Sweden	18 km	2 m	0.0001	NE-SW	reverse			Lagerbäck 1979
Lansjärv Fault	Sweden	50 km	22 m	0.0004	NE-SW	reverse	7.9		Lagerbäck 1979
Burträsk-Bastuträsk fault	Sweden	60 km	c. 10 m	0.0002	NE-SW N-S	??		two separate sections	Lagerbäck 1979
Stuoragurra Fault	Norway	80 km	7 m	0.0001	NE-SW	reverse	7.7	three separate sections	Olesen 1988
Nord-mannvik-dalen Fault	Norway	2 km	1 m	0.0005	NW-SE	normal			Tolgens-bakk & Sollid 1988

The major faults are NE-SW trending reverse faults and occur within a 400x400 km large area in northern Fennoscandia. The Nordmannvikdalen and Vaalajärvi faults are minor faults trending perpendicular to the reverse faults. The former is a normal fault and the latter is a potential normal fault. The scarp height/length ratio is generally less than 0.001. The Meras-järvi Fault has a scarp height/length ratio of 0.002. This fault represents, however, an antithetic fault to the major Pärve Fault.

A more extensive comparison of the postglacial faults within the Lapland Province is planned for the remaining NEONOR Project period. Field plans for 1999 are listed below in Section 4) Geological and geophysical investigations.

2) Mapping of recent offshore faulting

Two 3D surveys in the northern North Sea and one in Nordland VI have been interpreted in the shallow parts by IKU. Up to four horizons (including sea bed) have been interpreted in the North Sea surveys, while only seabed has been interpreted on the Nordland VI survey (NH9604, mainly in block 6710/6) due to thin Quaternary overburden and processing problems. In the North Sea, no conclusive observations have been made with regards to late tectonic activity (as reported at the meeting in Alta), while in the Nordland VI area, some seabottom trends may be connected to deeper faults. The seabed map shows several interesting features. One set of features runs in a northeast-southwest direction. A seismic line across one of these trends shows a gentle ridge on the seafloor, with the amplitude of approximately 10 ms. The ridge coincides with the continuation of a deeper fault. The fault seems to have caused a rupture through the shallow sediment layers, indicating a late movement of the fault. Below a glacially eroded trough in the north-eastern part of the survey, another fault causing a seabed event could be observed. The offset of seafloor in this area is clearly an evidence of a postglacial tectonic event. The interpretation of the 3D seismic surveys has been reported by Stein Fanavoll, IKU and will be included in the 1998 NEONOR Annual Technical Report.

The 3D seismic surveys SG9603M and BPN9401 in the northern North Sea and the ST9203 survey from the Nordland II area (Norne) have been loaded into seismic work station at NPD and interpreted. The interpretations of the two former surveys have been merged with data from NH9202 and NH9405 (interpreted by IKU) to generate a continuous coverage in the northeastern North Sea area. A total of eight 3D surveys have now been interpreted within the frame of the NEONOR Project. Two surveys were reported last year by NPD. Interpretation of the other six surveys is reported jointly by IKU, NGU and NPD.

Hovland (1983) reported faulting of Quaternary deposits on the western slope of the Norwegian Channel (to the west of Bergen). Studies of 2D exploration seismic surveys at NPD have shown that there are no faults at depth below the shallow faulting indicating that the deformation may be of superficial character.

The survey vessel M/S Sjømåleren from the Norwegian Mapping Authority (SK) has collected multibeam echo sounding data from two neighbouring localities along the Øygarden Fault Zone, immediately to the northwest of the mouth of Sognefjorden. Combined interpretation of 2D seismic and bathymetry data has been completed at Phillips Petroleum, NPD and NGU. Preliminary results were presented at the Alta meeting. Landslides can be observed along the scarp, but no evidence of young faulting has been observed.

An application for exchange of neotectonic information between the NEONOR and Seabed projects has been sent to the NEONOR partners. Hilmar Bungum, NORSAR has sent a similar application to the Seabed partners.

3) Database and national map (1:3 mill.) of reported phenomena

The work on the next draft of the neotectonic map has been continued. Compilation of precision levelling data from Norway, northern Sweden and northern Finland is finished. These data are combined with uplift data from GPS, gravity, tide stations, and historic mean sea level marks to produce new apparent uplift contours for Fennoscandia. The map does also include earthquakes, focal plane solutions, *in situ* stress measurements, postglacial faults, offshore Plio-Pleistocene wedges and Neogene domes. The base map constitutes bathymetry-/topography data set of Fennoscandia and adjacent ocean areas. Detailed bathymetric contours

for Svalbard and the Barents Sea have been delivered from the Norwegian Mapping Authorities (Sjøkartverket). A 3D bathymetric model in Arc/Info was produced to improve the detail on the Neonor map. We are hoping to receive more bathymetric contours for the Greenland Sea from the US Naval Research Laboratory. Offshore structures from NPD have been added to the database.

The NEONOR-Web page has been updated. General information as project proposal etc. is open file data. Other project data is now accessible only with password. NEONOR participants can now decide their own password and report it to John.Dehls@ngu.no who will register it in our system. Remember to keep the password confidential.

A project web site is available:

http://geofysikk.ngu.no/neonor

The neotectonic map (enclosed in the NEONOR Annual Technical Report) can be provided in Arc/Info and ER-Mapper format on request. Internet access to the NEONOR database has been tested and the confidentiality is now secured. The NEONOR steering committee should decide if the data may be accessible over internet.

The final version of the neotectonic map will be produced during the first half of 1999. Interpretation of the compiled data-sets will be given higher priority during the last year of the project period.

4) Geological and geophysical investigations (Lebesbye, Masi, Kåfjord and Østerdalen)

Two successful trenches across the Stuoragurra Fault in the Fidnajåkka area were carried out in August, 1998. A wealth of new information was acquired. The Stuoragurra Fault does seem to be a blind thrust since the 3-4 m thick overburden is folded around the uplifted block. There were also an abundance of liquefaction structures in the trenches. The precise age of the faulting is not known, but the structures and stratigraphy of the overburden show that the fault developed either during the very last part of the last deglaciation i.e. c. 9,300 ^{14}C-yr BP or shortly afterwards, possibly after a short phase of pedogenesis. Lars Olsen did a careful sampling of the paleo-surface to try to extract pollen for C14 dating.

Structural geological mapping and ground penetrating radar (GPR) were carried out in the Kåfjord area in the beginning of August. John Dehls and Jan Steinar Rønning concluded that the southeastward dipping GPR reflectors are representing the actual Nordmannvikdalen Fault and not the schistosity of the mica schists in the area. Two separate groups visited the Nordmannvikdalen fault on 19 and 21 Aug. (after the NEONOR Project Meeting in Alta): Lars Harald Blikra, Alvar Braathen, John Dehls, Philip Goldsmith, Odleiv Olesen and Arthur Sylvester. There was unanimity among the participants that the structure represents a true neotectonic fault of postglacial age. The opinions of the dip of this normal fault varied from 50 to 85 degrees. We have ordered a digital terrain model and an ortho-photograph from Fjellanger Widerøe to help determine the dip of the fault near the surface.

Geological studies of rock avalanches in Troms by Lars Harald Blikra demonstrate a surprisingly high number of events in the Kåfjord area. There are also several large-scale gravitational features in this area, characterised by large faults and crevasses. Horizontal displacements of as much as 10 m have been observed. The most probable trigger mechanism of those events is thought to be large-scale earthquakes. Attempts at dating some of the rock-avalanche events have thus been given priority. Seismic surveys on one avalanche in Sørfjorden, the fjord west of the Lyngen peninsula, indicate that this event occurred shortly after the deglaciation (ca. 10000-9500 years BP). Mapping of a large rock avalanche close to the Nordmannvik postglacial fault revealed evidence of marine abrasion and formation of beach terraces on high

altitudes, demonstrating that the event occurred shortly after the deglaciation. Geophysical investigations have been done on these deposits in order to map the relationship between blocky rock-avalanche deposits and the marine sediments. A large bedrock collapse west of Salangen formed huge blocky rock-avalanche deposits. Road cuts through this avalanche exposed marine sediments with mollusc-shells on relatively high altitudes, also indicating an old age. The conclusions from these studies may have a bearing on estimating the hazard related to developing petroleum fields at the continental margin offshore Norway, e.g. the Ormen Lange gas field below the Storegga slide.

The preliminary conclusions of this study indicate that the rock avalanches in Troms are concentrated in specific zones, and that they are old, formed shortly after the deglaciation. This implies that there were major earthquakes in the period 10000 to 9500 years BP, which might also be correlated with the postglacial faulting in Nordmannvikdalen.

David Roberts carried out a 3-day spell of fieldwork restricted to examining drillholes (boreholes) in road-cuts over a wide area extending from western Porsangerfjord to eastern Laksefjord, and even as far east as Varangerfjord. A drillhole displaced in a reverse-fault (thrust) sense along a slaty cleavage surface had been described earlier from a locality near Lebesby, Laksefjord, and some time was spent in re-examining this road-cut as well as other road-cuts in the same district. Two other, comparable, thrust-fault, drillhole offsets were encountered, both with roughly ESE to SE displacement vectors. Drillholes were also examined in many localities for axial fractures, which are considered to represent the local, and perhaps regional, stress relief axis — tensional fractures broadly parallel to the thrust trend and the contemporary S-max (horiz.). Some time was spent in and adjacent to the slate quarries at Friarfjord, innermost Laksefjord, measuring well-defined axial fractures and searching for potential drillhole offsets. Axial fractures in drillholes were particularly numerous in c. N-S to NNE-SSW oriented quarry faces, and showed mainly WNW-ESE to NW-SE trends. The data has been plotted during the autumn and an assessment of their significance made for the annual technical report.

The fieldwork by Morten Thoresen in Nord-Østerdalen in 1998 has focused on establishing a network and to find localities for detailed GPS-measurements in 1999. The main idea is to use the glacial dammed lake Nedre-Glåmsjø beachridges and lateral drainage systems (approx. 660 m above sea level) to establish isobase curves for the area. This will reveal if there are other processes than the normal isostatic uplift involved in the land uplift. Holmsen (1916) reported distortions of shorelines in Nord-Østerdalen from levelling data. The main challenge in 1998 has been to find localities with an exact measurable sea level. Both landforms as terraces, lateral drainage systems and beach ridges appear, but they sometimes have a complex origin and not all of them are possible localities to measure. So far the lateral drainage systems seem to be the most usable phenomena, mainly because they can be traced over long distances. But not all of them are necessarily made during an ice dammed lake stage, so also other landforms have to be measured.

A 3D gravity interpretations of the Sjona and Høgtuva tectonic windows in the Ranafjord area is planned to find out if the registered shallow earthquakes occur within the Caledonian nappes or the underlying Precambrian basement.

NEONOR field plans for 1999

a. Percussion drilling of the fifth well near the Stuoragurra Fault, which was originally planned for 1998, but has to be postponed because of the wet terrain which could not support the heavy drilling rig: April.

b. Trenching of a new locality at the Stouragurra Fault, north of Masi: August

c. Mapping of shore lines along the lake Iesjavri in Finnmark to test the hypothesis of subsidence of the Finnmarksvidda area in postglacial time. This work is depending on good weather conditions: August

d. Trenching of the Nordmannsvikdalen postglacial fault in Kåfjord, Troms for studies of deformation and dating of faulting. The excavator has to be transported with an helicopter into the field. Combined with NEONOR Project Meeting and excursion: August

e. Mapping and dating of rock avalanches in Troms (joint work with another NGU R&D project in the area).

f. Re-measurements of the GPS nets in Masi, Finnmark and Bremangerlandet, Sogn og Fjordane.

g. Surveying of shore lines (ice dammed lakes) in northern Østerdalen to check observed deflections by Holmsen.

h. Field checking of postglacial claims on Grythorga, Hardangervidda and Vassøyna in Ytre Byrknesøyna, Hordaland (to the west of Mongstad, reported by Michelsen *et al.* 1986).

i. Field checking of postglacial claims at Spronget, Krossvatn, Rogaland.

j. Mapping of faults on Bremangerlandet, Sogn og Fjordane

5-7) Geodetic measurements; GPS, triangulation and relevelling (Masi, Rana, Nordfjord, Yrkje and Ølen)

The GPS measurements by the Norwegian Mapping Authorities (SK) at Masi and Bremanger have so far been completed only once, and therefore no information is yet available concerning significant deformations. Indications of deformations will only begin to emerge once additional observations and computations are completed in 1999. Meanwhile, the reduction of the GPS observations at Bremanger are not yet complete, and no results are therefore included in the present report.

The standard Ashtech reduction software was used throughout for computing the vectors, which were subsequently adjusted in a horizontal network by means of the Norwegian Mapping Authority's program "GUNDA". A total of 49 vectors, all observed over a period of at least four hours, were included in the network adjustment. The standard errors for the horizontal and vertical components were approximately 1 mm and 3 mm, respectively. First indications are that the observations could reveal horizontal and vertical deformations of 3 mm and 9 mm per year respectively. These values however can only be confirmed by further observations in 1999, assuming that observational errors can be avoided so that there is consistency from year to year.

The two shortest vectors directly over the fault at Masi and Fidnajåkka were reduced and computed separately:

NM01 to NM02:   175.549 m ± 0.001

NM05 to NM06:   767.810 m ± 0.003

The above results however appear somewhat indecisive, and it is open to question whether an interval of only two years between observations is in fact too short to be able to properly identify the deformations that are suspected.

The Institute of Geodesy and Photogrammetry, University of Trondheim, carried out remeasurements of the Rana GPS net in September. The net was established in 1994 and the results of calculated deformation will be reported in the 1998 Annual Technical Report. No significant deformation has been recorded during the three year period.

The computations of triangulation measurements by the Norwegian Mapping Authorities at Yrkjesvågen are in hand, using a number of different and independent programs for network adjustment. So far, these are producing differing results that need to be examined further. Final results are expected early in 1999. The apparent co-ordinate shifts for all points are less than 0.2 mm per year.

Seven levelling lines were observed during 1997 over assumed moraines at Yrkevågen. Six of these levellings showed no significant height changes with respect to earlier observations. A significant height change is however apparent on the seventh levelling line, at Skjoldstraumen Bridge, although this needs to be confirmed by further observations.

Relevelling of the primary levelling line along the main road E134 from Haugesund through Ølen in 1988 showed an anomalous uplift pattern, which has been interpreted by Anundsen (1989) to represent an active halfgraben. Benchmark B36N0063 appeared to have moved vertically by 16 mm in the period from 1965 to 1988. The most recent relevelling in 1998 showed a further movement of 7 mm. Careful examination of the area around the benchmark indicates that it was emplaced in an unstable block or slab of rock. Similar vertical movements were not found at the extra benchmarks that were established in 1988, and this serves to further confirm that the suspect benchmark was originally founded at an unstable location.

The GPS nets in Masi and Bremangerlandet will be re-measured in 1999.

8-9) Drilling through faults; In situ stress measurements and trenching (Masi)

The NEONOR Project received an additional 100.000 NOK funding from NGU's Network Project (a project to encourage increased NGU collaboration with Norwegian universities and research institutes). We had applied for the extra funding to finance part of the *in situ* stress measurements in wells through the Stuoragurra postglacial fault in Masi by Ægir Jóhannsson, SINTEF and Arne Myrvang, NTNU. A total of five wells (percussion drilling) were planned in the Masi area for the 1998 field season. Three 3" diameter wells to a depth of 50-60 metres were drilled for *in situ* stress measurements, one on each side of the fault and one within the fault complex. Two 5.5" wells were planned to penetrate the fault to investigate the fault at depth. These two wells should also be utilised for groundwater test pumping and sampling. The drilling of one of these two wells had to be postponed to April 1999 because the ground was to wet for driving with the heavy drilling rig. The drilling company, Nord-Norsk Brønnboring, will drill the well on frozen ground in April when they also plan to do other drilling in Kautokeino. This drilling will be carried out without any increase in costs (relative to the contract). Temperature, conductivity, pH and CO_2-content of the groundwater were measured in the field. Samples for chemical analysis were also collected. An extraordinary high ground-water yield was found in the fault; more than 13.000 litres per hour, which was the maximum pumping capacity of the pump. The high content of CO_2 (100 times higher than in ordinary ground water) has been a matter of further study. Further chemical analysis did, however, not reveal any other anomalous chemical composition of the water.

Because of the intense fracturing of the bedrock, even at a distance of several kilometres from the fault scarp, it was not possible to get a hydraulic splitting of fresh bedrock within the wells. Hydraulic jacking of existing cracks occurred in all tested sections, which was selected from the electrically most resistive parts of the wells (from well logging).

The fault gouges in the Stuoragurra Fault have sealing properties. Ground water has earlier been encountered in BH4 at a depth of 35 m (2 m above the main fault zone). After penetration of the fault gouges at a depth of 37 m the ground water was drained but appeared again at a depth of 40 m. The fault gouges did consequently cause a 'hanging' ground water surface above the main fault zone.

Results from fieldwork in Finnmark and Troms have been reported from NGU and Sintef and will be included in the Annual Technical report.

Several groundwater springs occur along the fault scarp and one of them causes poisoning of the soil along a 25 m long and 3-5 m wide zone with no vegetation other than the flower *Viscaria alpina* and some moss. More than 1% copper content is detected in the soil.

There are also indications that the magnitude 4.0 earthquake on 21 January 1996 had influence on the groundwater in the Masi area. Large amounts of water had poured out of the fault escarpment at Stuoragurra some time between 23 January and 20 August 1996. The Norwegian Water Resources and Energy Administration (NVE) in Narvik (R. Sværd, pers. comm. 1998) has provided river flow data for the period 1989-1997 from the Iesjakka River which is draining the area where the M. 4 earthquake occurred on 21 January 1996. The gauge is located in Jergul, 20 km to the west of Karasjok. The flow rate was reduced by c. 30% during the week after the earthquake and stayed low during the months of February, March and April till the snow melting started in the middle of May. Reduced water flow after reverse fault earthquakes is also reported from Alaska and Japan. Normal fault earthquakes do, on the other hand, cause increased water flow. The fault plane mechanism (by NORSAR) from the 1996 earthquake shows that it is a reverse fault earthquake.

10) Detailed seismicity monitoring

The seismic network in Rana has now been redesigned by Erik Hicks and Conrad Lindholm to a network of 4 stations using a remote data acquisition system based on the UiB SEISLOG technology, with dial-up connection via modem from NORSAR. This will save the costs of a dedicated line, as used earlier. The first data indicate a successful installation and a stable operation. It is expected that the detection threshold will be only marginally affected as compared to the earlier 6-station network, but with somewhat lower location precision. The transmission costs are reduced to almost zero. This new (redesigned) data acquisition system has been a success, approximately 50 earthquakes were located during the autumn. A new group of earthquakes has appeared under Handnesøya in the western part of the Sjona fjord. The ~25 events have magnitudes ranging from under 1 to 2.5. Several of the quakes have been noticed by the local inhabitants as loud cracking/banging sounds, indicating a shallow hypocenter depth. Similar observations were reported during the Meløy earthquake swarm in 1978. The epicenters show a similar NW-SE orientation as the other groups north of the Sjona fjord.

The installation of the new 6-station seismic network in Bremanger started Sept. 29, based on the same technical solution as in Rana. There were some logistical planning problems related to line-of-sight, road and power access, etc., but a solution was found which is hoped to be acceptable without losing any of the initially planned network apertures (resolution).

The new network in Bremanger has had some technical problems, possibly related to a defective power supply, which means there is currently no data available. Erik Hicks made a maintenance trip to the network in Bremanger in November. The main problem that caused loss of data from all channels in October was caused by water in the amplifier box at the central station, which shorted out the power supply. Two of the radio receivers had also malfunctioned, it is unclear if this was connected to the power supply problems or due to lightning. The mo-

dem had also malfunctioned. Unfortunately, the new modem developed the same symptoms a few days later, meaning very little data is available. Norsar is working on diagnosing this problem so reliable communications may be established. The data acquisition system appears to be running, and has adequate disk space for several thousand detections, so data for November and December will be available at a later date.

Bremangerlandet constitutes an on-land part of the highly seismic area in the northern North Sea (Sogn Graben - northern Viking Graben area) and is therefore of particular interest to the petroleum industry. Interpretation of bathymetry, base Elster and base Quaternary reflectors from four 3D seismic surveys in the northern North Sea have been merged and will found an underlay for the new earthquake locations.

A new tectonic map from the area is produced by NGU within the frame of the project 'Onshore-offshore tectonic links in western Norway' (sponsored by NFR, Mobil Exploration, Phillips Petroleum) and is now released for publication. These data will make up an improved tectonic base map for the new and more precise epicentre locations.

11) Regional and local modelling

Quantitative modelling of the new compilation of uplift data will be carried out during 1999 by Willy Fjeldskaar at Rogalandsforskning. Glacio-isostatic modelling will reveal local areas that have a significant difference between the observed uplift and the calculated uplift. These may represent regions that experience tectonic movements today.

12) Reporting

The NEONOR Project Meeting was carried out according to the plans on 17-18 August with a total of 23 participants. A status report of the NEONOR activities in the first half of 1998 was produced for the meeting. A visit to the Stuoragurra postglacial fault was included. The project had a good press both in national and local newspapers and radio. Linn Arnesen and Hilmar Bungum were interviewed on the NRK national news; 'Her og nå' and 'Dagsnytt 18'. NRK made also a program in the popular science series 'Verdt å vite'. An excursion guide for the field trip to Masi and Kåfjord was prepared.

The NEONOR Annual Technical Report of 1997 has been sent to Dr. John Adams, Geological Survey of Canada and Professor Arthur Sylvester, University of California for review. The referee's reports were included in the NEONOR Status Report and were taken into account in the planning of the field season and further work within the NEONOR Project.

Professor Arthur Sylvester was invited as keynote speaker to the Alta meeting. He presented examples of quantification of crustal deformation in the western United States.

The editor (Halfdan Carstens) of the new Norwegian geological magazine, GEO, has offered to write an article about the NEONOR Project. John Dehls has received an invitation to publish the results from the NEONOR Project in a special neotectonics volume of the Quaternary Science Reviews. These matters will be discussed at the NEONOR meeting in Stavanger.

Geoscientists at the Geological Survey of Finland and University of Potsdam have expressed their interest in collaborating with the NEONOR Project. The Geological Survey of Finland has launched a similar project to the NEONOR Project in northern Finland. Professor Frank Scherbaum at the University of Potsdam has contacted NORSAR and expressed their interest in doing a multi-disiplinary study of the postglacial faults in Finnmark and Troms. The practical arrangement of the collaborations will be discussed at the NEONOR Steering Committee meeting in Stavanger.

Deadline for submitting contributions by the NEONOR participants to the Annual Technical

Report was 30 November. Drafts of most contributions have been received.

The NEONOR Project will be represented by four papers at the Norwegian Geological Society (NGF) Meeting in Stavanger, January 1999. We aim at presenting a total of four papers emphasising different aspects of the project. The NEONOR abstracts (which have been approved by the sponsors) are enclosed at the end of the present report.

The next NEONOR Project Meeting will be arranged at NPD, in Stavanger on 5 January, which is the day before the Annual Meeting of the Norwegian Geological Society.

A project web site has been constructed:

  http://geofysikk.ngu.no/neonor

Presently the site contains information from various project documents, information about the project members, minutes from meetings and status reports. Internet access to the NEONOR database has been tested and will be implemented when the confidentiality is secured.

NORSAR has constructed a web-page for the seismicity part of the NEONOR-Project and reports results from the seismic network in the Rana area:

  http://www.norsar.no/NEONOR/

Odleiv Olesen (NEONOR Project leader) was granted one sabbatical year from his position at NGU as Project Manager of Regional Geophysics. He has continued to work on the NEONOR Project at the Norwegian Petroleum Directorate in Stavanger and will manage the project from the NPD premises during the period 01.09.98 - 01.08.99.

Abstracts from the 16th Winter Meeting of the Norwegian Geological Society, Stavanger 5-7 Janauary, 1999.

POSTGLACIAL FAULTS IN TROMS AND FINNMARK: NEW EVIDENCE FROM GPR, PERCUSSION DRILLING AND TRENCHING

Dehls, John, Olesen, Odleiv, Olsen, Lars, Rønning, Jan Steiner

Norges geologiske undersøkelse, P.O. Box 3006, 7002 Trondheim

The Nordmannsvika postglacial fault is a NW-SE trending normal fault, dipping to the NE. The fault offsets glacial till material on the NW slope of Nordmannvikdalen. The escarpment varies in height from 0.5 to 1.5 metres, with a trench often present between the hanging wall and the footwall. The fault locally splits into 2 subparallel branches, however this is probably only in the glacial overburden. Ground penetrating radar (GPR) profiles were made during the 1997 and 1998 field seasons. Two prominent reflectors can be seen in the bedrock, dipping approximately 40° to the NE. An upward extrapolation of the northernmost reflector through the overburden coincides with the position of the surface scarp. The bedrock is well exposed along a stream bed parallel to the GPR profiles. The rocks are folded, with the foliation varying in dip between 20° to the SW and 35° to the N, and thus cannot be responsible for the reflectors visible in the GPR profiles.

The Stuoragurra postglacial fault can be followed, in several discontinuous sections, for 80 km, in a NE-SW direction. Since 1983, the Stuoragurra Fault has been the subject of numerous field mapping, seismological and geophysical studies, as well as both percussion and core

drilling. The fault is a reverse fault, with up to 10 metres of displacement. During August, this summer, two trenches were made across the Stuoragurra Fault, between Kautokeino and Masi. For the first time, the fault was directly observed in the bedrock. The hanging wall was seen to be thrust upwards over the footwall, with 7 metres vertical displacement evident from displaced glacial contacts. The fault did not penetrate the overlying glacial materials, but rather folded them, forming a blind thrust. Large liquefaction structures were found in the glacial material in both trenches. These liquefaction structures were probably formed in the minutes following the earthquake that formed the fault.

LOCAL SEISMICITY AND STRESS DATA FROM SELECTED AREAS IN NORWAY

Hicks, E.C (1,2), C.D. Lindholm (1) & H. Bungum (1,2)

(1) NORSAR, Box 51, N-2007 KJELLER

(2) Department of Geology, University of Oslo, Box 1014 Blindern, 0316 OSLO

erik.hicks@norsar.no/Fax: +47-63818719

As part of the NEONOR (Neotectonics in Norway) project, three areas in Norway are currently under close scrutiny regarding seismic activity, primarily aimed at mapping a possible correlation between neotectonics and earthquakes. A six-station local seismic network was installed in the Rana area in Northern Norway in July 1997, later in September 1998 reduced to four stations. A similar six-station network was installed in the Bremanger area in Northwest Norway in October 1998. There are also plans to study the seismic activity of the Stuoragurra fault area in Masi, Finnmark in 1999.

The seismic network in Rana has provided data surpassing all expectations, as several hundred earthquakes with magnitudes in the range ML 0.1 to 2.8 were located during the first year. Hypocenter depths are shallow, mainly around 5-12 km, which is consistent with other onshore earthquakes in the region. Four main clusters in time and space with large numbers of earthquakes have been observed. Nine earthquake focal mechanism solutions were determined, consistently showing up to 90° rotation of the principal stress axis with regard to the regional stress field. The network was planned to be disassembled in 1998, but the excellent results inspired a continued presence in the area. The four remaining stations provide virtually the same lower magnitude threshold of detection, albeit with a slightly reduced location precision.

The Bremanger area in Northwest Norway is situated close to areas with high levels of seismic activity in the Northern North Sea, and new data from the network will be presented. The network will provide significantly improved location accuracy for these offshore areas, thereby giving better possibilities for one-to-one correlation of earthquakes and faults, and an improved understanding of the deformation mechanisms at work. New focal mechanism stress data will also provide new and better information about the stress pattern in this area, where there are local indications of an exchange between the maximum and minimum horizontal stress directions.

The Stuoragurra fault in Finnmark is a spectacular postglacial fault of approx. 80 km length with an offset of up to ten metres and a surface scarp up to seven meters high. This fault has been trenched as part of the NEONOR project, with interesting results. Earlier microseismicity studies using existing seismic installations a correlation, albeit unclear, of microearth-

quakes in a zone parallel to the fault scarp. An extended study using new instruments is planned for 1999.

NEOTECTONICS IN NORWAY - NEONOR

Olesen, Odleiv[1], Dehls, John[1], Olsen, Lars[1], Rise, Leif [1], Bungum, Hilmar[2], Hicks, Erik[2], Lindholm, Conrad[1], Riis, Fridtjof[3], Bockmann, Lars[4], Blikra, Lars Harald[1], Braathen, Alvar[1], Fjeldskaar, Willy [5], Fanavoll, Stein [6], Longva, Oddvar[1], Myrvang, Arne[7], Roberts, David[1], Skogseth, Terje[7]

[1]Norges geologiske undersøkelse, P.O. Box 3006, 7002 Trondheim

[2]NORSAR, P.O. Box 51, 2007 Kjeller

[3]Oljedirektoratet, P.O. Box 600, 4001 Stavanger

[4]Statens kartverk, Kartverksvn. 3500 Hønefoss

[5]Rogalandsforskning, P.O. Box 2503 Ullandhaug

[6]IKU Petroleum Research, 7034 Trondheim

[7]NTNU, 7034 Trondheim

The NEONOR project represents a national effort by several research and mapping institutions to investigate neotectonic phenomena in Norway, through a multidisciplinary approach. The project is funded by the Norwegian Research Council, the Geological Survey of Norway (NGU), the Norwegian Petroleum Directorate (OD), the Norwegian Mapping Authority (SK), Amoco Norway, Norsk Hydro, Phillips Petroleum, Statkraft and NORSAR. Representatives from the Norwegian University of Science and Technology (NTNU), IKU Petroleum Research and Rogaland Research are participating in the project. The main objectives of the NEONOR Project are to systematically collect data and to provide answers to the questions: 1) How can recent crustal deformation be characterised in time and space? 2) What processes cause neotectonic crustal deformation? 3) What are the implications for migration and occurrence of fluids (especially hydrocarbons and groundwater) in bedrock? 4) What implications exist for geohazards related to construction of sensitive installations, such as pipelines, gasterminals and hydropower-plants? The initial phase of the project has included a systematic compilation and characterisation of reported deformation. Neotectonic crustal deformation has been reported at a large number of locations in Norway (both on local and regional scales). New geological, geodetic and seismological data has, however, also been acquired. The project includes the production of a 1:3,000,000-scale neotectonic map of Norway and adjacent ocean areas. In northern Norway there is now good evidence of postglacial crustal deformation in Rana, Melfjord, Steigen, Kåfjord and Masi. Many of the other reported neotectonic claims in Norway can, however, be attributed to other effects than tectonic, such as: 1) gravitationally induced faults 2) erosion along older zones of weakness 3) overburden draping of underlying bedrock features and 4) stress release features. The detailed studies have shown that there exist two systems of postglacial faults; one set of large scale (up to 10 metre) NE-SW trending reverse faults and another set of minor (1-2 metres offset) NW-SE trending normal faults. The faults are interpreted to represent a conjugate set, with normal faults perpendicular to the extensive system of NE-SW trending reverse faults in northern Fennoscandia.

The reverse faults are generally characterised by increased seismicity, reactivation of regional zones of weakness, high ground water yield and anomalous land uplift. A new seismic mini-array in the Ranafjord area has revealed an area of increased seismicity. Nearly 300 earth-quakes have been detected in less than a year. Studies of commercial 3D seismic data from offshore western and northern Norway have unveiled evidence of Quaternary deformation.

The final phase of the NEONOR project will involve an integrated interpretation of the compiled neotectonic data sets. Glacio-isostatic modelling reveals local areas that have a significant difference between the observed uplift and the calculated uplift. These are assumed to be areas that experience tectonic movements today.

Olsen, Lars, Dehls, John, Olesen, Odleiv, and Rønning, Jan Steinar

Norges geologiske undersøkelse, Boks 3006 - Lade, 7002 Trondheim

LATE QUATERNARY FAULTING AND PALEOSEISMICITY IN FINNMARK, NORTHERN

NORWAY.

The Stuoragurra postglacial fault can be followed on Finnmarksvidda, Northern Norway, in several discontinuous sections, for 80 km, in a NE-SW direction. (See Dehls et al., same issue, for further details.)

During August, this summer, two trenches were made across the Stuoragurra Fault, between Kautokeino and Masi. For the first time, the fault was directly observed in the bedrock. The hanging wall was seen to be thrust upwards over the footwall, with 7 metres vertical displacement evident from displaced glacial contacts (ablation material, including glaciofluvial sediments, overlying lodgement till). The fault did not penetrate the overlying glacial materials, but rather folded them, forming a blind thrust. Large liquefaction and other deformation structures were found in the glaciofluvial sediments in both trenches.

Veins of angular and subangular pebbles from the local bedrock (Masi Quartzite) penetrate more than 10 metres laterally from the thrust plane and into the sediments in the footwall. It is thought that these veins were possibly injected during the fault activity. The overall deformation may have taken place in one or more phases, but the major deformation of the sediments has a décollement plane that continues laterally in the E/B horizon contact of the modern soil on top of the footwall. This may indicate that an initial pedogenesis had taken place before the fault activity occurred, however no macro plant fossils to support this were found in the possible buried soil.